INVESTIGATING METHODS OF VISUALISING TRANSLATION

IN *SCHIZOSACCHAROMYCES POMBE*

Tina McLeod

Supervised by Dr Saverio Brogna

March 2016

School of Biosciences
The University of Birmingham
Birmingham, B15 2TT

This thesis is submitted for the degree of
DOCTOR OF PHILOSOPHY

Abstract

Gene expression is compartmentalised in eukaryotes due to the nuclear envelope separating the nuclear processes of transcription and pre-mRNA processing from cytoplasmic translation. While ribosome biosynthesis takes place in the nucleus, it is understood that a number of mechanisms keep them inactive until they reach the cytoplasm, where they mature to become translation-competent. However, this accepted view is being challenged by an increasing number of reports which suggest that translation may also occur in the eukaryotic nucleus. Recently, a new technique termed ribopuromycylation (RPM), claimed to report the presence of translating ribosomes in the nuclei of human cells. RPM involves immunodetection of puromycin-labelled nascent peptides on ribosomes that have been immobilised on mRNAs with translation elongation inhibitors. The aim of this study was to assess whether translating ribosomes are present in the nuclei of the fission yeast *Schizosaccharomyces pombe*. This possibility was suggested by a previous study in the Brogna lab which reported that many ribosomal proteins are present at transcription sites in *S. pombe*. This report details the optimisation of RPM conditions for use in fission yeast and how RPM was combined with chromatin immunoprecipitation (ChIP) to investigate whether translating ribosomes may be present at gene loci. The results of these investigations were, however, inconclusive. An in-depth analysis of the RPM technique was then conducted to assess whether it does report nascent peptides as claimed. In contrast to that reported in the original study in human cells, the results of these investigations suggest that immobilising ribosomes with translation elongation inhibitors does not lead to retention of puromycylated peptides on ribosomes in either *S. pombe* or *Drosophila melanogaster* S2 cells. However, preliminary immunofluorescence data suggests

that despite puromycylated peptides being released from the ribosome, immunodetection of puromycin-labelled peptides might still be used to visualise the sub-cellular localisation of ribosomes in *S. pombe*, along with other approaches which are also described here.

Acknowledgements

I would like to give my sincere thanks to my supervisor, Dr Saverio Brogna, for allowing me to experience the world of research and for his constant advice, encouragement and patience throughout my PhD.

A special mention to Kim Piechocki, who I shadowed as an intern, for providing an excellent grounding to start my PhD, and for her continued friendship since. To Marija Petric, who has gone to extraordinary lengths to provide practical help with preparing figures and proof-reading this thesis, but mostly for the emotional support and friendship that has ensured I made it through the difficult times. To Jianming Wang, with whom I shared my PhD journey, for his support and friendship throughout. Thanks to Anand Singh for help with microscope imaging. To all the other members of 6th floor past and present, Samira, Joe, Ming Li, Tom, Subhendu, Pinar, Uli and everyone else with whom I have shared travels, evenings out and general chats that have created so many wonderful memories. I have met so many people with such commitment, determination and resilience; I am truly inspired by you all.

Thanks also to the BBSRC for funding my PhD and for travel funds to attend conferences, to the University of Birmingham for excellent research and teaching facilities and to Dr Alicia Hidalgo and Dr Yun Fan for sharing reagents. I must also acknowledge the role the Open University played in getting me here, for being a flexible route into higher education for those of us who missed the opportunity first time round and who juggle their studies alongside other commitments, and to the excellent tutors who made science accessible and gave me the belief that I could take my studies further.

Last, but by no means least, thank you to all the people in my life outside of academia. To my friends who have been there for me despite me becoming so unreliable. To my mom and sister for the enormous sacrifices they made to help with childcare, which allowed me to work the unusual hours that research demands. I cannot express how much I appreciate your support - I could not have done this without you both. Finally, to my two daughters, Heather and Libby, for adjusting to our rather erratic routine so well and taking everything in your stride. I am proud and extremely fortunate to have you both in my life.

I would like to dedicate this work to my dad, Ian McLeod.

I would have loved for him to be here to share my journey in science.

Abbreviations used in this thesis

40S	Eukaryotic small ribosomal subunit
60S	Eukaryotic large ribosomal subunit
80S	Eukaryotic ribosomes
90S	90S pre-ribosome
BBP	Branch point binding protein
BiFC	Bimolecular fluorescence complementation
BPS	Branch point sequence
BSA	Bovine serum albumin
CBC	Cap binding complex
CBP	Cap binding protein
CDS	Coding sequence
Cryo-EM	Cryo-electron microscopy
CTD	C terminal domain
ChIP	Chromatin immunoprecipitation
DEPC	Diethylpyrocarbonate
DFC	Dense fibrillar component
DNA	Deoxyribonucleic acid
DSCAM	Down syndrome cell adhesion molecule
DSE	Downstream sequence element
EDTA	Ethylenediaminetetraacetic acid
eEF	Eukaryotic translation elongation factor
eIF	Eukaryotic translation initiation factor
EJC	Exon junction complex
EM	Electron microscopy

ER	Endoplasmic reticulum
eRF	Eukaryotic polypeptide release factor
ES	Expansion segments
ESE	Exonic splicing enhancers
ETS	External transcribed spacers
FC	Fibrillar centre
FISH	Fluorescence *in situ* hybridisation
GFP	Green fluorescent protein
GC	Granular component
ITS	Internal transcribed spacers
MHC	Major histocompatibility complex
NMD	Nonsense-mediated mRNA decay
ORF	Open reading frame
PABPC	Poly(A) binding protein (cytoplasmic)
PBS	Phosphate buffered saline
PEG	Polyethylene glycol
PTC	Premature translation termination codon
PMSF	Phenylmethanesulfonyl fluoride
Pol (I, II and III)	RNA polymerases (I, II and III)
RNA	Ribonucleic acid
RP	Ribosomal protein
RPM	Ribopuromycylation
RRM	RNA recognition motifs
RT-PCR	Reverse transcriptase polymerase chain reaction
SDS	Sodium dodecyl sulphate
SMG	Suppressor with morphogenic effects on genitalia

SS	Splice site
SF	Splicing factor
U2AF	U2 auxiliary factor
UPF	Up frameshift
UTR	Untranslated region
YFP	Yellow fluorescent protein

Contents

Chapter 1: Introduction

Expression of protein-coding genes involves transcription of double-stranded DNA into a single-stranded messenger RNA (mRNA), and its subsequent translation into protein. In prokaryotes, the processes of transcription and translation are coupled; ribosomes assemble on mRNAs still undergoing synthesis by RNA polymerase. However, the presence of the nuclear envelope in eukaryotes introduces an added level of complexity; mRNAs transcribed and matured in the nucleus must be transported through the nuclear pore complex to the cytoplasm, where functional ribosomes reside and translation can take place. Additionally, a number of covalent modifications, namely 5' capping, splicing and 3'-end processing and polyadenylation, must be undertaken whilst the primary transcript (pre-mRNA) is still within the nucleus (Fig 1.1).

1.1 Transcription

In eukaryotes, transcription of DNA into mRNA is performed by a multi-subunit enzyme, RNA polymerase II (Pol II). Recruitment of Pol II to the promoter of a gene is by means of transcription factors that bind to core promoter elements in the DNA template (Shandilya and Roberts, 2012). Subject to the presence of stimulatory signals, including the phosphorylation status of the C-terminal domain (CTD) of Pol II and the methylation status of histone proteins in flanking nucleosomes, transcription proceeds from the initiation phase, during which the initiation complex unwinds a short stretch of the DNA, to the elongation phase, during which Pol II establishes productive RNA synthesis (Shandilya and Roberts, 2012). Transcription terminates upon recognition of a specific sequence (discussed

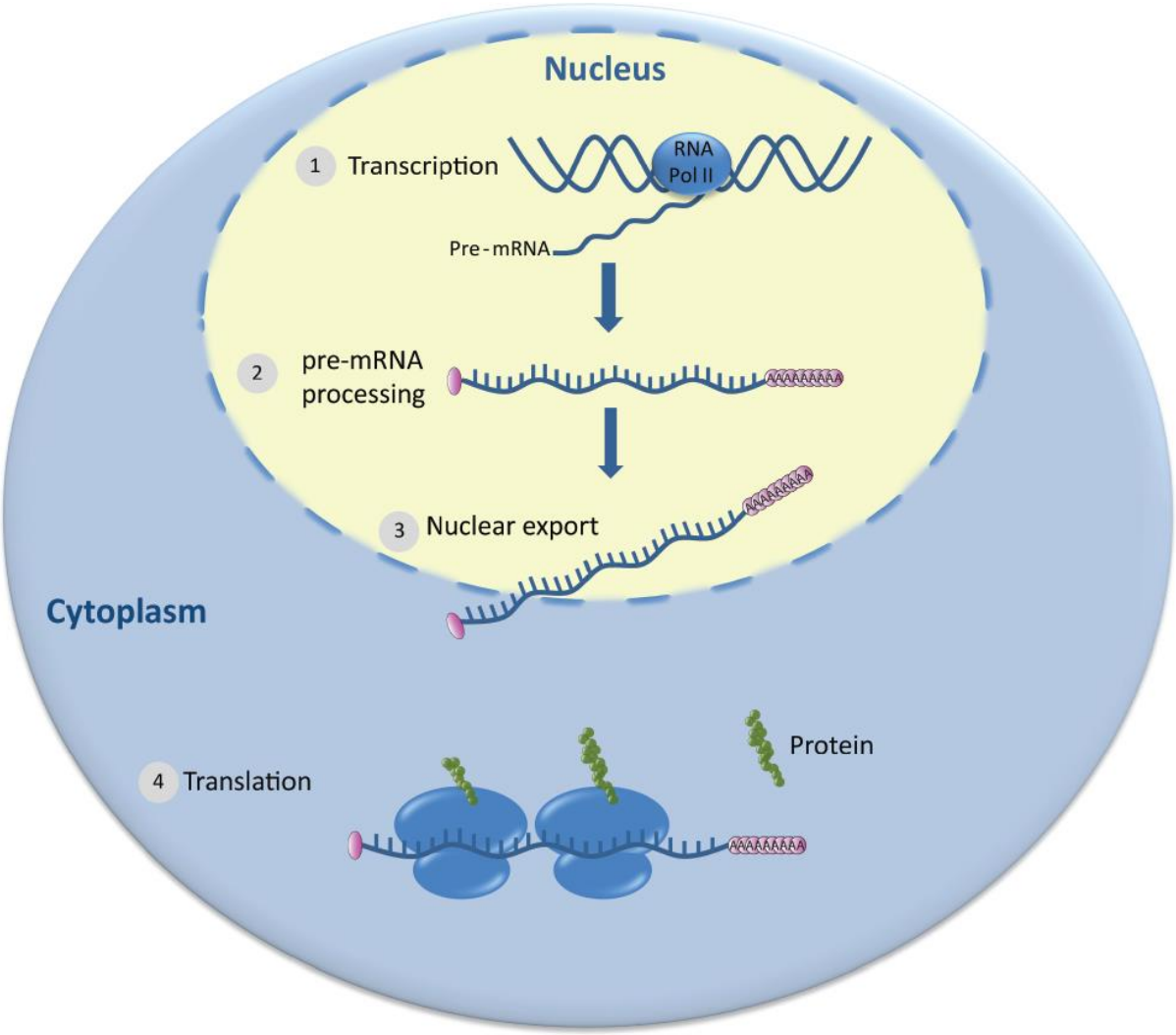

Figure 1.1 Schematic of eukaryotic gene expression. (1) Transcription of DNA into mRNA is carried out by RNA Polymerase II in the nucleus, producing a precursor mRNA (pre-mRNA). (2) The pre-mRNA is processed co-transcriptionally (shown here separately for simplicity) while still in the nucleus, by the addition of a cap at the 5' end (pink oval), a poly(A) tail at the 3' end, which is bound by poly(A) binding protein (pink circles) as well as the removal of intronic sequences. (3) The mature mRNA is transported 5' end first to the cytoplasm, where it is translated into protein by cytoplasmic ribosomes (4).

further in Section 1.2.3) which signals the recruitment of factors that lead to cleavage of the transcript, and subsequent processing of the 3' end (Nag et al., 2007).

1.2 Pre-mRNA processing

1.2.1 5' capping

Capping of the 5' end of an mRNA occurs co-transcriptionally, taking place when the nascent mRNA emerges from Pol II, once it reaches around 25 nucleotides in length (Topisirovic et al., 2011). Correct capping is thought to be a prerequisite for Pol II to escape promoter-proximal stalling, and serves as a checkpoint before the commitment to productive elongation (Saunders et al., 2006). Capping involves the addition and subsequent methylation of a modified guanine base to the 5' end of the mRNA. Two cap binding proteins, CBP20 and CBP80, form the cap binding complex (CBC), of which CBP20 directly binds the cap (Shatkin, 1976). The cap functions to stimulate splicing, direct nuclear export and protect the mRNA from 5'-3' exonuclease degradation (Topisirovic et al., 2011).

1.2.2 Splicing

Splicing, the process of removing introns from the primary transcript (pre-mRNA), is mediated by the spliceosome, a large ribonucleoprotein (RNP) consisting of five uridine-rich small nuclear RNAs (snRNAs) which in humans associate with around 45 discrete proteins, forming the U1, U2, U4/U6 and U5 snRNPs (Brow, 2002, Will and Luhrmann, 2011, Wahl et al., 2009). Between 150 and 300 additional proteins are found to copurify with the spliceosome in mammalian cells, interacting during different stages of the splicing process.

Introns are defined by particular consensus sequences, namely the 5' splice site (SS), branch point sequence (BPS) and a 3' SS (Will and Luhrmann, 2011, Wahl et al., 2009). The majority

of introns also possess a polypyrimidine tract, a pyrimidine-rich region between the BPS and 3' SS, that assists with spliceosome assembly (Brock et al., 2008). Intron excision is a step-wise process, with the spliceosome forming five distinct complexes which arise due to the association and disassociation of the five snRNPs at different stages (Fig 1.2).

Only 3% of *Saccharomyces cerevisiae* yeast genes are spliced and the majority of these have only one intron of around 270nt in length (Ram and Ast, 2007). Approximately one third of these spliced genes encode ribosomal proteins. In contrast, around 45% of genes are spliced in the fission yeast, *Schizosaccharomyces pombe*, with intron lengths of 40-70nt, and around half of these genes having more than one intron (Ram and Ast, 2007). The majority of genes in multicellular species are spliced and introns tend to be longer than in yeast. Genes of higher eukaryotes also possess multiple introns, with humans having 8.4 introns per gene on average (Ram and Ast, 2007). Alternative splicing in higher eukaryotes generates multiple proteins from a single gene (Matlin et al., 2005, Wahl et al., 2009). Exons can be removed along with introns during splicing and as such a number of different protein isoforms can be produced, particularly for genes with multiple exons, which can be retained or excised in different combinations (Breitbart et al., 1987).

1.2.3 3' end processing

The 3' end of the mRNA carries multiple adenine residues (around 250 in mammalian cells) to form a poly(A) tail, to which poly(A) binding proteins (PABPs) subsequently bind, both in the nucleus and in the cytoplasm (Goss and Kleiman, 2013). Formation of the 3' end and poly(A) tail occurs as a coupled cleavage reaction specified by flanking upstream and downstream sequence elements. The key cleavage and polyadenylation determinant is the

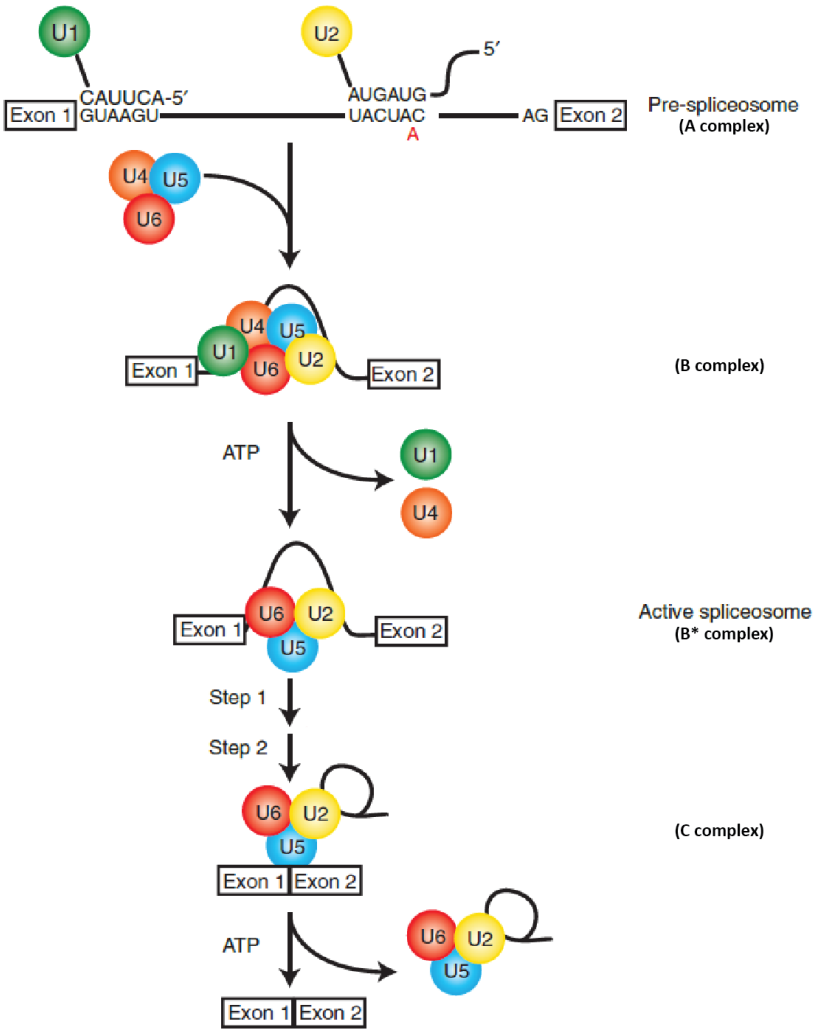

Figure 1.2 Spliceosome assembly and splicing. The pre-spliceosome A complex consists of the U1 and U2 snRNPs bound to the 5'SS and BPS respectively, via base pairing of their snRNAs with the conserved sequences on the pre-mRNA. The U4/U6 and U5 snRNPs are then recruited as a trimeric complex to form the still inactive B complex. Spliceosome activation is concomitant with release of U1 and U4; this rearrangement forms the B* complex. This activated complex performs the first catalytic step of splicing, whereby the BPS connects with the 5' SS to create an intron lariat, generating the C complex. The second catalytic step of exon ligation and excision of the intron lariat is then performed (Abelson et al., 2010).

upstream AAUAAA sequence, also known as the polyadenylation signal, which is recognised by cleavage/polyadenylation stimulation factor (CPSF) (Colgan and Manley, 1997). Binding of CPSF to the signal sequence is stabilised by cleavage stimulation factor (CstF) which binds a GU-rich region downstream of the CPSF binding site (Perez Canadillas and Varani, 2003). Together with cleavage factors I and II (CFI/II), the complex catalyses the cleavage of the mRNA from the transcription complex upon which poly(A) polymerase (PAP) adds adenine residues to the 3' end to form the poly(A) tail (Colgan and Manley, 1997). Similar to the cap at the 5' end, polyadenylation stabilises the mRNA (Zorio and Bentley, 2004). In the cytoplasm, the 5' cap and cytoplasmic PAB (PABPC) have been shown to interact, causing the mRNA to form a closed-loop structure; this is thought to enhance translational efficiency, as translating ribosomes are recycled back to the start of the transcript, where they can resume further rounds of translation (Jackson et al., 2010). This will be discussed in more detail in section 1.3.5.

1.2.4 Transcription and pre-mRNA processing are coupled

Pre-mRNA processing was originally considered to be independent of transcription, however, it is now understood that these processes are coupled. An early indication of this was electron microscopy visualisation of the *Drosophila* chorion gene. This revealed that nascent transcripts appear to shorten while in association with the chromatin, suggesting that splicing occurs co-transcriptionally (Beyer and Osheim, 1988). Subsequent observations that truncation of the CTD of Pol II caused defects in pre-mRNA processing (McCracken et al., 1997) demonstrated that transcription and pre-mRNA processing do not merely occur simultaneously, but are functionally and physically linked. It is now known that the CTD serves as a platform upon which pre-mRNA processing factors assemble (Buratowski, 2009).

The Pol II CTD is composed of numerous heptad repeats with the consensus sequence YSPTSPS (Buratowski, 2009). The number of repeats varies between organisms, with fission yeast possessing 29, *Drosophila* having 45 and vertebrates having 52 repeats (Corden, 2013, Hsin and Manley, 2012). The activity of Pol II depends upon cycles of phosphorylation/dephosphorylation of the serine residues of these heptads (Komarnitsky et al., 2000). Chromatin immunoprecipitation studies in budding yeast reported that the serine residues at positions two and five of the heptads undergo phosphorylation at different stages of transcription, for instance Ser 5 is more commonly phosphorylated while Pol II is in the promoter region and may be required for the dissociation of initiation factors, while Ser 2 phosphorylation is strictly associated with Pol II in the elongation phase of transcription (Komarnitsky et al., 2000). In addition, different regions of the CTD were identified as being independently involved in stimulating different mRNA processing events (Fong and Bentley, 2001).

The key role of the CTD of Pol II in coupling transcription with pre-mRNA processing is therefore essential to the assembly of a stable messenger ribonucleoprotein (mRNP) that is capable of being efficiently exported, localised and translated (Moore and Proudfoot, 2009).

1.3 Ribosomes and translation

Mature mRNAs are transported 5' end first (Mehlin et al., 1992), via the nuclear pore, to the cytoplasm, where they are translated into a specific protein product. The nucleotide sequence of an mRNA determines the order of amino acids in the final protein and decoding of the sequence is orchestrated by the ribosome, a macromolecular complex of ribosomal RNA (rRNA) and proteins (Yusupova and Yusupov, 2014). The ribosome provides a structural platform upon which the various factors involved in translation assemble, and also contains

a catalytic centre that facilitates the joining of amino acids to produce the resultant polypeptide (Kapp and Lorsch, 2004, Jackson et al., 2010, Dever and Green, 2012). Ribosomes associate with mRNAs and possess an entry site where charged transfer RNAs (tRNAs) bring amino acids to the growing peptide. tRNAs pair with nucleotide triplets (codons) on the mRNA via a complementary anticodon sequence (Kapp and Lorsch, 2004). Studies into the structure of the ribosome have increased our understanding of how it performs these functions (Maguire and Zimmermann, 2001, Schuwirth et al., 2005, Ben-Shem et al., 2011, Selmer et al., 2006, Armache et al., 2010, Anger et al., 2013). Details of ribosome biogenesis, ribosomal structure and the molecular basis of translation are outlined in the following sections.

1.3.1 Ribosome structure

Both prokaryotic and eukaryotic ribosomes are composed of a small and a large subunit, each consisting of its own complement of rRNA and proteins (Jackson et al., 2010). The unit of measurement for ribosomes, individual subunits and rRNAs is the Svedberg (S), a measure of the rate of sedimentation under ultracentrifugation which is determined by both the size and shape of a particle (Erickson, 2009). The prokaryotic 70S ribosome has a 30S small subunit, which contains a 16S rRNA and 21 proteins, and a large 50S subunit with two rRNAs of 5S and 23S, as well as 33 proteins (Melnikov et al., 2012). The larger eukaryotic 80S ribosome is composed of a 40S small subunit which has an 18S rRNA and 33 ribosomal proteins, and a 60S large subunit composed of three different rRNAs, 5.8S, 28S (25S in yeast) and 5S, plus 47 proteins (Ben-Shem et al., 2011, Yusupova and Yusupov, 2014). At the interface of the two subunits are three sites that bind transfer RNA (tRNA), the A, P and E sites. The A (acceptor) site houses the decoding centre, where the anticodons of

incoming aminoacylated tRNAs pair with mRNA codons. The growing peptide is tethered to the P (peptidyl transfer) site which provides the catalytic activity for peptide bond formation between the peptide and the incoming amino acid in the A site (Melnikov et al., 2012). The nascent peptide passes through a tunnel in the 60S subunit, the entrance to which is adjacent to the P site. Deacylated tRNAs are discharged from the P site into the third tRNA binding site, the exit (E) site (Melnikov et al., 2012). Details of the stages of translation will be reviewed further in section 1.3.5.

The ribosomal proteins and segments of the rRNA that are involved in forming the functional sites of the ribosome were initially identified by biochemical analyses in bacteria (Maguire and Zimmermann, 2001). Higher resolution X-ray crystallography and cryo-electron microscopy have together provided a much more detailed insight into the three-dimensional structure of both prokaryotic and eukaryotic ribosomes (Fig 1.3). The crystal structure of bacterial ribosomes has been resolved at 3.5 Å (Schuwirth et al., 2005), and at 2.8 Å when complexed with tRNA and mRNA (Selmer et al., 2006). The yeast 80S crystal structure has been resolved at 3.0 Å (Ben-Shem et al., 2011) while cryo-EM imaging of translating ribosomes from the wheat germ plant, *Triticum astivum,* was undertaken at 5.5 Å (Armache et al., 2010). Most recently, cryo-EM imaging has revealed the structure of *Drosophila* 80S at 5.4 to 6.0 Å, and human 80S at 3.8 to 9.0 Å (Anger et al., 2013).

Comparative analysis of the various models across species has shown the eukaryotic ribosome to be more complex than that of prokaryotes, however, the ribosomal core, which houses the functional centres, is composed of 34 proteins and around 4,400 rRNA bases that are highly conserved across bacterial and eukaryotic species (Yusupova and Yusupov, 2014). It was postulated that the catalytic activity required for peptide bond formation

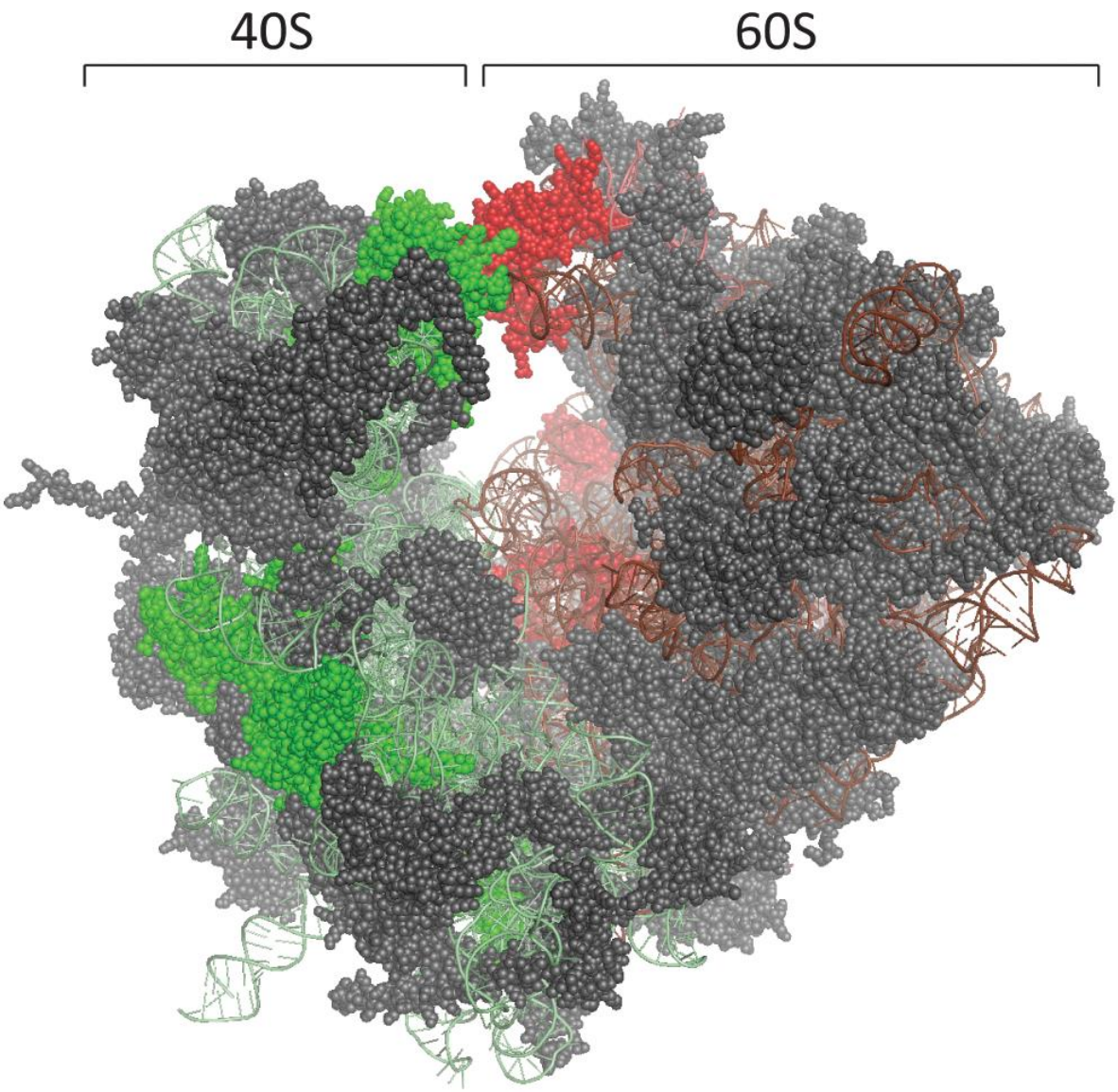

Figure 1.3 3D structure of the eukaryotic ribosome. Front view of the eukaryotic 80S ribosome. The structure was generated with PyMol, by modifying a PyMol Session downloaded from http://www.mol.biol.ethz.ch/groups/ban_group/Ribosome, which visualizes PDB files 2XZM (40S) and PDB 4A17, 4A19 (60S).

might be provided solely by the rRNA component of the ribosome, and bacterial studies seeking to resolve this identified a highly conserved region on the 23S rRNA that was integral to peptidyl transferase activity (Barta et al., 1984). However, the contribution of ribosomal proteins to this activity could not be ruled out, although further studies of catalytically active purified ribosomal particles eliminated all but two RPs (Noller et al., 1992). A more detailed analysis of the architecture of the ribosomal active site, from the crystal structure of the bacterial large subunit at 2.4 Å resolution, revealed that it is composed solely of rRNA, providing the most conclusive evidence to date that the ribosome is indeed a ribozyme (Cech, 2000). As well as the core conserved proteins, bacterial and eukaryotic ribosomes have numerous additional domain-specific proteins that are located at the solvent side. Bacterial 70S ribosomes possess 20 specific ribosomal proteins, 6 of which are found on the small subunit, and 14 of which are located on the large subunit (Yusupova and Yusupov, 2014) while the eukaryotic 80S has 18 additional eukaryotic-specific ribosomal proteins on its 40S subunit, and 28 in the 60S subunit. It is thought that the different repertoires of RPs between bacteria and eukaryotes function to regulate the initiation, termination and recycling stages of translation (discussed further in Section 1.3.5), which operate differently between the domains (Yusupova and Yusupov, 2014). Further divergence between the bacterial and eukaryotic ribosomes is evidenced through the presence of expansion segments (ESs), additional rRNA segments that have been acquired by serial accretion onto the conserved rRNA core, without disrupting the structures that the core forms (Petrov et al., 2015). Although a full characterisation of the roles of ESs is yet to be undertaken, their location predominantly at the solvent side of each of the ribosomal subunits suggests that they may increase the range of interactions the ribosome can make (Melnikov et al., 2012). One study which investigated ESs in the eukaryotic 25S rRNA

revealed that their deletion impinges upon 25S processing, demonstrating that ESs have a role in ribosome biogenesis (Ramesh and Woolford, 2016). Expansions are also found in some eukaryotic ribosomal proteins by acquisition of additional amino acids (Parker et al., 2014). These have been found to mainly increase the basicity of these RPs, which is thought to assist in their association with intracellular membranes, for instance during protein synthesis at the ER and during their transport to the nucleolus for ribosomal assembly (discussed further in section 1.3.3), as well as for increasing stability of the larger eukaryotic ribosome (Parker et al., 2014). The interaction between the small and large subunits is stabilised during translation by intersubunit bridges that are mainly, but not exclusively, between the rRNAs of each subunit. In bacteria there are 13 such bridges, which are conserved throughout evolution (Kietrys et al., 2009). Eukaryotes possess five additional bridges, many of which arise from their domain-specific RPs located at the periphery of the subunits (Ben-Shem et al., 2011), some of which were visualised in *Drosophila* by tagging pairs of RPs with split fragments of fluorescent proteins, which form a functional fluorophore only when the interaction between subunits bring the RPs into close proximity ((Al-Jubran et al., 2013) and Brogna lab unpublished data). The conservation within the core of bacterial and eukaryotic ribosomes explains the universality of the process of protein synthesis across domains, while the evolution of the eukaryotic ribosome towards increasing size and complexity helps to explain how translation has been refined and enhanced in higher organisms.

1.3.2 RPs with extraribosomal functions

Several studies have reported that some RPs have functions outside of their role as part of the ribosome. Many of these extraribosomal roles of RPs are in the regulation of their own

expression. For instance, human RPS14 regulates its own expression by binding intron 1 of its own mRNA and inhibiting its transcription (Tasheva and Roufa, 1995) and this was similarly found to be the case for yeast Rps14 (Fewell and Woolford, 1999). Other RPs, including yeast RPL32, RPL-12 in *Caenorhabditis elegans*, and human RPS26 and RPS13, have been reported to repress their own expression by inhibiting splicing (Warner and McIntosh, 2009, De et al., 2011) while Rps28b and Rpl2 regulate their own expression by accelerating turnover or degradation of their own transcripts in *S. cerevisiae* (Presutti et al., 1991, Badis et al., 2004). RpS3, in addition to regulating its own expression by binding its own mRNA in the cytoplasm, appears to possess a remarkable array of functions outside of its role in the ribosome. *Drosophila* and human RpS3 were shown in vitro to possess an affinity for damaged DNA bases and display N-glycosylase activity, which is required for base excision repair (Graifer et al., 2014). Overexpression of yeast RpS3 and transfection of recombinant RpS3 into mammalian cell lines led to increased resistance to DNA damaging agents. It therefore appears that RpS3 has a role in DNA repair (Graifer et al., 2014). RpS3 is also involved in the regulation of the expression of genes associated with various processes including development, apoptosis, immune responses and cell proliferation. It achieves this by binding nuclear factor-kappa B (NF-κB), which regulates the activity of such genes, facilitating the binding of NF-κB to the promoter region of its targets (Graifer et al., 2014). Other RPs that are reported to have roles outside of the ribosome or their own expression include RpS27a, which enhances cell proliferation and inhibits apoptosis in leukaemia cells (Wang et al., 2014), and RpL11 which binds the promoters of genes targeted by c-Myc, an oncoprotein that promotes cell growth, thereby regulating cell proliferation (Dai et al., 2007).

1.3.3 Ribosome biogenesis

Although functional ribosomes are thought only to be present in the cytoplasm, their assembly occurs in the nucleolus (Panse and Johnson, 2010). The nucleolus, the most apparent sub-nuclear structure, is not a membrane-bound compartment, but rather an organised centre, arising from the assembly of the components of ribosome biogenesis around specific regions of the chromosomal DNA that encode the ribosomal RNA (rRNA) (McClintock, 1934, Heitz, 1931, Shaw and Brown, 2012, Buratowski, 2009, McLeod et al., 2014). Three distinct sub-nucleolar regions are visible by electron microsocopy (Fig 1.4 and (McLeod et al., 2014)). Typically, around 17% of the nucleolus is made up of the dense fibrillar component (DFC), which is where transcription of ribosomal RNA (rRNA) most likely takes place. More lightly stained fibrillar centres (FCs), which constitute around 2% of the nucleolus, are found within the DFC, with some rRNA transcription taking place at their periphery. The majority of the nucleolus is composed of the granular component (GC) which is the site of pre-ribosomal assembly (Shaw and Jordan, 1995, Shaw and Brown, 2012, McLeod et al., 2014). The 18S, 5.8S and 28S rRNAs are transcribed from numerous tandem rDNA repeats (~150 in yeast) (Kobayashi et al., 2001) by RNA polymerase I, producing a single polycistronic pre-rRNA ranging in size from 35S in yeast to 45S in mammalian cells (Venema and Tollervey, 1999, Kopp et al., 2007) (Fig 1.5 A). This pre-rRNA particle is flanked at either end by external transcribed spacers (ETS) and the three rRNA sequences are separated by internal transcribed spacers (ITS), all of which are removed by numerous cleavage steps during pre-rRNA processing (Venema and Tollervey, 1999). The 5S rDNA is transcribed by RNA Pol III and is also found in tandem repeats that usually occupy a separate region of the genome in most organisms, a notable exception being yeast in which

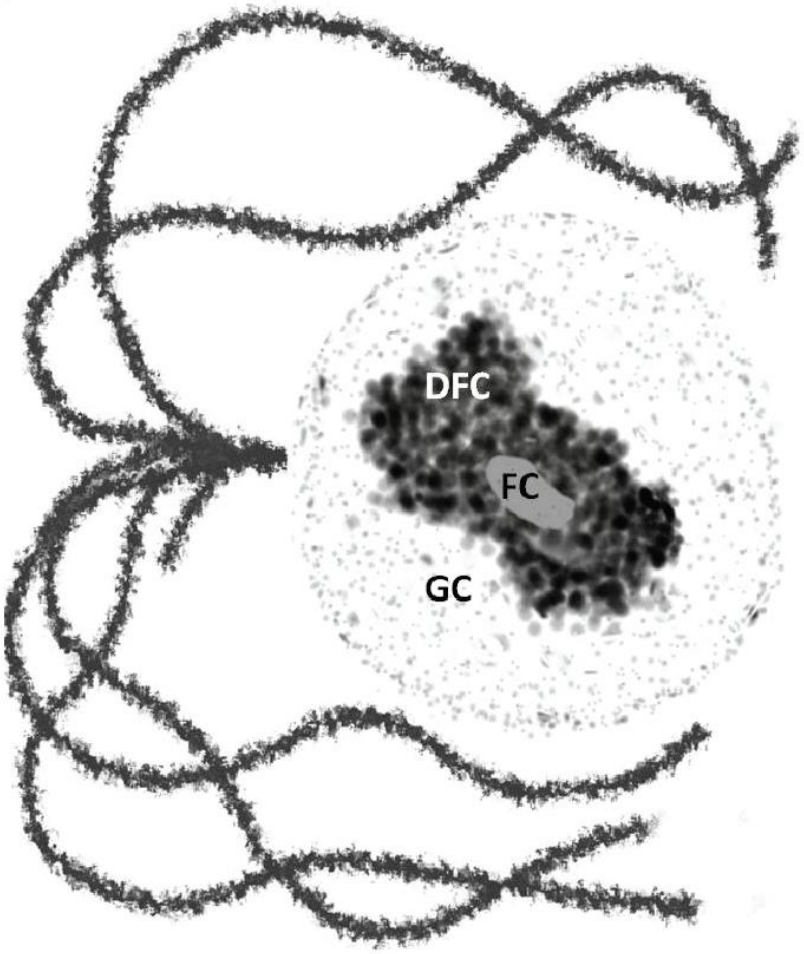

Figure 1.4 Schematic of the nucleolus. The granular component (GC) forms the majority of the nucleolus, with the dense fibrillar component (DFC) and fibrillar centres (FC) contained within. The chromosomes are shown surrounding the nucleolus (taken from McLeod et al., 2014).

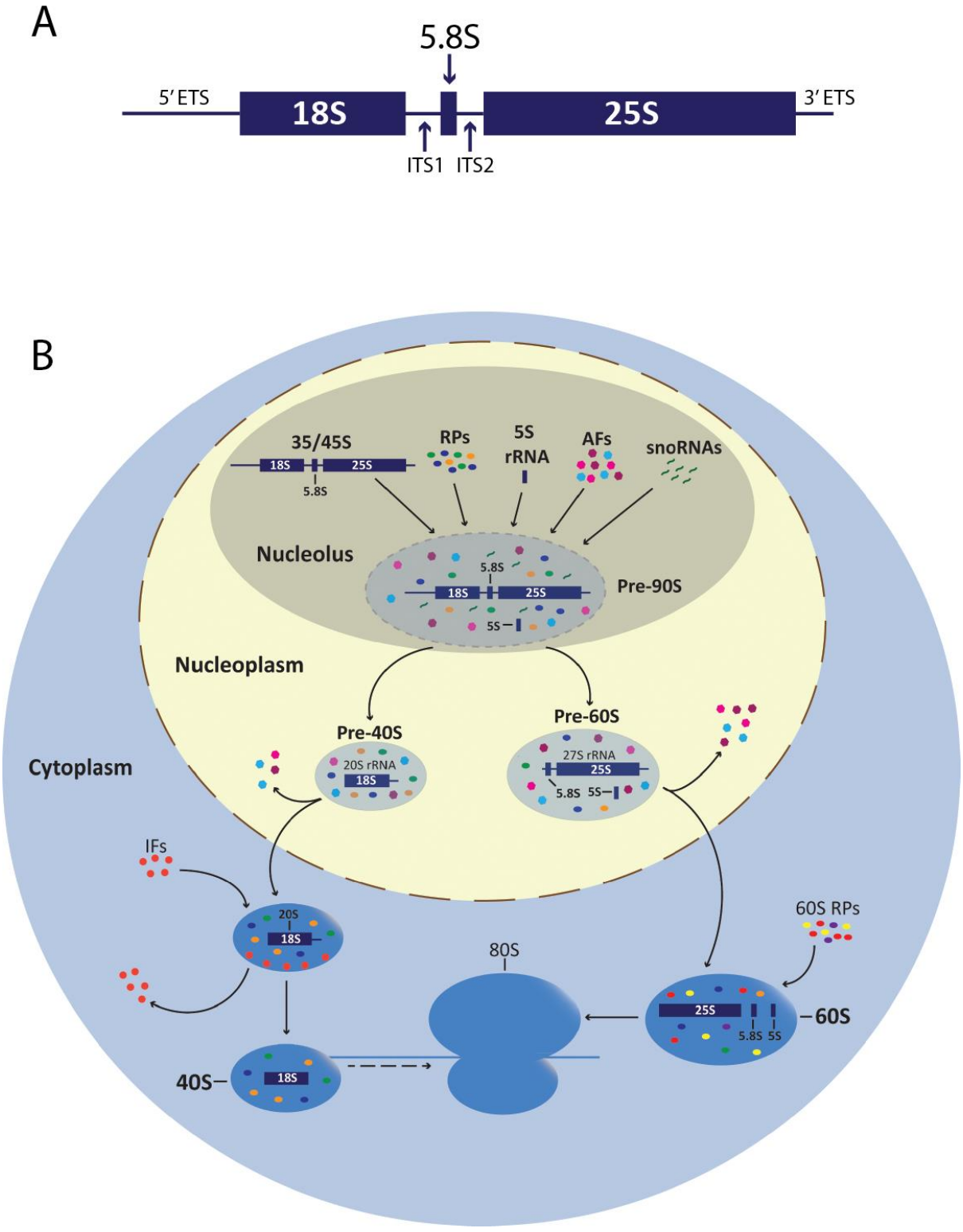
A
5.8S
5′ ETS
18S
25S
3′ ETS
ITS1
ITS2
B
35/45S
18S
25S
5.8S
RPs
5S
rRNA
AFs
snoRNAs
Nucleolus
5.8S
18S
25S
5S
Pre-90S
Nucleoplasm
Pre-40S
20S rRNA
18S
Pre-60S
27S rRNA
25S
5.8S
5S
Cytoplasm
IFs
20S
18S
60S RPs
80S
25S
5.8S
5S
60S
40S
18S

Figure 1.5 Ribosome biogenesis. (A) Schematic of the 35/45S polycistronic precursor rRNA showing the location of the three regions coding for the 18S, 5.8S and 25S, along with the 5' and 3' external transcribed spacers (ETS) and the two internal transcribed spacers (ITS1 and ITS2). (B) The 35/45S pre-rRNA is transcribed in the nucleolus where it assembles with the 5S rRNA, ribosomal proteins (RPs), assembly factors (AFs) and small nucleolar RNAs (snoRNAs) to form a pre-90S particle. Pre-90S assembly occurs cotranscriptionally but is shown here separately for simplicity. Cleavage of the pre-RNA leads to partitioning of the 90S pre-ribosome into a pre-40S particle containing 20S rRNA and a pre-60S particle containing a 27S rRNA and the 5S rRNA. These precursor subunits are processed separately, each traversing the nucleoplasm, shedding some assembly factors, and exiting to the cytoplasm. A number of inhibitory factors (IFs) associate with the pre-40S subunit to prevent it from prematurely engaging in translation. Cleavage of the 20S is the final maturation step that allows the 40S to initiate translation. The 27S rRNA in the pre-60S is cleaved to produce 25S and 5.8S rRNAs, which, along with the 5S rRNA, must associate with the majority of the 60S RPs in the cytoplasm to achieve functionality.

the 5S is found along with the other tandem rDNA repeats (Rubin and Sulston, 1973). Ribosome assembly begins on the nascent pre-rRNA, with the association of the 5S rRNA, snoRNAs, ribosomal proteins and a myriad of trans-acting factors, leading to the formation of a 90S pre-ribosome (Tschochner and Hurt, 2003) (Fig 1.5 B). Non-ribosomal factors which associate at this point include those involved in the pre-rRNA modifications described, endonucleases,exonucleases, RNA helicases and nucleo-cytoplasmic transporters (Venema and Tollervey, 1999). Tandem affinity purification studies revealed that while the 90S contains the majority of the 40S ribosomal proteins, it is surprisingly lacking in those of the 60S (Grandi et al., 2002). A study in *S. cerevisiae* showed that initial processing of the 90S pre-ribosome begins with cleavage of the 3' ETS of the pre-rRNA, releasing the nascent transcript. Cleavage at the 5' ETS then occurs (Veinot-Drebot et al., 1988), followed by exonucleolytic processing at the ITS between the 18S and 5.8S sequences, separating the 35S into a 20S and a 27S particle (Tschochner and Hurt, 2003) (Fig 1.5 B). The 20S is partitioned, along with its complement of ribosomal proteins and assembly factors, into a pre-40S subunit while the 27S, together with the 5S and associated factors, forms a pre-60S subunit. The two are transported separately to the cytoplasm, via the nuclear pore complex, where further maturation takes place to produce the 40S and 60S subunits (Tschochner and Hurt, 2003) (Fig 1.5 B). The final maturation of the 40S subunit is achieved by cleavage of the 20S rRNA to the final 18S (Udem and Warner, 1973), while the 60S forms following a series of cleavage steps that release the 5.8S and 25S rRNAs from the 27S, along with assembly of the ribosomal proteins of the large subunit (Tschochner and Hurt, 2003). The result is mature 40S and 60S subunits that are now capable of participating in translation (Fig 1.5 B).

Although the biogenesis of ribosomal subunits begins in the nucleolus, it is largely accepted that a number of mechanisms keep them inactive until they have fully matured in the cytoplasm (Panse and Johnson, 2010). The 60S subunit is bound by a number of non-ribosomal factors during nuclear export that must be released before the subunit is able to engage in translation. Rlp24 (ribosomal L24-like protein) is one such example; this protein shares sequence homology with the ribosomal protein Rpl24, and is thought to occupy the same site on the ribosome. It therefore appears that binding of this protein prevents the association of Rpl24, which is necessary for ribosome functionality due to enabling the recruitment of other factors that ultimately lead to the release of Tif6, a protein which prevents the joining of ribosomal subunits (Panse and Johnson, 2010). Several assembly factors also associate with the 40S at the late maturation stage in the cytoplasm. These were found to bind regions of the pre-40S that specifically block the binding of initiation factors, mRNA and the 60S, in order to prevent premature engagement in translation (Strunk et al., 2011). It was also discovered in both *S. cerevisiae* and mammalian cells, that processing of the 20S rRNA to 18S is a cytoplasmic event and this was interpreted as being a central means by which the 40S is prevented from prematurely engaging in translation (Udem and Warner, 1973, Rouquette et al., 2005). However, more recent work in *S. cerevisiae* showed that impairment of the processing of 20S rRNA still allows immature 40S subunits to engage with translation initiation factors and that they are detected in 80S and polysomal fractions, although degraded more rapidly than mature 80S (Soudet et al., 2010). It has even been suggested that the association of the pre-40S with initiation factors and the 60S is necessary for the final processing of the 20S rRNA (Strunk et al., 2011, Lebaron et al., 2012). However, these 80S do not contain initiator tRNA and so it was proposed that they must dissociate before they can bind mRNA and begin translation (Strunk et al., 2012).

Nevertheless, it appears that ribosomal subunits are not as stringently kept separated as was initially thought.

1.3.4 Differentiated ribosomes

Since ribosome biogenesis and maturation is a complex and highly-regulated process, ribosomes might be considered to be homogeneous entities that must contain the same complement of RPs and rRNAs in order to function correctly. However, examples of altered ribosomes that have specialised functions or are operational in certain tissues have been described in both prokaryotes and eukaryotes. In *E. coli*, the MazF toxin, produced in response to stress, was known to cleave single-stranded mRNAs at ACA codons, thus inhibiting the translation of the majority of mRNAs, although selective translation of around 50 mRNAs still occurs (Vesper et al., 2011). These mRNAs were found to have been cleaved at or near the AUG start codon, generating leaderless mRNAs (lmRNAs) that lack the Shine-Dalgarno sequence, a short consensus sequence located just upstream of the start codon, which recruits the ribosome to prokaryotic mRNAs. MazF also cleaves at an ACA sequence on the 16S rRNA, resulting in the loss of 43 nucleotides from the 3' end of the 16S sequence. This region forms a part of the decoding centre that binds the Shine-Dalgarno sequence and its absence leads to the generation of 30S subunits which become part of 70S ribosomes that preferentially translate lmRNAs. In eukaryotes, two-dimensional polyacrylamide gel electrophoresis analysis of RPs in the amoeba *Dictyostelium discoideum*, demonstrated the heterogeneity of ribosomes at different developmental stages; two RPs were specific to vegetative cells, and three were specific to differentiated spores (Ramagopal and Ennis, 1981). Analysis of proteome-wide data on the distribution of mouse RPs revealed that ribosomal proteins can have very different expression levels across different tissues such as

the heart, brain, kidney and liver (Kislinger et al., 2006). Often, deletion or loss-of-function mutations of RPs have tissue-specific effects that reflect this expression pattern. One such example is *Rpl38*, which is highly expressed in mouse somites and also in the neural retina and tissues that form the upper lip and palate of mouse embryos. *Rpl38* mutant mouse embryos develop cleft palates and eye and skeletal defects (Kondrashov et al., 2011). In the Brogna lab, visualisation of fluorescently-tagged RPs revealed that RpL41, although abundant in most cell types, is not present in enteroendocrine cells and differentiated enterocytes of *Drosophila* larvae (Brogna lab, unpublished data).

1.3.5 The mechanism of translation

Translation occurs in four stages; initiation, elongation, termination and ribosome recycling (Kapp and Lorsch, 2004). At the initiation stage, ribosomes bound by an initiator tRNA assemble at a translation start codon. The elongation phase involves the decoding of the mRNA sequence by aminoacylated tRNAs, and the ribosome-catalysed formation of peptide bonds between incoming amino acids and the nascent peptide. Termination occurs upon recognition of a translation stop codon, which triggers the release of the completed polypeptide. Ribosome recycling involves the processing of post-termination complexes (post-TCs) to make the ribosomal subunits available for new rounds of translation.

Translation Initiation

In eukaryotes, the initiation stage of translation begins with the formation of a 43S pre-initiation complex (PIC) which is composed of the 40S subunit, bound by three eukaryotic initiation factors, eIF1, eIF1A and eIF3, the ternary complex comprising eIF2, GTP and a specialised, methionine-charged, initiator tRNA ($tRNA_i^{Met}$) which occupies the peptidyl (P)

site on the 40S, and eIF5 (Jackson et al., 2010, Hinnebusch and Lorsch, 2012). The nuclear cap binding complex (CBC) at the 5' end of the mRNA is replaced in the cytoplasm by eIF4F, a complex of three individual factors, eIF4A, eIF4G and eIF4E. eIF4G is a scaffold protein to which eIF4A, eIF4E and other factors involved in translation bind (Prevot et al., 2003, Jackson et al., 2010). eIF4E binds the cap directly, while eIF4A serves as a helicase, removing secondary structures from the mRNA 5' end; this generates a platform upon which the PIC can load (Jackson et al., 2010). eIF3 promotes recruitment of the PIC to the cytoplasmic cap binding complex, while eIF1 and eIF1A induce an open conformation of the mRNA binding channel on the 40S, facilitating mRNA loading (Kapp and Lorsch, 2004, Passmore et al., 2007). The PIC then scans in the 5' to 3' direction until an AUG start codon is encountered, with which the anticodon of $tRNA_i^{Met}$ binds (Jackson et al., 2010, Kapp and Lorsch, 2004). eIF1 is bound near the P site on the 40S, preventing incorrect base pairing between $tRNA_i^{Met}$ and the mRNA, and is only displaced upon correct pairing with an AUG (Hinnebusch and Lorsch, 2012). The resulting intermediate is termed the 48S (Dever and Green, 2012). Hydrolysis of eIF2-bound GTP is then stimulated by eIF5; this leads to the release of $tRNA_i^{Met}$ into the 40S P site and the dissociation of eIF2 (Kapp and Lorsch, 2004). eIF5B joins the complex and, following the release of other initiation factors, promotes the joining of the 60S subunit to form the translation-competent 80S (Kapp and Lorsch, 2004, Hinnebusch and Lorsch, 2012).

Translation initiation in prokaryotes is significantly different to that in eukaryotes. Firstly, there is no temporal or spatial separation between transcription and translation as there is in eukaryotes, and prokaryotic ribosomes are recruited to mRNAs co-transcriptionally (McGary and Nudler, 2013). Bacterial translation involves only three initiation factors, IF1,

IF2 and IF3. IF1 is the bacterial ortholog of eukaryotic eIF1A and prevents the initiator tRNA from incorrectly binding the A site (Passmore et al., 2007, Kapp and Lorsch, 2004). Structurally, IF2 is the ortholog of eIF5B, but functionally shares features of both eIF2 and eIF5B. As with eIF2, IF2 binds GTP, and its hydrolysis causes the transfer of the initiation tRNA (which in bacteria is formylated to give fMet-$tRNA_i$) into the P site of the small subunit (Kapp and Lorsch, 2004). Similar to eIF5B, IF2 also promotes the joining of the large subunit following start codon recognition (Kapp and Lorsch, 2004). There does not appear to be any eukaryotic ortholog of IF3, but functionally IF3 is similar to eIF1, ensuring the fidelity of initiator tRNA binding at the start site (Kapp and Lorsch, 2004). Bacterial initiator complexes bind mRNAs not through binding to a 5' cap as in eukaryotes, but rather by base pairing between the 16S rRNA and the Shine-Dalgarno sequence just upstream of the AUG (Kozak, 1999).

Translation elongation

The elongation stage of translation, during which synthesis of the peptide chain occurs, is highly conserved between prokaryotes and eukaryotes and requires the action of three elongation factors (Kapp and Lorsch, 2004, Saini et al., 2009). The initiator complex at the AUG start codon has a vacant A site poised over the second mRNA codon (Dever and Green, 2012). Aminoacyl-tRNAs complexed with GTP-bound elongation factor 1A (eEF1A, EF-Tu in bacteria) enter the A site, but only cognate tRNAs that correctly pair with the mRNA elicit a conformational change in the small ribosomal subunit that leads to hydrolysis of GTP by eEF1A/EF-Tu, and the full accommodation of the tRNA into the ribosomal A site (Saint-Leger and Ribas de Pouplana, 2015, Kapp and Lorsch, 2004, Dever and Green, 2012). The peptidyl transferase site then catalyses peptide bond formation between the amino acid bound to

the tRNA in the A site and the nascent peptide chain that emerges from the P site (Beringer and Rodnina, 2007). The ribosome now contains tRNAs existing in a hybrid state; the deacylated tRNA, with its anticodon in the P site, has its acceptor arm positioned in the ribosomal E site, while the growing peptide is now tethered to a tRNA with its acceptor arm in the P site but its anticodon in the A site (Dever and Green, 2012). The re-positioning of the anticodons into the P and E sites occurs by translocation of the complex so that the ribosome is now positioned three nucleotides further along the mRNA, with its A site positioned at the next codon (Kapp and Lorsch, 2004); this process is catalysed by eEF2 (EF-G in bacteria) which associates with the 28S/23S rRNA of the large subunit and hydrolyses GTP (Dever and Green, 2012, Ling and Ermolenko, 2016). Translocation appears to be driven by movement of the tRNAs rather than that of the ribosome or the mRNA, with studies reporting that tRNAs must be present in both the A and P sites in order for translocation to occur, and that tRNAs can translocate through the ribosome in the absence of an mRNA template (Ling and Ermolenko, 2016). The deacylated tRNA, now positioned in the ribosomal E site, is released from the ribosome, while a new aminoacyl-tRNA enters the now vacant A site. A third elongation factor, eIF5A (EF-P in bacteria) is also involved in translocation although its molecular function is not known (Saini et al., 2009). While its role in ribosome translocation in a subset of transcripts has been reported (Pereira et al., 2016), whether eIF5A has a universal function in translation elongation is yet to be shown, although yeast studies concluded that it is essential since polysomes accumulated and ribosome transit times increased, when eIF5A was deactivated (Saini et al., 2009). Elongation continues until one of three translation termination codons (UAA, UAG or UGA) is reached.

Translation termination

Termination codons are not recognised by charged tRNAs, but instead by proteins, termed release factors, which morphologically resemble tRNAs (Dever and Green, 2012, Petropoulos et al., 2014). In bacteria there are two class 1 release factors, RF1 and RF2. Both can recognise UAA stop codons but UAG is recognised only by RF1, and UGA only by RF2 (Kapp and Lorsch, 2004). Eukaryotes on the other hand possess only one class 1 release factor, eRF1. Both prokaryotic and eukaryotic class 1 release factors enter the ribosomal A site where they appear to recognise stop codons via a tripeptide sequence (Ito et al., 2000, Chavatte et al., 2002). In *E. coli*, domain swapping between RF1 and RF2 revealed that the tripeptide resides within a central domain (Ito et al., 2000), and recognition is supported by an induced-fit structural change in the small ribosomal subunit (Youngman et al., 2007). Peptide release in prokaryotes is stimulated by a conformational change in the peptidyl transferase centre of the ribosome following stop codon recognition by the class 1 release factors (Korostelev et al., 2008). Bacterial class 2 release factor, RF3, binds GTP and destabilises RF1/RF2, stimulating their release from the ribosome following peptide release and subsequently hydrolyses GTP, which results in its own release (Kapp and Lorsch, 2004). In eukaryotes, analysis of digested mRNA following photoactivatable crosslinking of purified mammalian reticulocyte ribosomes revealed that eukaryotic eRF1 binds the mRNA codon via a tripeptide in its N terminal domain (Chavatte et al., 2002). Similar to prokaryotes, eukaryotes also possess a single class 2 release factor, eRF3 (Dever and Green, 2012). eRF1 and eRF3 interact via their C-terminal domains, and peptide release in eukaryotes is promoted by GTP hydrolysis by eRF3; this causes the middle domain of eRF1 to move into

peptidyl transferase centre of the ribosome, leading to hydrolysis of the nascent peptide (Dever and Green, 2012, Susorov et al., 2015).

Ribosome recycling

Upon termination, ribosomes are recycled for use in further rounds of translation. This process is best-understood in bacteria, which are known to possess a specific ribosome recycling factor (RRF) that works in concert with EF-G and IF3 to make ribosomal subunits available for new initiation events (Kiel et al., 2007, Gao et al., 2005, Dever and Green, 2012, Hirokawa et al., 2002, Zavialov et al., 2005). The precise functions of these factors in ribosome recycling are not fully understood, however a number of studies have provided insights into the process. Following the dissociation of the release factors required for translation termination, RRF binds the A site of ribosomes that now have a deacylated tRNA in the hybrid P/E state (Dever and Green, 2012). RRF is structurally a mimic of tRNA, and it appears that, as in the elongation stage of translation, EF-G stimulates its translocation into the P site, causing the deacetylated tRNA to be released (Hirokawa et al., 2002). Cryo-EM studies suggest that RRF also disrupts intersubunit bridges, thereby destabilising the ribosome (Gao et al., 2005). Both RRF and EF-G are required for the catalysis of subunit dissociation, and the hydrolysis of GTP by EF-G has also been shown to be necessary for the release of subunits from the mRNA, since polysome profiling in the presence of non-hydrolysable analogues does not result in the breakdown of polysomes (Hirokawa et al., 2002). Although IF3 is not necessary for the dissociation of subunits (Zavialov et al., 2005), it is required to keep them apart until a new initiation event (Kiel et al., 2007).

The recycling of eukaryotic ribosomes is less well-understood. Post-termination ribosomes are still bound by eRF1, deacylated tRNA and mRNA; although no specific ribosome recycling

factor has been identified, the initiation factors eIF3 and the ATP-binding cassette protein, ABCE1, are known to be important in the process of splitting ribosomal subunits (Nurenberg and Tampe, 2013). *In vitro* experiments with purified mammalian translation extracts showed the release of deacylated tRNA from post termination ribosomes by eIF1, while eIF3 elicits ribosome release at low Mg^{2+} concentrations, a process that is enhanced by eIF1 and eIF1A (Pisarev et al., 2007). However, at least 20-25% of mRNA remained associated with the 40S subunit, and its release is mediated by a subunit of eIF3, eIF3j (Pisarev et al., 2007). At higher Mg^{2+} concentrations, ABCE1 mediates the dissociation of ribosomal subunits, in a manner requiring ATP hydrolysis (Pisarev et al., 2010). Similar to eIF3, this yields free 60S subunits and 40S still bound by tRNA and mRNA, with eIF1 and eIF3j performing the same functions in their release as in eIF3 mediated subunit dissociation (Pisarev et al., 2010). eIF3 remains associated with the solvent side of the 40S following subunit dissociation, and appears to induce a conformational change in the small subunit that prevents it from associating with the 60S (Jackson, 2010). eIF6 appears to serve a similar anti-association function by binding to the 60S (Groft et al, 2016 crystal structures of ribosome anti-association factor IF6).

Several studies of eukaryotic translation have determined that the recycling of ribosomes may not be explained solely by their complete dissociation from the mRNA. Since their discovery, both the 5’ cap and the poly(A) tail were known to enhance translational efficiency and in vitro translation analysis of eukaryotic lysates showed that the poly(A) tail binds the 5’ cap binding proteins (Gallie and Tanguay, 1994, Tarun and Sachs, 1996). A subsequent study in yeast translation extracts found that this interaction was mediated by the yeast poly(A) binding protein, Pab1p (Tarun and Sachs, 1995, Tarun and Sachs, 1996). An

interaction between the two ends of an mRNA results in a closed-loop formation, and terminating ribosomes are therefore in close proximity to their starting position. It was postulated that in such circumstances the closed loop may facilitate subsequent translation initiation events, since the 40S subunit may not dissociate from the mRNA upon termination and may instead undertake new rounds of translation by shuttling across the poly(A) tail back to the 5' end (Jackson et al., 2010, Dever and Green, 2012). This closed-loop model of eukaryotic translation was substantiated somewhat by the discovery that eRF3 interacts via its N-terminus with the C-terminus of PABP bound to the poly(A) tail (Hoshino et al., 1999), thereby evidencing a direct link between terminating ribosomes and the poly(A) tail, which in turn interacts with the 5' cap. Indeed it was already known that ribosomes are able to reinitiate after translation of upstream open reading frames (uORFs), although this appears to be more efficient when uORFs are shorter (Kozak, 2001). More recently, a global analysis of closed-loop translation in yeast has been published, in which mRNAs associated with 5' cap and poly(A) binding proteins were identified by RNA immunoprecipitation sequencing (Costello et al., 2015). Many mRNAs, particularly those encoding RPs or proteins involved in ribosome biogenesis, were enriched with the components that form the closed-loop conformation, and since these are highly expressed, this suggests that the closed loop is a means of enhancing the initiation of subsequent rounds of translation when demand is high. However, another population of heavily translated mRNAs showed no enrichment with the 5' cap binding proteins but were enriched with Pab1p. Therefore efficient translation is not only orchestrated through mRNAs being in a closed-loop formation (Costello et al., 2015). It has also been reported that, although advantageous under competitive conditions, the association of PABPC and eIF4G is nonessential (Dever and Green, 2012, Jackson et al., 2010). This aspect of ribosome recycling is therefore the subject of continued debate and

further research is required to understand the full extent to which it regulates translation, as well as the precise mechanism by which it occurs.

1.4 Cellular location of translation

As outlined earlier, a number of aspects of ribosome maturation only take place following export of the ribosomal subunits from the nucleus, therefore translation is considered to be a strictly cytoplasmic process. However, a number of studies have published findings which raise the possibility that translation may also occur in the nucleus. In the 1950s, the uptake of radioactively labelled amino acids was reported in isolated calf thymus nuclei (Allfrey, 1954) and a later study described the release of elongation-competent polyribosomes from HeLa cell nuclei (Goidl et al., 1975). However, estimates that protein synthesis in isolated calf thymus nuclei (Allfrey, 1954, Allfrey et al., 1964) and HeLa cell nuclei (Goidl et al., 1975) accounted for 30% and 10% of total protein synthesis respectively were disputed on the basis that the nuclear fractionation methods used were insufficient to completely remove cytoplasmic ribosomes, particularly those associated with the perinuclear endoplasmic reticulum, or even that whole cells contaminated nuclear fractions (Goidl and Allen, 1978). Indeed an investigation into whether protein synthesis could occur in the nuclei of sea urchin blastulae cells, in which a higher degree of purification was achieved, reported that nuclear protein synthesis accounted for a maximum of 0.2% of the total, with the authors conceding that there may be no nuclear translation at all (Allen and Wilt, 1976). If nuclear translation were to take place, it might seem more efficient that the types of proteins synthesised in the nuclear compartment were those that were functional there. However, studies into protein synthesis kinetics have concluded that the classic nuclear histone proteins are in fact synthesised in the cytoplasm and rapidly transported to the nucleus (Wu

and Warner, 1971, Robbins and Borun, 1967). The nuclear translation hypothesis was therefore shelved, and particularly in light of the discovery that eukaryotic transcripts undergo extensive processing, and in particular splicing (Berget et al., 1977, Chow et al., 1977), it is generally considered that the separation of transcription and translation by the presence of a nuclear envelope is an evolutionarily adaptive means by which eukaryotic cells ensure that only fully processed mRNAs undergo translation (Martin and Koonin, 2006).

1.4.1 Nonsense-mediated mRNA decay

Nonsense-mediated mRNA decay (NMD) is one of many cellular mechanisms that serve to maintain the integrity of gene expression, by identifying mRNAs that harbour a premature translation codon and targeting them for rapid degradation (Muhlemann et al., 2008, Brogna and Wen, 2009). NMD operates at the translational level and has been shown to be dependent upon active translation; NMD substrates are stabilised following translation elongation inhibition by cycloheximide, or by the introduction of secondary structures such as a hairpin in the 5'UTR which prevent ribosomes from initiating translation (Belgrader et al., 1993, Gonzalez et al., 2000). PTCs may be present in mRNAs due to inherited mutations in the DNA or may originate by errors during DNA replication, transcription, or pre-mRNA processing, in particular splicing (Muhlemann et al., 2008). The traditional view of NMD is that it is a mechanism that evolved specifically to protect the cell against the potentially harmful effects the resultant truncated proteins may have, such as interacting with other proteins in a dominant-negative manner or leading to loss of function in proteins that form dimers. This was observed in *C. elegans*, where NMD mutants with PTCs in the gene for the myosin heavy chain became paralysed (Muhlemann et al., 2008, Brogna et al., 2016, Hodgkin et al., 1989). Estimates are that around one third of all human inherited genetic

conditions are due to the acquisition of PTCs caused by nonsense mutations (Mendell and Dietz, 2001). Indeed, the selective degradation of nonsense transcripts is why, in conditions such as β-thalassemia, individuals inheriting one PTC-containing copy of the β-globin gene are usually healthy, presumably since the aberrant mRNA is degraded before it can be translated (Hall and Thein, 1994). This was further substantiated in a study of symptomatic β-thalassemia patients in which the PTC was found to be present in the final exon of the β-globin gene. mRNAs arising from this allele escaped NMD, resulting in comparable levels of normal and mutant β-mRNA which can be translated and lead to dominant-negative effects (Hall and Thein, 1994). Conversely around 5% of cystic fibrosis cases arise due to inherited nonsense mutations (Bedwell et al., 1997) that are downregulated by NMD, yet it is suggested that truncated proteins could be at least partially functional, as evidenced by the observation that the amino-terminus of the cystic fibrosis transmembrane conductance regulator can form a functional chloride ion channel (Frischmeyer and Dietz, 1999, Sheppard et al., 1994). This implies that NMD may be detrimental for the patient in some circumstances. As well as inherited conditions, NMD is also significantly implicated in the development of human cancers, for instance, 77% of mutations in *BRCA1*, a tumour suppressor gene that is associated with the development of breast cancer, are nonsense mutations. NMD of the resulting transcripts essentially leads to loss-of-function of this gene (Culbertson, 1999).

Although NMD was traditionally considered to be a means of detecting and specifically rapidly degrading faulty transcripts, mRNA profiling in *S. cerevisiae* (Guan et al., 2006, Lelivelt and Culbertson, 1999), *C. elegans* (Ramani et al., 2009), *Drosophila* (Rehwinkel et al., 2005) and human cells (Mendell et al., 2004) demonstrated that many physiological mRNAs,

with wide-ranging functions, are upregulated in NMD mutants (Fatscher et al., 2015). These studies were key to the understanding that NMD has an important role in regulating global gene expression, with estimates that between 3 and 10% of all mRNAs are affected (Schweingruber et al., 2013). The coupling of NMD with alternative splicing plays a significant part in this regulation of gene expression; retention of introns during alternative splicing may generate mRNA isoforms with PTCs, which lead to their degradation by the NMD machinery (Hamid and Makeyev, 2014). This alternative splicing coupled NMD may even regulate the expression of components of the splicing machinery themselves. For instance, it has been reported that when high levels of U1C, a component of the U1 snRNP, are expressed, the U1 snRNP associates with a cryptic splice site in the mRNA of another U1 snRNP protein, U1-70K (Hamid and Makeyev, 2014). The result is the inclusion of an exon that induces NMD of U1-70K, thereby also regulating the expression of the U1 snRNP (Hamid and Makeyev, 2014). This demonstrates a cross-regulatory circuit that achieves stoichiometric levels of the proteins required for the formation of the spliceosomal snRNPs (Hamid and Makeyev, 2014).

The means by which PTCs are distinguished from normal translation termination codons has been the subject of intense research. Studies across eukaryotic species have identified a number of factors that are required for NMD to take place and several models have been proposed to explain how these factors function to elicit NMD upon premature translation termination. An overview of these findings is presented in the following section.

1.4.1 NMD mechanisms

The means by which aberrant mRNAs are identified and targeted for rapid degradation are still poorly understood, however genetic screens have identified a number of trans-acting

factors involved in NMD (Hodgkin et al., 1989). The screen in *S. cerevisiae* was conducted in a tRNA frameshift suppressor genetic background which allowed low level read-through of a *his4-38* frameshift mutation at 30°C, although the His^- phenotype was observed at 37°C (Culbertson et al., 1980). However, mutations in three genes were found to suppress the His^- phenotype at 37°C, and these genes were named *UPF1*, *UPF2* and *UPF3* (for up-frameshift). Further studies showed that these mutations led to the stabilisation of nonsense transcripts (Leeds et al., 1991, Leeds et al., 1992). A similar screen in *C. elegans* identified six suppressors of three different genes which were named *smg1-6* (for suppressor with morphogenic effects on genitalia, due to the male morphological phenotype also observed in these mutants) (Hodgkin et al., 1989). A seventh *smg* suppressor was subsequently discovered and named *smg-7* (Cali et al., 1999). *smg-2, smg-3* and *smg-4* have since been found to be homologous to yeast *UPF1, UPF2 and UPF3* respectively (Muhlemann et al., 2008) while the other *smg* genes encode proteins that are involved in the phosphorylation and dephosphorylation of upf1, which is crucial to the regulation of NMD in higher eukaryotes (Ohnishi et al., 2003, Grimson et al., 2004, Isken et al., 2008).

A yeast two-hybrid screen revealed that the three Upf proteins form a trimeric complex, with Upf2p forming a bridge between Upf1p and Upf3p (He et al., 1997) and this complex was also detected by co-immunoprecipitation studies in human cells (Lykke-Andersen et al., 2000). Characterisation of purified yeast Upf1 protein established both RNA and DNA dependent ATPase activity and ATP dependant helicase activity on both RNA and DNA duplexes (Czaplinski et al., 1995). The absence of ATP led to stable binding of UPF1 to both RNA and DNA. These features were later confirmed in the human Upf1 protein

(Bhattacharya et al., 2000). Mutations in the helicase and ATPase regions were found to inactivate NMD and prevent suppression of nonsense phenotypes in yeast (Weng et al., 1996). UPF1 has also been shown to associate with prematurely terminating ribosomes via eRF1 and eRF3 (Czaplinski et al., 1998). Extensive work has been undertaken, using known NMD targets and various reporter constructs, to understand how these factors operate to distinguish premature from normal translation termination. As detailed below, three different models have been proposed over the years to explain how NMD substrates can firstly be identified, then targeted for rapid degradation.

1.4.1.1 The DSE model of NMD

The first study into NMD in *S. cerevisiae* reported a polarity effect with regards to the location of a PTC and the efficiency of NMD (Losson and Lacroute, 1979); those nonsense mutations nearer to the 5' end resulted in lower levels of URA3 mRNA than when the PTC was nearer to the 3' end. This phenomenon was confirmed in a subsequent study of the *PGK1* gene in *S. cerevisiae* (Peltz et al., 1993). It was initially proposed that this polarity effect was due to the presence of a specific downstream sequence element (DSE), which was more likely to be present when translation termination occurred nearer the 5' end (Fig 1.6 ii). This was supported by the observation that deletion of sequences 3' of an early PTC stabilised the mRNA. The DSE was later proposed to be a TGYYGATGYYYYY (Y = either pyrimidine) motif since several other yeast genes were found to possess this motif, and its deletion led to stabilisation of PTC-containing mRNAs in the *PGK1*, *ADE3* and *HIS4* genes (Zhang et al., 1995). The DSE was thought to recruit RNA binding proteins (RBPs) which then trigger NMD. Consistent with the DSE model, subsequent investigations reported that the

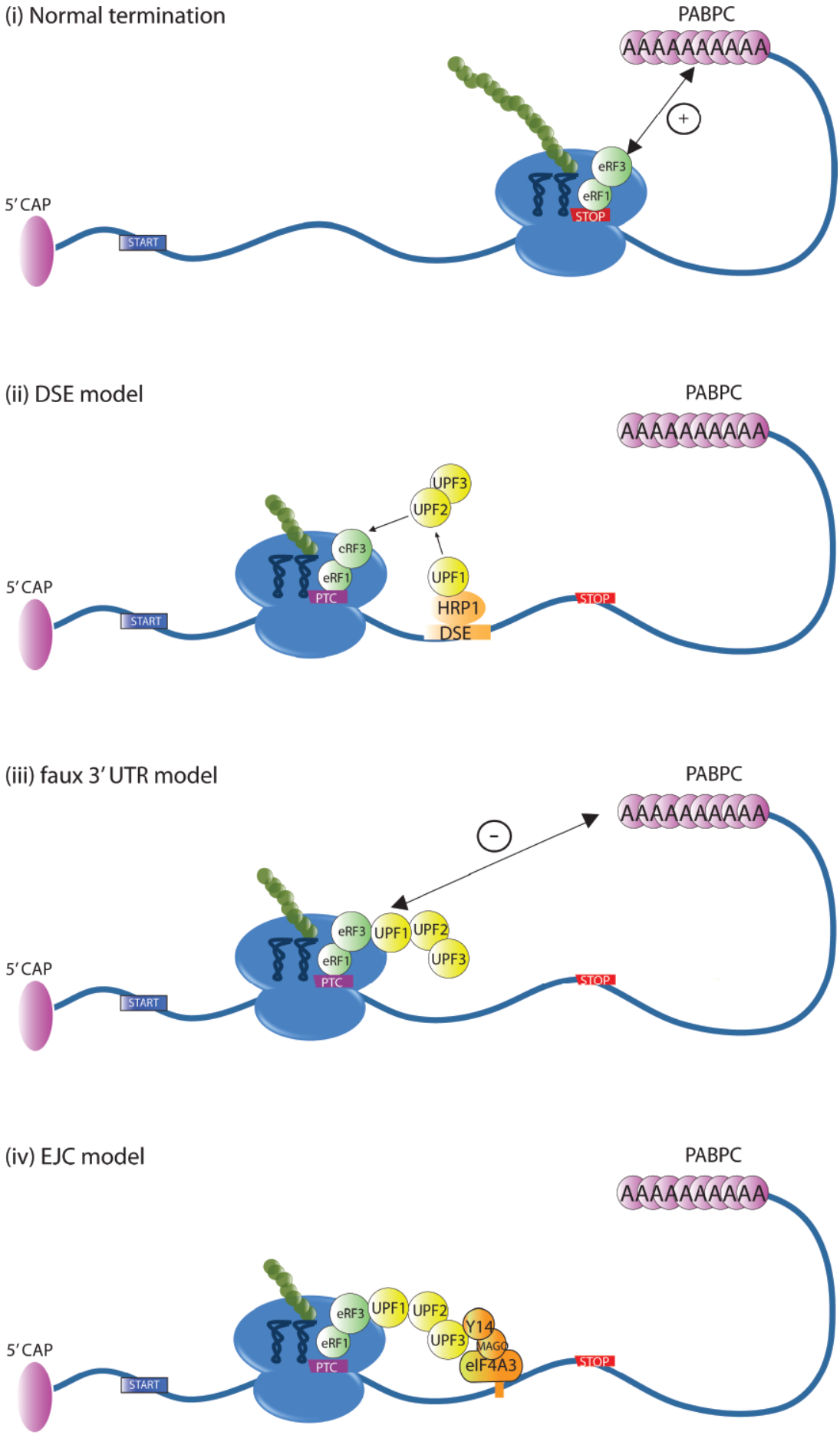
(i) Normal termination
PABPC
AAAAAAAAAA
+
eRF3
eRF1
STOP
5′CAP
START
(ii) DSE model
PABPC
AAAAAAAAAA
UPF3
UPF2
eRF3
eRF1
PTC
UPF1
HRP1
DSE
STOP
5′CAP
START
(iii) faux 3′UTR model
PABPC
AAAAAAAAAA
−
eRF3
UPF1
UPF2
eRF1
PTC
UPF3
STOP
5′CAP
START
(iv) EJC model
PABPC
AAAAAAAAAA
eRF3
UPF1
UPF2
eRF1
PTC
UPF3
Y14
MAGO
eIF4A3
STOP
5′CAP
START

Figure 1.6 NMD models. (i) Normal translation termination at the canonical stop codon. Eukaryotic release factors (eRF1 and eRF3) are recruited to the terminating ribosome. (ii) The DSE model. Translation termination at a PTC is recognised as premature due to the presence of a downstream sequence element (DSE) that is not present in the normal 3' UTR. HRP1 binds the DSE, interacting with UPF1 and UPF2/UPF3 which trigger degradation of the mRNA. (iii) The faux 3' UTR model. Premature translation termination is identified due to a lack of interaction between eRF3 on the terminating ribosome and PABPC bound to the poly(A) tail that usually occurs during normal termination as in (i). Instead, UPF1, and in turn UPF2 and UPF3, are recruited to the terminating ribosome, stimulating mRNA decay. (iv) The EJC model. If the ribosome terminates upstream of an exon-exon junction, demarcated by the presence of an exon junction complex (EJC) that has been deposited during splicing, an interaction between ribosome-bound UPF1 and UPF2 and UPF3 which bind the EJC, initiates a sequence of events that result in degradation of the mRNA.

RBP, Hrp1p, can bind to DSE-containing substrates, and can also interact with UPF1 (Gonzalez et al., 2000). Mutations in the *HRP1* gene were found to stabilise PTC-containing mRNAs. It was thought that upon translation termination, a surveillance complex comprising UPF1, UPF2 and UPF3 assembles and scans for the DSE-bound HRP1 (Ruiz-Echevarria and Peltz, 1996, Peltz et al., 1993, Zhang et al., 1995). However, the DSE model was abandoned as it became apparent that there was little consensus between the putative downstream sequences of different mRNAs (Hilleren and Parker, 1999, Hagan et al., 1995, Zhang et al., 1995, Ruiz-Echevarria and Peltz, 1996, Peltz et al., 1993).

1.4.1.2 The faux 3' UTR model

Although the initiation of NMD could no longer be explained by the presence of a specific downstream sequence, the polarity effect in yeast was still apparent, and it was found that aberrant mRNAs with increased 3'UTR length, arising from mutations in the polyadenylation signal, were stabilised when Upf1, Upf2 or Upf3 were absent (Muhlrad and Parker, 1999). This indicated that the distance between the stop codon and the 3' end of the mRNA, rather than a putative DSE, allowed discrimination between normal and aberrant mRNAs. The DSE model was subsequently superseded by the *faux* 3' UTR model, first proposed by a later study which reported that translation termination is aberrant when it fails to occur in the context of a properly configured 3' UTR and the regulatory elements associated with it (Amrani et al., 2004) (Fig 1.6 iii). In this case the key regulatory factor was found to be the yeast ortholog of PABPC, Pab1p, since PTC-containing mRNAs were stabilised when Pab1p was tethered near to the PTC. It had been previously identified that Pab1p interacts with Sup35p (the yeast ortholog of eRF3), which associates with terminating ribosomes (Cosson et al., 2002), as does the mammalian homologue, PABPC (Hoshino et al., 1999). The faux 3'

UTR model proposes that PTCs are recognised as such due to ribosomal bound eRF3 failing to interact with PABPC when the 3' UTR is lengthened. Ribosomes terminating at a PTC instead interact with UPF1 (Amrani et al., 2006, Baker and Parker, 2006) and this association leads to the subsequent recruitment of UPF2 and UPF3, which together trigger degradation of the mRNA.

The polarity effect of PTCs had also been observed in the *Adh* gene of *Drosophila* (Brogna, 1999) and was subsequently identified in human cells using Ig-μ gene constructs (Buhler et al., 2006). Lengthening of the 3' UTR was also found to elicit NMD, while tethering of PABPC1 near to a PTC inhibited NMD in both *Drosophila* and human cells (Behm-Ansmant et al., 2007, Eberle et al., 2008), suggesting an evolutionarily conserved means by which PTC-recognition may take place.

1.4.1.2 The influence of splicing on NMD in mammalian cells and the EJC model of NMD

NMD is coupled to translation, yet many studies in mammalian systems reported that the presence of one or more introns downstream of a PTC is required for NMD. Introns were first implicated in NMD during studies of the human TPI gene which showed that termination codons in the final exon (exon 7) produced normal mRNA levels, whilst PTCs in exon 6 led to a dramatic reduction in mRNA (Cheng et al., 1994). Notably, artificially introducing an intron downstream of a normal termination codon in the T-cell receptor-β (TCR-β) gene was also observed to trigger NMD (Carter et al., 1996). Further studies substantiated the splicing-dependent nature of mammalian NMD; a number of intronless genes were shown to be resistant to NMD, including the naturally intronless heat shock protein 70, human histone H4 and melanocortin 4-receptor genes, as well as the human *HEXA* minigene in which NMD was greatly reduced in an intronless construct when

compared to the intron-containing gene (Rajavel and Neufeld, 2001, Brocke et al., 2002, Maquat and Li, 2001). In light of these observations, a mediator between the nuclear process of splicing and cytoplasmic NMD was sought. Analysis of cross-linked mRNAs from HeLa nuclear extracts showed a splicing-dependent deposition of a set of proteins on mRNAs that remain bound during export to the cytoplasm (Le Hir et al., 2000b). The site of deposition was found to be 20-24 nt upstream of the exon-exon junction since this region was protected during RNase H cleavage (Le Hir et al., 2000a). The discovery that this exon junction complex (EJC) serves as a platform to which Upf2 and Upf3 bind provided the connection between the EJC and NMD (Le Hir et al., 2001). The core EJC proteins have since been identified as eIF4AIII, Y14, MAGOH and MLN51 (Shibuya et al., 2004, Andersen et al., 2006, Bono et al., 2006). UPF3 was found to interact with the EJC via association of its C-terminus with Y14 (Gehring et al., 2003, Buchwald et al., 2010). Deletion of this region of UPF3 inhibited NMD (Gehring et al., 2003), as did RNAi depletion of MAGO, eIF4AIII and MLN51 (Ferraiuolo et al., 2004, Palacios et al., 2004, Shibuya et al., 2004) and tethering of RNPS1, another EJC component, to the 3' UTR of β globin mRNA (Lykke-Andersen et al., 2001).

A number of studies have envisaged the means by which the known NMD factors might work together in conjunction with the EJC and translational machinery to bring about PTC recognition and degradation of NMD substrates (Fig 1.6 iv). EJCs are thought to be displaced by translating ribosomes (Dostie and Dreyfuss, 2002), but the EJC model predicts that a transient complex, comprising SMG1, which catalyses the phosphorylation of UPF1, unphosphorylated UPF1 and the translation release factors eRF1 and eRF3 (the so-called SURF complex), assembles on ribosomes terminating upstream of an EJC (Kashima et al.,

2006) (Fig 1.6 iv). Whilst bound to SURF, the CH domain of UPF1 at its N-terminus acts as a *cis* inhibitor of its helicase and ATPase activity (Chamieh et al., 2008). In the case of premature termination, a bridge is established between ribosome bound UPF1 and UPF2/UPF3 which are bound to the EJC, forming the decay inducing complex (DECID) (Kashima et al., 2006). Upon formation of DECID, UPF1 is phosphorylated by SMG1, and although it exists only briefly in this state, phosphorylation is essential for NMD to occur (Anders et al., 2003). Upon UPF1 phosphorylation, SMG-5 and SMG-7 are recruited as a heterodimer, and these proteins lead to the dephosphorylation of UPF1 (Anders et al., 2003, Ohnishi et al., 2003) which is required for the activation of UPF1 (Okada-Katsuhata et al., 2012, Fiorini et al., 2013). Activated UPF1 then dissociates the ribosome and eRF1/eRF3 (Kashima et al., 2006). Cryo-electron microscopy demonstrated that upon binding to EJC bound UPF2 and UPF3, the EJC/UPF complex is remodelled so that UPF1 is positioned toward the EJC 3' end, enabling it to perform its helicase activity downstream of the EJC (Melero et al., 2012).

1.4.1.3 Current models do not fully explain all observations of NMD

The faux 3' UTR model of PTC recognition was originally based upon observations in yeast, while the EJC model was formulated and developed in the context of mammalian NMD. However, subsequent studies suggest that these models do not apply exclusively to particular classes of organisms. EJC components are conserved in *D. melanogaster*, *C. elegans*, *Arabidopsis thaliana* and *S. pombe* (Gatfield et al., 2003, Longman et al., 2007, Pendle et al., 2005, Wen and Brogna, 2010) although depletion of these components in flies and nematodes found that the EJC was not required for NMD and that PTC discrimination was independent of splicing (Gatfield et al., 2003, Longman et al., 2007). The authors

concluded from these studies that the EJC model was restricted to vertebrates and that the faux 3' UTR was a more reliable model of NMD in invertebrates, however from the reporter constructs used, it cannot be ruled out that both systems operate in the same organism. Indeed, both modes of NMD were demonstrated in *Arabidopsis* (Nyiko et al., 2013) while a study in *S. pombe* showed that as well as the polarity effect leading to more efficient degradation of mRNAs containing PTCs closer to the 5' end in intronless reporters, PTCs further along the coding region elicit strong NMD when an intron is introduced (Wen and Brogna, 2010). This study also found that splicing-dependent NMD occurred in an EJC-independent manner, but most intriguingly, that splicing enhanced NMD even when the intron was placed upstream of a PTC (Wen and Brogna, 2010).

Even in mammalian NMD, the EJC model cannot explain all observations since several studies have shown that downstream introns are not a prerequisite for recognition of PTCs in a number of instances (Delpy et al., 2004, Buhler et al., 2006, Eberle et al., 2008). One of these studies in particular found that extending the distance between a normal termination codon and the 3' UTR by the insertion of a sequence between them in the mini-μ reporter construct triggered NMD, and that this could be suppressed by either tethering poly (A) binding protein nearer to the termination codon or folding the mRNA so that the poly (A) tail was more proximal (Eberle et al., 2008). While this study demonstrates that NMD can occur in the absence of downstream introns, the NMD reporters which were used carried an intron upstream of the PTC, as in the *S. pombe* study, therefore the effect of splicing could not be ruled out. Furthermore, two recent studies reported that the EJC can also bind other non-canonical sites on the mRNA which do not correlate with splice sites (Singh et al., 2012,

Sauliere et al., 2012). Therefore it could be possible that non-canonical EJCs could account for splicing-dependent NMD, particularly when splice sites are upstream of a PTC.

1.4.2 Can NMD occur in the nucleus?

As described, NMD is dependent upon translation and therefore is considered to be a cytoplasmic process. However, a number of observations of NMD in mammalian cells suggest that PTC recognition may take place within the nucleus. Fractionation of cells into nuclear and cytoplasmic components had shown that the nonsense transcript levels of the dihydrofolate reductase (Urlaub et al., 1989), human β-globin (Baserga and Benz, 1992), triosephosphate isomerase (TPI) (Cheng and Maquat, 1993, Belgrader et al., 1993), mouse major urinary protein (Belgrader et al., 1994) and T-cell receptor-β mRNAs were all reduced while still associated with the nucleus. Moreover, some of these studies reported that the fraction of PTC-containing mRNA that escapes nuclear-associated NMD has a cytoplasmic half-life comparable to that of its wild type counterpart (Urlaub et al., 1989, Baserga and Benz, 1992, Cheng and Maquat, 1993). These results were paradoxical to the idea that only ribosomes located in the cytoplasm could recognise PTCs and one explanation was that ribosomes may also operate within the nucleus. The possibility that the fractionation process yielded nuclear fractions that were contaminated with cytoplasmic components was addressed in the TPI studies by carrying out a blot hybridisation of *c-myc* cDNA, which was barely detectable in the nuclear fraction (Belgrader et al., 1993), while electron microscopy showed nuclei to be free of cytoplasmic tags following stringent detergent washes (Cheng and Maquat, 1993). The results of these investigations suggested that cytoplasmic contamination could not explain the extent of the reduction of TPI mRNA that was observed in the nuclear fraction, although an alternative proposal was that the nuclear reduction of

NMD substrates could be due to cytoplasmic ribosomes associating with mRNAs as they exit the nuclear pore (Belgrader et al., 1994) in a so-called 'pioneer' round of translation (Maquat, 1995). Electron microscopy had previously revealed the co-translational export of the *Chironomun tentans* Balbiani ring granule mRNA which exits the nucleus 5' end first and associates with cytoplasmic ribosomes whilst still partially within the nucleus (Mehlin et al., 1992). Support for the pioneer round of translation came from a report that in human cells, β-globin mRNAs with nonsense mutations underwent NMD while still bound by the nuclear cap binding protein, CBP80, and that mRNAs are stable once this is replaced by the cytoplasmic cap binding protein, eIF4E (Ishigaki et al., 2001). Additional evidence came from the finding that UPF2, UPF3 and EJC components only purified with CBP80-bound and not with eIF4E-bound mRNAs (Lejeune et al., 2002). CBP80 was also found to directly interact with UPF1 and promote UPF1 binding to UPF2 to stimulate NMD (Hosoda et al., 2005). Immunoprecipitation of UPF1 in HeLa cells showed an enrichment of CBP20 and CBP80 which was greatly reduced upon nuclease treatment, demonstrating that the ribosome:SURF complex assembles on CBP20 and CBP80 bound mRNAs. A recent study into the decay kinetics of PTC-containing β-globin mRNA further supported the pioneer round model of NMD (Trcek et al., 2013). Fluorescent in situ hybridisation (FISH) was used to detect PTC+ (TER) and PTC- (NORM) mRNAs coexpressed in the same cell. TER and NORM mRNAs accumulated at the same rate within the nucleus, and upon blocking transcription depleted at similar rates, attributable to their export to the cytoplasm (Trcek et al., 2013). However, 60% less TER β-globin accumulated in the cytoplasm compared to NORM mRNA. The half-life of TER mRNA was similar to that of NORM mRNA (around 7.2 h), therefore the relative depletion of TER mRNA in the cytoplasm must be due to its rapid decay during a pioneer round of translation (Trcek et al., 2013). However, in contrast to the pioneer round

of translation NMD model, other studies have reported that both eIF4E and CBC associated mRNAs are equally affected by NMD (Rufener and Muhlemann, 2013, Durand and Lykke-Andersen, 2013). In addition to this, a study in human cells showed that TCR-β NMD substrates were still subjected to NMD when nuclear export of mRNA was blocked (Bühler et al., 2002), although blocking nuclear export of mRNAs in *S. cerevisiae* was found to have no impact on NMD (Kuperwasser et al., 2004). In *Arabidopsis*, EJC components, aberrant mRNAs and NMD factors were found to accumulate in the nucleolus, providing further support to the proposal that NMD may occur in this region of the cell (Pendle et al., 2005, Kim et al., 2009). A FISH assay of PTC+ and PTC- immunoglobulin (Ig)-μ and TCR-β reporters, and later, fluorescence recovery after photobleaching (FRAP) of Ig-μ PTC+ and PTC- mRNA reported accumulation of PTC+ mRNAs at the site of transcription (Muhlemann et al., 2001, de Turris et al., 2011), indicating that PTC discrimination occurs within the nucleus. The retention of the Ig-μ transcript was found to be dependent upon UPF1 and SMG and the transcripts were found to be unspliced (de Turris et al., 2011). A more recent FISH study of smad and β-globin reporters also found that PTC-containing transcripts were preferentially retained in the nuclei of HeLa cells and that this was dependent on the presence of the AUG start codon and an intact Kozak sequence, indicating that nuclear PTC recognition is dependent upon the ability of ribosomes to engage with the mRNA (Shi et al., 2015).

1.4.3 Do nonsense mutations affect pre-mRNA processing?

Although the pioneer round of translation may account for nucleus-associated NMD, a number of studies had indicated that nonsense mutations influenced pre-mRNA splicing, which further substantiated claims that nuclear scanning by ribosomes may occur. One such study was in the parvovirus minute virus of mice (MVM) in which R1 mRNA is spliced to

produce R2 mRNA. It was found that a PTC in exon 2 of R2 interfered with the splicing of R1 to R2 mRNA, indicating a possible change in splice site definition induced by the presence of a nonsense codon (Naeger et al., 1992). Similarly, in a study of a patient homozygous for a nonsense mutation in exon 6 of the Fanconi anaemia group C gene, a proportion of mRNA transcripts lacked exon 6, indicating that the nonsense codon had influenced pre-mRNA splicing to induce exon skipping (Gibson et al., 1993). Exon skipping when a nonsense mutation was present in the skipped exon was also observed in mature transcripts of the *FBN1* gene of a patient with Marfan syndrome (Dietz et al., 1993) as well as in the human TCRβ gene. Additionally, removal of PTCs in intronic sequences led to activation of a downstream latent 5' SS in a CAD minigene system, indicating that 5' SS identification is altered in the presence of nonsense codons (Li et al., 2002). Although these findings were originally interpreted as evidence that PTC-recognition takes place within the nucleus, it was later realised that the nonsense mutation in the FBN1 transcript induced exon skipping by disrupting exonic splicing enhancers (ESEs) (Caputi et al., 2002). However other instances of nonsense altered splicing, such as in the MVM and TCR-β genes, were found not be due to disruption of ESEs, since nonsense mutations altered splicing but missense mutations did not (Maquat, 2002).

Changes in pre-mRNA processing caused by nonsense mutations appear to be not only restricted to humans, but also occur in flies, since a study of the *Adh* gene in *Drosophila* reported that those transcripts harbouring PTCs had longer poly (A) tails and that this applied to both pre-mRNA and mature mRNA (Brogna, 1999).

1.5 Revisiting the case for nuclear translation

Since translation is a pre-requisite for NMD, the observations that NMD occurred in association with the nuclear fraction, and that PTCs affected mRNA processing, revived the debate over whether translation itself could occur in the nucleus. Several groups turned their attention to investigating whether components of the translation machinery, or evidence of protein synthesis, could be detected in the nuclear compartment. In 2001 a prominent paper reported the transcription and translation-dependent incorporation of lysine from biotin and BODIPY tagged lysine-tRNAs into nascent peptides in the nuclei of permeabilised HeLa cells, as well as in purified nuclei (Iborra et al., 2001). The conclusion from this study was that, as in prokaryotes, translation could occur co-transcriptionally in eukaryotes. The authors later reported the copurification of the NMD factors UPF1, UPF2 and UPF3, and also the translation initiation factors eIF4E and eIF4G, with the phosphorylated CTD of Pol II as well as visualisation of their colocalisation by electron microscopy (Iborra et al., 2004). This provided additional support to the proposal that the processes of translation and NMD are coupled with transcription. However, as with the studies several decades earlier, concerns were raised about whether these observations could be accounted for by the transfer of cytoplasmic components to nuclei during permeabilisation, and whether purified nuclei were contaminated by retention of the endoplasmic reticulum at the cytoplasmic surface of the nuclear envelope (Nathanson et al., 2003).

Results from a study in *Drosophila* provided further support for the proposal that translation may occur cotranscriptionally. The study reported that immunofluorescence of polytene chromosomes revealed the presence of 20 ribosomal proteins at transcriptionally active

sites, as identified by Pol II staining (Brogna et al., 2002). Similarly, translation factors and rRNAs belonging to both ribosomal subunits were found at such sites, the latter being detected by both immunofluorescence and in situ hybridisation (Brogna et al., 2002). Additionally this study showed that radioactive amino acids were rapidly incorporated at transcription sites, as well as in the nucleolus. The results of this study were received with scepticism since the antibodies used were against human RPs which, as discussed, despite being evolutionarily well-conserved, possess a certain degree of variation between species (Dahlberg and Lund, 2004). The presence of RPs at transcription sites does not necessarily indicate the presence of functioning ribosomes in any case, since some RPs are known to have separate functions that are independent of the ribosome (see section 1.3.2). However, the known extraribosomal roles of RPs are independent of other RPs and it might be argued that it is unlikely that 20 different RPs would have independent roles at the same loci. However, it could alternatively be that a sub-ribosomal particle with an as yet unknown function exists; indeed antibodies against 27 RPs were used in the study, but only 20 stained transcribed regions of the chromosome (Brogna et al., 2002), suggesting that the RPs being detected were not part of a complete ribosome. The authors however argue that the co-localisation of the RPs along with translation factors and rRNAs, as well as the incorporation of radioactive amino acids, adds weight to their interpretation that they are detecting translation at the polytene chromosomes (Brogna et al., 2002). A later study, again in *Drosophila*, confirmed that several RPs are present at the chromosomes: this study circumvented the concerns surrounding antibody cross-reactivity by visualising a number of fluorescently-tagged RPs, and these were detected both in the nuclei of salivary gland cells and at transcriptionally active loci on polytene chromosomes (Rugjee et al., 2013). Again, unknown extraribosomal functions of these RPs cannot be ruled out and this study provided

no evidence for the presence of other components of translation at transcription sites. Ribosomal proteins have also been detected at the chromosomes in both budding and fission yeast (Schroder and Moore, 2005, De et al., 2011). In *S. cerevisiae*, ChIP of four RPs, followed by radioactive PCR of several loci showed the association of these RPs with several genes (Schroder and Moore, 2005). This association was RNA-dependent at two protein-coding genes, *ADH1* and *PYK1*, and conjecture might be that these RPs belong to a ribosome that is translating nascent transcripts. However, the same RPs were also found at loci encoding tRNAs and snRNAs and this association was also RNA-dependent, therefore the role of these RPs at the chromosomes appears to be unrelated to translation. Additionally, the introduction of a hairpin structure in the 5' UTR, which had been shown to block cytoplasmic translation, did not affect the level of association of these proteins at the loci at which they were detected (Schroder and Moore, 2005), providing a further indication that extraribosomal functions may explain the presence of these RPs at the chromosomes. The fission yeast study reported a genome-wide ChIP-chip analysis of three RPs, RpL7, RpL11 and RpL25, and found that all three colocalise in an RNA-dependent manner at the same actively transcribed genes (De et al., 2011). The authors postulated that the remarkable similarity in the distribution of the three RPs across the genome may indicate that they were recruited as part of a larger complex, possibly a functional ribosomal subunit such as the 60S or pre-60S. However, as in the *S. cerevisiae* study, the RPs tested were also present at nonprotein-coding loci, particularly at tRNA genes (De et al., 2011); the function of a ribosomal subunit at such loci is difficult to envisage.

The topic of nuclear translation remained controversial and it was apparent that the detection of RPs and translation factors in the nucleus or at the chromosomes was

insufficient to settle the debate. More direct evidence of translation itself, without the potential for cytoplasmic contamination, was demanded, and recently new methods have been developed which claim to have achieved this. The bimolecular fluorescence complementation method (BiFC) reportedly allowed the visualisation of the joining of ribosomal subunits, the hallmark of translation initiation. This method, which was developed in *Drosophila*, involved tagging pairs of RPs on different ribosomal subunits with complementary halves of fluorescent proteins (Al-Jubran et al., 2013). Tagged RPs that are in close proximity when the ribosomal subunits join to form the 80S would be expected to bring the two halves together to form a functional fluorescent protein, however RPs that are not adjacent on the 80S should not produce a fluorescent signal. The fluorescent signal was apparent when RpS18 on the 40S and RpL11 on the 60S were tagged with the N- and C-terminal halves of the fluorescent protein respectively (Al-Jubran et al., 2013). These two RPs are located at the head region on each of the ribosomal subunits and are adjacent upon ribosomal subunit joining. The signal was apparent throughout the cytoplasm of S2 cells, but intriguingly, a nucleolar signal was also present in around 10% of cells. The cytoplasmic and nucleolar signals were also visualised in whole salivary glands. The authors argue that this assay reports the presence of translating ribosomes, since treatment with emetine, a translation elongation inhibitor that increases the density of ribosomes on mRNAs, increased the intensity of the fluorescent signal in cell extracts. Conversely, fluorimetric analysis of polysome fractions showed that treatment with puromycin, which causes ribosomal subunits to detach from mRNAs, caused a shift in the fluorescent signal from polysomes to those fractions corresponding to individual ribosomal subunits. Other pairs of RPs that are adjacent upon subunit joining, such as RpS6 and RpL24, also produced a cytoplasmic signal, while pairs that are on opposite sides of the ribosome, such as RpS13,

located on the solvent-facing side of the 40S, paired with RpL11, did not (Al-Jubran et al., 2013). One exception to this was when RpL11 was paired with RpS9, which is located on the solvent-facing side of the body of the 40S. This pair of tagged RPs produced a weak cytoplasmic signal but a strong nucleolar signal despite not being adjacent on the 80S. Since the nucleolus is the site of ribosome biogenesis, it might be that the nucleolar signal arising from non-adjacent RPs is generated when they are part of a nucleolar pre-ribosomal particle that has a different arrangement of RPs to that of the mature subunits and 80S. Although the translation dependence of the RpS18/RpL11 signal was shown, the same was not done for RpL11/RpS9.

Another method, developed in human cell lines, rests upon the detection of puromycin that has been incorporated into nascent peptides on immobilised ribosomes ((David et al., 2012) and (Fig 1.7). HeLa cells and human monocytes were treated with translation inhibitors such as emetine and cycloheximide, which immobilise elongating ribosomes on mRNAs (Grollman, 1968). Cells were subsequently treated with puromycin, an antibiotic that is structurally similar to the 3' end of an aminoacylated tRNA (Pestka, 1971) (Fig 1.7 A). Puromycin enters the ribosomal A site and the ribosome catalyses its incorporation into the C-terminus of the nascent peptide. Without prior elongation inhibition, so-called puromycylated peptides are released from the ribosome (Grollman, 1968, Baliga et al., 1970), however the authors show through Western blotting of polysomal fractions that puromycylated peptides are retained on the ribosome following emetine or cycloheximide pre-treatment, referring to this process as ribopuromycylation (RPM) (David et al., 2012). Immunodetection with an anti-puromycin antibody revealed that ribopuromycylated peptides are found not only in the cytoplasm, as would be expected, but surprisingly also in

A

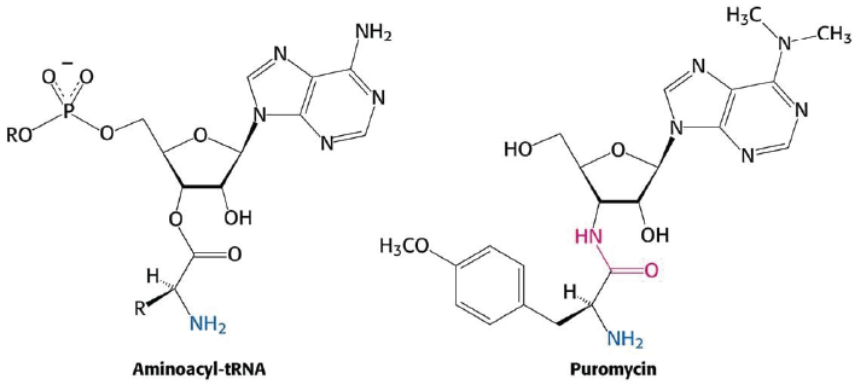
Aminoacyl-tRNA
Puromycin

B

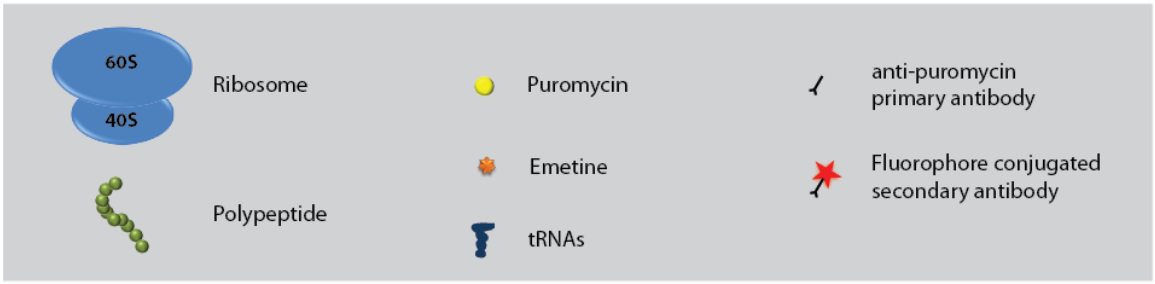
60S
40S
Ribosome
Polypeptide
Puromycin
Emetine
tRNAs
anti-puromycin primary antibody
Fluorophore conjugated secondary antibody

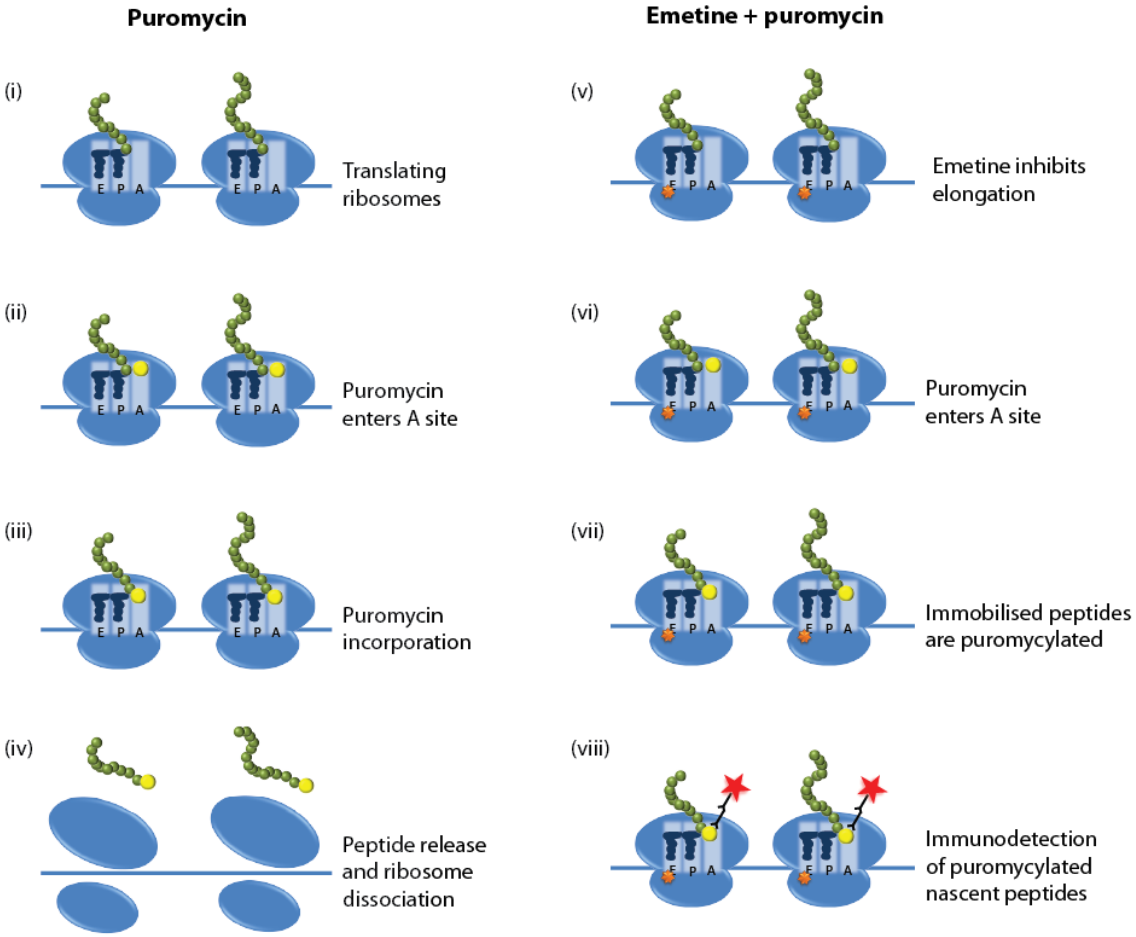
Puromycin
Emetine + puromycin
(i)
Translating ribosomes
(ii)
Puromycin enters A site
(iii)
Puromycin incorporation
(iv)
Peptide release and ribosome dissociation
(v)
Emetine inhibits elongation
(vi)
Puromycin enters A site
(vii)
Immobilised peptides are puromycylated
(viii)
Immunodetection of puromycylated nascent peptides

Figure 1.7 The RPM technique. (A) Structural comparison of the 3' end of an aminoacylated tRNA and puromycin. (B) Translating ribosomes (i) treated with puromycin (ii) will catalyse the incorporation of the drug into the C-terminus of the nascent peptide (iii) which results in the release of the puromycylated peptide (iv). If ribosomes are pre-treated with a translation elongation inhibitor such as emetine (v), which immobilises ribosomes on the mRNA, subsequent treatment with puromycin (vi) will still lead to its incorporation at the C-terminus of the peptide (vii) but the peptide is not released. These ribopuromycylated peptides can be visualised by immunofluorescence using a primary antibody against puromycin (viii) (David et al., 2012).

the nucleus, particularly the nucleolus. Western blotting showed that puromycin incorporation into nascent peptides was abolished when translation initiation was blocked using inhibitors such as pactamycin, demonstrating that the signal was dependent on translation and not representative of non-specific association of puromycin with ribosomal subunits (David et al., 2012). The nuclear RPM signal was also inhibited when cells were pretreated with anisomycin, an antibiotic that competes with puromycin for occupation of the ribosomal A site, demonstrating that puromycin incorporation is dependent upon catalysis by the ribosome. The development of the RPM method was therefore an important contribution to the debate surrounding the controversial issue of nuclear translation, since it claims to enable the visualisation of actively translating ribosomes in intact cells. The RPM method has also been used in *Drosophila* polytene chromosomes, where it revealed staining at transcriptionally active sites (Al-Jubran et al., 2013), suggesting the presence of translating ribosomes in association with nascent transcripts.

The central questions are now what biological function nuclear ribosomes serve and what proteins would be synthesised in the nucleus. A very recent study has proposed that nuclear translation generates peptides for immunosurveillance in human cells (Apcher et al., 2013). It had been observed that inserting an antigenic peptide sequence upstream of a PTC in a β-globin NMD reporter led to antigen presentation in the major histocompatibility complex (MHC) class I pathway (Apcher et al., 2011). Inhibiting eIF4E interaction with the cap structure did not interfere with antigen presentation, suggesting that the peptides were produced during the pioneer round of translation. This work was followed up by inserting two different antigenic peptide sequences into intronic regions of the β-globin gene, which are removed in the nucleus during splicing. Antigen presentation of the peptide from the

intronic region was at levels comparable to presentation when the peptide was expressed from an exonic region, thus antigenic peptides might have been produced from translation of the pre-mRNA in the nucleus (Apcher et al., 2013). It is unlikely that nuclear translation has a similar role in *Drosophila* or yeast since these organisms do not possess this antigen presentation pathway (Danchin et al., 2004). One seemingly plausible suggestion is that it would be more energetically favourable for cells to produce proteins local to where they are required. Indeed, examples of localised translation have been reported in other cellular contexts. Polyribosomes have been isolated from neuronal dendrites and the translation of particular mRNAs that are localised to synapses and growth cones is proposed to enable rapid responses to external stimuli (Holt and Schuman, 2013, Shigeoka et al., 2013, Xue and Barna, 2012). Work by others in the Brogna lab, using the BiFC method described above, reported the presence of 80S in the axons of photoreceptor cells (Abdullahi, 2014). Evidence that mitochondrial proteins are also synthesised close to their outer membranes has also been via the detection of ribosomes and specific mRNAs to this location (Lesnik et al., 2015). However, evidence for such localised translation of nuclear proteins within the nucleus has not been found. As described earlier, kinetic studies concluded that histone proteins are synthesised solely in the cytoplasm and are then rapidly transported to the nucleus (Robbins and Borun, 1967). However, histone proteins are just one example of numerous nuclear proteins, therefore it may be that other proteins with nuclear functions are synthesised in the nuclear compartment.

Whether nuclear translation can occur, and its potential role, are questions that remain unanswered. Identification of the transcripts with which nuclear ribosomes are associated will be central to answering the question of the functional relevance of nuclear translation.

One possibility for achieving this would be to combine RPM, which has been used to visualise the cellular locations of translating ribosomes, with chromatin immunoprecipitation, which allows identification of genes associated with given proteins of interest, to assess whether translating ribosomes are associated with nascent transcripts.

Aims of this study

Although it is generally thought that translation occurs only in the cytoplasm in eukaryotes, a number of observations suggest that translation may also occur in the nucleus, however these reports have either been overlooked or dismissed by the wider scientific community. It has also been reported in several organisms that nuclear mRNA is surprisingly reduced by nonsense-mediated mRNA decay (NMD), a process that is translation-dependent, and therefore expected to occur only in the cytoplasm. The Brogna lab, and other groups, have also reported the presence of many ribosomal proteins (RPs) at transcription sites in both yeast and *Drosophila*. The initial aim of this project was to investigate whether these RPs are part of a functional ribosome that is engaged in co-transcriptional translation in the fission yeast *Schizosaccharomyces pombe*. To do this, a recently developed technique known as ribopuromycylation (RPM) was used. This technique, which reportedly detects translating ribosomes, was developed in human cells, where both cytoplasmic and nuclear signals were visualised. In this study, RPM was combined with chromatin immunoprecipitation (ChIP) with the aim of identifying genes that are potentially co-transcriptionally translated in fission yeast. However, nascent peptides were not detected at most of the transcriptions sites assayed. To investigate the reasons behind this, the project was refocused on fully characterising RPM in in *S. pombe* and *Drosophila* S2 cells, by polysome profile analysis. The findings of these investigations were that RPM does not retain peptides on ribosomes as previously reported in HeLa cells, therefore this technique does not report sites of translation.

Chapter 2: Materials and Methods

2.1 *S. pombe* media and culturing methods

Yeast extract with supplements (YES) and Edinburgh minimal media (EMM) were used in the culturing of cells, details of which can be found in Appendix 1. Methods for working with S. pombe were taken, or adapted, from the Fission Yeast Handbook (available from http://research.stowers.org/baumannlab/documents/Nurselab_fissionyeasthandbook_000.pdf). Strains were streaked to single colonies on agar media plates, which were then grown at 30°C for 2-4 days. Single colonies were inoculated into a 1-2 mL start-up overnight liquid culture and grown. This was subsequently scaled up, typically by diluting to OD_{600} 0.02, for further overnight growth to achieve the desired final volume. Strains were stored long-term by growing a 1 mL culture to OD_{600} ~0.5, to which 667 µL of 80% glycerol was added, mixed and stored at -80°C.

2.2 *S. pombe* strains

Details of *S. pombe* strains used in this study can be found in Appendix 2.

2.3 Growth/recovery assay

1 mL YES media was inoculated with a fixed number of wild-type *S. pombe* cells from a start-up culture and translation inhibitors were added to the desired concentrations as indicated in the relevant figures. Cultures were grown at 30°C in a shaking incubator for 16 hours and cell counts were taken using a haemocytometer (Section 2.5). 1000 cells were spread onto agar plates and grown at 30°C for two days, after which the number of colonies was counted.

2.4 Mating of *S. pombe* strains

The two strains to be mated were cultured until growth was visible and 5 µL of each were mixed together on a SPAS mating plate (recipe in Appendix 1). Plates were incubated at 25°C and after 3 days a small amount was placed on a slide and checked for spores under the microscope. Around 1/3 of the colony was resuspended in 50 µL sterile purified H_2O (Elga PURELAB flex system) and incubated at 55°C in a water bath for 30 minutes to kill residual vegetative transient diploid cells, and possibly break asci. Cells were then spread on selective agar plates (Khare et al., 2011) .

2.5 Counting *S. pombe* cells

Cells were counted using a haemocytometer as described in http://www.abcam.com/protocols/counting-cells-using-a-haemocytometer. A coverslip was placed over the counting chamber and 10 µL of a 1 in 10 dilution of cells was pipetted onto the space just in front of the coverslip. The cell suspension was allowed to run underneath the slip. The chamber was then placed under the microscope and cells in the squares marked X (Figure 2.1) were counted. In case of cells touching the border, only cells on two sides of the square were counted. The value was multiplied by 2, then by the dilution factor and then by 10^4 to give the total number of cells per mL.

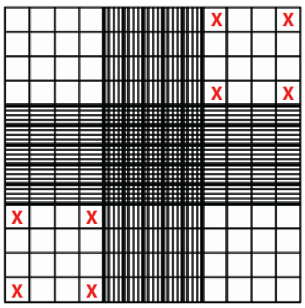

Figure 2.1 The haemocytometer grid as viewed under the microscope

2.6 Extraction of proteins from *S. pombe* cell cultures

Proteins were extracted using the sodium hydroxide method (Matsuo et al., 2006). 5 mL of *S. pombe* culture was grown to OD_{600} ~0.5, pelleted by centrifugation at 3000 rpm for 3 minutes at room temperature, the media removed and the cells washed by resuspending in 1 mL purified H_2O. Cells were pelleted again and resuspended in 300 µL of fresh purified H_2O and 300 µL of 0.6M NaOH was added to the sample to give a final concentration of 0.3M. Samples were gently mixed, incubated at room temperature for 10 minutes, and then centrifuged at 3000 rpm for 3 minutes at room temperature. The NaOH was removed and the pellet resuspended in 70 µL of 1X SDS loading buffer (60mM Tris HCl, pH 6.8, 4% β-mercaptoethanol, 4% SDS, 0.01% bromophenol blue, 5% glycerol and 1 mM phenylmethanesulfonylfluoride (PMSF), prepared in purified H_2O). Samples were boiled for 3 minutes and either loaded on the gel straight away or stored at -20°C.

2.7 SDS-PAGE and Western blotting

Samples were run on a 10% SDS-PAGE gel unless otherwise stated (Green and Sambrook, 2012). 15 µL of total protein extract in 1X SDS loading buffer was loaded per well. Gels were run at 100 V for 90 minutes at room temperature in a Bio-Rad Mini-PROTEAN Tetra Cell system using 1X SDS running buffer, pH 8.3 (0.025 M Tris, 0.19 M glycine, 0.1% SDS). Proteins were transferred to a nitrocellulose membrane using a Bio-Rad Mini PROTEAN II wet electrotransfer system at 350 mA for 2 hours in a cold room in 1X transfer buffer (0.2 M glycine, 0.025 M Tris, 10% methanol). To check transfer of proteins, membranes were stained with Ponceau S (Sigma) for 5 minutes at room temperature, with gentle agitation, and the excess was rinsed off. Membranes were blocked with 10 mL of 5% skimmed milk in

TBST (50 mM Tris, 150 mM NaCl, 0.05% Tween) on a rocker at room temperature for 30 mins, unless otherwise stated, then incubated overnight with the primary antibody (puromycin detection was with mouse anti-puromycin clone 5B12 and HA detection was with mouse anti-HA 12CA5), diluted 1:5000 in 5 mL TBST and placed on a rocker in the cold room. Membranes were washed the following day by 2 quick rinses and 3 x 5 min washes in TBST on a rocker at room temperature. The secondary antibody was a 1:10000 dilution of horseradish peroxidase (HRP) conjugated anti-mouse (Sigma) which was incubated with the membrane on a rocker at room temperature for 1 hour. Washes were carried out as for the primary antibody. The signal was developed with the ECL Prime Western Blotting Detection Reagent (GE Healthcare). 500 µL of Luminol Enhancer Solution and 500 µL of Peroxide Solution were mixed, applied evenly across each membrane and incubated for 5 minutes at room temperature. The developing solution was then drained off and the membrane was wrapped in Saran Wrap. A Geneflow G:Box Documentation system was used to visualise the signal.

2.8 Chromatin Immunoprecipitation Protocol I

The chromatin immunoprecipitation methods used were taken or adapted from (Aparicio et al., 2005).

2.8.1 Crosslinking and sample preparation

A 200 mL culture of the desired strain was grown to OD ~0.5. Cells were fixed by addition of 10% methanol-free, UltraPure EM grade formaldehyde (Polysciences, Inc) to a final concentration of 1% and cultures were transferred to a 27°C incubator with gentle shaking for 20 minutes. Glycine was then added to a final concentration of 330 mM to block fixation

and cultures were returned to the shaking incubator for a further 5 min. Cultures were transferred to 500 mL plastic Nalgene bottles and centrifuged at 4°C, 4000 rpm, 5 min to pellet cells. The media was discarded and the pellet was washed twice in 100 mL ice cold TBS and centrifuged again to pellet. The pellet was resuspended in 10 mL ice cold FA lysis buffer (50 mM HEPES-KOH pH 7.5, 150 mM NaCl, 1 mM EDTA, 1% Triton X-100, 0.1% Na deoxycholate) with 0.5% SDS, and transferred to a 15 mL Falcon tube. Cells were pelleted at 4°C, 3000 rpm, 5 min. The supernatant was discarded and the pellet resuspended in 1 mL FA lysis buffer with 0.1% SDS, 2mM PMSF and Roche EDTA-free protease cocktail inhibitor (half a tablet was used per 5 mL lysis buffer). 500 µL of the sample was added to 1.5 mL of glass beads in a 2 mL screw cap tube, ensuring the sample settled completely through the beads (if necessary by shaking the tube). Cell lysis was carried out in a Precellys cell lysis machine at 6500 rpm, with three rounds of 30s on, 30s off, 30s on, placing on ice in between cycles to achieve >90% lysis, as confirmed by a visual check under the microscope. The sample was recovered by piercing the bottom of the screw cap tube 3 times with a 25 gauge needle, placing the tube into the barrel of a 5 mL syringe and the syringe into a 15 mL Falcon tube. The lysate was collected by centrifuging at 1000 rpm, for 1 minute at 4°C and the beads were washed with a further 500 µL FA lysis buffer with 0.1% SDS, 2mM PMSF and protease inhibitor cocktail, and centrifuged again. Like samples were combined to reduce any variance and then aliquoted into two 1.5 mL eppendorf tubes. Samples were then centrifuged at 13200 rpm for 15 min at 4°C, the supernatant removed and the pellet resuspended in 1 mL FA lysis buffer with PMSF/SDS/protease inhibitor.

2.8.2 Sonication

Shearing of the chromatin was carried out by sonication with a Misonix Ultrasonic Processor The sonicator was set to level 3 and tuned to a frequency of 10%. The probe was inserted so that it was above, but not touching, the bottom of the tube. Sonication was for 3 cycles of 20s, with at least 20s on ice in between cycles. Sonicated samples were centrifuged at 13200 rpm for 30 minutes at 4°C. The supernatant containing the chromatin was transferred using filter tips to a fresh LoBind Eppendorf tube (~450 µL chromatin should be obtained from 500 µL sample). Samples can be frozen in liquid nitrogen and stored at -80°C at this stage along with any unused lysate.

2.8.3 Immunoprecipitation and decrosslinking

50 µL of Protein G Dynabeads (Life Technologies) was added to 1 mL of freshly prepared 1X PBS (137 mM NaCl, 2.7 mM KCl, 10 mM Na_2HPO_4, 1.8 mM KH_2PO_4, adjusted to pH 7.4) with 5 mg/mL bovine serum albumin (BSA), vortexed and centrifuged briefly to bring down any beads from the top of the tube. The beads were washed by placing the tubes in a magnetic rack, allowing the beads to migrate to the magnetic surface and rotating the tube 6 times. The PBS was then removed and washing was repeated a further 3 times. After the final wash the beads were resuspended in 500 µL PBS/BSA. 10 µg of antibody (mouse anti-puromycin clone 5B12 or mouse anti-HA 12CA5 as required) was added to each tube and then incubated overnight at 4˚C with rotation. The tubes were placed in the magnetic rack and the beads were washed twice with 1 mL PBS containing BSA as before to remove any unbound antibody. The antibody coated beads were then resuspended in 50 µL FA lysis buffer with 0.1% SDS, 400 µL of the chromatin sample was added and the remaining 50 µL was kept as input (stored at -20°C). The samples were incubated overnight at 4°C. The

following day the input samples were thawed on ice whilst the immunoprecipitated (IP) protein-DNA complexes were eluted from the beads. The IP samples were spun briefly and placed into the magnetic rack, the supernatant was discarded and the beads were washed for 5 mins on a rotator at room temperature sequentially with 1 mL of each of wash buffer 1 (FA lysis buffer with 0.1% SDS and 275 mM NaCl), wash buffer 2 (FA lysis buffer with 0.1% SDS and 500 mM NaCl), wash buffer 3 (10 mM Tris-HCl, pH 8.0, 0.25 mM LiCl, 1 mM EDTA, 0.5% Igepal CA-630, 0.5% Na deoxycholate), TE buffer (10 mM Tris-HCl pH 8.0, 1 mM EDTA). To elute the protein-DNA complexes the beads were resuspended in 100 µL of ChIP elution and the samples were incubated in a 65°C water bath for 10 min, spun briefly and placed back into the magnetic rack. The supernatant was transferred to a clean LoBind tube. 50 µL of ChIP elution buffer was added to the input samples to give an equal volume to the IP samples. Decrosslinking was done by overnight incubation at 65°C with 15 µL of 20 mg/mL Proteinase K and 1 µL of 20 mg/mL RNase A.

2.8.4 Purifying ChIP DNA using AMPure XP beads

1.8 volumes of AMPure XP beads was added to each sample (ChIP and Input), vortexed well and incubated on a rotator for 10 min at room temperature. Samples were spun briefly and placed on the magnetic rack, the supernatant was discarded and the beads were washed three times with 300 µL of freshly prepared 70% ethanol. Ethanol was removed after the final wash and the beads were allowed to air dry in laminar flow until there was visible cracking. The DNA was eluted by resuspending the beads in 50 µL of 0.1X TE, placing the tubes on the magnetic rack and transferring the supernatant to a new LoBind tube using filter tips. The tube containing the eluted DNA was placed back on the magnetic rack to separate any residual beads and the supernatant was again transferred to a fresh tube. This

process was repeated until the sample was clear of beads. Input samples were typically diluted in 1400 µL 0.1X TE and IP samples were diluted in between 200 and 600 µL 0.1X TE and kept at -80°C.

2.9 Chromatin Immunoprecipitation Protocol II

A modified ChIP protocol was used when RNase treatment was undertaken. This was based on the first protocol, but with the following amendments. Fixation of cells was with 37% formaldehyde (Sigma) to a final concentration of 1% for 5 minutes at 27°C. Cells were lysed by vortexing with beads for 10 cycles of 20s on, 20s off, 20s on, with 2 min on ice in between each cycle. Sonication was for 6 pulses of 20 s, with 20 s on ice between each cycle. 150 µL of the resulting chromatin, diluted in 150 µL purified H_2O, was used for each ChIP.

2.10 Chromatin Immunoprecipitation Protocol III

Further modifications were made to the above protocol; 400 µL of chromatin was used per ChIP. Elution of the DNA from Protein G Dynabeads was repeated by resuspending the beads in 100 µL elution buffer and incubating for 10 min in a 65°C water bath. Decrosslinking was by incubation at 65°C overnight and 5 µL 20 mg/mL Proteinase K was added the following day and incubated at 37°C for 2 hours. Purification of the DNA was with a QIAquick PCR Purification Kit, as per supplied protocol, with the sample being passed through the column twice. Eluted DNA was diluted in 50 µL 0.1X TE to which 1 µL of 20 mg/mL RNase A was added. This was incubated at 37°C for 1 hour and 25 µL was diluted with a further 175 µL 0.1X TE to bring the final volume up to 200 µL for use in qRT-PCR.

2.11 Quantitative real-time PCR (qRT-PCR)

qRT-PCR of purified input and immunoprecipitated DNA was carried out using an ABI Prism 7000 real-time PCR thermocycler. 20 µL PCR reactions were prepared on ice in triplicate for each sample, containing 1X SensiFAST SYBR Hi-ROX mix (Bioline), 0.4 µM of each of the forward and reverse primers for the region of interest, and 4 µL of template DNA. The programme used was 2 min at 50°C, 5 min at 95°C, followed by 35 cycles of 15 s at 95°C and 1 min at 60°C.

2.11.1 Calculation of fold enrichment from qRT-PCR data

Analysis of fold enrichment of proteins of interest at chosen loci was carried out using the ΔΔct method. The baseline level was set to read the cycle at which all samples were being amplified exponentially (the Ct, or cycle threshold, level). The average Ct value was calculated for the triplicate repeats of each sample, removing any outliers from the calculation. The difference between the Ct values of the test gene and control gene (in this case an intergenic region) was calculated for both the input and immunoprecipitated samples and the difference between these two values was then calculated to give the ΔΔct value. The fold enrichment was calculated as 2^ΔΔct.

2.12 Polysome profiling

The polysome profiling method used in this study was adapted from (Wen, 2009).

2.12.1 Preparation of sucrose gradients

50% and 10% sucrose solutions were prepared in polysome buffer (10 mM Tris acetate pH7.4, 70 mM ammonium acetate, 4 mM magnesium acetate in DEPC-treated purified H_2O).

A gradient mixer was used to prepare 10-50% (w/v) gradients from the stock solutions, which were dispensed into SW41 polyallomer centrifuge tubes (Beckman Coulter). Where gradients were to be used for fractionation of samples treated with the translation elongation inhibitors cycloheximide and emetine, the relevant concentrations of these drugs were also added to the gradients. Gradients were cooled to 4°C before use.

2.12.2 Cell extract preparation

50 mL of *S. pombe* cell culture at OD ~0.5 was used per sample. Cells were treated with translation elongation inhibitor drugs according to desired experimental conditions (see results chapters). An equivalent volume of ice-cold water was added to the cell culture following drug treatment to halt the reaction and cultures were immediately placed on ice. All subsequent steps were carried out on ice or at 4°C. Cells were pelleted by centrifugation at 3000 rpm, washed in 10 mL HEPES buffer (10 mM HEPES pH 7.4, 2 mM magnesium chloride, 2 mM magnesium acetate, 100 mM potassium acetate, prepared in DEPC treated purified H_2O), pelleted again, then resuspended in 300 µL lysis buffer (HEPES buffer with 1mM phenylmethylsulfonyl fluoride, 1 mM dithiothreitol, 1.2 µL RNAse inhibitor Ribolock and Roche EDTA free protease inhibitor cocktail). The cell suspension was transferred to pre-cooled 2 mL screw-cap tubes to which pre-cooled acid-washed, glass beads (0.5 mm diameter) were added until they reached the meniscus. Cells were lysed by vortexing in a Precellys lysis machine for 5 rounds of 15 seconds at 5500 rpm, with 2 minutes on ice between each round. Lysis was checked under the microscope before proceeding. An additional 300 µL of lysis buffer was then added to the tube. The bottom of the screw-cap tube was pierced 3 times with a 25 gauge needle and the tube was then inserted into a 5 mL syringe placed in a 15 mL Falcon tube, and centrifuged at 4000 rpm for 5 minutes to collect

the lysate. The lysate was transferred to pre-cooled 1.5 mL tubes and cleared by centrifugation at 13200 rpm for 10 minutes. The supernatant was transferred to fresh tubes and cleared again. The absorbance at 260 nm was read using a NanoDrop spectrometer (ND-100 NanoDrop) with a typical reading being somewhere between 20 and 80.

2.12.3 Fractionation

20 OD_{260} units of lysate (~350-600 µL) were carefully loaded onto the sucrose gradient. DEPC treated purified H_2O was added to the top of each gradient where necessary to balance the tubes before centrifugation. The gradient tubes were then loaded into the buckets of a Beckman SW41 rotor and centrifuged at 38000 rpm for 160 minutes at 4°C. A steel capillary needle was carefully lowered to the bottom of the gradient tube, through which the gradient was pumped using a Pharmacia P-1 peristaltic pump. The gradient passed through an Isco UA-6 absorbance detector, and the absorbance at 254 nm was plotted with a Pharmacia LKB REC 102 plotter. Gradients were dispensed as 15 ~800 µL fractions using a Pharmacia FRAC-100 collector.

2.12.4 Protein purification from sucrose gradients

Proteins were precipitated from sucrose gradients using the methanol/chloroform method (http://www.mitosciences.com/PDF/sg.pdf). A 200 µL aliquot of each fraction was taken, to which 800 µL of methanol was added and mixed thoroughly by inverting several times. 200 µL chloroform was then added and the samples were vortexed, followed by 400 µL of purified H_2O after which samples were vortexed thoroughly again. The samples were centrifuged at 13200 rpm for 5 minutes and the upper aqueous phase was removed. 867 µL of methanol was added to the tubes which were then inverted three times. The tubes were

centrifuged at 13200 rpm for 5 minutes and the supernatant was removed. The protein-containing pellets were air dried and resuspended in 35 µL of 1X SDS-loading buffer as described in 2.6.

2.13 Colony PCR

S. pombe strains were confirmed by PCR of single colonies using primers specific for the region of interest. 25 µL reactions were prepared on ice in sterile purified H_2O containing 1X GoTaq buffer, 1.5 mM $MgCl_2$, 200 µM dNTP mix, 0.4 µM of each of the forward and reverse primers and 0.025 units/µL GoTaq polymerase (Promega), into which a small amount (just visible on the end of a 2 µL tip) of colony was resuspended. Reactions were carried out in a thermocycler with a typical programme being an initial 10 minutes at 95°C to break the cells, followed by 35 cycles of denaturing for 30 s at 95°C, annealing for 30 s at 52°C and extension for 1 minute at 72°C, and a final 5 minutes at 72°C. The temperature of the annealing step and the duration of the extension step were calculated according to the melting temperatures of the primers and the length of the region being amplified respectively.

2.14 DNA cloning in *Escherichia coli*

A number of proteins were C-terminally tagged with GFP for episomal expression. The plasmid vector used in this study was pREP41 containing the GFP ORF under the control of the nmt41 (no message thiamine) promoter, which gives a moderate level of expression in the absence of thiamine (Wen and Brogna, 2010) (Appendix 9). Cloning was at an Nhe1 restriction site immediately downstream of the ATG start codon in the GFP ORF. The plasmid contains the *LEU2* gene from *S. cerevisiae* which serves as a selection marker.

2.14.1 Strains

The *E. coli* strain used for all cloning procedures was XL1-Blue with the genotype *recA1 endA1 gyrA96 thi-1 hsdR17 supE44 relA1 lac [F´ proAB lacIq ZΔM15 Tn10 (Tetr)]*.

2.14.2 *E. coli* media and culturing methods

LB liquid and agar media were used in the culturing of *E. coli*, details of which can be found in Appendix 1. Colonies were grown overnight on 10 cm LB agar plates in a 37°C incubator and liquid cultures were grown in a 37°C shaking incubator at 220 rpm.

2.14.3 Bacterial transformation

Plasmid vectors were amplified before use. 1 µL of plasmid DNA was mixed with 50 µL of competent cells and kept on ice for 30 minutes. Cells were heat shocked in a 42°C water bath for 90 seconds then placed on ice for 2 minutes. 450 µL of NZY media was added to the cells which were then kept at 37°C for 1 hour. The mixture was split, with one tenth being spread onto a LB + 100 µg/mL ampicillin plate and nine tenths on a separate plate. Plates were grown overnight in a 37°C incubator.

2.14.4 Large-scale plasmid preparation

Bacterial transformants were inoculated from single colonies into 2 mL of LB media in the morning, incubated at 37°C for ~8 hours, and the 2 mL then added to a further 50 mL of LB media and grown to saturation overnight. Plasmid DNA was typically purified using an Invitrogen midi-prep kit as per kit protocol. The resulting plasmid DNA pellet was resuspended in 200 µL TE buffer and the plasmid concentration measured using a Nanodrop ND-1000 spectrometer.

2.14.5 Restriction enzyme digestion of plasmid DNA

Restriction enzyme digestion of 5 µg of plasmid DNA at the Nhe1 site was carried out in 50 µL reactions. All restriction enzymes used in the study were obtained from New England Biolabs (NEB) and conditions of the digestion were followed according to NEB enzyme instructions typically for 2 hours at 37°C.

2.14.6 Dephosphorylation of digested plasmid

Antarctic phosphatase (NEB) was used to remove the 5' terminal phosphates of digested plasmid DNA. This procedure was applied to prevent self-ligation of the digested plasmid. Following restriction enzyme digestion, 1 µL of Antarctic phosphatase (5 units/µL) and 1 µL of 10X Antarctic phosphatase buffer were added to a 50 µL reaction and incubated at 37°C for 1 hour. The enzyme was then inactivated by incubating the tube in a 65°C water bath for 15 minutes.

2.14.7 PCR for cloning

The DNA sequence to be cloned was amplified from yeast genomic DNA that had been purified using commercially available kits (Fermentas, K0512); primers used for cloning are listed in Appendix 8. Typically the forward primer was the ~20 base sequence immediately downstream of the start codon of the gene sequence being amplified, flanked at the 5' end with the Nhe1 restriction site to allow in-frame insertion in the GFP CDS after the ATG. The reverse primer was the reverse complement of ~20 bases immediately upstream of the stop codon of the gene being amplified, with the Nhe1 digestion site at the 5' end of the primer. Typically, 50 µL reactions were prepared on ice in sterile purified H_2O containing 20 ng of genomic DNA, 1X HF buffer, 200 µM dNTP mix, 0.4 µM of each of the forward and reverse

primers and 0.25 units/µL of Phusion DNA polymerase (NEB). The reaction was carried out in a thermocycler with a typical programme being an initial of denaturing step for 5 minutes at 95°C, followed by 35 cycles of denaturing at 95°C for 30 seconds, annealing at 55°C for 30 seconds and extension for 1 minute at 72°C, and a final extension at 72°C for 5 minutes. The temperature of the annealing step and the duration of the extension step were calculated according to the melting temperatures of the primers and the length of the region being amplified respectively.

2.14.8 Purification of digested plasmid and PCR-amplified fragments

Digested and dephosphorylated plasmid DNA was run on a 1 % agarose gel. The section of the gel containing the DNA fragment was sliced out and placed in a 1.5 mL Eppendorf tube. DNA was purified using a Fermentas Silica Bead DNA Gel Extraction Kit as per kit protocol. Digested PCR fragments were purified using a QiAgen PCR purification kit as per kit protocol.

2.14.9 Digestion of PCR fragments

Restriction digestion of the purified PCR fragments with Nhe1 was carried out for two hours at 37°C in a 50 µL reaction according to NEB enzyme instructions. The digested product was purified again using a QiAgen PCR purification kit as per kit protocol.

2.14.10 Ligation of vector and fragment DNA

Ligation of DNA fragments was typically performed in a 15 µL reaction containing 100 ng of linearized plasmid and a 10:1 ratio of fragment to vector DNA, with 10 units of T4 DNA ligase and 1.5 µL T4 DNA ligase buffer (NEB). The ligation reaction was kept at 18°C overnight. 7.5 µL of the ligation mix was used to transform *E. coli* competent cells as previously described and colonies were screened by colony PCR as for *S. pombe* colony PCR,

with a forward primer specific for the nmt41 promoter region and a reverse primer specific for the gene insert. Further verification was by restriction digestion with NEB restriction enzymes. Plasmid stocks were made by amplification in *E. coli* and harvesting by midi-prep as described.

2.15 *S. pombe* plasmid transformation

Transformation of S. pombe cells was carried out using the lithium acetate method, adapted from (Forsburg and Rhind, 2006). 2.5 mL of *S. pombe* cells grown to OD_{600} 0.8 were used per transformation. Cells were pelleted by centrifugation at 3000rpm for 5 minutes and washed in 2.5 mL sterile purified H2O. Cells were rendered competent by resuspension in 50 µL sterile purified H_2O plus an equal volume of Lithium Acetate buffer (10 mM Tris-HCl pH 8.0, 1 mM EDTA, 0.1 M Lithium acetate) and incubation at room temperature for 30 minutes. 2 µL of plasmid DNA and 3 µL denatured salmon sperm DNA was added to the cell suspension, resuspended gently and the sample was kept at room temperature for a further 30 minutes. 220 µL of PEG 3350 and 40 µL Lithium Acetate buffer was added to the sample, resuspended gently and incubated at 30°C for 1 hour, with gentle resuspension halfway through. Samples were heat shocked in a 42°C water bath for 30 minutes and cells were pelleted at 3000rpm for 5 minutes. The pellet was washed once in 1 mL sterile purified H_2O and pelleted again. The final pellet was resuspeded in 100 µL sterile purified H_2O, spread onto selective agar media and grown at 30°C for 3-5 days until colonies formed.

2.16 Immunofluorescence

Protocol available at

http://users.ox.ac.uk/~kearsey/resources/protocolsmirror/pombe%20immunofluorescence.pdf

A 1 mL culture of cells was grown to OD_{600} ~0.5 and fixed with 3.7% formaldehyde for 30 minutes in a 27°C shaking incubator at 160 rpm. The cells were pelleted by centrifugation at 3000 rpm and washed 3 times in 1 mL PBS. Cells were then spheroplasted by resuspending in 100 µL of PBSSorb (PBS with 1.2 M sorbitol) containing 14 µL of 100 mg/mL Zymolyase® 20T (Amsbio) and 2 µL of β-mercaptoethanol, and incubating in a 37°C water bath for 90 minutes, vortexing every 20 minutes. Cells were pelleted again, resuspended in 100 µL PBSSorb with 1% Triton X-100 and incubated for 10 minutes at room temperature. Cells were resuspended in ~100 µL of PBS and 5 µL was pipetted onto a well of a 10-well microscope slide (Marienfeld) that had been coated with Concanavalin A (see below). The cells were left on the slide for 10 minutes, the excess was pipetted off and the remainder was allowed to dry. Immediately upon drying, the slide was placed into a 9 cm petri dish with PBS for 5 minutes, then transferred to PBSBAL (PBS with 100 mM lysine hydrochloride, 0.01% NaN_3 and 1% BSA) with 0.3% Triton X-100 overnight at 4°C. The slide was removed from the PBSBAL and the excess drained away. The required primary antibody was diluted 1:125 PBSBAL with 0.3% Triton X-100 and 1.5 µL was pipetted onto each well of the slide. A cover slip was gently placed on the slide and the slide was inverted and incubated in a humidity chamber at 30°C for 2 hours. The slide was then transferred back to the petri dish and excess antibody was washed by two quick rinses in 20 mL PBSBAL (during the first rinse the cover slip was allowed to detach from the slide and was carefully removed), followed by three 5 minute washes in 20 mL PBSBAL with 0.3% Triton X-100. The slide was then removed from the PBSBAL, the excess drained away and 1.5 µL of secondary antibody, diluted 1:125 in PBS with 0.3% Triton X-100, was pipetted onto the well. A cover slip was carefully placed over the well and the slide was inverted and placed in a humidity chamber at 30°C for 1 hour. All remaining steps were carried out with minimum exposure to light.

The slide was transferred back to the petri dish and excess antibody washed away by two quick rinses in 20 mL PBS (removing the cover slip as before) followed by two 5 minute washes in 20 mL PBS with 0.3% Triton X-100 and 1 wash in 20 mL PBS alone. Slides were mounted by the addition of 2 µL of 80% glycerol, containing 0.1 µg/mL of DAPI to stain the DNA (to counterstain the nucleus), to each well, gently lowering a coverslip onto the slide and allowing adhere in the dark, typically overnight. The coverslip was then sealed with nail polish and the slide kept at 4°C.

2.16.1 Coating of microscope slides

20 µL of 500 mg/mL Concanavalin A (Sigma) was pipetted onto each well of a 10 reaction well microscope slide (Marienfeld). Slides were covered and left at RT for 2 hours after which the excess Concanavalin A was pipetted off and they were allowed to dry completely in a laminar flow hood.

2.16.2 Counterstaining cells with an RNA selective dye

The RNA-selective dye, E36 (Chemical BioImaging Lab, (Li et al., 2006)) was used to counterstain RNA where indicated. A 10 mM stock was prepared in DMSO which was diluted to a 5 µM working concentration in PBS. 20 µL of this was placed on the well of each slide and was incubated at RT for 20 minutes in the dark immediately before the final two 5 mins PBS washes in the immunostaining procedure.

RESULTS

Chapter 3: Can ribopuromycylation detect co-transcriptional translation in *Schizosaccharomyces pombe*?

3.1 Introduction

The increasing number of studies reporting evidence in support of nuclear translation are at odds with the conventional view that translation occurs solely within the cytoplasm. The ribopuromycylation (RPM) technique, which rests upon the immunodetection of puromycin that has been incorporated into nascent peptides on immobilised ribosomes (Introduction, Fig 1.7), was developed in human cells, where it reported a signal not only in the cytoplasm, but also in the nucleus (David et al., 2012). In the Brogna lab, a bimolecular fluorescence complementation (BiFC) assay reported the joining of ribosomal subunits in the nuclei of *Drosophila* S2 cells and salivary glands, while immunostaining of *Drosophila* polytene chromosomes following RPM also reported the incorporation of puromycin at active transcription sites (Al-Jubran et al., 2013). ChIP-chip analysis in *S. pombe* has also revealed that three ribosomal proteins (RPs) co-localise at numerous loci across the whole of the genome, raising the question of the role of these RPs at such sites and whether they belong to a larger complex, for instance a functional ribosome or ribosomal subunit (De et al., 2011). This chapter presents further work carried out in *S. pombe* to address this question, combining RPM with chromatin immunoprecipitation (ChIP) to investigate whether ribosomes may be co-transcriptionally translating nascent mRNAs (Fig 3.1 (i)).

(i)

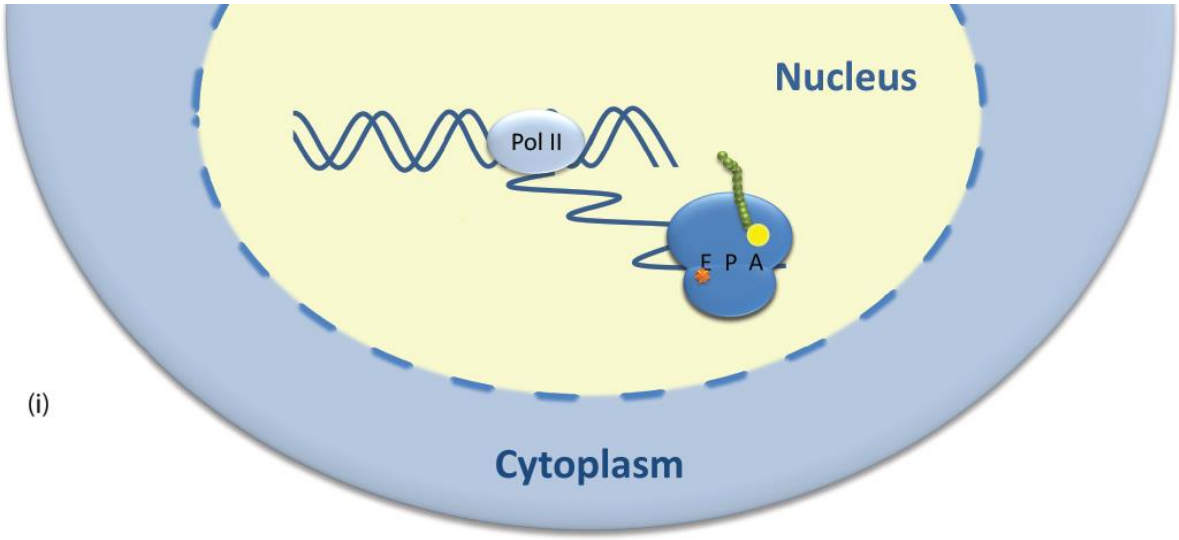

(ii) lyse cells

(iii) shear chromatin by sonication

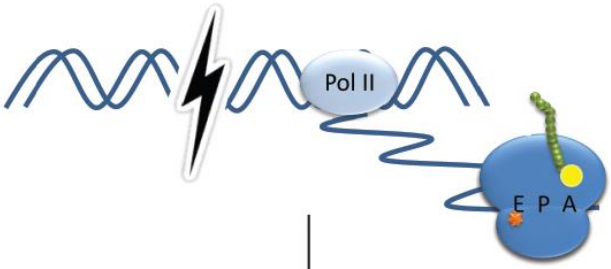

(iv) immunoprecipitate target

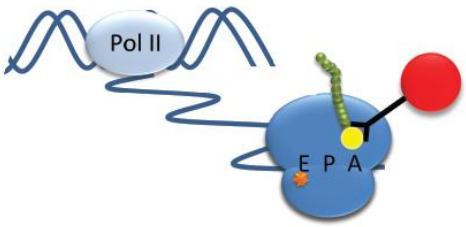

(v) degrade RNA and proteins

(vi) analyse DNA by qRT-PCR

Figure 3.1 Analysis of co-transcriptional translation by chromatin immunoprecipitation (ChIP). (i) Schematic of hypothesised co-transcriptional translation within the cell. Treatment of cells with translation elongation inhibitors (orange star) immobilises ribosomes and subsequent treatment with puromycin (yellow circle) labels nascent peptides. (iii) Cells are lysed and the chromatin sheared by sonication. (iv) The sheared chromatin is incubated with Protein G beads (red circle) which are bound by an anti-puromycin antibody, resulting in the precipitation of any regions of the chromatin that are indirectly associated with ribosomes translating nascent mRNAs. The chromatin is sheared by sonication and then incubated with Protein G beads (red circle) bound by an anti-puromycin antibody, to immunoprecipitate chromatin fragments that are associated with ribopuromycylated peptides. (v) DNA/protein/RNA complexes are washed from the beads and the sample is treated with proteinase and RNase to isolate the DNA. (vi) The purified DNA is then analysed by qRT-PCR to identify regions that are enriched with ribopuromycylated peptides compared to a non-transcribed intergenic region.

S. pombe cells are known to be resistant to a number of drugs due to the presence of effective efflux pumps that prevent the accumulation of drugs inside the cell (Lage, 2003, Paulsen et al., 1996), therefore drug concentrations and treatment times were first optimised before carrying out RPM. ChIP, using an antibody against puromycin, was subsequently performed on ribopuromycylated *S. pombe* cells followed by quantitative real-time PCR (qRT-PCR) (a schematic of the procedure is shown in Fig 3.1) to analyse a number of gene loci which were highly enriched with the three RPs in the previous ChIP-chip study (De et al., 2011). Enrichment of puromycylated peptides at these loci was compared to that of an intergenic region which does not encode any protein or RNA product, and hence which should not immunoprecipitate with ribopuromycylated peptides. The results of this optimisation and ChIP analysis are presented in this chapter.

3.2 Results

3.2.1 Analysis of the effect of translation elongation inhibitors on cell growth in *S. pombe*

RPM requires that ribosomes are first immobilised on mRNAs by treating cells with a translation elongation inhibitor such as emetine or cycloheximide (David et al., 2012). To assess the efficacy of the drugs required for RPM in the inhibition of protein synthesis in *S. pombe*, the growth of wild type cells (TLM001, see table of strains used in this study and their genotypes in Appendix 2) treated with different concentrations of each drug were compared with control wild-type cells grown without any drug.

All emetine concentrations assayed resulted in a significant inhibition of cell growth when compared to the control (Fig 3.2 A (i)). After 16 hours' growth in the presence of 25 and 50

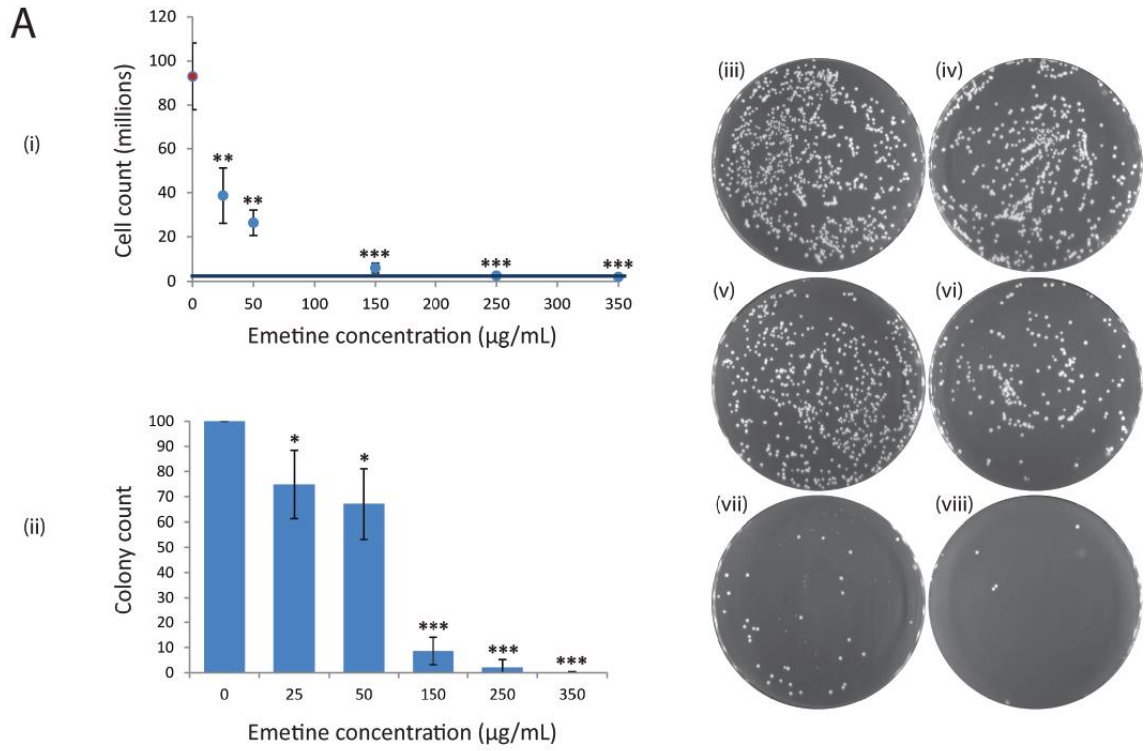
A
(i)
Cell count (millions)
Emetine concentration (µg/mL)
(ii)
Colony count
Emetine concentration (µg/mL)
(iii)
(iv)
(v)
(vi)
(vii)
(viii)

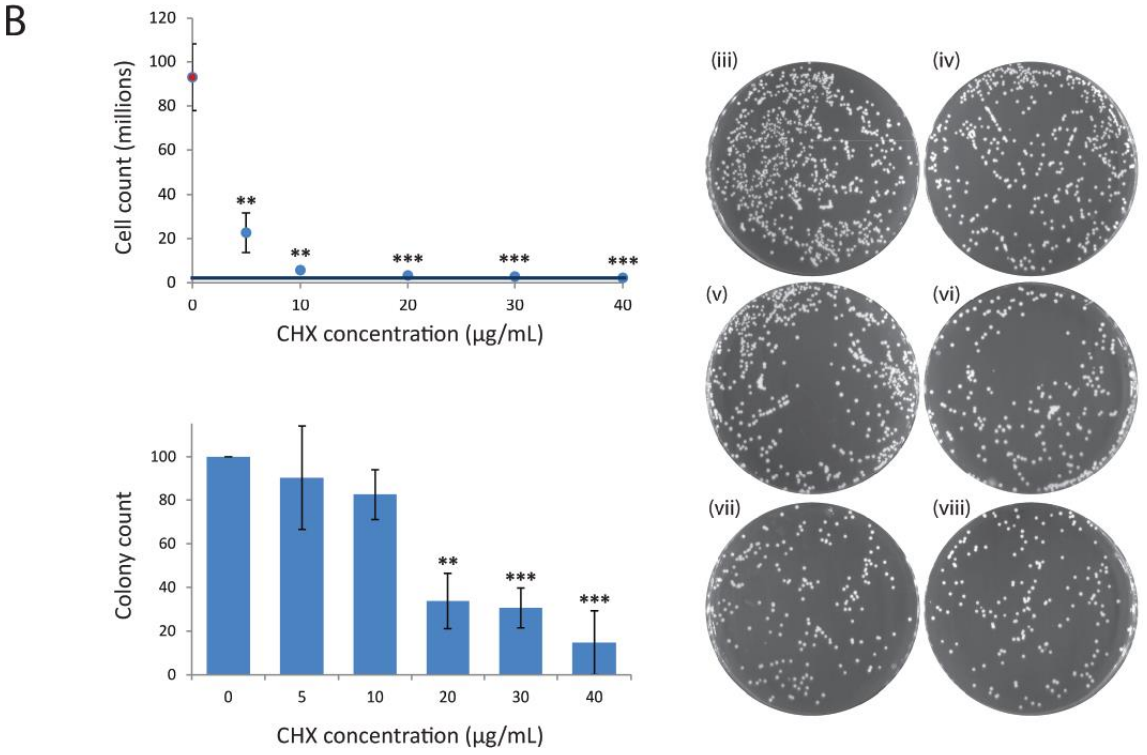
B
Cell count (millions)
CHX concentration (µg/mL)
Colony count
CHX concentration (µg/mL)
(iii)
(iv)
(v)
(vi)
(vii)
(viii)

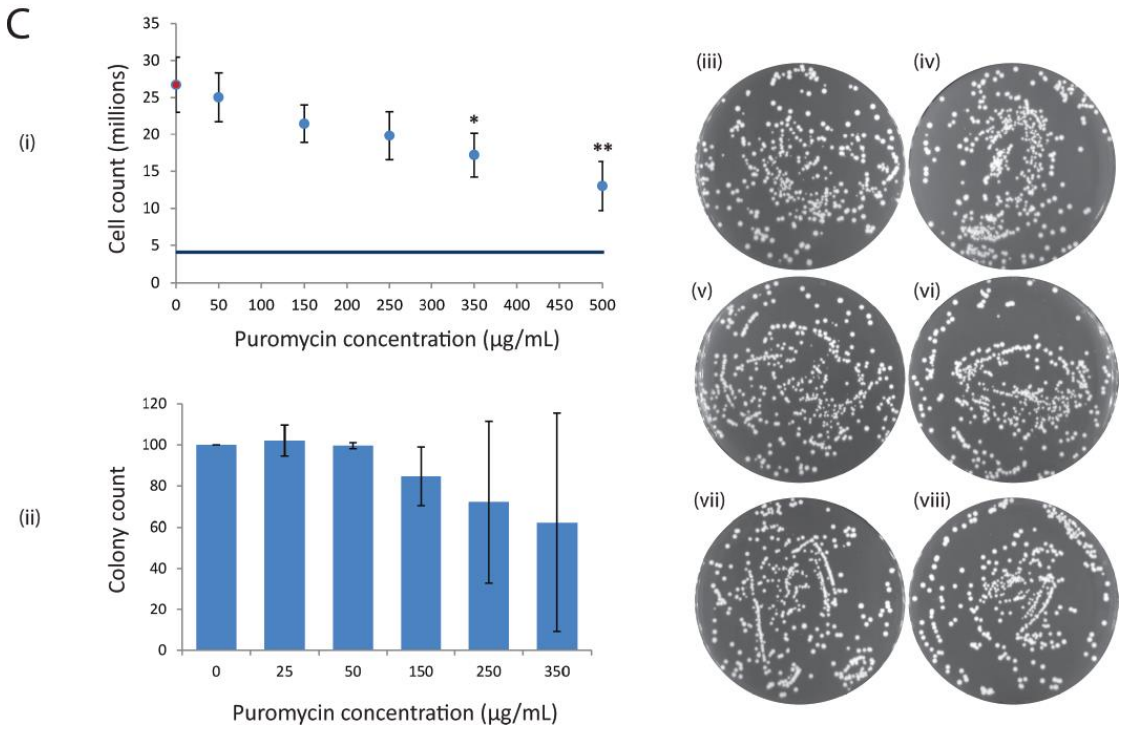

Figure 3.2 Analysis of the effect of translation inhibitor drugs on *S. pombe* growth. (A) One mL wild-type *S. pombe* cultures (TLM001, Appendix 2) were inoculated with 3 million cells (horizontal blue line) and grown in YES liquid media in the presence of 0, 25, 50, 150, 250, and 350 µg/mL emetine at 30 °C. Cell counts were taken after 16 hours (i). One thousand cells were then plated onto YES agar media, grown for 2 days at 30 °C and the number of colonies was counted (iii-viii). (ii) Number of colonies formed on agar media, expressed as a percentage of those from untreated cells. (B) As in (A) but cells were instead treated with 0, 5, 10, 20, 30 and 40 µg/mL cycloheximide (CHX). (C) As in (A) but cultures were inoculated with 4 million cells and treated with 0, 50, 150, 250, 350 and 500 µg/mL puromycin. All data are the result of three biological repeats and error bars show +/- standard deviation (SD). Statistical significance was determined by carrying out a t-test to compare the means of the three biological repeats for each condition, and is demonstrated by asterisks (* = $p < 0.05$, ** = $p < 0.01$, *** = $p < 0.001$).

µg/mL of emetine, the initial population of 3 million cells on average doubled between 3 and 4 times, which was a significant reduction ($p < 0.01$) compared to untreated cells, which doubled on average 5 times during the same period (Figure 3.2 A (i)). Cells grown in the presence of 150 µg/mL emetine and above doubled only once ($p < 0.001$) during the 16 hour period, while at 250 and 350 µg/mL emetine no cell growth was observed at all ($p < 0.001$). To determine whether cells could recover from emetine treatment, cells from each of the cultures assayed above were plated on agar media without any drug and colony formation was assessed. Colony formation was significantly reduced for all concentrations of emetine assayed compared to those from untreated cultures (Fig 3.2 A (ii-viii)). Recovery of cells from cultures treated with 25 and 50 µg/mL emetine was only 75% ($p < 0.05$) and 67% ($p < 0.05$) respectively compared to colony formation from untreated cultures (Fig 3.2 A (ii-v)). The reduction in recovery of cells treated with emetine at concentrations of 150 µg/mL and above was even more marked; at 150 µg/mL and 250 µg/mL emetine, recovery was 9% ($p < 0.001$) and 2% ($p < 0.001$) compared to the growth of cells from untreated cultures (Fig 3.2 A (ii) and compare (iii) to (vi) & (vii)), while the rate of recovery from cells that had been grown in the presence of 350 µg/mL was less than 1% ($p < 0.001$) (Fig 3.2 A compare (ii) & (viii)). These results reveal that low concentrations of emetine are tolerated in *S. pombe* and are therefore insufficient to inhibit translation elongation. That cells from cultures grown at low concentrations of the drug partially recover when plated onto media without emetine indicates that at these concentrations the drug possibly fails to reach the intracellular levels required to act as an irreversible elongation inhibitor as was previously reported in mammalian cells (Grollman, 1968). RPM demands that ribosomes are immobilised in order to ensure that sites of translation, and not released puromycylated peptides, are detected, therefore low concentrations of 25 and 50 µg/mL emetine are unsuitable for these

purposes. Higher concentrations of 250 µg/mL and above of emetine do however inhibit cell growth and recovery when transferred to drug-free media and are therefore suitable for RPM.

A similar assay using different concentrations of cycloheximide to inhibit translation elongation was carried out in parallel (Figure 3.2 B). Cycloheximide had a much more pronounced effect on cell growth than emetine, with inhibition of growth being more greatly reduced at much lower concentrations of the drug than that required of emetine to give a similar effect (Fig 3.2 compare A (i) with B (i)). Over the 16 hour incubation period, the initial population of three million cells doubled only three times when grown in the presence of a low concentration of 5 µg/mL cycloheximide (Fig 3.2 B (i), which represents a significant inhibition compared to untreated cells ($p < 0.01$). In the presence of 10 µg/mL cycloheximide, cells doubled only once ($p < 0.01$) while cultures treated with 20, 30 and 40 µg/mL cycloheximide produced no growth at all ($p < 0.001$) (Figure 3.2 B (i)), demonstrating that translation is completely inhibited at these concentrations. However, the extent of cell recovery when plated onto drug-free agar media was different from those treated with emetine (compare Fig 3.2 A (ii) and (iii) to (viii) with Fig 3.2 B (ii) and (iii) to (viii)). Although strong inhibition of growth was observed at concentrations of 5 and 10 µg/mL cycloheximide, the subsequent formation of colonies on drug-free agar media was not significantly different to that of the no-drug control (Figure 3.2 (ii-iv)). Recovery of cells that had been treated with 20, 30 and 40 µg/mL cycloheximide, although significantly reduced compared to the no-drug control, was observed at a rate of 34, 31 and 15% respectively ($p < 0.001$) (Fig 3.2 B (ii) and (vi-viii)). These results are consistent with cycloheximide being a reversible inhibitor of eukaryotic translation elongation (Grollman, 1968), with cells being

able to recover when cycloheximide inhibition is released even when growth had been strongly inhibited. Although the reversible nature by which cycloheximide inhibits translation may appear to make it a less desirable option for ensuring effective immobilisation of the ribosome during RPM, the growth assay demonstrates that at concentrations of 20 μg/mL and above it does completely inhibition growth, and therefore translation. Therefore cycloheximide is also suitable for RPM.

The same assay, using puromycin to inhibit translation elongation, showed that this drug is less effective than emetine at inhibiting cell growth at similar concentrations (compare Fig 3.2 A (i) with 3.2 C (i)). Although a general trend of reduced growth with increasing puromycin concentration was observed, there was no significant difference in cell growth between the control untreated cultures and those treated with 50, 150 or 250 μg/mL puromycin (Fig 3.2 C (i)). Only at a concentration of 350 μg/mL puromycin was a significant reduction in cell growth seen ($p < 0.05$) although cells had still undergone two rounds of doubling, while at 500 μg/mL growth was inhibited further, with cells on average doubling 1.9 times ($p < 0.01$) (Fig 3.2 C (i)). Puromycin treatment appears to be reversible as when transferred to drug-free agar media, no significant difference was observed in the recovery of cells that were treated with any of the concentrations of puromycin assayed, although again a general trend was observed in that those treated at higher concentrations on average recovered less well (Figure 3.2 C (ii-viii). However, the results here represent three biological repeats, one of which showed greatly reduced recovery of cells from those cultures that had been treated with 250 μg/mL puromycin and above, while in the other two repeats, cell recovery was similar to that of the wild type control for all concentrations of puromycin assayed, resulting in large standard deviations. Puromycin is reportedly a

reversible translation inhibitor (Wagner and Huang, 1965), thus cells might be expected to recover once translation inhibition has been released. It may therefore be that this variation is due either to a difference between batches of the drug or a technical error when counting or plating the cells.

3.2.2 Puromycin is incorporated into peptides in *S. pombe*

The puromycin growth/survival assay described above demonstrates that *S. pombe* cells are sensitive to the drug at concentrations of 350 μg/mL and above when exposed for a 16 hour duration. Whether incorporation of puromycin into nascent peptides can occur during the brief incubation periods required for RPM was assessed via Western blotting of protein extracts from wild-type (TLM001, Appendix 2) cell cultures that had been treated with increasing concentrations of puromycin for two different time periods (Figure 3.3). Upon puromycin treatment, ribosomes at various positions along an open reading frame (ORF) will incorporate puromycin into the C-terminus of the nascent peptide, therefore a ladder of proteins of different sizes should be apparent on a Western blotting if puromycylation has been effective. The anti-puromycin antibody used to detect ribopuromycylated peptides is specific for puromycin since no signal is present in the no-drug control (Fig 3.3 (i)). The results show no statistical significance between the intensity of the signals from protein extracts of cultures treated with 50 and 150 μg/mL, for either a 15 minute or a 30 minute incubation period (Fig 3.3). Treatment with 250 μg/mL for 15 minutes however produced a 2.7-fold increase in signal intensity relative to that of the extract from cultures treated with 50 μg/mL puromycin for 15 mins ($p < 0.05$). Although treatment with 250 μg/mL puromycin for 30 minutes gave an average 2.2-fold increase in signal intensity, this was not found to be statistically significant; it may be that degradation of puromycylated peptides begins during

(i)

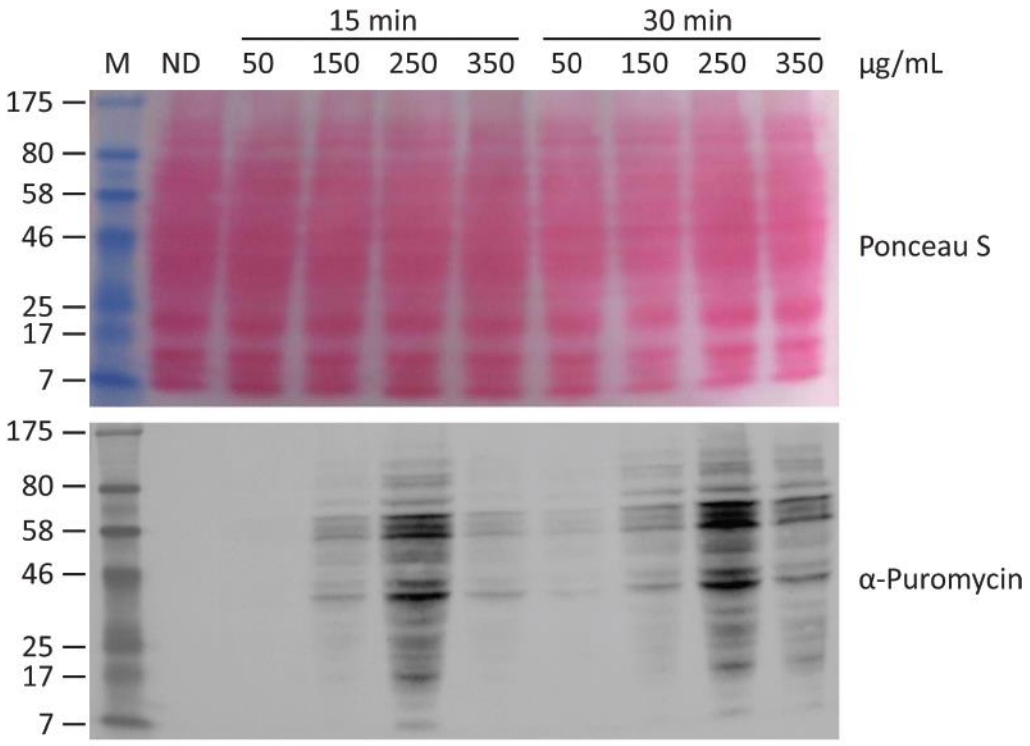
15 min
30 min
M
ND
50
150
250
350
50
150
250
350
µg/mL
175
80
58
46
25
17
7
Ponceau S
175
80
58
46
25
17
7
α-Puromycin

(ii)

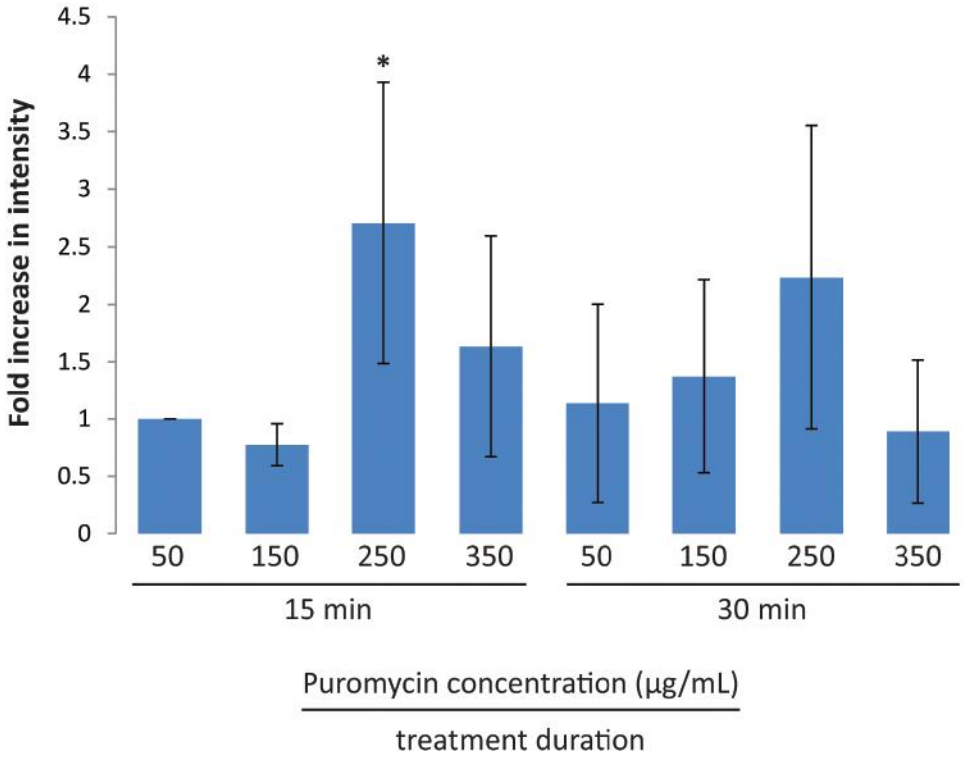
Fold increase in intensity
4.5
4
3.5
3
2.5
2
1.5
1
0.5
0
*
50
150
250
350
50
150
250
350
15 min
30 min
Puromycin concentration (µg/mL)
treatment duration

Figure 3.3 Puromycin is incorporated into nascent peptides in *S. pombe*. (i) Western blot of protein extracts from wild-type *S. pombe* cells (TLM001, Appendix 2) that had been treated with puromycin at concentrations of 50, 150, 250 and 350 µg/mL for 15 minutes and 30 minutes. A no drug (ND) control was also loaded. Top panel shows Ponceau S staining as a transfer and loading control. Bottom panel shows puromycin detection with a mouse anti-puromycin antibody (clone 5B12, see Material and Methods). The bands of the protein ladder (M) (NEB prestained protein marker, broad range, P7708) are labelled with their sizes in kDa. (ii) Fold intensities of the puromycin signal for each condition. The intensity of the puromycin signal for each lane was determined using Image J software and these were normalised against the intensity of the corresponding Ponceau S signal. Fold increase in intensity for each lane is in comparison to the sample treated with the lowest concentration of 50 µg/mL for the shortest time of 15 minutes. All data is representative of three biological repeats and error bars show +/- standard deviation (SD). Statistical significance is demonstrated by an asterisk (* = $p < 0.05$).

this longer incubation period. Protein extracts of cells treated with 350 µg/mL puromycin for both 15 and 30 mins showed reduced levels of puromycin incorporation compared to 250 µg/mL puromycin, and there was no significant difference between the signals from these samples and the sample treated with the 50 µg/mL puromycin for 15 minutes. This effect was reproduced in three biological repeats but the reasons for this reduction remain unclear. On the basis of these results, a concentration of 250 µg/mL puromycin, and an incubation period of 15 minutes, was selected for subsequent experiments since this produces a reproducibly intense band, demonstrating that puromycin incorporation is effective under these conditions.

3.2.3 Puromycylation is inhibited by cycloheximide but not by emetine in *S. pombe*

To determine whether puromycylation occurs effectively on immobilised ribosomes, Western blotting of protein extracts from wild-type cultures treated with different concentrations of either emetine or cycloheximide, before treatment with` 250 µg/mL puromycin, was carried out (Figure 3.4). The results show that emetine pretreatment does not significantly affect the incorporation of puromycin into nascent peptides at any of the concentrations assayed relative to that of cells treated with puromycin alone (Fig 3.4 A). This is consistent with previous reports that emetine does not interfere with puromycin incorporation into nascent peptides in both cell-free mammalian protein-synthesis extracts and HeLa cells (Grollman, 1968, Pestka, 1971, Baliga et al., 1970). Cycloheximide pretreatment on the other hand results in significant inhibition of puromycin incorporation to a similar degree at concentrations of 50, 100, 250 and 350 µg/mL (between 10 and 14% of that of cells treated with puromycin only ($p < 0.05$)) (Fig 3.4 B). This was similarly

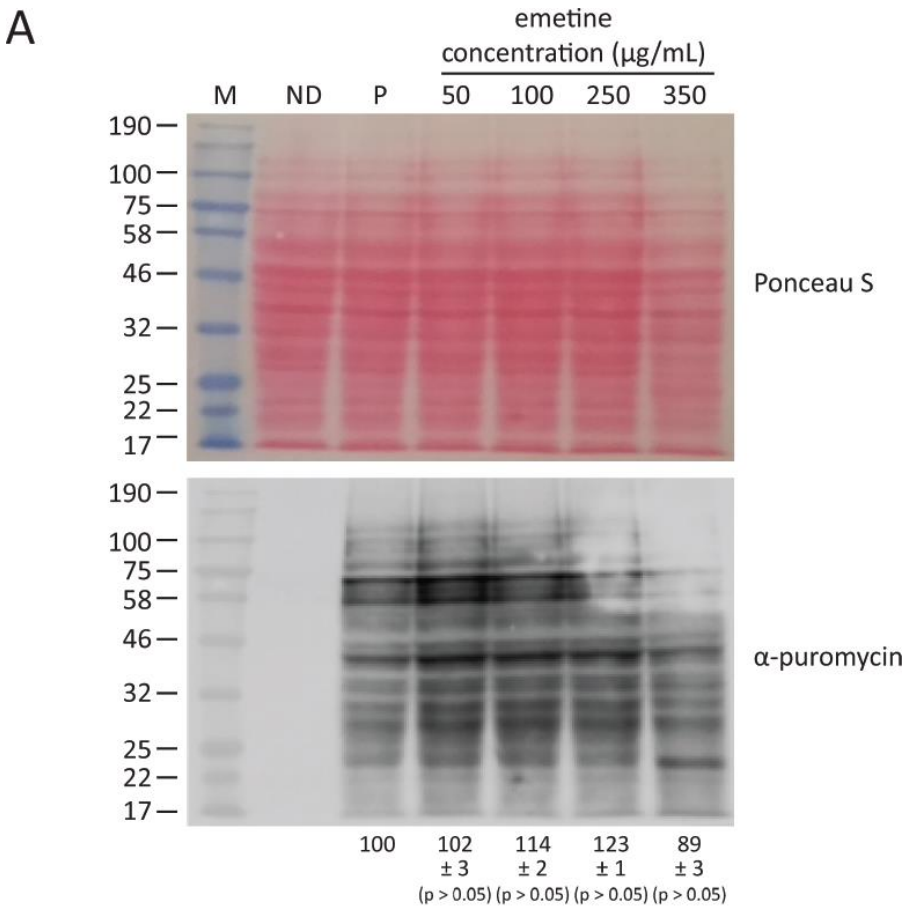
A
emetine
concentration (μg/mL)
M
ND
P
50
100
250
350
190
100
75
58
46
32
25
22
17
Ponceau S
α-puromycin
100
102 ± 3 (p > 0.05)
114 ± 2 (p > 0.05)
123 ± 1 (p > 0.05)
89 ± 3 (p > 0.05)

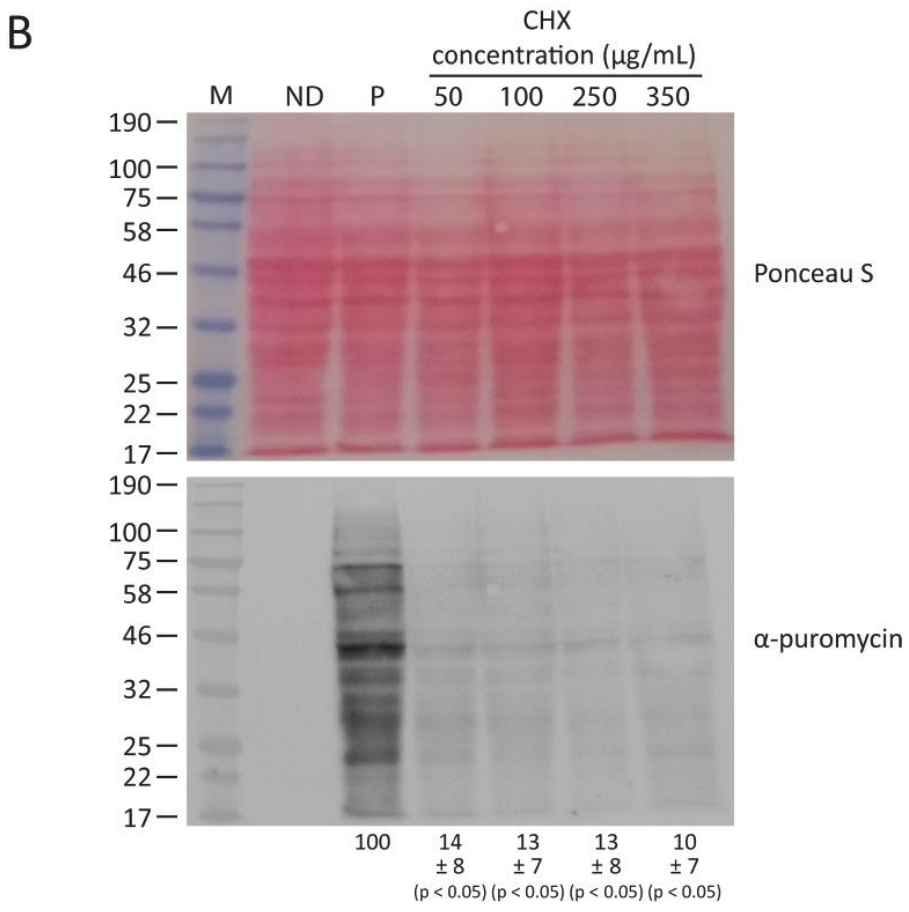
B
CHX
concentration (μg/mL)
M
ND
P
50
100
250
350
190
100
75
58
46
32
25
22
17
Ponceau S
α-puromycin
100
14 ± 8 (p < 0.05)
13 ± 7 (p < 0.05)
13 ± 8 (p < 0.05)
10 ± 7 (p < 0.05)

Figure 3.4 Puromycylation is inhibited by cycloheximide but not by emetine in *S. pombe*. (A) Western blot of protein extracts from wild-type *S. pombe* cultures that had been treated with 50, 100, 250 and 350 µg/mL emetine for 30 minutes, followed by treatment with 250 µg/mL puromycin for 15 minutes. (B) Western blot of protein extracts from wild-type S. pombe cultures that had been treated with 50, 100, 250 and 350 µg/mL cycloheximide for 30 minutes, followed by treatment with 250 µg/mL puromycin for 15 minutes. A no-drug (ND) control was also loaded for each blot. The top panel of each figure shows Ponceau S staining as a transfer and loading control while the bottom panel shows puromycin detection with a mouse anti-puromycin antibody as described in Figure 3.3. Statistical analysis was carried out by normalising the intensity of the puromycin signal against that of the respective Ponceau S signal, then calculating the percentage of signal for each lane relative to that of a sample that had been treated with 250 µg/mL puromycin only (P). The values below each lane show these percentages +/- standard deviation (SD) with statistical significance shown in brackets below.

observed in two earlier studies which concluded that cycloheximide prevents translocation of the mammalian ribosome in cell-free protein synthesis extracts, and that this translocation is required for puromycin incorporation (Baliga et al., 1970, McKeehan and Hardesty, 1969). The more recent study, which described the development of the RPM technique in human cells, reported different effects of emetine and cycloheximide on puromycin incorporation to these earlier studies, with emetine reportedly enhancing puromycin incorporation, while cycloheximide pretreatment maintained puromycylation at the level of that observed in cells treated only with puromycin (David et al., 2012). In *Drosophila* S2 cells on the other hand, emetine was shown to reduce the level of puromycin incorporation relative to that observed in cells treated with puromycin alone (Al-Jubran et al., 2013). The results presented here are more consistent with the older studies than with either of these recent publications; it maybe that these differences reflect species-specific variations in the actions of emetine, cycloheximide and puromycin on the ribosome, although despite the ribosome becoming increasingly complex in higher organisms, the core structure which contains the peptidyl transferase centre is highly conserved. It therefore seems likely that these antibiotics would have the same mode of action across eukaryotes. Alternatively, it could be that variations in the experimental conditions, such as drug concentration or treatment time, or in the *in vitro*, *ex vivo* and *in vivo* environments of the different studies, account for the differences observed in each system. The authors of the HeLa study argue that irreversibly immobilising ribosomes with emetine facilitates the puromycylation reaction (David et al., 2012). On the other hand, since treatment with puromycin alone leads to the release of puromycylated peptides and the dissociation of ribosomes, which are then free to engage in further rounds of translation, it may be that immobilising ribosomes, thus preventing the subunits from dissociating, limits the potential

for ribosomes to incorporate puromycin into additional peptides as they re-engage in new rounds of translation. This could explain why reduced puromycylation was observed in the *Drosophila* study in which ribosomes were immobilised with emetine (Al-Jubran et al., 2013). In light of both the growth/survival assay and the Western blot results, it was decided that emetine would be used at a concentration of 200 µg/mL for the ChIP experiment, since it was inferred from the growth assay (Fig 3.2 A) and Western blot (Fig 3.4 A) that this concentration reproducibly inhibits cell growth due to effectively and irreversibly immobilising ribosomes, without impeding puromycylation.

3.2.4 Anisomycin blocks ribopuromycylation in *S. pombe*

Anisomycin is a translation elongation inhibitor that competes with puromycin for binding to the A site of the ribosome (Ioannou et al., 1998); pretreatment with anisomycin should therefore block puromycylation and serves as a control to verify that any puromycin signal observed is due to its incorporation via the ribosome. To optimise the level of anisomycin required to impede puromycin incorporation, Western blotting of protein extracts from wild-type cells that had been treated with both emetine and anisomycin at several different concentrations prior to puromycin treatment was performed (Figure 3.5 A). Anisomycin reduces puromycin incorporation in a dose dependent manner on ribosomes that have been immobilised by emetine pretreatment, although a statistically significant effect was only observed at a concentration of 50 µg/mL and above, at which puromycin incorporation was 7.3% ± 6% ($p < 0.05$) that of cells treated with emetine and puromycin alone. At 150 µg/mL, puromycin incorporation reduced further to 3.1% ± 2% ($p < 0.05$) while at 250 µg/mL, puromycin incorporation was negligible at 1.6% ± 1% ($p < 0.05$). Anisomycin also reduces puromycin incorporation on ribosomes that have not been immobilised (Fig 3.5 B). At a

A

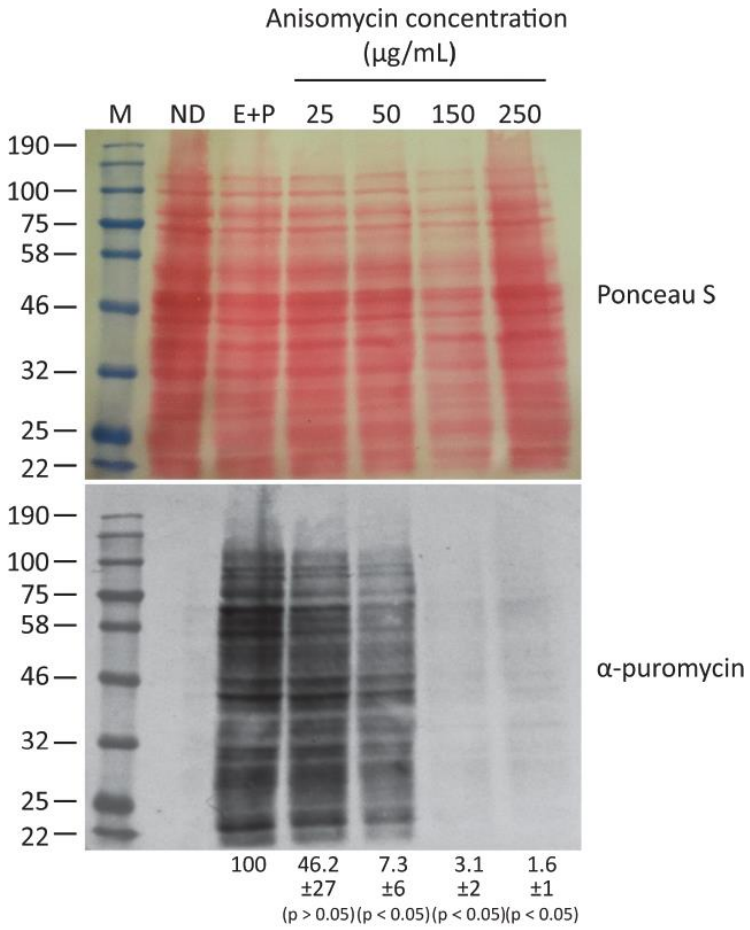
Anisomycin concentration (µg/mL)
M
ND
E+P
25
50
150
250
190
100
75
58
46
32
25
22
Ponceau S
α-puromycin
100
46.2 ±27
7.3 ±6
3.1 ±2
1.6 ±1
(p > 0.05)
(p < 0.05)
(p < 0.05)
(p < 0.05)

B

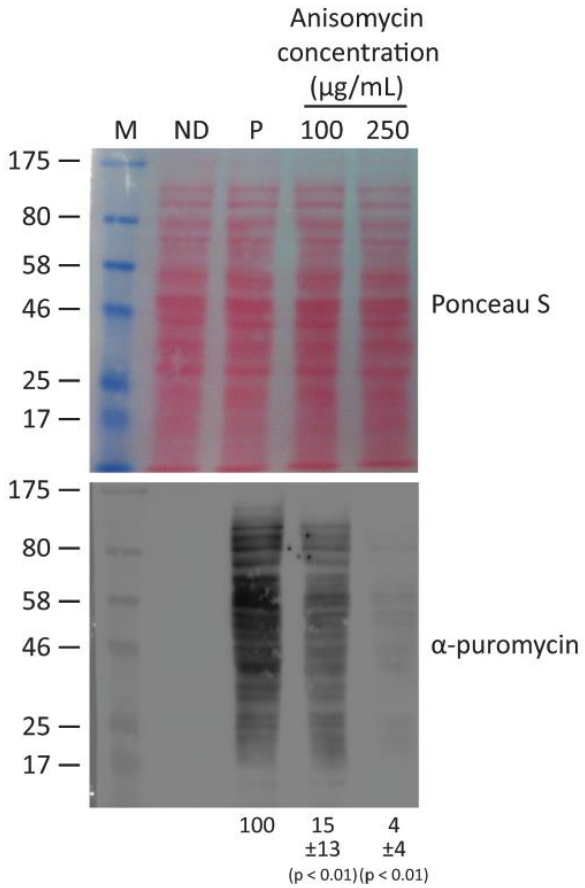
Anisomycin concentration (µg/mL)
M
ND
P
100
250
175
80
58
46
25
17
Ponceau S
α-puromycin
100
15 ±13
4 ±4
(p < 0.01)
(p < 0.01)

Figure 3.5 Anisomycin blocks puromycylation in *S. pombe*. (A) Western blot of protein extracts from wild-type *S. pombe* cells that had been treated with emetine at a concentration of 200 µg/mL, along with anisomycin for 30 minutes at concentrations of 25, 50, 150 and 250 µg/mL. Emetine/anisomycin pretreatment was followed by treatment with 250 µg/mL puromycin for 15 minutes. A no drug (ND) control was also loaded and a sample treated with emetine and puromycin only (E+P) is also shown. (B) Western blot of protein extracts from *S. pombe* cells that had been pretreated with anisomycin alone at concentrations of 100 and 250 µg/mL before puromycin treatment. A no drug (ND) negative control was also loaded and a sample treated with puromycin only (P) is also shown. The top panel of each figure shows Ponceau S staining as a transfer and loading control while the bottom panel shows puromycin detection with a mouse anti-puromycin antibody as described in Figure 3.3. Statistical analysis was carried out by normalising the intensity of the puromycin signal against that of the respective Ponceau S signal, then calculating the percentage of signal for each lane relative to that of (E+P) in (A) and (P) in (B). The values below each lane show these percentages +/- standard deviation (SD) with statistical significance shown in brackets below.

concentration of 100 µg/mL, anisomycin reduced puromycin incorporation to 15% ± 13% ($p < 0.01$) that of cells treated with puromycin only, while at 250 µg/mL, anisomycin reduced puromycin incorporation to 4% ± 4% ($P < 0.01$). A concentration of 250 µg/mL anisomycin was selected for subsequent experiments as this concentration was shown to almost completely exclude puromycin incorporation at the ribosome.

3.2.5 Chromatin immunoprecipitation standardisation in *S. pombe*

Chromatin immunoprecipitation is a powerful technique to assess whether a protein of interest associates with DNA, either directly or via nascent RNA (Fig 3.1). To assess the interaction of factors that are tethered to DNA via an association with nascent RNA, a previous study in the Brogna lab indicated that the optimal DNA fragment size is ~500-1000 bp (De et al., 2011). Standardisation of the sonication conditions was carried out using a strain in which the Cbc2 protein was tagged with 3HA at the carboxy terminal (TLM093, Appendix 2). Cbc2 is the *S. pombe* homologue of the nuclear human cap binding complex small subunit, CBP20, which co-transcriptionally binds the 5' cap of nascent mRNAs as they emerge from Pol II; the enrichment of Cbc2 at certain gene loci has previously been established in the Brogna lab (De et al., 2011). Optimisation of the ChIP procedure with this strain therefore allows standardisation of the conditions required to detect targets that are associated with nascent RNA. These conditions can then be used to detect regions of the chromatin that are bound indirectly by ribosomes that are co-transcriptionally translating nascent mRNAs. Sonication was initially carried out for four, six and eight pulses of 20 seconds; the resulting chromatin fragments from each condition were similar in size, peaking at around 500 bp (Figure 3.6 (i)). In order to reduce the possibility that nascent RNA could be sheared in the process, the number of sonication pulses was reduced further.

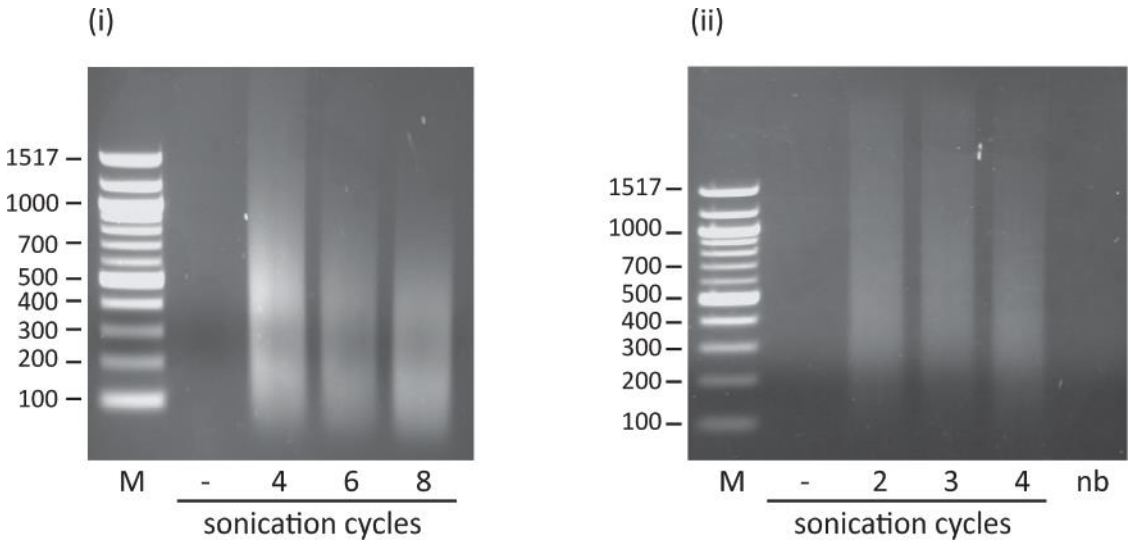

Figure 3.6 Chromatin immunoprecipitation optimisation in *S. pombe*. (i) A 500 µL chromatin sample from a Cbc2-3HA strain (TLM093, Appendix 2) was sonicated for 4, 6 or 8 cycles of 20s using a Misonix Ultrasonic Processor. 250 µL of each sample was diluted in 250 µL ChIP elution buffer and treated with 20 µL of 20 mg/mL Proteinase K and decrosslinked overnight at 63 °C. DNA was purified as per Materials and Methods and the pellet was diluted in 30 µL of TE buffer with 1 µL of 20 mg/mL RNase A. 15 µL was run on a 1% agarose gel. (ii) as in (i) but sonication was carried out for 2, 3 or 4 cycles of 20s. A control without sonication is also shown for each gel (-). A sample which had not been lysed with beads is shown in (ii) (nb) and the first lane of each gel shows a 100 bp ladder (NEB).

Chromatin fragment size was also within the desired range after only two, three and four 20 second pulses (Figure 3.6 (ii)).

A preliminary ChIP of the Cbc2-3HA strain was carried out to assess whether the number of sonication cycles impacts on the level of enrichment of Cbc2 at different regions of two gene loci, *pma1* and *act1*, which had previously been shown to be enriched with this protein The fold enrichment of Cbc2 at these loci was analysed by qRT-PCR and expressed as relative to that of an intergenic region which is not transcribed and shows no enrichment with Pol II or any of the three RPs investigated in the previous ChIP-chip analysis (De et al., 2011) and (Fig 3.7 A). The results of this initial experiment showed that the greatest enrichment was achieved when sonication was carried out for three cycles (see histogram in Appendix 3), therefore this was the condition used in subsequent experiments.

3.2.6 Analysis of RPM at gene loci

To assess whether translation may occur on nascent transcripts in *S. pombe*, the optimised ChIP protocol, using an antibody against puromycin, was carried out in wild-type cells that had undergone RPM. Different regions of three genes, *pma1*, *fba1* and *gpd3*, were subsequently analysed by qRT-PCR for their enrichment with puromycylated nascent peptides (Fig 3.7). These loci were selected as the previous ChIP-chip data showed that they were highly enriched with Pol II, demonstrating that they are actively transcribed, and also with Rpl7, Rpl11 and Rpl25 (De et al., 2011), making them potential candidates for co-transcriptional translation. Fold enrichment was calculated relative to an intergenic region as described above (Fig 3.7 A). There was no significant evidence of RPM at most of these loci (Fig 3.7), however a 7.7-fold enrichment ($p < 0.01$) was detected at the middle of the

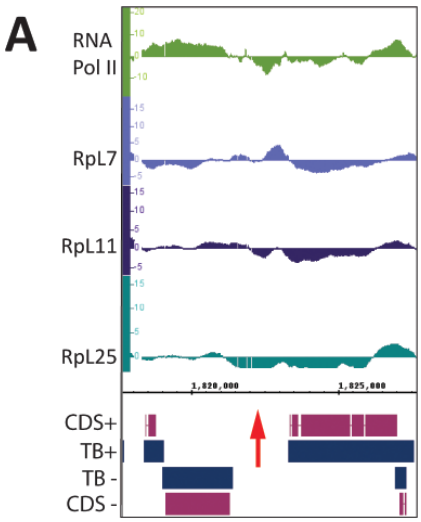
A
RNA Pol II
RpL7
RpL11
RpL25
CDS+
TB+
TB -
CDS -

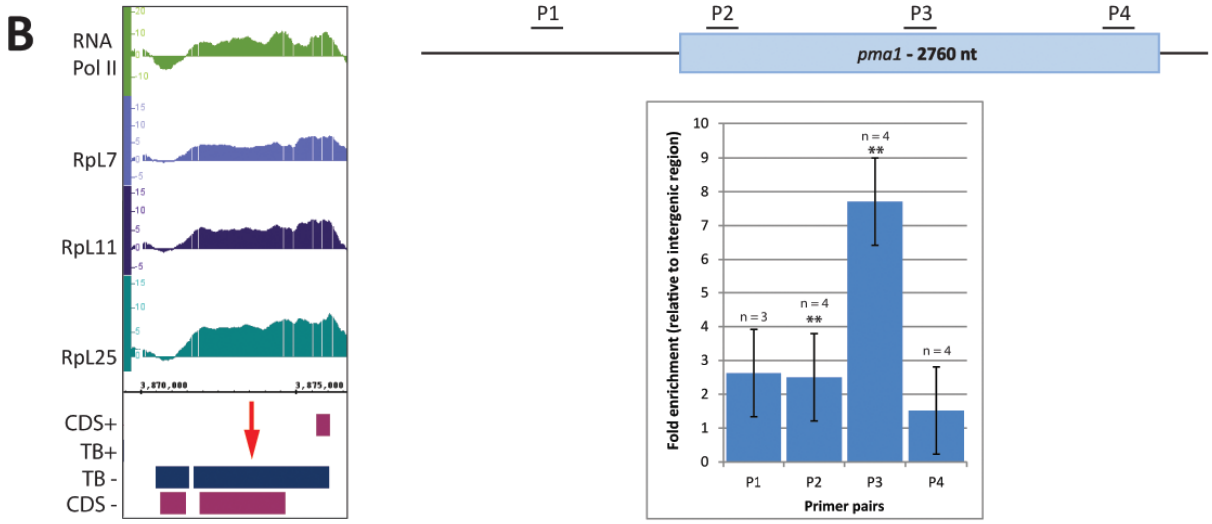
B
RNA Pol II
RpL7
RpL11
RpL25
CDS+
TB+
TB -
CDS -
P1
P2
P3
P4
pma1 - 2760 nt
Fold enrichment (relative to intergenic region)
n = 3
n = 4
**
n = 4
**
n = 4
Primer pairs

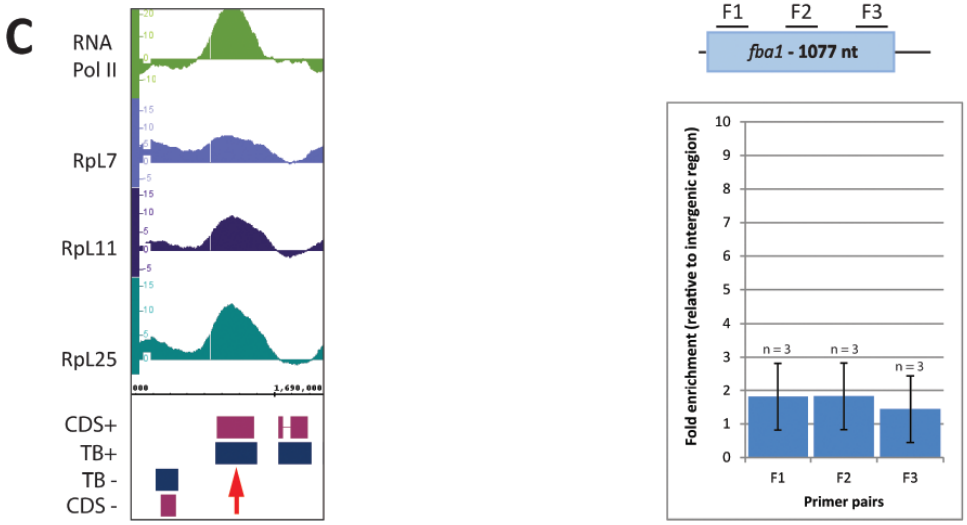
C
RNA Pol II
RpL7
RpL11
RpL25
CDS+
TB+
TB -
CDS -
F1
F2
F3
fba1 - 1077 nt
Fold enrichment (relative to intergenic region)
n = 3
n = 3
n = 3
Primer pairs

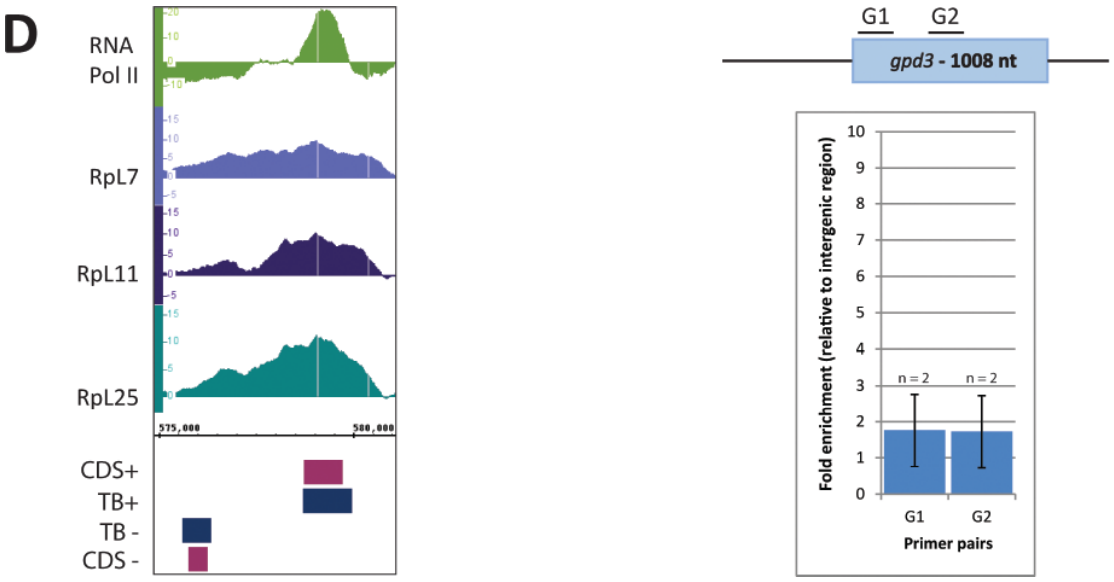

Figure 3.7 The enrichment of ribopuromycylated peptides at gene loci does not reflect the enrichment with ribosomal proteins. Enrichment profiles of Pol II, RpL7, RpL11 and RpL25 at several *S. pombe* loci, as determined by analysis of ChIP-chip data (De et al., 2011). Histograms in each panel show qRT-PCR analysis of enrichment of ribopuromycylated peptides at (A) an intergenic region (B) *pma1*, (C), *fba1* and (D) *gpd3* (see Appendix 4 for primer details). Wild-type cultures were treated with 200 µg/mL emetine for 30 minutes followed by 250 µg/mL puromycin for 15 minutes, and ChIP was then carried out with an anti-puromycin antibody (clone 5B12) using ChIP protocol I (Materials and Methods). Schematic of each gene shows the locations of primer pairs used at each locus. The fold enrichment of puromycylated peptides at different regions of each locus was calculated using the ΔΔct method (described in Materials and Methods) and expressed as relative to the intergenic region in (A) with error bars showing ± SD. The number of biological repeats for each primer pair is displayed on the above each bar on the histograms. Statistical significance was calculated for all values with 3 or more repeats and is denoted by asterisks where applicable (** = $p < 0.01$).

coding region of the *pma1* locus (Figure 3.7 B). To determine whether this enrichment is dependent upon an interaction via RNA, rather than the association of puromycylated peptides directly with the chromatin, ChIP was carried out again in ribopuromycylated wild-type cells along with a control RNase treated sample, which should reduce the enrichment if the hypothesis is correct. A modified version of the ChIP protocol that had been optimised by another member of the lab (Jianming Wang, PhD student) was used; this method was shown to aid RNase digestion without negatively affecting ChIP efficiency (ChIP protocol II in Materials and Methods). As with the original ChIP method, the middle of the coding region of the *pma1* locus was enriched with ribopuromycylated peptides (Fig 3.8), but this time to a much greater extent (44-fold ($p < 0.05$) compared to 7.7-fold ($p < 0.01$), compare Figure 3.8 with Figure 3.7 B)). This does not appear to be an artefact of the modified protocol itself as no greater enrichment was detected at the start of the CDS of *pma1*. RNase treatment resulted in a significant reduction in the enrichment detected at the middle of the CDS to 3.8-fold ($p < 0.01$) (Figure 3.8), suggesting that RPM followed by ChIP allows detection of peptides that are in association with the RNA, possibly the nascent transcript.

Despite these promising initial results, a number of other observations did not support the hypothesis that the presence of RPs at the chromosomes indicates that translating ribosomes are also present there. Firstly, although an enrichment of ribopuromycylated peptides was observed at the middle of the *pma1* coding region in this study, other regions of the *pma1* CDS were not significantly enriched (Figs 3.7 and 3.8). This is in contrast to the ChIP-chip study, which detected an enrichment of RPs across the whole of the *pma1* CDS, including at the promoter region (De et al., 2011). Additionally, the *fba1* and *gpd3* loci,

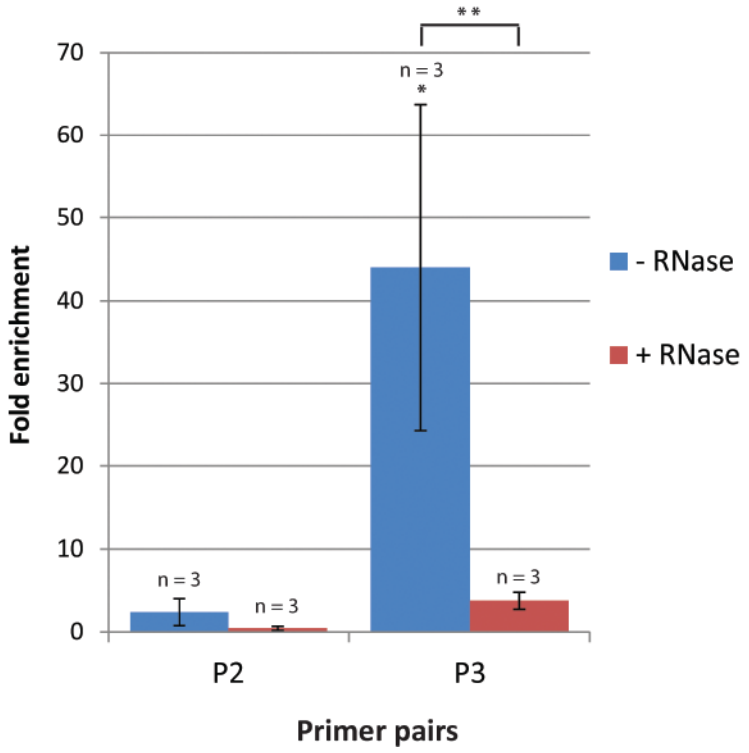

Figure 3.8 The enrichment of ribopuromycylated peptides at the *pma1* locus is RNA-dependent. qRT-PCR analysis of the *pma1* locus with and without RNase treatment, following ChIP using the modified protocol (Protocol II in Materials and Methods). RNase treatment was by incubating the eluted DNA with 1 µL 20 mg/mL RNase A for 1 hour at 37 ˚C. Fold enrichment was calculated as in Figure 3.7. Statistical significance of enrichment of puromycylated peptides relative to the intergenic region is shown (* = $p < 0.05$). Statistical significance of the change in fold enrichment following between no RNase and RNase treatment is also shown for the P3 region (** = $p < 0.01$).

which were reportedly enriched with all three RPs, showed no enrichment with ribopuromycylated peptides in this study (Fig 3.7). If the presence of RPs was due to the presence of functional ribosomes at these loci, then the enrichment of ribopuromycylated peptides would be expected to be similar; that this was not the case suggested that either the RPs were not part of a functional ribosome, or that RPM was not enabling detection of the ribosome. As well as these reproducible observations, a preliminary analysis of RPM at several other gene loci which were enriched with RPs in the previous ChIP-chip study also showed no enrichment in this study, although these were assessed only once and therefore no statistical significance can be derived from this data (Appendix 5 A). Several other loci did show an enrichment of ribopuromycylated peptides in a preliminary experiment, however anisomycin, which competes with puromycin for occupation of the A site of the ribosome, and therefore should deplete a genuine puromycin-mediated ChIP enrichment, failed to reduce the enrichment observed at these loci (Appendix 5 B). Although these latter observations were made in a small set of pilot experiments, the conclusion was that together they suggest that RPM may not work in *S. pombe* as reported in HeLa cells (David et al., 2012) and *Drosophil*a (Al-Jubran et al., 2013). Therefore the RPM technique should be carefully characterised to assess whether it can also be used to detect nascent peptides in yeast.

3.3 Discussion

The aim of the work in this chapter was to use RPM (David et al., 2012) to assess whether translation occurs at transcription sites in *S. pombe*. To implement this technique, the concentrations at which puromycin and other translation inhibitor drugs inhibit growth in *S. pombe* were firstly assessed. Although *S. pombe* cells possess features that confer resistance

to a number of drugs, this study has established the conditions under which emetine, cycloheximide and puromycin are taken up into the cell and are effective as inhibitors of translation.

The data presented in this chapter support previous reports that emetine is an irreversible translation elongation inhibitor, while cycloheximide inhibition of translation elongation is reversible (Grollman, 1968), since a degree of recovery is observed when cells are transferred to an environment without the drug.

These results are also consistent with puromycin incorporation into nascent peptides being via the ribosome since it is almost completely eliminated by anisomycin, which competes with puromycin for binding to the ribosomal A site (Ioannou et al., 1998). Although emetine was shown here to effectively inhibit translation in *S. pombe*, it showed no significant effect on the efficiency of puromycin incorporation. This is in agreement with older studies conducted in HeLa cells and *in vivo* mammalian translation extracts (Grollman, 1968, Baliga et al., 1970). However it contrasts with more recent works, such as the original RPM paper which claims that emetine enhances puromycin incorporation in HeLa cells (David et al., 2012), and a study in *Drosophila* which reported that puromycin incorporation is reduced following prior treatment with emetine (Al-Jubran et al., 2013). The reasons for these differences remain unclear but may be accounted for by differences in the systems and experimental conditions used in each study. A recent structural analysis of emetine bound to the 80S of the human malaria parasite, *Plasmodium falciparum*, reported that it binds the ribosomal E site on the small subunit and posits that this impedes mRNA/tRNA translocation (Wong et al., 2014). Since puromycin incorporation is dependent on ribosome movement (Grollman, 1968), it might be expected that inhibiting this would prevent puromycylation.

However the older studies conclude that emetine does not prevent translocation of tRNAs from A to P sites (Pestka, 1971), which may be sufficient to allow continued puromycin incorporation over the short incubation periods used in this study. Cycloheximide pretreatment on the other hand strongly reduced the level of puromycin incorporation in this study; this is in agreement with earlier studies which found that cycloheximide inhibits translocation of the ribosome, which is a requirement for puromycin incorporation (Baliga et al., 1970, McKeehan and Hardesty, 1969). However the recent study in which RPM was developed (David et al., 2012) reported that the level of puromycin incorporation is preserved in HeLa cells that have been pretreated with cycloheximide. Again, variations in experimental conditions and systems may account for the differences observed.

The conclusion from these findings is that emetine appears to be the preferable choice of drug to inhibit translation elongation in *S. pombe*, since it is irreversible, but most importantly, immobilises ribosomes without interfering with the incorporation of puromycin into nascent peptides.

This study also presents the results of chromatin immunoprecipitation experiments carried out to investigate whether nascent peptides associate with sites of transcription. The results were largely negative. Several gene loci which were previously reported to be enriched with RPs at these sites showed no evidence of RPM. Possible explanations are that i) the RPs have some other function at these loci ii) RPM-ChIP does not work to identify loci that are co-transcriptionally translated, for instance the anti-puromycin antibody is not effective in ChIP iii) co-transcriptional translation does not occur and therefore no enrichment will be observed following RPM-ChIP. Explanation ii) can be eliminated since a consistent enrichment was seen at the middle of the *pma1* CDS, therefore it appears that the antibody

does precipitate puromycin-associated targets. It may however be that the RPM conditions used in this study do not prevent the release of puromycylated peptide from the ribosomes. This could explain the enrichment seen at the *pma1* locus, since released puromycylated peptides could have diffused from translation sites to other regions of the cell, or may even have been transported into the nucleus where they could bind *pma1* or other genes either directly or indirectly, leading to spurious enrichment by ChIP. This is perhaps the most critical point to address before proceeding further with ChIP, therefore the next chapter presents the results of polysome profiling that was carried out to directly assess whether the translation elongation inhibitors used in RPM prevent the release of puromycylated peptides from immobilised ribosomes.

Chapter 4: Inhibition of translation elongation does not prevent release of nascent peptides upon puromycylation

4.1 Introduction

The ribopuromycylation (RPM) method reportedly allows detection of nascent peptides that are bound to immobilised ribosomes (David et al., 2012). The group that developed the technique demonstrated this by carrying out Western blotting of proteins that had been extracted from polysome fractions, showing the presence of puromycin labelled peptides in those fractions corresponding to translating polysomes, and not with the 80S (David et al., 2012). Polysomal fractionation separates mRNAs complexed with multiple translating ribosomes (polysomes) from individual ribosomes, ribosomal subunits or sub-ribosomal lighter fractions, by centrifugation of cell extracts through a sucrose gradient (Fig 4.1). This chapter presents the results of an in-depth investigation in *S. pombe*, as well as in *Drosophila* S2 cells, into the effects of the various translation elongation inhibitors used in RPM, on the stability of polysomes, puromycylation efficiency and on the association of puromycylated peptides with different polysomal fractions.

4.2 Results

4.2.1 Polysomes are stabilised by cycloheximide but not emetine treatment in *S. pombe.*

During optimisation of the polysome profiling procedure, an initial analysis of the association of puromycylated peptides with the polysomal fractions revealed that the vast majority of puromycylated peptides were present in the soluble fractions, indicating that

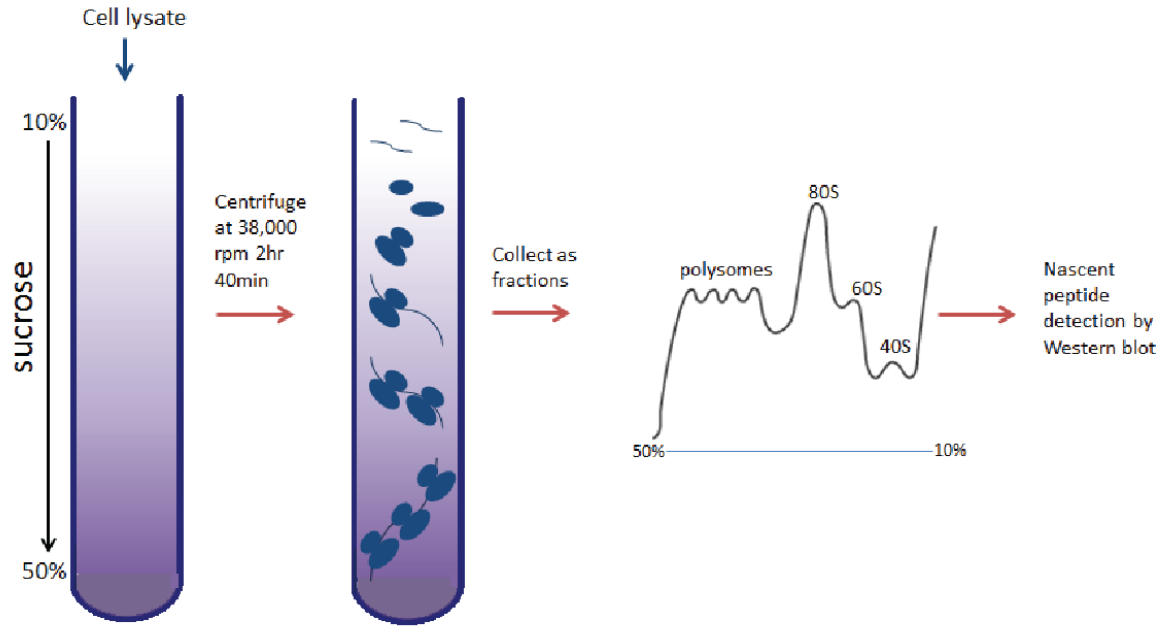

Figure 4.1 Schematic of the polysome profiling procedure. Cell lysates are loaded onto a sucrose gradient (purple column) and centrifuged at high speed to separate polysomes, which sediment through the gradient at faster rates, from lighter monosomes, individual ribosomal subunits and soluble RNAs, which are retained further up the gradient (left diagram). The gradient is collected through a capillary needle, inserted through the gradient to the bottom of the centrifuge tube, and pumped through a flow-cell UV recorder (OD_{254}), producing a profile of the relative RNA reading in different parts of the gradient (right diagram). Fractions, each correlating to a specific part of the gradient, are collected and analysed by Western blotting to assess the association of the protein of interest, in this case puromycylated peptides, with different regions of the gradient.

peptides had not been retained on the ribosome and were instead released (Appendix 6 (ii)). The RPM conditions for this initial experiment were those which were optimised as reported in Chapter 3 (pretreatment with 200 μg/mL emetine for 30 min to immobilise ribosomes followed by 250 μg/mL puromycin for 15 min to label nascent peptides). While this initial observation could indicate that puromycylated peptides are released from ribosomes under these conditions, analysis of the levels of ribosomal RNA (rRNA) in each fraction showed that 25S and 18S rRNA in the 80S/60/40S fraction (Appendix 6 (i) lanes 6-10) was observably greater that that present in polysomal fractions (Appendix 6 (i) lanes 1-5). This suggested that the release of puromycylated peptides may be an artefact of insufficient stabilisation of polysomes by emetine.

In light of this preliminary data, the ability of emetine to stabilise polysomes in *S. pombe* was subsequently assessed using different concentrations and incubation periods with the drug. Initial polysome profiling of cells treated with emetine for 15 minutes at concentrations of 350 and 20 μg/mL was carried out alongside that of cells that were untreated. Visual analysis of these initial polysome profiles suggested a higher proportion of 80S, 60S and 40S to polysomes in cells treated with both concentrations of emetine (Appendix 7 A (i) and (ii)) relative to untreated cells (Fig 4.2 (iii)), indicating that rather than having a stabilising effect, emetine in fact causes polysomes to break down. The incubation time with both of these concentrations of emetine was reduced to 5 minutes to determine whether this improved polysome stabilisation (Fig 4.2 (i) and (ii)). Statistical analysis of three independent biological repeats reveals no significant difference in the proportion of polysomes to 80S/60S/40S between cells treated with either of these concentrations of emetine for 5 minutes and untreated cells. A comparison of the mean

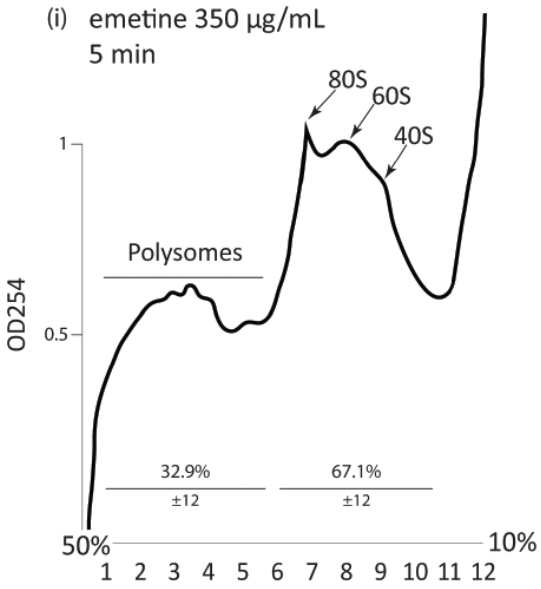
(i) emetine 350 µg/mL
5 min
80S
60S
40S
Polysomes
OD254
1
0.5
32.9%
±12
67.1%
±12
50%
10%
1 2 3 4 5 6 7 8 9 10 11 12

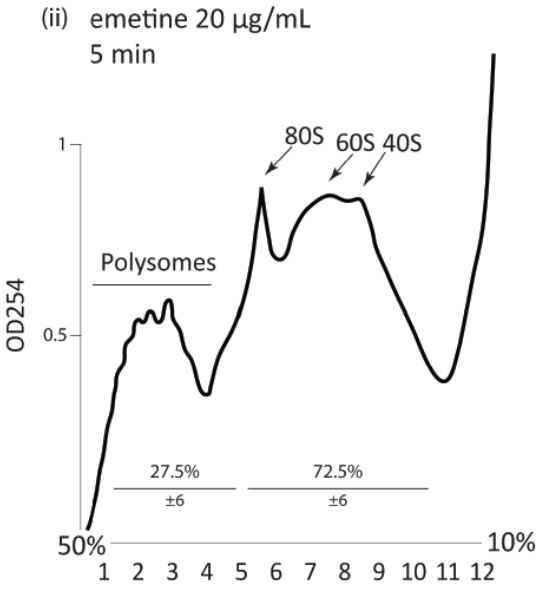
(ii) emetine 20 µg/mL
5 min
80S
60S
40S
Polysomes
OD254
1
0.5
27.5%
±6
72.5%
±6
50%
10%
1 2 3 4 5 6 7 8 9 10 11 12

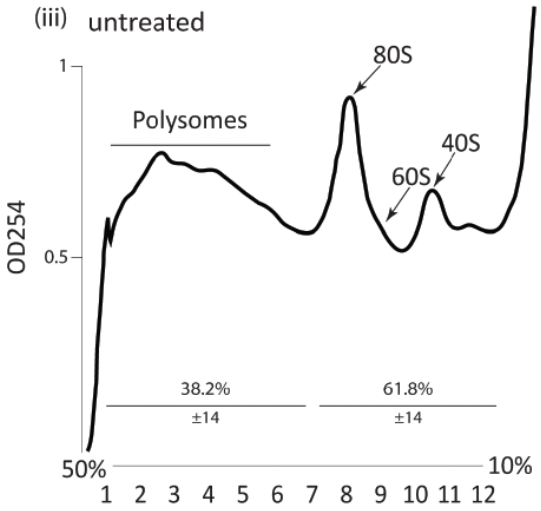
(iii) untreated
80S
Polysomes
40S
60S
OD254
1
0.5
38.2%
±14
61.8%
±14
50%
10%
1 2 3 4 5 6 7 8 9 10 11 12

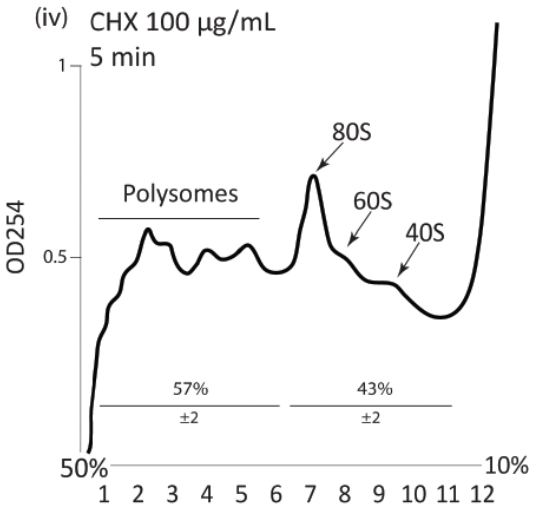
(iv) CHX 100 µg/mL
5 min
80S
Polysomes
60S
40S
OD254
1
0.5
57%
±2
43%
±2
50%
10%
1 2 3 4 5 6 7 8 9 10 11 12

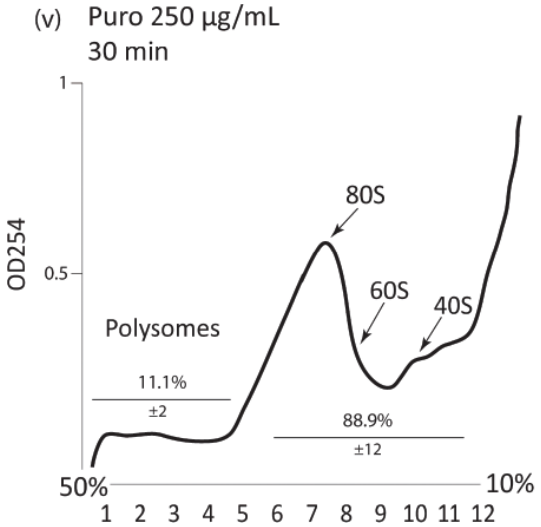
(v) Puro 250 µg/mL
30 min
80S
60S
40S
Polysomes
OD254
1
0.5
11.1%
±2
88.9%
±12
50%
10%
1 2 3 4 5 6 7 8 9 10 11 12

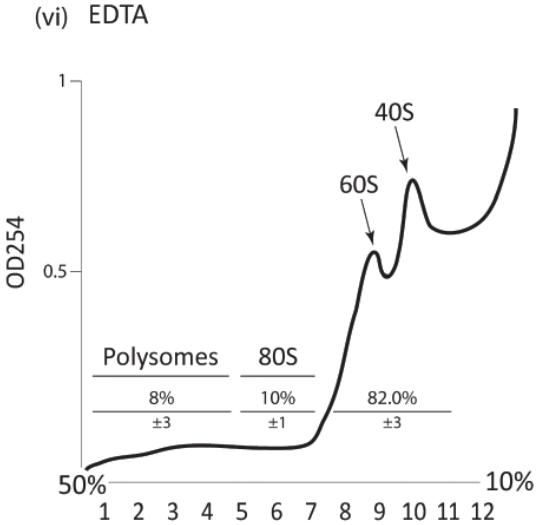
(vi) EDTA
40S
60S
Polysomes
80S
OD254
1
0.5
8%
±3
10%
±1
82.0%
±3
50%
10%
1 2 3 4 5 6 7 8 9 10 11 12

Figure 4.2 The effect of translation elongation inhibitors on polysome stabilisation in *S. pombe*. 50 mL cultures were treated with 350 µg/mL (i) or 20 µg/mL (ii) emetine or with 100 µg/mL cycloheximide (CHX) (iv) for 5 minutes and polysome profiling (Materials and Methods) was then carried out to assess the stabilisation of polysomes. Profiling of a control untreated culture was also carried out for comparison (iii). To determine that translating ribosomes were being detected, cleared lysates were treated with 250 µg/mL puromycin (v) or 30 mM EDTA (vi) to assess the dissociation of ribosomes. The horizontal axis on each plot shows the polysomal fraction number and the vertical axis is a relative measurement of the relative optical density (OD) at 254 nm reading. Areas under the curve were calculated for the polysomal and 80S/60S/40S regions using Image J software. The figures on each profile represent the mean area for each region, calculated from three biological repeats and expressed as a percentage of the total area ± SD. Statistical analyses discussed in the text were determined by carrying out a t-test to compare the means of three biological repeats for the described conditions.

values however shows that following treatment with emetine, more RNA is found on average in the 80S/60S/40S region (67.1% ± 12 when treated with 350 μg/mL emetine and 72.5% ± 6 when treated with 20 μg/mL) compared to that found in the 80S/60S/40S region of untreated cells (61.8% ± 14) (compare Fig 4.2 (i) and (ii) with (iii)). Emetine therefore appears to elicit a tendency towards polysome breakdown rather than stabilisation. This is in contrast to previous studies which have shown that emetine stabilises eukaryotic polysomes (Grollman, 1968). Cycloheximide at a concentration of 100 μg/mL on the other hand, although also not leading to a statistically significant difference between the proportion of polysomes to 80S/60S/40S when compared with untreated cells, causes a trend in the opposite direction to that of emetine, with more of the RNA being detected in the polysomal region (57% ± 2) than in the 80S/60S/40S (43% ± 2) (Fig 4.2 compare (iv) with (iii)). The difference between cycloheximide and emetine treatment on the proportion of polysomes to 80S/60S/40S (compare Fig 4.2 (i) with (iv)) is however significant ($p < 0.05$). This is in agreement with early studies which reported the stabilisation of eukaryotic polysomes following cycloheximide treatment (Grollman, 1968). The polysome profiling method used in this study is reporting translating ribosomes and not non-ribosomal RNA/protein complexes as treatment of lysates with puromycin (Fig 4.2 (v)) or EDTA (Fig 4.2 (vi)), which both lead to the dissociation of ribosomal subunits from mRNAs (Morozov et al., 2012, Blobel and Sabatini, 1971, Calzone et al., 1982), causes the loss of polysomes, with the vast majority of RNA instead being present in the 80S/60S/40S region (88.9% ± 12 for puromycin treatment and 82.0% ± 3 for EDTA treatment ($p < 0.001$ for both compared to cycloheximide treated cells)).

4.2.2 Peptides are released from immobilised *S. pombe* ribosomes immediately upon puromycylation

The previous results indicate that emetine does not stabilise polysomes in *S. pombe* and this may therefore explain why puromycylated peptides were observed in the soluble fractions in the preliminary analysis (Appendix 6). It could also be that the 15 minute incubation period with puromycin is too long, therefore shorter incubation periods with the drug were investigated to determine whether this abrogates the release of puromycylated peptides following both cycloheximide and emetine pretreatment (Fig 4.3). An initial analysis of cycloheximide pretreated cells which were subsequently treated with puromycin for two minutes before carrying out polysome profiling, showed that even this greatly reduced incubation period led to the majority of puromycylated peptides being detected in the soluble fractions (Appendix 7 A (iii)). All subsequent investigations were therefore carried out with puromycin treatments of only 30 seconds. Statistical analysis showed no significant difference in the proportion of polysomes to 80S/60S/40S between cells that had been treated with cycloheximide and those treated with cycloheximide + puromycin (Fig 4.3 (i)) compared with Fig 4.2 (iv)), therefore puromycin treatment does not cause the breakdown of polysomes following immobilisation of ribosomes with cycloheximide. The majority (68.4% ± 11) of puromycylated peptides are found in the soluble fractions that correspond to released proteins (Fig 4.3 (i) lower panel). This indicates that the immobilisation of ribosomes does not preclude the release of puromycylated peptides upon subsequent puromycin treatment, which is in contrast to the conclusions of the paper which reported the development of RPM (David et al., 2012). There is also no significant difference in the

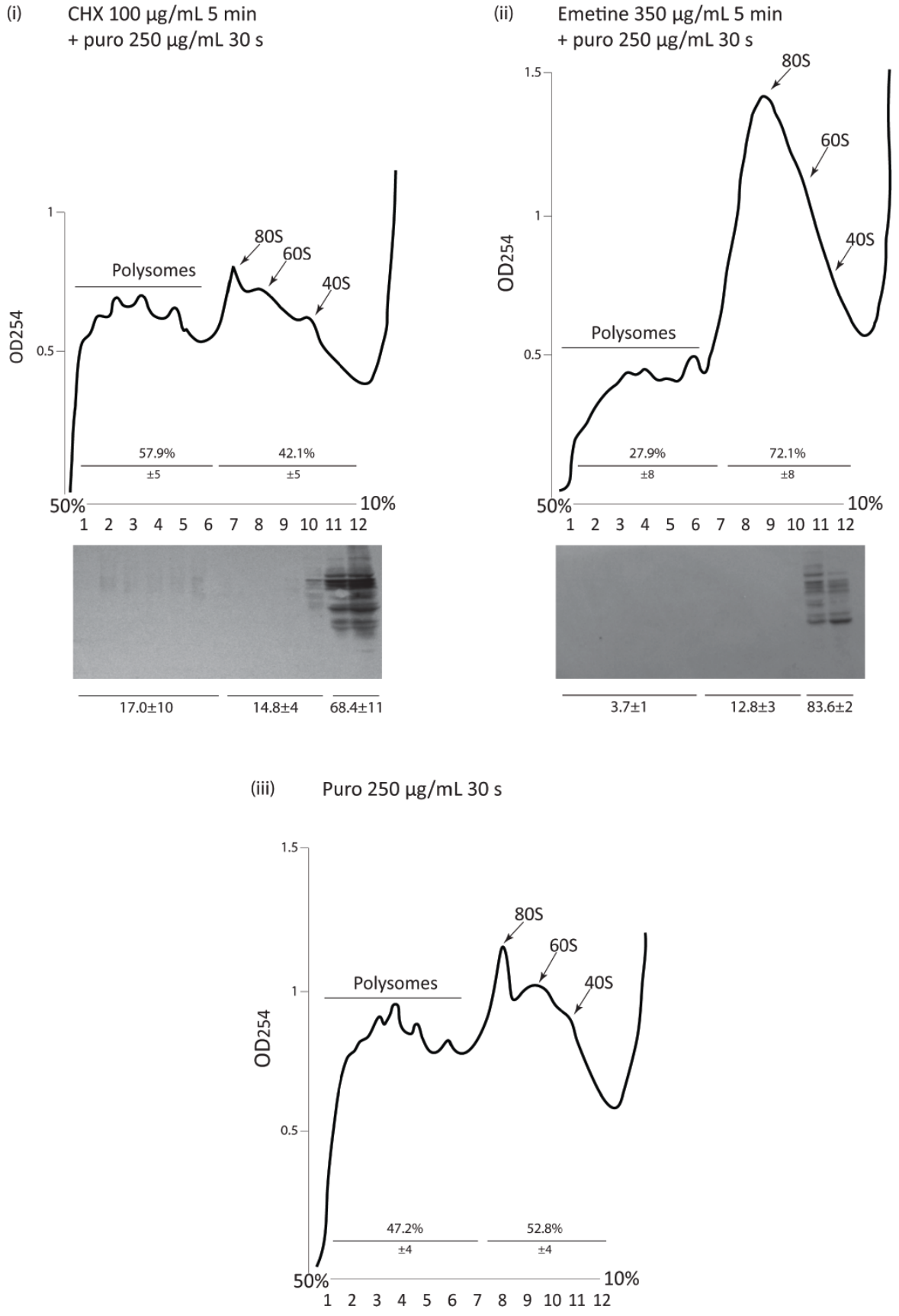
(i)
CHX 100 µg/mL 5 min
+ puro 250 µg/mL 30 s
OD254
1
0.5
Polysomes
80S
60S
40S
57.9%
±5
42.1%
±5
50%
10%
1 2 3 4 5 6 7 8 9 10 11 12
17.0±10
14.8±4
68.4±11
(ii)
Emetine 350 µg/mL 5 min
+ puro 250 µg/mL 30 s
OD254
1.5
1
0.5
80S
60S
40S
Polysomes
27.9%
±8
72.1%
±8
50%
10%
1 2 3 4 5 6 7 8 9 10 11 12
3.7±1
12.8±3
83.6±2
(iii)
Puro 250 µg/mL 30 s
OD254
1.5
1
0.5
80S
60S
40S
Polysomes
47.2%
±4
52.8%
±4
50%
10%
1 2 3 4 5 6 7 8 9 10 11 12

Figure 4.3 Puromycylated peptides are released regardless of whether ribosomes are immobilised on mRNAs. *S. pombe* cell cultures were treated with 100 µg/mL cycloheximide (i) or 350 µg/mL emetine (ii) for 5 minutes, followed by 250 µg/mL puromycin for 30s. Polysome profiling was carried out and the association of puromycylated peptides with polysomes was analysed by Western blotting of protein extracts from polysomal fractions in (i) and (ii) lower panels. A separate culture was treated with 250 µg/mL puromycin only for 30 s (iii). Detection of puromycylated peptides was performed by probing the nitrocellulose membrane with a mouse anti-puromycin antibody (clone 5B12, see Material and Methods). Statistical analysis of the profiles was carried out as in Fig 4.2. Statistical analysis of the proportion of puromycin signal detected in the polysomal, 80S/60S/40S and soluble fractions was also carried out and is expressed below each Western blot as a percentage of the total puromycin signal ± SD from three independent biological repeats.

proportion of polysomes to 80S/60S/40S between cells that had/had not been pretreated with cycloheximide before puromycin treatment (Fig 4.3 (i) and (iii)), further indicating that it is not the destabilisation of ribosomes by puromycin that causes peptides to be released.

Analysis of the effect of emetine pretreatment followed by a 30 second puromycin treatment (Fig 4.3 (ii)) corroborated the preliminary results (Appendix 6) since the majority 83.6% ± 2) of puromycylated peptides were detected in the soluble fractions (Fig 4.3 (ii) lower panel). This is unsurprising in light of the finding that emetine does not stabilise *S. pombe* polysomes (Fig 4.2 (i) and (ii)). Although a comparison of the mean values of three biological repeats indicates that a greater proportion of puromycylated peptides are released following emetine pretreatment than for cycloheximide pretreatment, and a corresponding greater proportion of puromycylated peptides are apparent in the polysomal fractions of cycloheximide treated cells (compare Fig 4.3 (i) and (ii)), statistical analysis shows that this difference is not significant. These results indicate that neither emetine nor cycloheximide pretreatment allows the retention of puromycylated peptides on ribosomes in *S. pombe*, therefore ChIP analysis following RPM will not provide any insight into whether translating ribosomes are present at the chromosomes in this organism.

4.2.3 Puromycylated peptides are also released from immobilised ribosomes in *Drosophila* S2 cells

To determine whether the findings in *S. pombe* are specific to fission yeast, or are a more general phenomenon, analysis of RPM was carried out in *Drosophila* S2 cells. Cells were untreated or treated with emetine or cycloheximide, both with and without subsequent puromycin treatment. A comparison between untreated cells and cells treated with 100

A

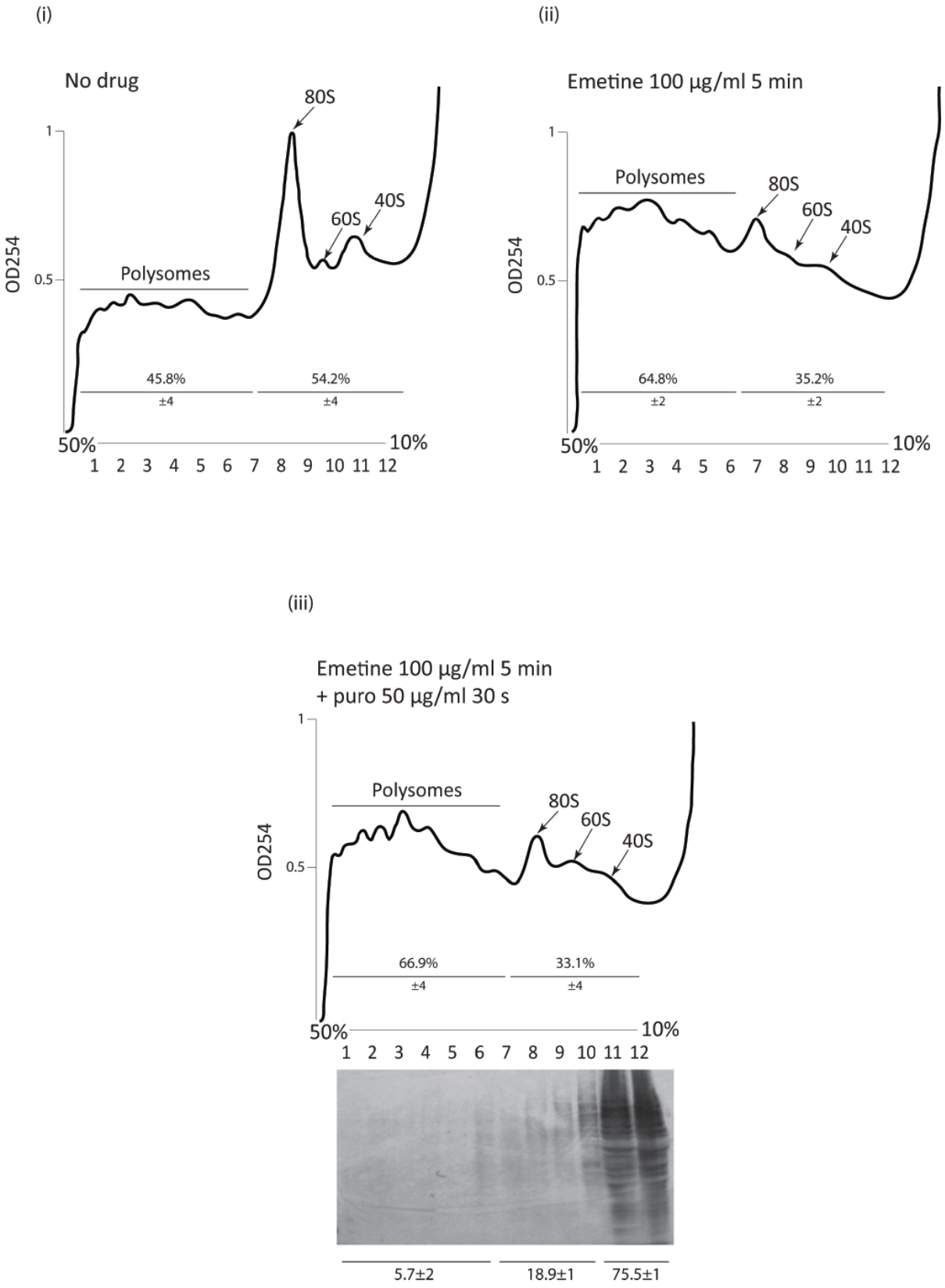
(i)
No drug
80S
60S
40S
Polysomes
OD254
1
0.5
45.8%
±4
54.2%
±4
50%
10%
1 2 3 4 5 6 7 8 9 10 11 12
(ii)
Emetine 100 µg/ml 5 min
Polysomes
80S
60S
40S
OD254
1
0.5
64.8%
±2
35.2%
±2
50%
10%
1 2 3 4 5 6 7 8 9 10 11 12
(iii)
Emetine 100 µg/ml 5 min
+ puro 50 µg/ml 30 s
Polysomes
80S
60S
40S
OD254
1
0.5
66.9%
±4
33.1%
±4
50%
10%
1 2 3 4 5 6 7 8 9 10 11 12
5.7±2
18.9±1
75.5±1

B

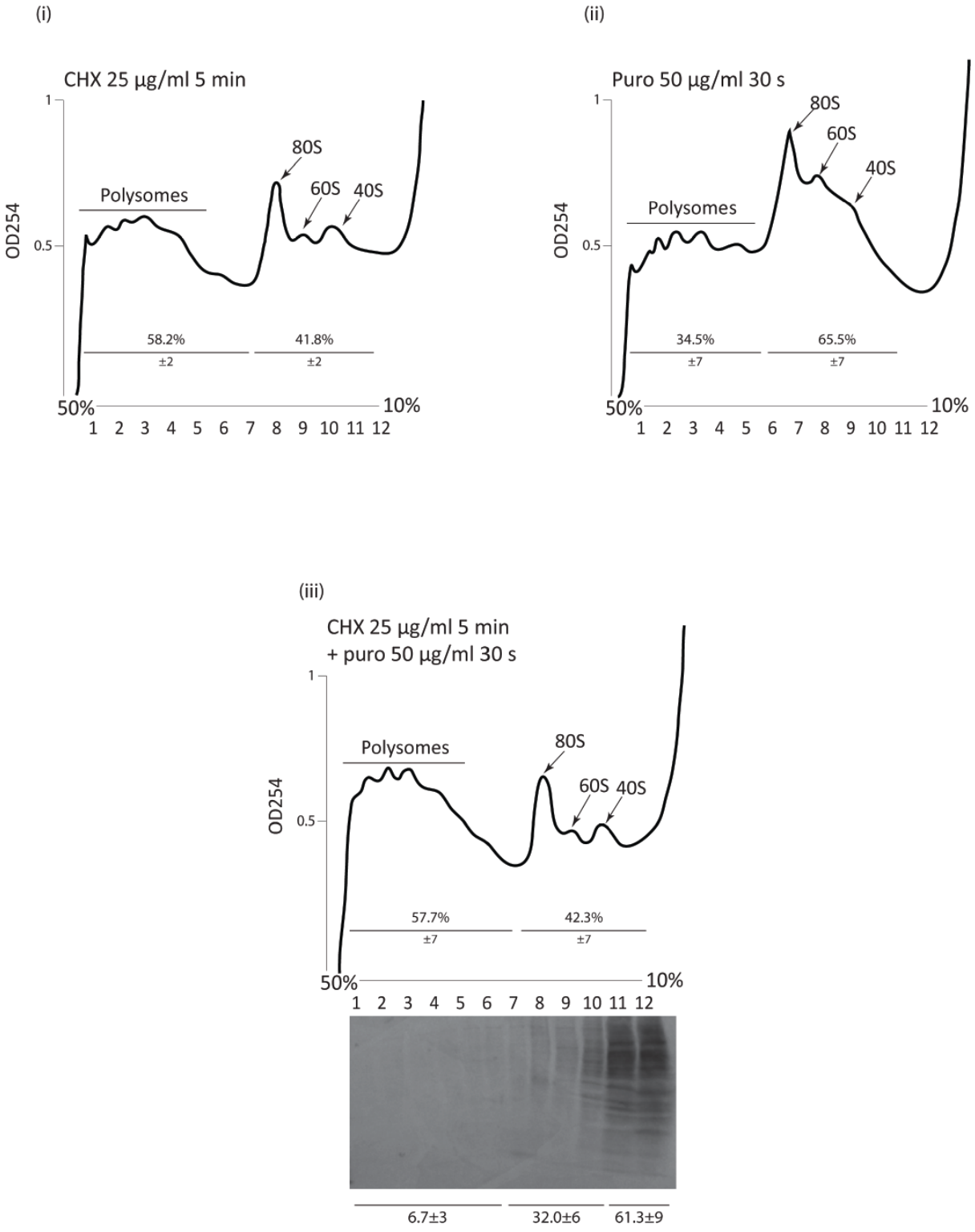
(i)
CHX 25 µg/ml 5 min
OD254
1
0.5
Polysomes
80S
60S
40S
58.2%
±2
41.8%
±2
50%
10%
1 2 3 4 5 6 7 8 9 10 11 12
(ii)
Puro 50 µg/ml 30 s
OD254
1
0.5
Polysomes
80S
60S
40S
34.5%
±7
65.5%
±7
50%
10%
1 2 3 4 5 6 7 8 9 10 11 12
(iii)
CHX 25 µg/ml 5 min
+ puro 50 µg/ml 30 s
OD254
1
0.5
Polysomes
80S
60S
40S
57.7%
±7
42.3%
±7
50%
10%
1 2 3 4 5 6 7 8 9 10 11 12
6.7±3
32.0±6
61.3±9

Figure 4.4 Emetine and cycloheximide stabilise polysomes in S2 cells but puromycylated peptides are still released. (A) Polysome profiles of S2 cells without drug treatment (i), treated with 100 μg/mL emetine for 5 minutes (ii) and with 100 μg/mL emetine for 5 minutes followed by 50 μg/mL puromycin for 30 s (iii). Western blotting of puromycylated peptides from protein extracts of the fractions collected in (iii) is also shown. (B) Polysome profiles of S2 cells treated with 25 μg/mL cycloheximide for 5 minutes (i), with 50 μg/mL puromycin for 30 s (ii) and with 25 μg/mL cycloheximide for 5 minutes followed by 50 μg/mL puromycin for 30 s (iii). Western blotting of puromycylated peptides from protein extracts of the fractions collected in (iii) is also shown. Puromycylated peptides were detected as in Figure 4.3. Statistical analysis was carried out on polysome profiles and Western blots as in Figures 4.2 and 4.3.

µg/mL emetine reveals that in contrast to that observed in *S. pombe*, emetine does stabilise polysomes (Fig 4.4 A compare (i) to (ii)); in untreated cells, the polysomal region represents 45.8% ± 4 of the total profile, and the 80S/60S/40S region represents 54.2% ± 4, whereas emetine causes the polysomal region to significantly increase to 64.8% ± 2 and the 80S/60S/40S region to reduce to 35.2% ± 2 of the total profile ($p < 0.01$). This effect of emetine is in agreement with its known function as a translation elongation inhibitor (Grollman, 1968). Treatment with puromycin following emetine pretreatment does not significantly affect this stabilisation of polysomes (Fig 4.4 A (iii)). Analysis of the association of puromycylated peptides with the polysomal fractions shows that, as in *S. pombe*, the majority (75.5% ± 1) of puromycylated peptides are in the soluble fractions (Fig 4.4 A (iii) lower panel), with 18.9% ± 1 in the 80S/60S/40S region and only 5.7% ± 2 in association with polysomes. Therefore, although emetine does stabilise polysomes in S2 cells, this does not facilitate the retention of peptides on ribosomes upon subsequent puromycin treatment. This is in contrast to that reported in the RPM study (David et al., 2012).

Cycloheximide also significantly ($p < 0.01$) stabilised S2 polysomes compared to control untreated cells (Fig 4.4 B (i) compared with Fig 4.4 A (i)), with 58.2% ± 2 of the profile represented in the polysomal region and 41.8% ± in the 80S/60S/40S region, again in agreement with earlier studies that show it to be an effective translation elongation inhibitor (Grollman, 1968). As with puromycin treatment following stabilisation of polysomes with emetine, treatment with puromycin following cycloheximide pretreatment does not disrupt polysomes (Fig 4.4 B (i) compared with (iii)) and the majority (61.3% ± 9) of puromycylated peptides are found in the soluble fractions corresponding to released peptides (Fig 4.4 B (iii) lower panel). The difference between the level of release of

puromycylated peptides between emetine (75.5% ± 1) and cycloheximide (61.3% ± 9) is significant ($p < 0.05$). Cycloheximide therefore appears to more effective than emetine at abrogating the release of nascent peptides upon puromycin treatment, although since the majority of peptides are still released, it is unsuitable for both the visualisation of nascent peptides and to use in conjunction with ChIP to investigate the potential that nascent transcripts are cotranscriptionally translated.

4.3 Discussion

This chapter presents the results of an in-depth analysis of the effect of translation elongation inhibitors on polysomes in fission yeast and *Drosophila* S2 cells, as well as an assessment of how these drugs affect puromycylation and the release of the nascent peptide from the ribosome. Emetine is reported to inhibit translation elongation across eukaryotes by entering the E site of the ribosome and, by a poorly-understood mechanism, preventing the translocation of the ribosome, instead immobilising it on the mRNA (Grollman, 1968, Wong et al., 2014). The results of polysome profiling of *S. pombe* cells that have been treated with emetine suggest that this function of emetine is not universal across eukaryotes, as polysomes are not stabilised by emetine treatment in comparison to *S. pombe* cells that are untreated. Emetine does however stabilise polysomes in S2 cells. Cycloheximide on the other hand stabilises polysomes in both *S. pombe* and S2 cells. The effect of puromycin on ribosome stability in *S. pombe*, and *Drosophila* revealed that a short exposure to the drug at the concentrations used in this study does not significantly affect the stability of polysomes that have been immobilised by pretreatment with emetine or cycloheximide in both organisms. However, Western blotting of proteins extracted from polysome fractions revealed that pretreating *S. pombe* and S2 cells with cycloheximide or

emetine before treating with puromycin does not abrogate the release of the majority of puromycylated peptides from ribosomes in either organism as the majority are found in the soluble fractions and only a small percentage in the fractions corresponding to translating ribosomes. The group that developed RPM claimed that pretreatment with translation elongation inhibitor drugs immobilises polysomes and that they are not destabilised upon subsequent puromycin treatment (David et al., 2012). This has indeed been reported previously in cell-free mammalian translation extracts; emetine was shown to stabilise polysomes and subsequent puromycin treatment did not lead to polysome breakdown (Baliga et al., 1970). However, the same study reported that pretreatment with cycloheximide failed to stabilise polysomes as well as emetine, and inhibited puromycin incorporation into peptides.

These results show that puromycylated peptides are released from immobilised ribosomes even when puromycin treatment is as brief as 30s. It therefore appears that peptide released is concomitant with puromycylation, regardless of ribosome dissociation. This effect was reproducibly observed in both *S. pombe* and S2 cells, and was also seen in a preliminary study of HeLa cells (Appendix 7 B). Therefore it cannot be ruled out that the nuclear RPM signal detected in the original study (David et al., 2012) reflects the presence of proteins that were synthesised in the cytoplasm and have subsequently either diffused or been transported to other cellular sites. It therefore appears that sites of protein synthesis may not be detected with this technique.

Chapter 5: Utilisation of immunofluorescence to detect sites of protein synthesis in *Schizosaccharomyces pombe*

5.1 Introduction

Although the polysome analysis strongly suggests that puromycylated peptides are released from ribosomes (Chapter 4), there is evidence that newly synthesised peptides remain in the vicinity of the ribosome, making contacts with the S1, S2, S4, and possibly S3, RPs on the 30S subunit, which are located around the mRNA-decoding region of the ribosome (Choi and Brimacombe, 1998). The contacts made between the nascent peptide and the mRNA are thought to regulate the level of translation. This, together with observations made during some preliminary immunofluorescence analyses following ribopuromycylation (RPM) (described below), suggested that even if not strictly detecting nascent peptides tethered to ribosomes, the technique may still report on the location of newly synthesised peptides, which perhaps transiently concentrate in the sub-cellular region where they were made. This chapter describes work that has been started to investigate this possibility, as well as other methods that are being developed to investigate the sub-cellular localisation of ribosomes.

5.2 Results

5.2.1 Optimisation of immunofluorescence in *S. pombe*

Before the results of the polysome analysis which indicated that puromycylated peptides are released from the ribosome, immunofluorescence of ribopuromycylated *S. pombe* cells had been conducted, as in the original study in human cells (David et al., 2012). To

successfully identify the locations of target proteins in immunostaining, cells must first be fixed to preserve the native distribution of proteins across the cell, and then permeabilised to allow the antibody to access target proteins. The fixation reagents most commonly used are methanol and formaldehyde, both of which can affect the ability of subsequent immunolabelling to report the true nature of protein localisation *in vivo* (Schnell et al., 2012, Pollice et al., 1992, Hirata and Okamoto, 1987). Methanol both fixes and permeabilises cells, but in the process cytoplasmic, and some nuclear, proteins may be extracted from cells. Formaldehyde fixation preserves cellular structure well by comparison, although electron microscopy has shown that it can cause changes to, or loss of, organelles (Schnell et al., 2012). Additionally, cells need to be permeabilised following formaldehyde fixation to allow the penetration of antibodies. This can be achieved through the use of detergents, such as Triton X-100, to ensure permeabilisation of all cellular compartments, including the nucleus. Sequential permeabilisation with methanol is also used, with the prior formaldehyde fixation mitigating the extraction of proteins. Flow cytometry assays have confirmed this method to preserve the cellular content of proteins, although it cannot account for their localisation (Pollice et al., 1992, Hirata and Okamoto, 1987). Comparisons between live cells expressing GFP-labelled proteins and fixed cells immunolabelled with anti-GFP have demonstrated that formaldehyde fixation does not always allow immunodetection of the proteins at sites where the GFP signal is present, even when subsequent permeabilisation is carried out (Schnell et al., 2012). This can be explained by the high degree of cross-linking leading to obstruction of the antibody binding site.

Previous observations in the Brogna lab indicated that under standard conditions, immunostaining might not reveal all of the locations where a protein might be abundant (Al-

Jubran et al., 2013, Rugjee et al., 2013). This was particularly frequent with GFP-tagged ribosomal proteins, which are clearly abundant in the nucleus from the GFP signal, yet standard immunostaining typically shows a mostly cytoplasmic signal (Al-Jubran et al., 2013, Rugjee et al., 2013). The fixation and permeabilisation conditions were therefore optimised at the start of this work. To do this, immunofluorescence in the Rpl11-3HA strain (TLM097, Appendix 2) that had previously been used in the lab to study the association of RPs with gene loci via ChIP-chip (De et al., 2011), was used. The effects of methanol and formaldehyde fixation for 5, 15 and 30 minutes, with and without permeabilisation by 0.3% Triton-X100 were compared (see Materials and Methods for full protocol). A signal should be apparent where ribosomes are found, throughout the cytoplasm, but also, since ribosomal proteins assemble with ribosomal RNA in the nucleolus, an accumulation should be observed in this compartment. Cells were counterstained with E36 (see Material and Methods), an RNA selective dye which should stain ribosomal RNA and thus show a similar distribution to Rpl11, and also with DAPI, which defines the region of the nucleus containing the DNA.

Visual inspection of the fluorescent signal produced from cells fixed with formaldehyde or methanol for different lengths of time showed that formaldehyde fixation generally produces a weaker signal from Rpl11-3HA than methanol fixation (Figure 5.1 B) although permeabilisation with Triton X-100 did improve this following 30 minutes fixation (compare Figure 5.1 B with 5.1 C). The signal from both Rpl11-3HA and RNA was diffuse across the cell under methanol fixation, but in cells fixed with formaldehyde, the nuclei generally appeared darker; this was somewhat improved following permeabilisation. However, none of the conditions revealed an accumulation of either Rpl11 or RNA in the nucleolus. While the

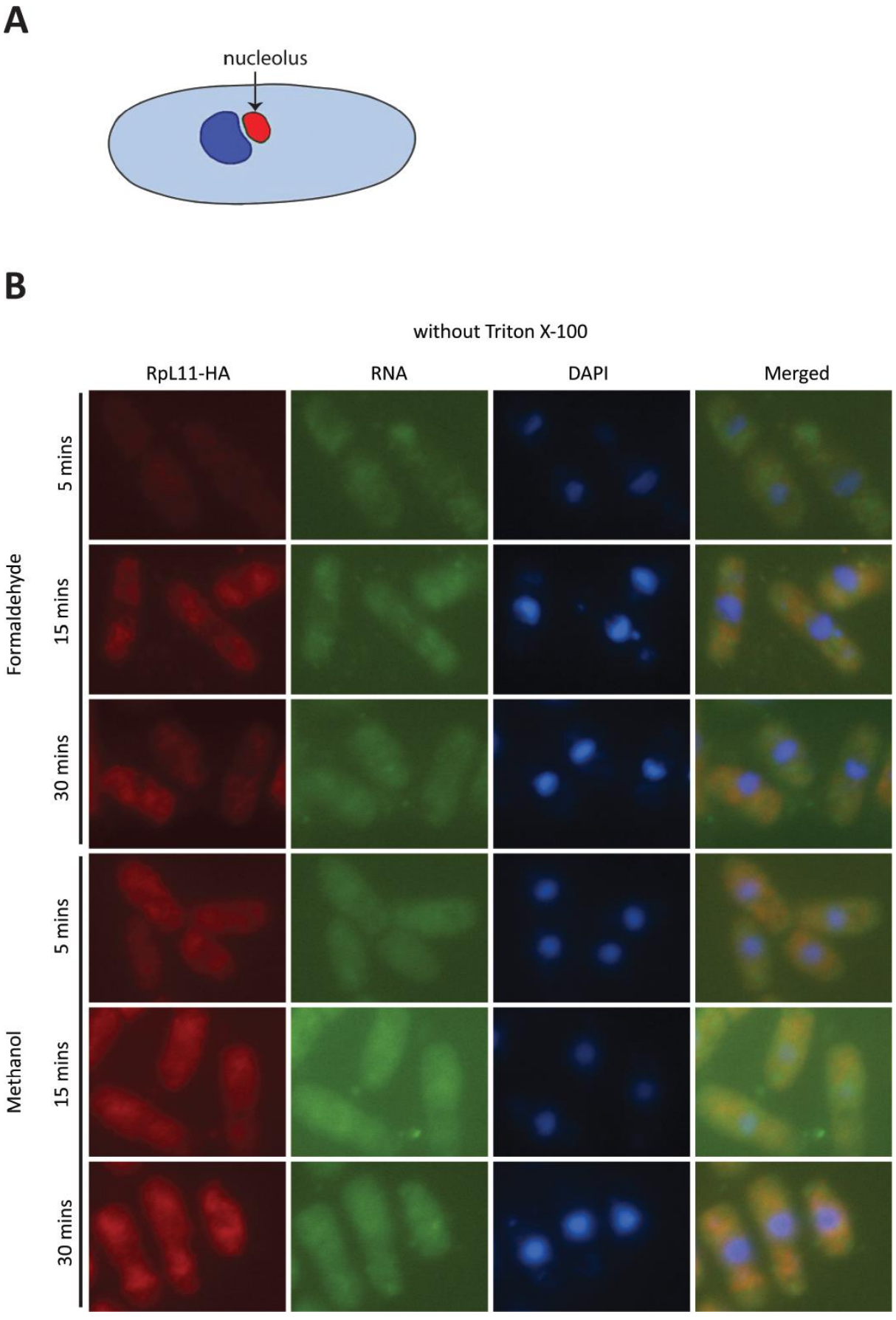
A
nucleolus
B
without Triton X-100
RpL11-HA
RNA
DAPI
Merged
Formaldehyde
Methanol
5 mins
15 mins
30 mins
5 mins
15 mins
30 mins

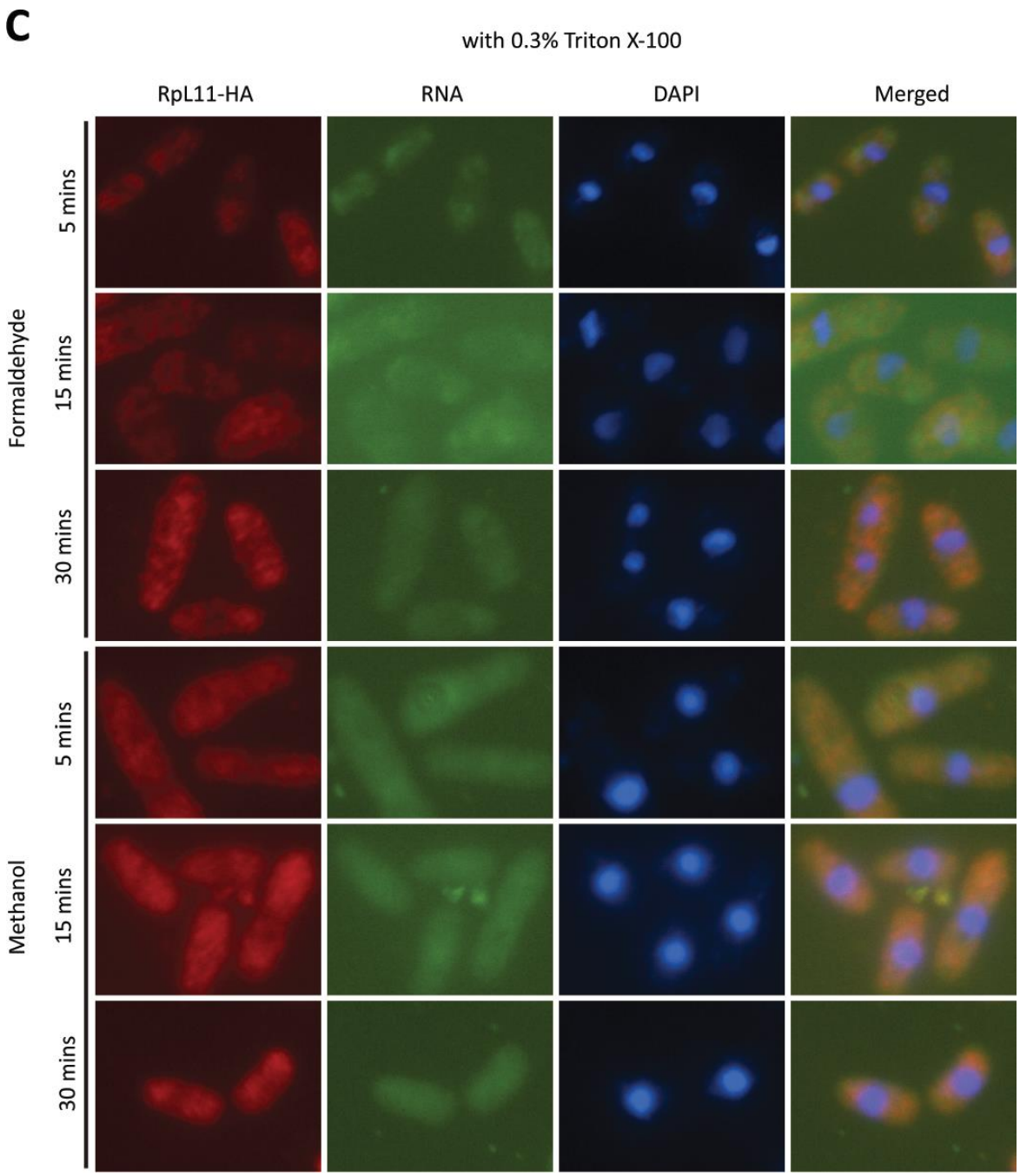
C
with 0.3% Triton X-100
RpL11-HA
RNA
DAPI
Merged
Formaldehyde
Methanol
5 mins
15 mins
30 mins
5 mins
15 mins
30 mins

Figure 5.1 Comparison of formaldeyhde and methanol fixation methods, with and without permeabilisation, on subsequent immunofluorescence. (A) Schematic of *S. pombe* cell, showing the nucleolus in red, adjacent to the characteristically crescent-shaped DAPI stained region of the nucleus containing the DNA in blue. (B and C) Immunofluorescence images of RpL11-3HA. Cells were fixed with either formaldehyde or methanol for 5, 15 or 30 minutes, both with (B) and without (C) subsequent permeabilisation with Triton X-100. Permeabilisation was carried out as in the immunofluorescence protocol in Materials and Methods. Cells were counterstained with RNA specific dye, E36 (green) and DAPI (blue). Detection of HA-tagged RpL11 was with a 12CA5 mouse anti-HA primary antibody (CRUK) and an anti-mouse Cy3-conjugated secondary antibody. Data represents one experimental run.

crescent shaped DAPI staining of cells fixed with formaldehyde is apparent (top three rows in Figure 5.1 B and C), that of methanol fixed cells is fuzzy and the boundary with the nucleolus is difficult to define (see bottom three rows in Figure 5.1 B and C). Since recent works have concluded that the nucleolus in particular is a site of potential nuclear translation, it is important that this sub-cellular location is apparent in fluorescent imaging. Methanol fixation is therefore unsuitable for these purposes, and formaldehyde fixation for 30 minutes, followed by permeabilisation with 0.3% Triton X-100 is the better option to allow clear visualisation of the DAPI/nucleolar boundary.

The absence of an accumulation of both RNA and ribosomal protein Rpl11 in the nucleoli of *S. pombe* cells using this method, indicated that the permeabilisation of the nucleus might be insufficient, since RPs are expected to accumulate particularly in the nucleolus, as this is where ribosome biosynthesis takes place. The method was further tested using a strain transformed with a pREP41 plasmid expressing green fluorescent protein (GFP) (Wen, 2009) into which the coding sequence (CDS) of *upf3* was cloned immediately downstream of the start codon in the GFP CDS (TLM011, Appendix 2), thus expressing Upf3 tagged at the C-terminus with GFP (Figure 5.2 A). Overexpression of fluorescently tagged Upf3 had been previously shown to lead to localisation of the protein in the *S. pombe* nucleolus (Matsuyama et al., 2006). The work carried out on the strain constructed in this study shows a similar pattern; Upf3-GFP is mostly apparent as an intense signal within the nucleolus (Figure 5.2 B). Immunofluorescence in this strain, using an anti-GFP primary antibody, following formaldehyde fixation for 30 minutes, with subsequent permeabilisation, showed a 100% ($p < 0.001$) overlap between the GFP and anti-GFP signals (Figure 5.2 C), therefore

A

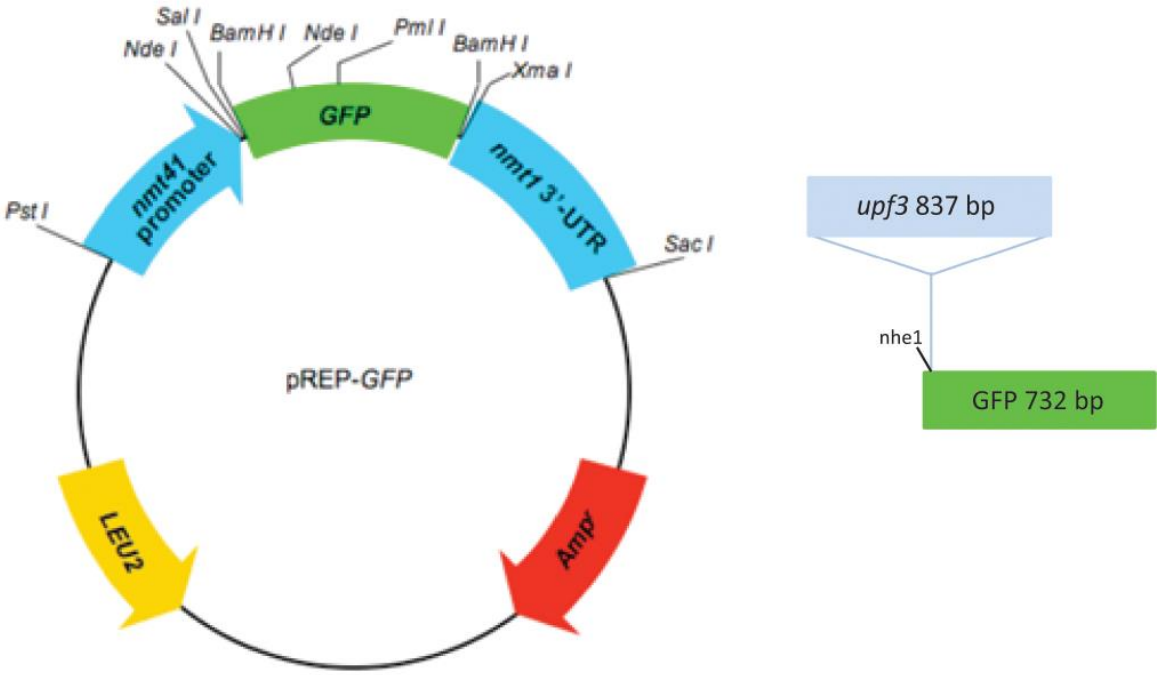
Sal I
Nde I
BamH I
Nde I
Pml I
BamH I
Xma I
GFP
nmt41 promoter
nmt1 3'-UTR
Pst I
Sac I
pREP-GFP
LEU2
Amp
upf3 837 bp
nhe1
GFP 732 bp

B

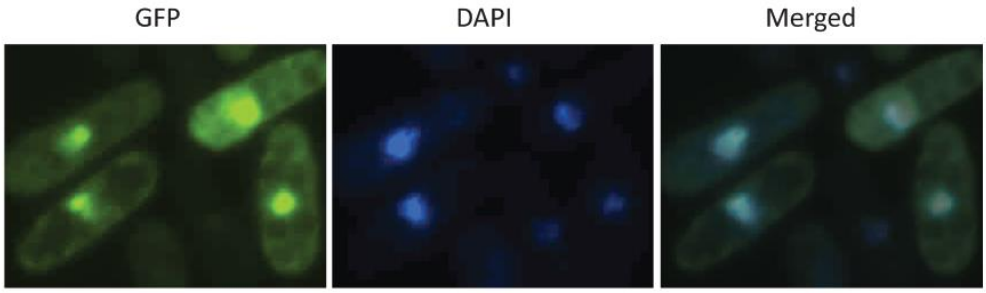
GFP
DAPI
Merged

C

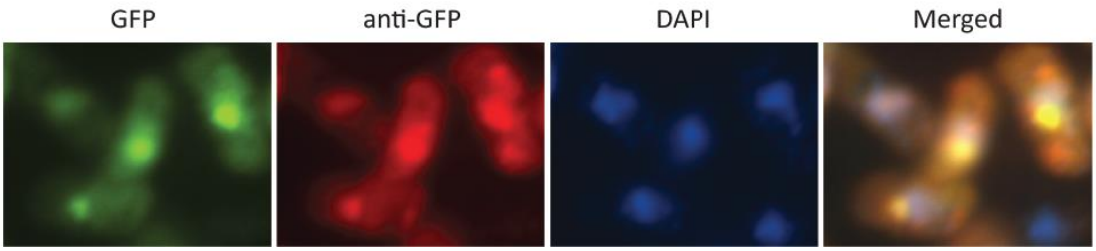
GFP
anti-GFP
DAPI
Merged

Figure 5.2 Nuclear targets can be identified by immunofluorescence. (A) Map of the plasmid used for tagging Upf3 with GFP (left) with schematic of the insert (right). Primers used for cloning are listed in Appendix 3 (B) Fluorescence microscope image of live *S. pombe* cells episomally expressing Upf3-GFP (TLM011, Appendix 2) (green) and stained with DAPI to show the region of the nucleus containing the DNA (blue). (C) Fluorescence microscope image of fixed *S. pombe* cells expressing GFP-tagged Upf3 (green), and GFP detected by immunofluorescence (red). Cells were counterstained with DAPI (blue). Immunodetection of GFP was with a rabbit anti-GFP primary antibody (Invitrogen A11122) and an anti-rabbit Alexa 647 secondary antibody. Statistical significance was determined by carrying out a t-test to compare the means of three biological repeats, counting a total of 82 cells.

the optimised immunofluorescence procedure is suitable for detecting nuclear targets.

5.2.2 Puromycylated peptides accumulate at the tips of *S. pombe* cells when nuclear export of RNA is blocked

The optimised immunofluorescence procedure was used to visualise puromycylated peptides in cells labelled by RPM using the conditions that had originally been determined in the growth assays and Western blotting described in Chapter 3. RPM was carried out in a strain expressing GFP-tagged Gar2 (TLM101, Appendix 2), which serves as a nucleolar marker (De et al., 2011), both with and without anisomycin. The results show that the puromycin antibody successfully detects puromycylated peptides (Fig 5.3 (i) top row and (ii) top profile) indicated by the presence of a relatively intense signal, and that anisomycin blocks this puromycin signal (Fig 5.3 (i) bottom row and (ii) bottom panel), consistent with the data from Western blotting in this study (Chapter 3) and previous reports (David et al., 2012).

Immunofluorescence following RPM was carried out in several strains that are temperature sensitive for nuclear export of RNA (TLM103, TLM105, TLM107 and TLM109, Appendix 2) (Azad et al., 1997, Yoon et al., 2000) to determine whether an accumulation of RNA in the nucleus leads to a corresponding increase of the RPM signal. However, in light of the polysome analysis, such a signal would not necessarily be representative of nuclear protein synthesis, and may instead reflect puromycylated peptides that have been transported into the nucleus after synthesis in the cytoplasm. The puromycin signal was of relatively low intensity in two of the mutants, ptr-1-1 (Fig 5.4 A (i)) and ptr4-1 (Fig 5.4 A (ii)), both when they had been grown at the permissive temperature of 25 °C and when they had been

(i)

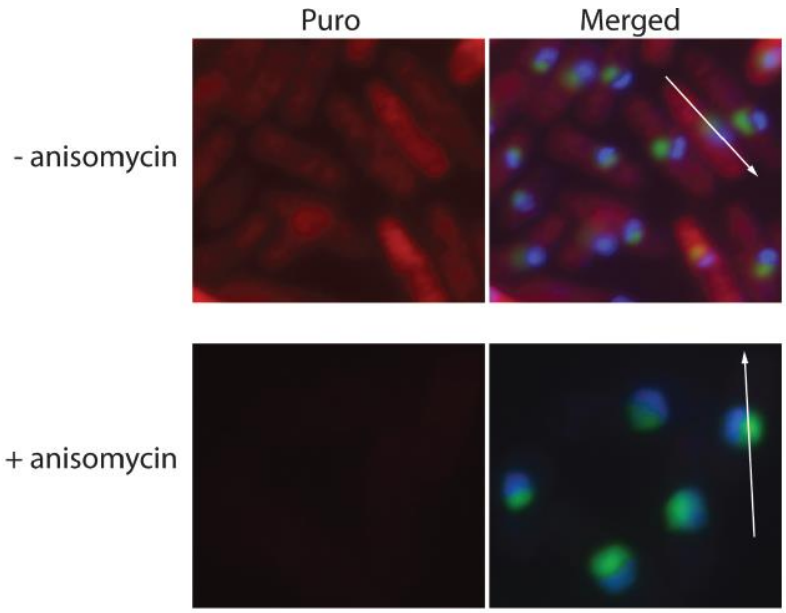
Puro
Merged
- anisomycin
+ anisomycin

(i)

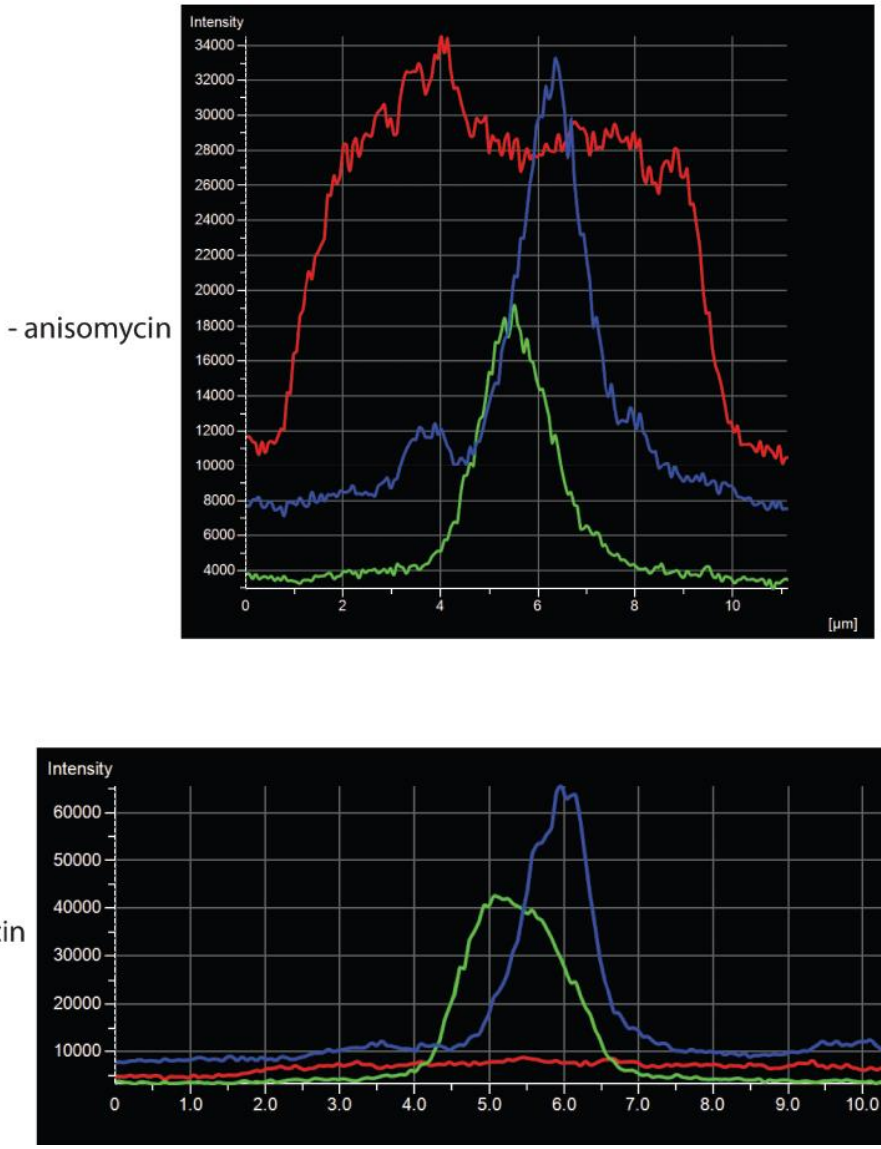
- anisomycin
Intensity
34000
32000
30000
28000
26000
24000
22000
20000
18000
16000
14000
12000
10000
8000
6000
4000
0
2
4
6
8
10
[µm]
+ anisomycin
Intensity
60000
50000
40000
30000
20000
10000
0
1.0
2.0
3.0
4.0
5.0
6.0
7.0
8.0
9.0
10.0
[µm]

Figure 5.3 Anisomycin blocks the immunofluorescence signal from puromycin. (i) Fluorescence microscope images following RPM in *S. pombe* cells expressing Gar2-GFP (TLM101, Appendix 2) which is a nucleolar marker (green). Cells were treated with 200 µL emetine for 30 mins followed by 250 µg/mL puromycin for 15 minutes, both without (top panels) and with (bottom panels) 250 µg/mL anisomycin alongside the emetine treatment. The puromycin signal (red) was detected with a mouse anti-puromycin primary antibody (clone 5B12) and an anti-mouse Cy3-conjugated secondary antibody. Cells were counterstained with DAPI (blue). White arrows show the path of the fluorescence intensity profiles shown in (ii). Intensity profiles show scale in µM on the x-axis and relative intensity on the y-axis. Colours reflect those in the immunofluorescent images. The data are representative of two independent biological repeats.

moved to the non-permissive temperature of 37 °C for 4 hours (see fluorescent images and compare puromycin signal on intensity profiles to that of DAPI). The growth of these strains was significantly slower at 25 °C than the usual doubling time for *S. pombe* cells, therefore the relatively low puromycin signal might reflect slower rates of translation in these mutants. The shift to 37 °C for 4 hours induces blockage of RNA export which would also lead to reduced level of cytoplasmic translation due to a reduction in available ribosomal RNAs and mRNAs; this might therefore account for the corresponding low signal from puromycin in these strains. At 25 °C a relatively low puromycin signal was also observed in the ptr3-1 ts mutant but at 37 °C the fluorescent images and intensity profile show the puromycin signal to be relatively intense at the tips of many of these cells (37% ± 12) (Fig 5.4 A (iii)). A relatively high puromycin signal was observed in the rae1-167 ts at both temperatures and a proportion of cells (26% ± 10) also showed a particularly intense signal at the tips (Fig 5.4 A(iv)). In an attempt confirm that RNA export from the nucleus had successfully been blocked in the temperature sensitive mutants, and also to determine whether the puromycin signal overlapped with that of RNA, an RNA dye had been used in some of these immunostaining experiments. Generally a signal from the RNA dye was not detectable, likely because formaldehyde fixation alters the RNA in such a way that it prevents the dye from binding (Evers et al., 2011). However, on one occasion, a signal from the RNA dye was observed in the rae1-167 ts mutant (Figure 5.4 B). Notably, the RNA had not only accumulated in the nucleus (white arrows) as should occur when RNA export has been effectively blocked, but additionally at the tips of the cells, which also corresponded to the localisation of puromycylated peptides (Figure 5.4 B). It is therefore likely that the same RNA distribution is present in the other cells in which the puromycin signal was present at the tips (Figure 5.4 A iii and iv). Since *S. pombe* cells grow from the tips, it is possible that the

A

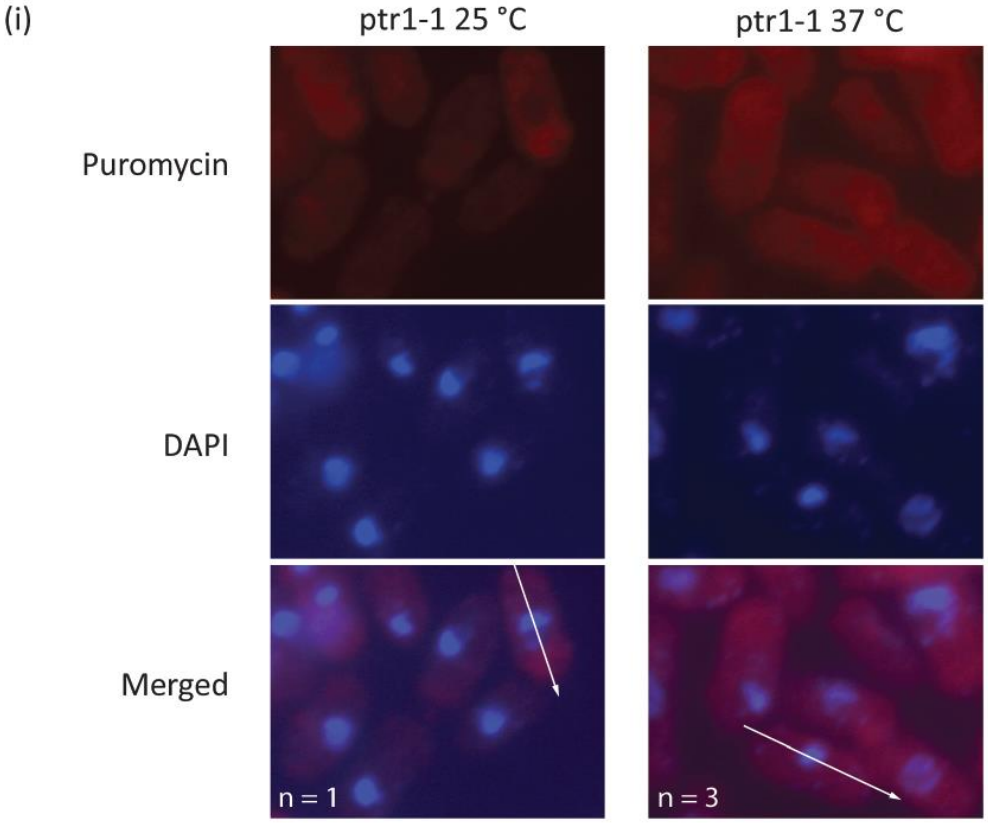
(i)
ptr1-1 25 °C
ptr1-1 37 °C
Puromycin
DAPI
Merged
n = 1
n = 3

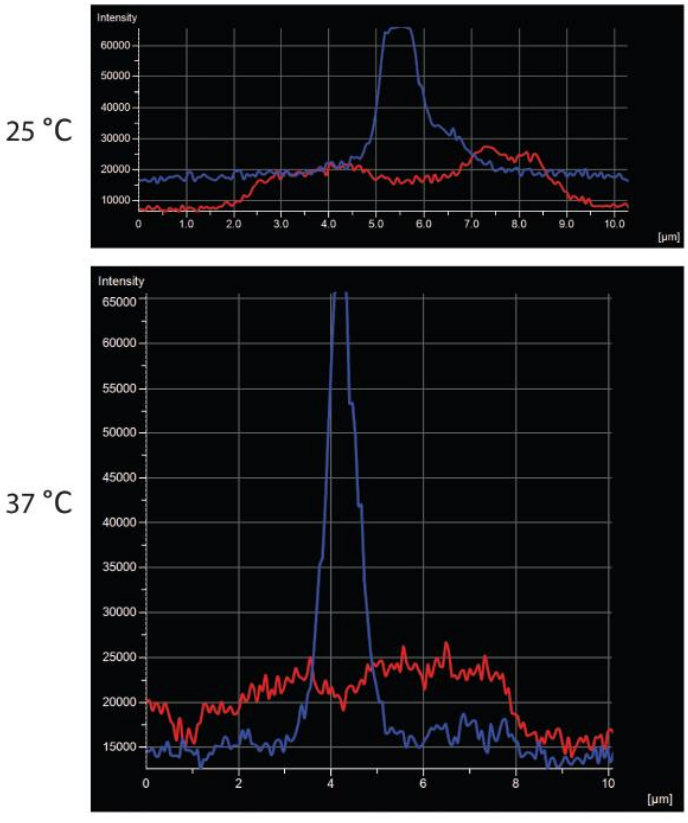
25 °C
Intensity
60000
50000
40000
30000
20000
10000
0
1.0
2.0
3.0
4.0
5.0
6.0
7.0
8.0
9.0
10.0
[µm]
37 °C
Intensity
65000
60000
55000
50000
45000
40000
35000
30000
25000
20000
15000
0
2
4
6
8
10
[µm]

(ii)

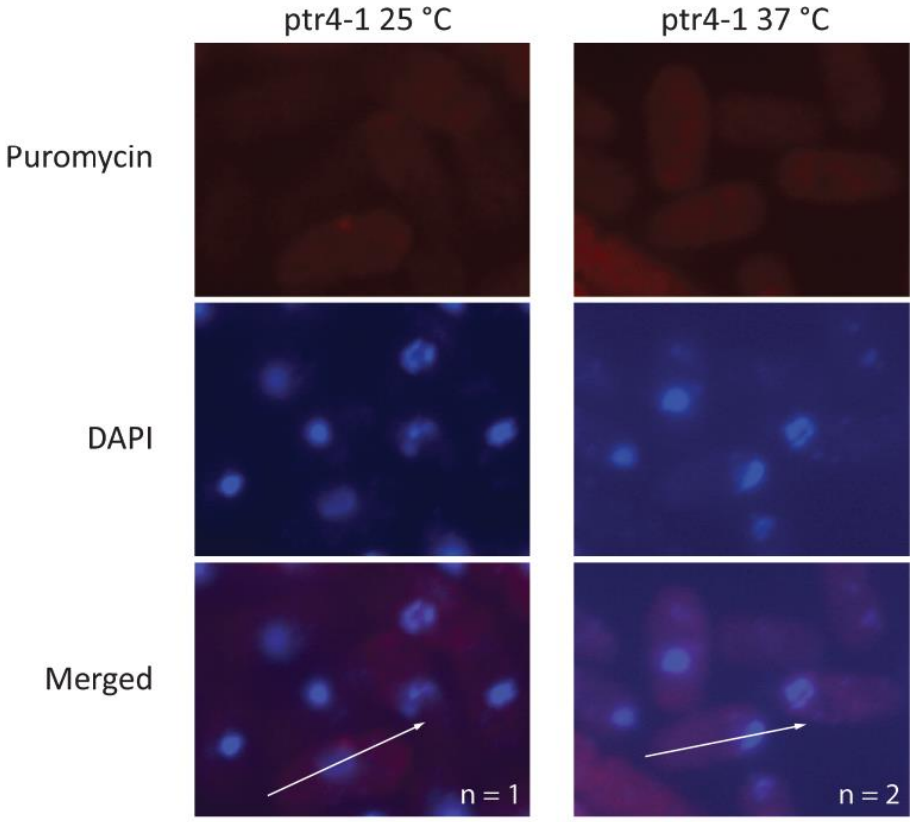
ptr4-1 25 °C
ptr4-1 37 °C
Puromycin
DAPI
Merged
n = 1
n = 2

25 °C

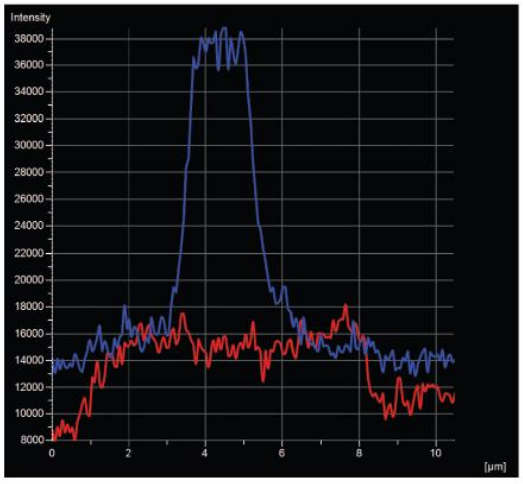
Intensity
38000
36000
34000
32000
30000
28000
26000
24000
22000
20000
18000
16000
14000
12000
10000
8000
0
2
4
6
8
10
[µm]

37 °C

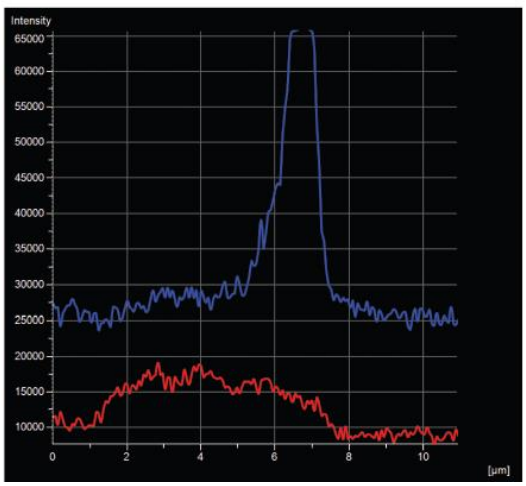
Intensity
65000
60000
55000
50000
45000
40000
35000
30000
25000
20000
15000
10000
0
2
4
6
8
10
[µm]

(iii)

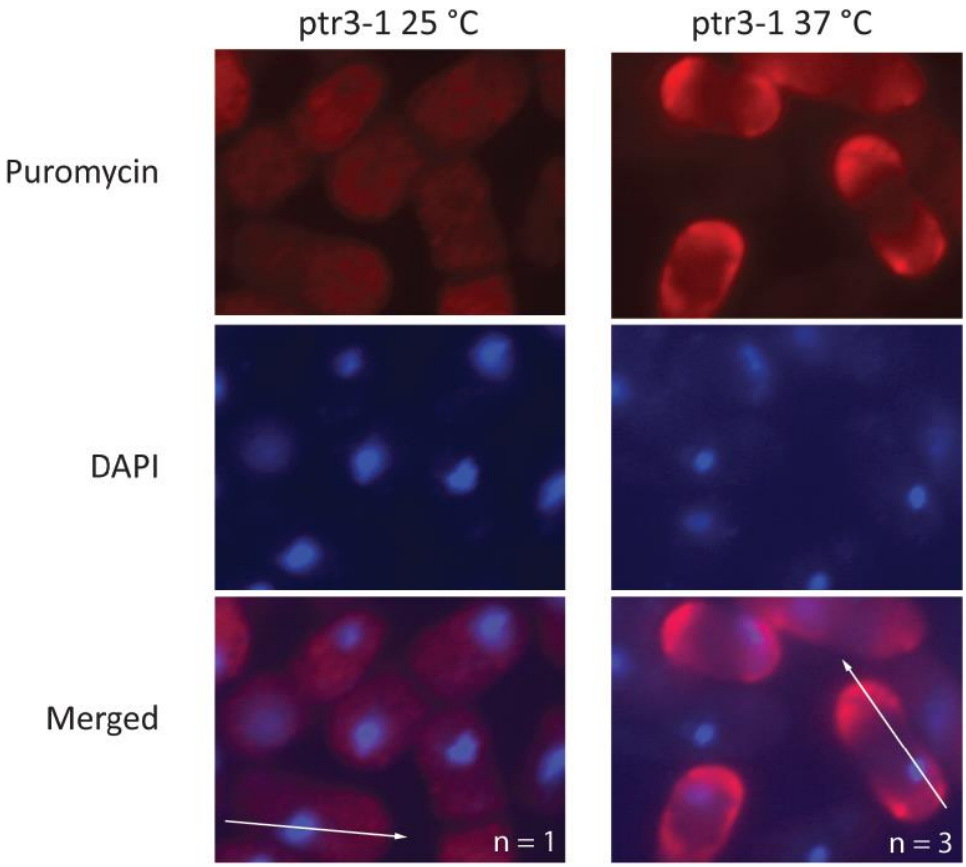
ptr3-1 25 °C
ptr3-1 37 °C
Puromycin
DAPI
Merged
n = 1
n = 3

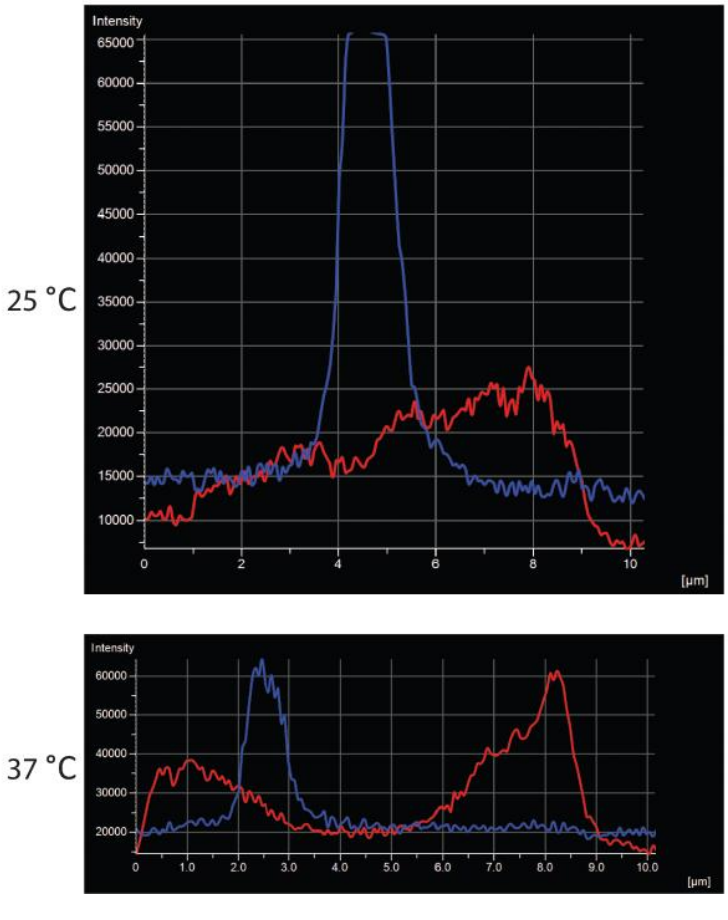
25 °C
Intensity
65000
60000
55000
50000
45000
40000
35000
30000
25000
20000
15000
10000
0
2
4
6
8
10
[µm]
37 °C
Intensity
60000
50000
40000
30000
20000
0
1.0
2.0
3.0
4.0
5.0
6.0
7.0
8.0
9.0
10.0
[µm]

(iv)

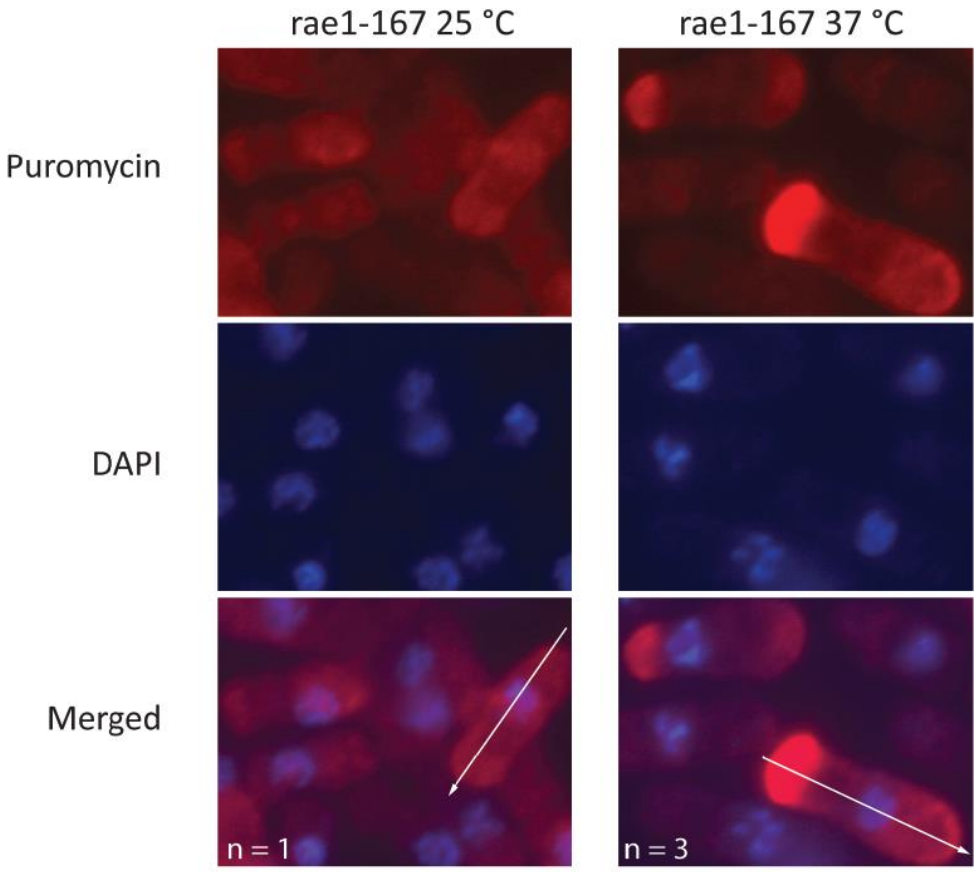
rae1-167 25 °C
rae1-167 37 °C
Puromycin
DAPI
Merged
n = 1
n = 3

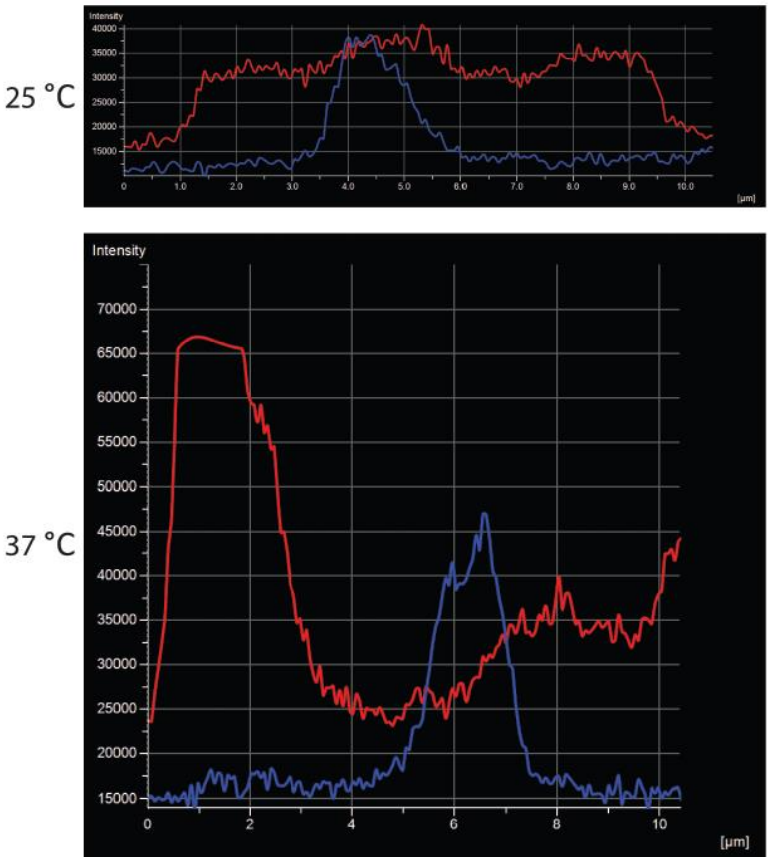
25 °C
37 °C
Intensity
[µm]

B

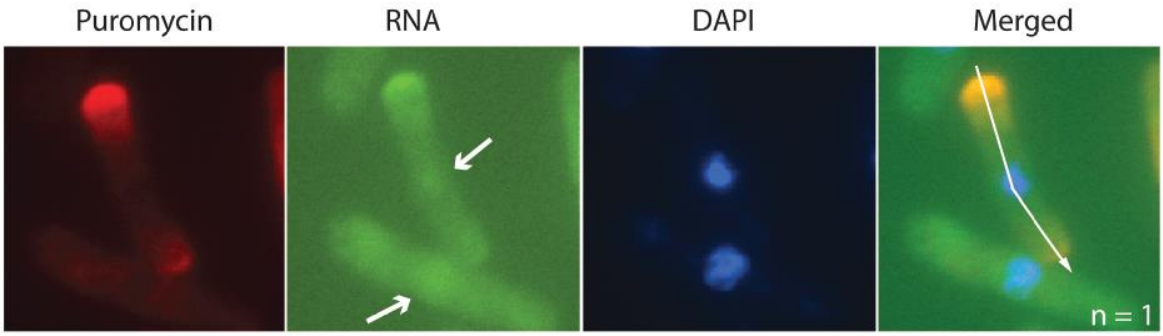
Puromycin
RNA
DAPI
Merged
n = 1

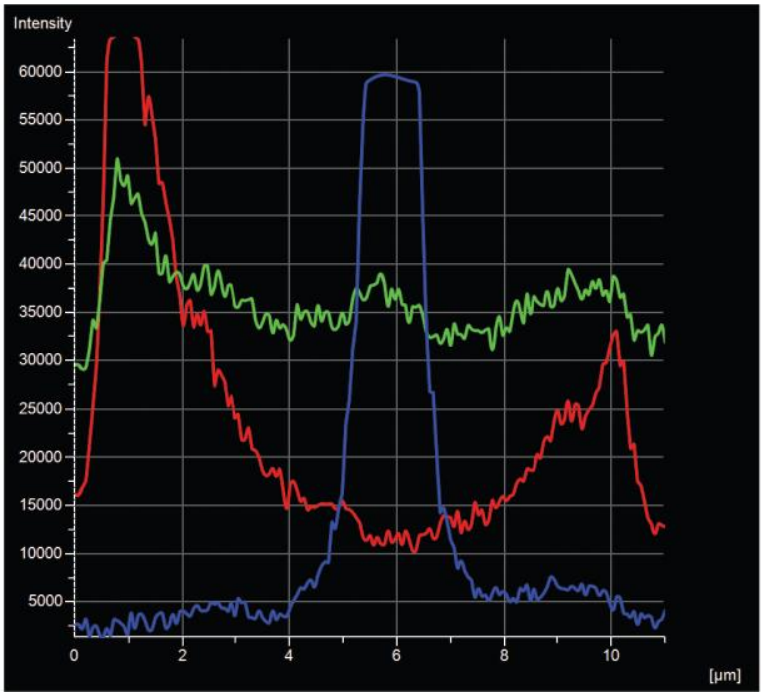
Intensity
60000
55000
50000
45000
40000
35000
30000
25000
20000
15000
10000
5000
0
2
4
6
8
10
[µm]

Figure 5.4 Blocking nuclear export of RNA leads to accumulation of puromycylated peptides at the tips of *S. pombe* cells. (A) Immunofluorescence of (i) ptr1-1, (ii) ptr4-1, ptr3-1 and (iv) rae1-167 *S. pombe* mutants, which are temperature sensitive for RNA export. 2mL liquid cultures of each mutant were grown at the permissive temperature of 25 °C and a 1 mL aliquot of each was then transferred to the non-permissive temperature of 37 °C for 4 hours. The remaining 1 mL was kept at 25 °C. RPM was carried out at the non-permissive temperature. Fluorescent images are shown in upper panels and lower panels are relative intensity profiles as in Fig 5.3. The number of independent biological repeats is shown in the bottom corner of the fluorescent images. A total of 160 cells were counted for the statistical to calculate the percentage of cells with intensity at the tips, as discussed in the text. Other images are representative of counts of between 56 and 180 cells. (B) Fluorescent microscope images of the rae1-167 mutant following RPM at the non-permissive temperature, counterstained with E36 RNA dye (green). Short white arrows show the site of RNA accumulation in the nuclear region. The data represents one experimental run. Long white arrow shows the path of the intensity profile in the lower panel. The puromycin signal was detected with mouse anti-puromycin primary antibody, clone 5B12 and an anti-mouse cy3-conjugated secondary antibody (red). Cells were counterstained with DAPI (blue).

concentration of RNA and puromycylated peptides observed at the tips of the cells might be a stress response induced by the blockage of RNA export to the cytoplasm. Under such conditions, cells might be unable to carry out normal levels of translation and may respond by diverting resources towards translating mRNAs that encode proteins essential for maintaining cellular growth. The RNA signal at the tips could correspond to ribosomes translating these mRNAs. It could be that under these stress conditions, the cell directs ribosomes and mRNAs to the tips, where localised protein synthesis then takes place.

5.2.3 Creation of strains for investigating ribosome and puromycin colocalisation

These findings raised the possibility that localised translation could be taking place in *S. pombe* cells, and that this could be detected using puromycylation under certain conditions. However, it remained possible that peptides were not being made at the tips, but rather had been synthesised across the cell and had transferred to the tips over the 15 minute puromycin incubation period. A time course experiment would be an appropriate means of tracking the puromycin signal following short, medium and longer incubation periods. Since puromycylated peptides are released from ribosomes (Chapter 4) a strain in which the ribosome could be visualised alongside the puromycin signal would allow nascent peptides to be distinguished from those that have been released. This could be achieved by crossing the rae1-167 and ptr3-1 ts mutants with those strains in which the ribosomal proteins were tagged with HA, as used in the ChIP-chip study (De et al., 2011). Since both the RNA export mutants and the Rpl-HA tagged strains are of the h^- mating type, the Rpl-HA strains were first crossed with a wild type strain with mating type h^+. Successful crosses would carry both the h^+ mating type and the G418 antibiotic resistance marker from the Rpl-HA tagged strain, therefore strains were selected on YES + G418 plates. The mating type was screened for by

colony PCR. Two h^+ colonies for each of Rpl7-HA and Rpl25-HA were isolated, however no Rpl11 h^+ mutants were identified. This is probably due to the *rpl11* gene and the mating type locus being only ~74 kb apart on chromosome II, meaning the two alleles are unlikely to recombine during meiosis, and the likelihood of the two desired alleles segregating together on the same chromosome is very low.

To test whether Rpl7-3HA and Rpl25-3HA in the h^+ background (TLM111 and TLM113, Appendix 2) produce functional RPs that form part of translation-competent ribosomes polysome profiling followed was carried out and Western blotting was performed to identify those fractions with which the tagged RPs were associated. This had been previously done for the three RPs during the ChIP-chip study (De et al., 2011), but was repeated in this study with copies of all three original h^-strains (TLM095, TLM097 and TLM099, Appendix 2) as well as the newly-made h^+ strains to determine whether the same pattern is observed. In agreement with the previous study, Rpl11 in the h^- background and Rpl25 in both the h^+ and h^- backgrounds were detected in the fractions corresponding to polysomes and 80S (Figure 5.5 lower three panels). However, in contrast to the previous study, reported that Rpl7-HA was in the polysomal fractions, here Rpl7 was detected only in the 80S and 60S fractions in both the h^+ and h^- backgrounds (Figure 5.5 top two panels). The published Western blot (De et al., 2011) appears overexposed compared to that of Rpl11 and Rpl25 and the signal is more intense in the 80S and 60S fractions. This suggests that RpL7-HA might not be functional. Additionally, the gene that was tagged in the previous study is in fact predicted to encode ribosomal protein-like Rlp7 rather than ribosomal protein Rpl7, and is predicted to play a role in ribosome biogenesis; this perhaps explains why it is not in the polysomal fractions but is in the 80S and 60S.

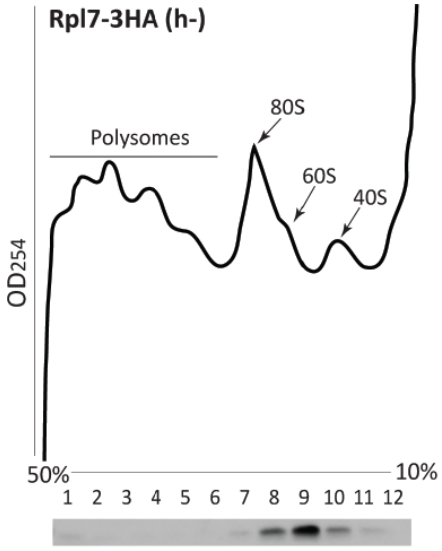
Rpl7-3HA (h-)
Polysomes
80S
60S
40S
OD254
50%
10%
1 2 3 4 5 6 7 8 9 10 11 12

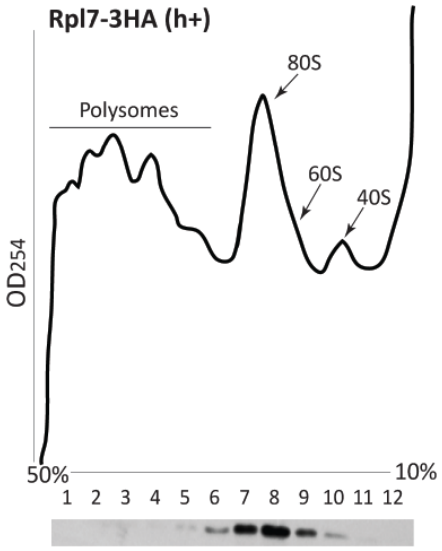
Rpl7-3HA (h+)
Polysomes
80S
60S
40S
OD254
50%
10%
1 2 3 4 5 6 7 8 9 10 11 12

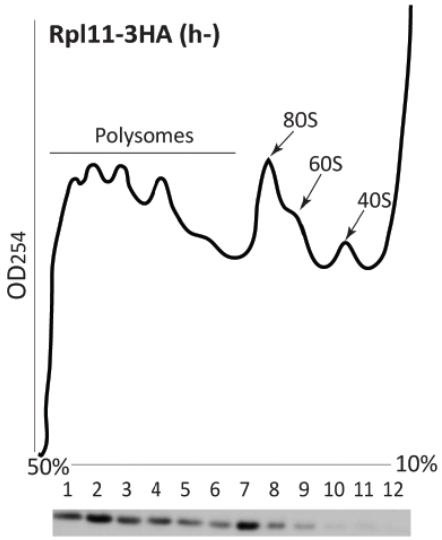
Rpl11-3HA (h-)
Polysomes
80S
60S
40S
OD254
50%
10%
1 2 3 4 5 6 7 8 9 10 11 12

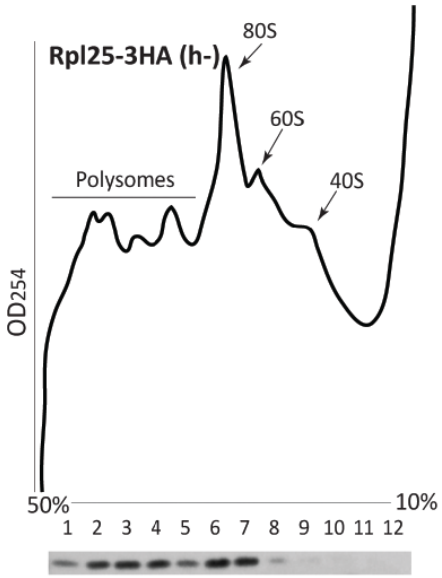
Rpl25-3HA (h-)
80S
60S
Polysomes
40S
OD254
50%
10%
1 2 3 4 5 6 7 8 9 10 11 12

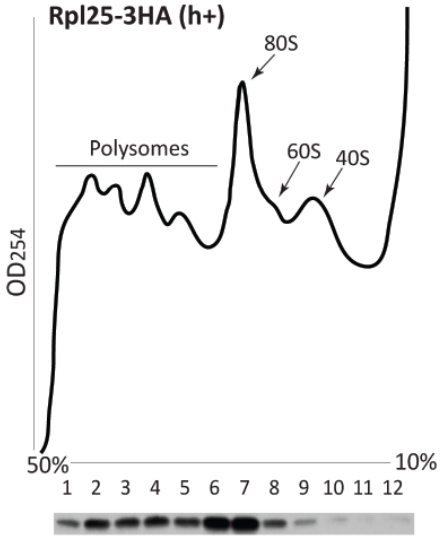
Rpl25-3HA (h+)
80S
Polysomes
60S
40S
OD254
50%
10%
1 2 3 4 5 6 7 8 9 10 11 12

Figure 5.5 Ribosomal protein RpL7 is not detected in polysomes. Polysome profiles of 3HA-tagged Rpl7, 11 and 25 strains with Western blotting analysis of HA-tagged RPs indicated in protein extracts from each fraction below each profile (TLM095, TLM097, TLM099, TLM111 and TLM113, Appendix 2). The horizontal axis on each plot shows the polysomal fraction and the vertical axis is a relative measurement of the optical density (OD) of RNA at 254 nm reading. HA-tagged RPs were detected with 12CA5 mouse anti-HA primary antibody (CRUK) and an anti-mouse HRP-conjugated secondary antibody.

Since Rpl7 appears not to be a ribosomal protein and no Rpl11 h^+ colonies were successfully identified, the Rpl25 h^+ strain was used in further work to cross it with the two ts mutants that had shown the puromycin signal at the tips of the cells. The strains were selected on YES + G418 agar media at the permissive temperature to select for the presence of Rpl25-3HA. Colonies were then spotted onto new plates and grown at the non-permissive temperature. Failure to grow at the non-permissive temperate indicates that the strain also possesses the ts mutation. Four Rpl25-3HA colonies with the rae1-167 mutation were identified and four with the ptr3-1 mutation (Figure 5.6). Although immunostaining was not carried out in these strains due to time constraints, they are now ready to be used for immunofluorescence following RPM to determine the relationship between the puromycin and Rpl25 signals following incubation with puromycin for different lengths of time. The conditions of puromycylation should be further optimised to increase the likelihood of detecting newly-made peptides in the vicinity of where they have been synthesised.

A better way to visualise the cellular locations of ribosomes might be to carry out puromycylation in a strain in which ribosomal proteins on both subunits are tagged with different epitopes. The signal from all three could then be visualised with a super-resolution microscope available at the UoB (STORM, Nikon). If newly-made puromycylated peptides colocalise with both RPs within the 20-50 nm radius that can be resolved by the microscope this may signify that nascent peptides are on or in the vicinity of ribosome. Although the majority of puromycylated peptides are released from ribosomes, the presence of the HA, GFP and puromycin signal within close proximity allowed by super-resolution microscopy will be more indicative of the presence of functional ribosomes. Nascent peptides might be released immediately upon puromycylation and thus not likely to be detected, yet this

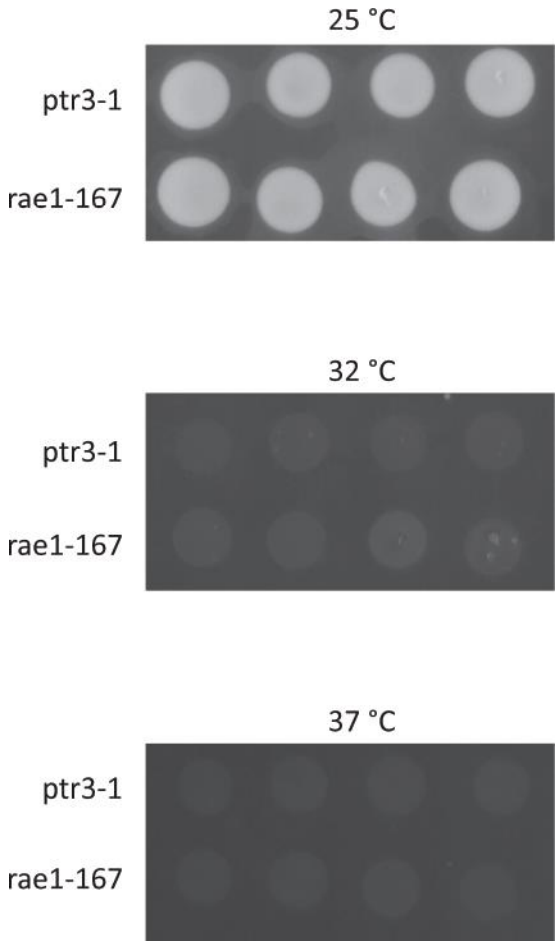

Figure 5.6 Rpl25-3HA strains have been crossed with mutants that are temperature sensitive for RNA export. Rpl25-3HA strain was crossed with the ptr3-1 and rae1-167 ts mutants and grown at the permissive temperature of 25 °C for 3 days on YES + G418 plates to select for the presence of Rpl25-3HA. Colonies were then spotted onto fresh YES + G418 plates and grown at the non-permissive temperatures of 32 °C and 37 °C. Failure to grow indicates that the strains also carry the temperature sensitive mutation.

approach should allow visualisation of the single 80S ribosomes as indicated by localisation of small and large subunit proteins. To this end work has been undertaken to tag several proteins on the small ribosomal subunit with GFP using the same cloning strategy used for tagging Upf3. The work is in the preliminary stages and *E. coli* transformants are being confirmed by colony PCR in collaboration with a Masters student under supervision (See Appendix 9 for plasmid maps and list of RPs being tagged). As soon the correct plasmids have been generated, these will be transformed into the three Rpl-HA strains described above.

5.2.4 Bioinformatic comparison of Rlp7 and Rpl7 in *S. pombe* and *S. cerevisiae*

In light of the finding that the previous ChIP-chip study had been with ribosomal protein-like Rlp7, rather than the ribosomal protein Rpl7, bioinformatical analyses of the protein structures of these proteins was conducted to investigate their relatedness. As mentioned in the introduction, some ribosomal-like proteins have similar structures to ribosomal proteins and block the premature association of RPs to prevent pre-ribosomal subunits from engaging in translation (Panse and Johnson, 2010). The ribosomal protein-like RLP7 is also present in *S. cerevisiae* but does not function to inhibit binding of RPL7 since it was found to simultaneously bind a different site on the ribosome (Babiano et al., 2013). Sequence alignment of this and *S. pombe* Rlp7 was conducted, along with the two *S. pombe* genes encoding the ribosomal protein, Rpl701 and Rpl702, (Figure 5.7 A). The *S. pombe*, Rpl701 and Rpl702 amino acids sequence similarity but there is some divergence between these and the Rlp7 sequence (Figure 5.7 A). However, the *S. pombe* Rpl7 and *S. cerevisiae* RPL7 sequences are much more divergent than those of *S. pombe* Rlp7 and the two ribosomal protein sequences, Rpl701 and Rpl702 (Figure 5.7 A). 3D modelling predicts that the two *S.*

pombe Rpl7 genes, the *S. pombe* Rlp7 gene and the two *S. cerevisiae* RPL7 genes (RPL7A and RPL7B) all encode proteins that have a high degree of structural similarity (Figure 5.7 B). The tertiary structure of *S. cerevisiae* RLP7 is predicted to be generally similar to that of the RPs, but with additional protein domains. Only further experimental analysis would enable identification of the role of Rlp7 in *S. pombe*.

A

```
S.cerevisiaeRLP7      -MSSTQDSKAQTLNSNPEILLRKRRNADRTRIERQELAKKKREEQIKKKRSNKNKFVRAE
S.pombeRlp7           --MAEDAPVVQQTMLEPEVLLKKRKVNERTRKERVEQAIAKKEAQKKNR---KETFKRAE
S.pombeRpl701         MAVASSTVPSKEQIFAPESLLKKKKTQEQSREQRVAAAAEKKAAQQKKR---ELIAKRAE
S.pombeRpl702         -MVASSTVPSVASIFAPESLLKKTKAQKQSREQIVAAAAEKKSARQKKR---ELIAKRAE
                         : .          ** **:* :  .::* :    *  *:  : *::   :    ***

S.cerevisiaeRLP7      SIVAKTLATSREKERIKRVSILEDKKAKNETQHIASGKDFILKITEKANGAEENSVDLEE
S.pombeRlp7           TFINNYRQRER-------------------------------------------ERIRLNR
S.pombeRpl701         SYDAEYRKAER-------------------------------------------EQIELGR
S.pombeRpl702         AYEAEYRAAER-------------------------------------------EQIELAR
                      :   :    .*                                            : : * .

S.cerevisiaeRLP7      TEEEEDDGLIREKTTYDGKPALLFIVRVRGPLAVNIPNKAFKILSLLRLVETNTGVFVKL
S.pombeRlp7           SAKNKG------DIFVPDETKLLFVIRIAGV--KNMPPKIRKVLRLLRLSRINNAVFVRN
S.pombeRpl701         KARAEG------NYYVPDETKLVFVIRIRGI--NNIPPKARKIMQLLRLIQINNGVFVKF
S.pombeRpl702         KARAEG------NYFVPHEPKLIFVVRIRGI--NNIPPKARKIMQLLRLLQINNGIFVKF
                      . . :       .     :  *:*::*: *    *:* *  *:: **** . *..:**:

S.cerevisiaeRLP7      TKNVYPLLKVIAPYVVIGKPSLSSIRSLIQKRGRIIYKGENEAEPHEIVLNDNNIVEEQL
S.pombeRlp7           NKAVAQMLRIVEPYVMYGIPNLHSVRELIYKRGFG------KINGQRIALSDNALIEEAL
S.pombeRpl701         NKATKEMLQVVEPYVTYGIPNLKTVRELLYKRGFG------KVNKQRIALSDNAIIEAAL
S.pombeRpl702         NKAIKEMLQVVEPYVTYGIPNHKTVRELIYKRGFG------KVNKQRIPLSDNAIIEAAL
                      .*    :*::: ***  * *.  ::*.*: ***        : : :.* *.** ::*  *

S.cerevisiaeRLP7      GDHGIICVEDIIHEIATMGESFSVCNFFLQPFKLNREVSGFGSLNRLRKIKQREAESRTR
S.pombeRlp7           GKYDVISIEDIIHEIYNVGSHFKEVTKFLWPFTLTPVKHSLMEKKVKHFNEGRKAG----
S.pombeRpl701         GKYSILSIEDLIHEIYTVGPNFKQAANFIWPFQLSSPLGGWRDRKFKHFIEGGDAG----
S.pombeRpl702         GKYSILSVEDLIHEIYTVGPNFKQAANFLWPFKLSSPLGGWRERKFKHFIEGGDAG----
                      *.: ::.:**:**** .:*  *.    *: ** *.    .  . :  :  :  .*

S.cerevisiaeRLP7      QFSNAATAPVIEVDIDSLLAKLN
S.pombeRlp7           ---------YCGEEINELIKKQV
S.pombeRpl701         ---------KRDEHINSLVRKML
S.pombeRpl702         ---------KRDEHINGLVQKML
                              .*: *: *
```

B

S. pombe Rpl701

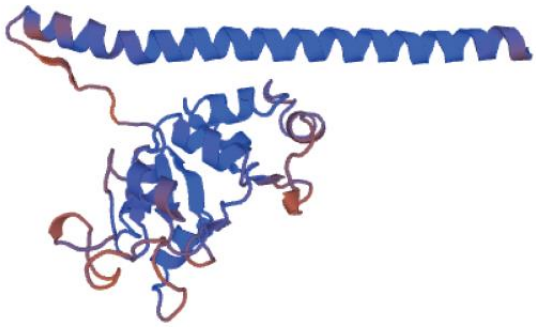

S. pombe Rpl702

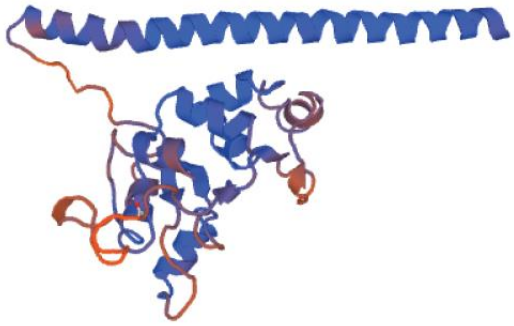

S. pombe Rlp7

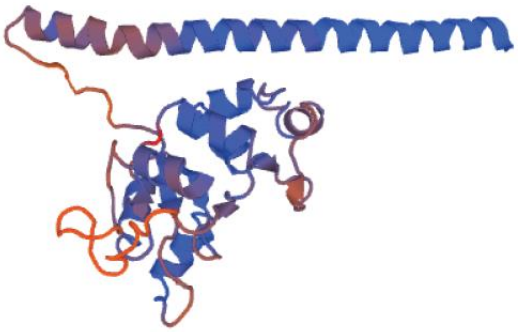

S. cerevisiae RLP7

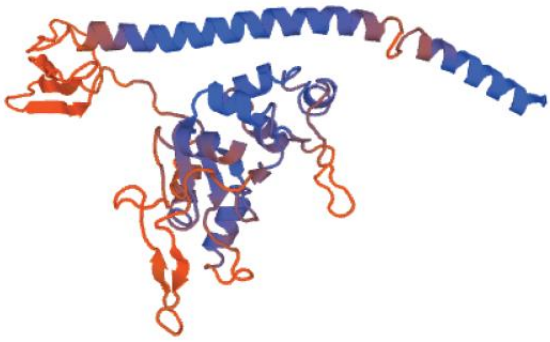

S. cerevisiae RPL7A

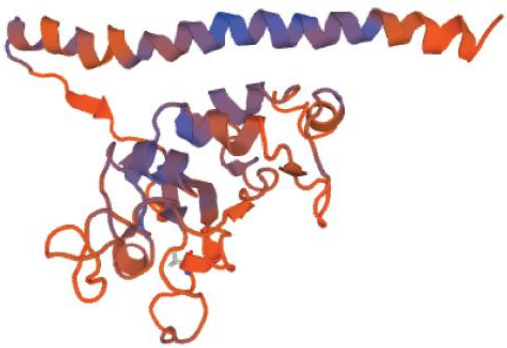

S. cerevisiae RPL7B

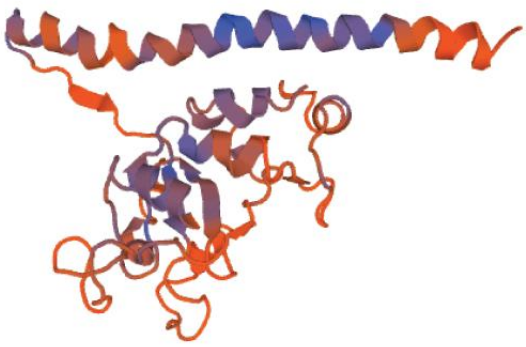

Figure 5.7 Bioinformatical analysis of Rlp7 and Rpl7 in *S. pombe* and *S. cerevisiae.* (A) Sequences alignment of the amino acid sequences of *S. cerevisiae* RLP7 and *S. pombe* Rlp7, Rpl701 and Rlp702. Alignment was with Clustal Omega Multiple Sequence Alignment software. (B) Predicted tertiary structures of *S. pombe* Rpl701, Rpl702 and Rlp7 and *S. cerevisiae* RLP7, RPL7A and RPL7B. Modelling was with Expasy Swiss Model Respository software.

5.3 Discussion

This chapter describes preliminary work carried out to optimise the immunofluorescence procedure in *S. pombe* to allow the detection of target proteins in all cellular locations, particularly in the nucleus. Initial immunofluorescence experiments, using RPM, prior to the finding that puromycylated peptides are released from ribosomes, suggested that translation becomes localised when cells are subject to certain stresses. Notably, when nuclear export of RNAs is blocked, puromycylated peptides accumulate at the tips of cells. Conjecture might be that under such stress/mutant conditions, the cell diverts its energy towards producing only those proteins essential for growth (Atilgan et al., 2015). That the bulk of the RNA was also localised in this region of the cell suggests that ribosomes (and some mRNAs) are present in that region rather than being distributed across the cell and proteins then diffusing from these sites to the tips.

With the aim of investigating further whether immunostaining of puromycylated peptides can used to visualise translation sites, strains expressing Rpl25-3HA in a background of the ts mutations have been produced. The ts mutants had produced the striking localised puromycin signal at the growing tips of the cell. RP/puromycin double-immunostaining followed by super-resolution microscopy can be carried out in these and other strains that episomally express ribosomal proteins of both the small and large subunits carrying different tags, and can be used to investigate whether the puromycin signal does in fact corresponded to that of the ribosomes. Additionally by imaging pairs of RPs, it should be possible to visualise 80S ribosomes in the absence of puromycylation.

Finally, if such analysis indicates that puromycylated peptides remain on or in the vicinity of the ribosome in these or other stress or mutant conditions, puromycin ChIP could be

attempted again to identify co-transcriptionally translated genes. However, one possibility is that the ChIP study of ribosomal proteins (De et al., 2011) may in fact have been reporting pre-ribosomes or ribosomal subunits that are yet to release the various assembly factors with which they associate to prevent premature engagement in translation. Nevertheless, their presence at the chromosomes is still intriguing, thus the issue will need to be investigated in future.

Chapter 6 Conclusion

Although, as reviewed in the Introduction, recent data from the Brogna lab and other groups provide support for the hypothesis that translation may also occur in the eukaryotic nucleus, many, possibly most, investigators remain sceptical. Specifically, the Brogna lab has reported that ribosomal subunits can join to form translating 80S in the *Drosophila* nucleus (Al-Jubran et al., 2013), which, together with previous reports that ribosome components are present on nascent transcripts in both *Drosophila* (Brogna et al., 2002, Rugjee et al., 2013), and *S. pombe* (De et al., 2011), indicates that ribosomes may translate nascent transcripts. The question at the start of this work was therefore what function nuclear translation would serve in eukaryotic cells. A new technique at the time, termed ribopuromycylation (RPM), reportedly allowed the visualisation of puromycin-labelled nascent peptides by immunofluorescence in human cells (David et al., 2012). With the aim of identifying co-transcriptionally translated genes, this study began by combining RPM with chromatin immunoprecipitation (ChIP) in *S. pombe*. While ChIP has more often been used to identify proteins that are either in direct contact with the DNA (such as RNA Pol II) or in indirect contact via protein-protein interactions (such RNA Pol II protein cofactors), the Brogna lab and others have used this technique to assess the association of proteins with nascent RNAs (Abruzzi et al., 2004, De et al., 2011). ChIP could therefore also potentially identify genes that are associated with ribopuromycylated nascent peptides tethered to ribosomes that are indirectly associated with the DNA via nascent RNAs. The puromycylation conditions were firstly optimised in *S. pombe*; this primarily involved determining the optimal concentrations of the different drugs required for RPM, and controls to confirm the specificity of the signal.

Many genes which were known to be both highly transcriptionally active and associated with ribosomal proteins (RPs) (De et al., 2011), were assessed by ChIP for their association with puromycylated peptides. After numerous attempts, the only gene that showed reproducible enrichment in an RNAase-dependent manner was *pma1* (Chapter 3, Fig 3.8), however, this enrichment was only detected in the middle of the *pma1* locus, making it difficult to draw strong conclusions at this stage. It was possible that RPM in *S. pombe* does not lead to retention of puromycylated peptides on ribosomes, as it reportedly does in HeLa cells; the ChIP results may simply be due to the association of puromycylated peptides that have been released from the ribosome and, for reasons which remain unclear, bind the *pma1* locus.

To investigate whether RPM does detect nascent peptides in *S. pombe* a detailed characterisation of puromycylation was carried out in this organism. The key assumption of the RPM technique is that puromycylated peptides remain attached to the ribosome when cells are pretreated with translation elongation inhibitors such as cycloheximide or emetine. This was assessed in this study by tracking the association of puromycylated peptides with ribosomes using polysomal fractionation of cells that had been treated with puromycin in the presence or absence of elongation inhibitors (Chapter 4). In contrast to that reported in the original study in mammalian cells (David et al., 2012) pretreatment with neither emetine nor cycloheximide retains nascent peptides on ribosomes upon puromycylation. Notably, comparable results were obtained in similar experiments carried out in *Drosophila* S2 cells, and also in a preliminary study in HeLa cells. The release of nascent peptides appears to be concomitant with puromycin incorporation, since the same effect was observed even though puromycin treatment was extremely brief at 30 seconds. While these findings are

not in agreement with those recently reported in mammalian cells (David et al., 2012), they are in line with an older study in HeLa cells which similarly reported that puromycin treatment causes the release of nascent peptides from ribosomes that have been stabilised with emetine (Grollman, 1968). Furthermore, this data clearly shows that cycloheximide significantly reduces puromycin incorporation, while emetine does not increase it. This also contrasts with that reported in HeLa cells (David et al., 2012), but the reduction caused is in agreement with a previous study which reported that cycloheximide pre-treatment reduces puromycin incorporation on mammalian ribosomes (Baliga et al., 1970). Blocking translation elongation most likely inhibits either tRNA translocation (Wong et al., 2014) which has been reported to be required for puromycin incorporation (Baliga et al., 1970) or peptidyl transferase activity (Grollman, 1966) upon which the catalytic incorporation of puromycin depends. The reduction in puromycylation following cycloheximide pretreatment could alternatively be explained by the prevention of the release/recycling of ribosomes, leading to a reduction in ribosomal subunits available to re-engage in further rounds of translation as would occur when puromycin is incorporated without prior elongation inhibition. However, the reason why emetine does not similarly inhibit puromycylation remains unclear.

Cumulatively the results of the characterisation of puromycylation in *S. pombe* and *Drosophila* S2 cells contradict the main conclusions of the RPM paper that elongation inhibitors can prevent release of nascent peptide following puromycylation (David et al., 2012). However, the means by which the authors confirmed that RPM allows detection of ribosome-bound nascent peptides may explain why these differences are observed. In the RPM study, rather than carrying out polysomal fractionation of cells that had undergone

both emetine and puromycin treatment, cells were instead fractionated after being treated only with emetine (David et al., 2012). Aliquots of each fraction were transferred to a PVDF membrane and subsequently treated with puromycin. This was followed by analysis of the association of puromycylated peptides with the polysomal fractions by enzyme-linked immunosorbent assay (ELISA). The authors reasoned that ribosomes within the fractions would bind the membrane and that only puromycin-labelled nascent peptides retained on ribosomes would be detected, since those that are released would be removed by subsequent washes. In view of the findings of this study, an alternative interpretation is that the PVDF membrane may bind any proteins in the fractions, including puromycylated peptides that have been released. The authors reported no puromycin signal in fractions corresponding to 60S, 40S and soluble fractions, which they cite as evidence that the method reports only nascent peptides (David et al., 2012). However, since puromycin incorporation into nascent peptides requires catalysis by the ribosome, no signal would be expected from fractions that do not contain complete ribosomes. The study subsequently used RPM to investigate the cellular location of translating ribosomes, yet in light of the findings of this study, it is possible that the reported nuclear signal may reflect the presence of proteins that had undergone puromycylation and release from the ribosome in the cytoplasm, and had then been transported into the nucleus. This could account for the stronger signal observed when permeabilisation of the nucleus with detergents was carried out.

The data produced during this study are of interest not only because the validity of the RPM technique is brought into question, but also the conclusion of several other published works which have used the RPM technique. In the Brogna lab, RPM has concluded that nascent

peptides are present at polytene chromosomes of *Drosophila* salivary glands (Al-Jubran et al., 2013). While the puromycin signal was RNase-sensitive, suggesting that nascent transcripts may be undergoing translation, the polysome analysis in this study has revealed that puromycylated peptides are also released from ribosomes in *Drosophila* cells, therefore the signal at the polytene chromosomes could reflect the presence of peptides, or almost fully translated proteins, that have been C-terminally labelled with puromycin in the cytoplasm and then transported into the nucleus where they associate with the chromosomes. This possibility is made more likely since the puromycin treatment was for 15 minutes and was simultaneous with emetine treatment, rather than being subsequent to it, according to the Materials and Methods outlined in the paper (Al-Jubran et al., 2013). Despite these findings, as reviewed in the Introduction, additional independent evidence strongly indicates that ribosomal subunits join to form 80S in a translation-dependent manner in the nucleus (Al-Jubran et al., 2013). Future studies will be needed to investigate this matter further.

In conclusion, based on evidence that released peptides do not immediately diffuse from their sites of translation (Choi and Brimacombe, 1998), it may be possible that the localised puromycin signal detected in *S. pombe* cells in which RNA export had been blocked (Chapter 5), as well as that reported in *Drosophila* (Al-Jubran et al., 2013), reflects that the RPM technique might still be useful for localising translation sites when labelling can be achieved with very a brief puromycin exposure time. It will therefore be interesting and informative to pursue puromycylation further as an assay to investigate whether localised translation occurs at the growing tips of *S. pombe* cells under stress conditions. Strains which carry both the temperature sensitive mutation for mRNA export and a tagged ribosomal protein have

been constructed. These strains can be puromycylated for different time periods followed by double-immunostaining for puromycin and the RP tag, to determine i) whether the puromycin signal changes over time and ii) how this signal relates to that of the tagged ribosomal protein. Additionally, construction of other strains in which ribosomal proteins on both subunits are tagged with different epitopes is under way. These strains can be used both with and without parallel puromycylation to visualise sites at which signals for both ribosomal subunits are in close proximity using the super-resolution microscope; this will be indicative of the presence of translating ribosomes.

References

ABDULLAHI, A. 2014. *Visualisation of Ribosomal Subunits Interaction Reveals 80S Ribosomes in the Nucleus of Drosophila Cells.* PhD, University of Birmingham.

ABELSON, J., BLANCO, M., DITZLER, M. A., FULLER, F., ARAVAMUDHAN, P., WOOD, M., VILLA, T., RYAN, D. E., PLEISS, J. A., MAEDER, C., GUTHRIE, C. & WALTER, N. G. 2010. Conformational dynamics of single pre-mRNA molecules during in vitro splicing. *Nat Struct Mol Biol,* 17**,** 504-12.

ABRUZZI, K. C., LACADIE, S. & ROSBASH, M. 2004. Biochemical analysis of TREX complex recruitment to intronless and intron-containing yeast genes. *EMBO J,* 23**,** 2620-31.

AL-JUBRAN, K., WEN, J., ABDULLAHI, A., ROY CHAUDHURY, S., LI, M., RAMANATHAN, P., MATINA, A., DE, S., PIECHOCKI, K., RUGJEE, K. N. & BROGNA, S. 2013. Visualization of the joining of ribosomal subunits reveals the presence of 80S ribosomes in the nucleus. *RNA,* 19**,** 1669-83.

ALLEN, W. R. & WILT, F. H. 1976. The amount of nuclear protein synthesis in sea urchin blastulae. *Exp Cell Res,* 97**,** 151-63.

ALLFREY, V. G. 1954. Amino Acid Incorporation by Isolated Thymus Nuclei. I. The Role of Desoxyribonucleic Acid in Protein Synthesis. *Proc Natl Acad Sci U S A,* 40**,** 881-5.

ALLFREY, V. G., LITTAU, V. C. & MIRSKY, A. E. 1964. Methods for the Purification of Thymus Nuclei and Their Application to Studies of Nuclear Protein Synthesis. *J Cell Biol,* 21**,** 213-31.

AMRANI, N., DONG, S., HE, F., GANESAN, R., GHOSH, S., KERVESTIN, S., LI, C., MANGUS, D. A., SPATRICK, P. & JACOBSON, A. 2006. Aberrant termination triggers nonsense-mediated mRNA decay. *Biochem Soc Trans,* 34**,** 39-42.

AMRANI, N., GANESAN, R., KERVESTIN, S., MANGUS, D. A., GHOSH, S. & JACOBSON, A. 2004. A faux 3'-UTR promotes aberrant termination and triggers nonsense-mediated mRNA decay. *Nature,* 432**,** 112-8.

ANDERS, K. R., GRIMSON, A. & ANDERSON, P. 2003. SMG-5, required for C.elegans nonsense-mediated mRNA decay, associates with SMG-2 and protein phosphatase 2A. *EMBO J,* 22**,** 641-50.

ANDERSEN, C. B., BALLUT, L., JOHANSEN, J. S., CHAMIEH, H., NIELSEN, K. H., OLIVEIRA, C. L., PEDERSEN, J. S., SERAPHIN, B., LE HIR, H. & ANDERSEN, G. R. 2006. Structure of the exon junction core complex with a trapped DEAD-box ATPase bound to RNA. *Science,* 313**,** 1968-72.

ANGER, A. M., ARMACHE, J. P., BERNINGHAUSEN, O., HABECK, M., SUBKLEWE, M., WILSON, D. N. & BECKMANN, R. 2013. Structures of the human and Drosophila 80S ribosome. *Nature,* 497**,** 80-5.

APARICIO, O., GEISBERG, J. V., SEKINGER, E., YANG, A., MOQTADERI, Z. & STRUHL, K. 2005. Chromatin immunoprecipitation for determining the association of proteins with specific gene sequences in vivo. *Curr. Protoc. Mol. Biol.*

APCHER, S., DASKALOGIANNI, C., LEJEUNE, F., MANOURY, B., IMHOOS, G., HESLOP, L. & FAHRAEUS, R. 2011. Major source of antigenic peptides for the MHC class I pathway is produced during the pioneer round of mRNA translation. *Proc Natl Acad Sci U S A,* 108**,** 11572-7.

APCHER, S., MILLOT, G., DASKALOGIANNI, C., SCHERL, A., MANOURY, B. & FAHRAEUS, R. 2013. Translation of pre-spliced RNAs in the nuclear compartment generates peptides for the MHC class I pathway. *Proc Natl Acad Sci U S A,* 110**,** 17951-6.

ARMACHE, J. P., JARASCH, A., ANGER, A. M., VILLA, E., BECKER, T., BHUSHAN, S., JOSSINET, F., HABECK, M., DINDAR, G., FRANCKENBERG, S., MARQUEZ, V., MIELKE, T., THOMM, M., BERNINGHAUSEN, O., BEATRIX, B., SODING, J., WESTHOF, E., WILSON, D. N. & BECKMANN, R. 2010. Cryo-EM structure and rRNA model of a translating eukaryotic 80S ribosome at 5.5-A resolution. *Proc Natl Acad Sci U S A,* 107**,** 19748-53.

ATILGAN, E., MAGIDSON, V., KHODJAKOV, A. & CHANG, F. 2015. Morphogenesis of the Fission Yeast Cell through Cell Wall Expansion. *Curr Biol,* 25**,** 2150-7.

AZAD, A. K., TANI, T., SHIKI, N., TSUNEYOSHI, S., URUSHIYAMA, S. & OHSHIMA, Y. 1997. Isolation and molecular characterization of mRNA transport mutants in Schizosaccharomyces pombe. *Mol Biol Cell,* 8**,** 825-41.

BABIANO, R., BADIS, G., SAVEANU, C., NAMANE, A., DOYEN, A., DIAZ-QUINTANA, A., JACQUIER, A., FROMONT-RACINE, M. & DE LA CRUZ, J. 2013. Yeast ribosomal protein L7 and its homologue Rlp7 are simultaneously present at distinct sites on pre-60S ribosomal particles. *Nucleic Acids Res,* 41**,** 9461-70.

BADIS, G., SAVEANU, C., FROMONT-RACINE, M. & JACQUIER, A. 2004. Targeted mRNA degradation by deadenylation-independent decapping. *Mol Cell,* 15**,** 5-15.

BAKER, K. E. & PARKER, R. 2006. Conventional 3' end formation is not required for NMD substrate recognition in Saccharomyces cerevisiae. *RNA,* 12**,** 1441-5.

BALIGA, B. S., COHEN, S. A. & MUNRO, H. N. 1970. Effect of cycloheximide on the reaction of puromycin with polysome-bound peptidyl-tRNA. *FEBS Lett,* 8**,** 249-252.

BARTA, A., STEINER, G., BROSIUS, J., NOLLER, H. F. & KUECHLER, E. 1984. Identification of a site on 23S ribosomal RNA located at the peptidyl transferase center. *Proc Natl Acad Sci U S A,* 81**,** 3607-11.

BASERGA, S. J. & BENZ, E. J., JR. 1992. Beta-globin nonsense mutation: deficient accumulation of mRNA occurs despite normal cytoplasmic stability. *Proc Natl Acad Sci U S A,* 89**,** 2935-9.

BEDWELL, D. M., KAENJAK, A., BENOS, D. J., BEBOK, Z., BUBIEN, J. K., HONG, J., TOUSSON, A., CLANCY, J. P. & SORSCHER, E. J. 1997. Suppression of a CFTR premature stop mutation in a bronchial epithelial cell line. *Nat Med,* 3**,** 1280-4.

BEHM-ANSMANT, I., GATFIELD, D., REHWINKEL, J., HILGERS, V. & IZAURRALDE, E. 2007. A conserved role for cytoplasmic poly(A)-binding protein 1 (PABPC1) in nonsense-mediated mRNA decay. *EMBO J,* 26**,** 1591-601.

BELGRADER, P., CHENG, J. & MAQUAT, L. E. 1993. Evidence to implicate translation by ribosomes in the mechanism by which nonsense codons reduce the nuclear level of human triosephosphate isomerase mRNA. *Proc Natl Acad Sci U S A,* 90**,** 482-6.

BELGRADER, P., CHENG, J., ZHOU, X., STEPHENSON, L. S. & MAQUAT, L. E. 1994. Mammalian nonsense codons can be cis effectors of nuclear mRNA half-life. *Mol Cell Biol,* 14**,** 8219-28.

BEN-SHEM, A., GARREAU DE LOUBRESSE, N., MELNIKOV, S., JENNER, L., YUSUPOVA, G. & YUSUPOV, M. 2011. The structure of the eukaryotic ribosome at 3.0 A resolution. *Science,* 334**,** 1524-9.

BERGET, S. M., MOORE, C. & SHARP, P. A. 1977. Spliced segments at the 5' terminus of adenovirus 2 late mRNA. *Proc Natl Acad Sci U S A,* 74**,** 3171-5.

BERINGER, M. & RODNINA, M. V. 2007. The ribosomal peptidyl transferase. *Mol Cell,* 26**,** 311-21.

BEYER, A. L. & OSHEIM, Y. N. 1988. Splice site selection, rate of splicing, and alternative splicing on nascent transcripts. *Genes Dev,* 2**,** 754-65.

BHATTACHARYA, A., CZAPLINSKI, K., TRIFILLIS, P., HE, F., JACOBSON, A. & PELTZ, S. W. 2000. Characterization of the biochemical properties of the human Upf1 gene product that is involved in nonsense-mediated mRNA decay. *RNA,* 6**,** 1226-35.

BLOBEL, G. & SABATINI, D. 1971. Dissociation of mammalian polyribosomes into subunits by puromycin. *Proc Natl Acad Sci U S A,* 68**,** 390-4.

BONO, F., EBERT, J., LORENTZEN, E. & CONTI, E. 2006. The crystal structure of the exon junction complex reveals how it maintains a stable grip on mRNA. *Cell,* 126**,** 713-25.

BREITBART, R. E., ANDREADIS, A. & NADAL-GINARD, B. 1987. Alternative splicing: a ubiquitous mechanism for the generation of multiple protein isoforms from single genes. *Annu Rev Biochem,* 56**,** 467-95.

BROCK, J. E., DIETRICH, R. C. & PADGETT, R. A. 2008. Mutational analysis of the U12-dependent branch site consensus sequence. *RNA,* 14**,** 2430-9.

BROCKE, K. S., NEU-YILIK, G., GEHRING, N. H., HENTZE, M. W. & KULOZIK, A. E. 2002. The human intronless melanocortin 4-receptor gene is NMD insensitive. *Hum Mol Genet,* 11**,** 331-5.

BROGNA, S. 1999. Nonsense mutations in the alcohol dehydrogenase gene of Drosophila melanogaster correlate with an abnormal 3' end processing of the corresponding pre-mRNA. *RNA,* 5**,** 562-73.

BROGNA, S., MCLEOD, T. & PETRIC, M. 2016. The Meaning of NMD: Translate or Perish. *Trends Genet,* 32**,** 395-407.

BROGNA, S., SATO, T. A. & ROSBASH, M. 2002. Ribosome components are associated with sites of transcription. *Mol Cell,* 10**,** 93-104.

BROGNA, S. & WEN, J. 2009. Nonsense-mediated mRNA decay (NMD) mechanisms. *Nat Struct Mol Biol,* 16**,** 107-13.

BROW, D. A. 2002. Allosteric cascade of spliceosome activation. *Annu Rev Genet,* 36**,** 333-60.

BUCHWALD, G., EBERT, J., BASQUIN, C., SAULIERE, J., JAYACHANDRAN, U., BONO, F., LE HIR, H. & CONTI, E. 2010. Insights into the recruitment of the NMD machinery from the crystal structure of a core EJC-UPF3b complex. *Proc Natl Acad Sci U S A,* 107**,** 10050-5.

BUHLER, M., STEINER, S., MOHN, F., PAILLUSSON, A. & MUHLEMANN, O. 2006. EJC-independent degradation of nonsense immunoglobulin-mu mRNA depends on 3' UTR length. *Nat Struct Mol Biol,* 13**,** 462-4.

BÜHLER, M., WILKINSON, M. F. & MÜHLEMANN, O. 2002. Intranuclear degradation of nonsense codon-containing mRNA. *EMBO Reports,* 3**,** 646-651.

BURATOWSKI, S. 2009. Progression through the RNA polymerase II CTD cycle. *Mol Cell,* 36**,** 541-6.

CALI, B. M., KUCHMA, S. L., LATHAM, J. & ANDERSON, P. 1999. smg-7 is required for mRNA surveillance in Caenorhabditis elegans. *Genetics,* 151**,** 605-16.

CALZONE, F. J., ANGERER, R. C. & GOROVSKY, M. A. 1982. Regulation of protein synthesis in Tetrahymena: isolation and characterization of polysomes by gel filtration and precipitation at pH 5.3. *Nucleic Acids Res,* 10**,** 2145-61.

CAPUTI, M., KENDZIOR, R. J., JR. & BEEMON, K. L. 2002. A nonsense mutation in the fibrillin-1 gene of a Marfan syndrome patient induces NMD and disrupts an exonic splicing enhancer. *Genes Dev,* 16**,** 1754-9.

CARTER, M. S., LI, S. & WILKINSON, M. F. 1996. A splicing-dependent regulatory mechanism that detects translation signals. *EMBO J,* 15**,** 5965-75.

CECH, T. R. 2000. Structural biology. The ribosome is a ribozyme. *Science,* 289**,** 878-9.

CHAMIEH, H., BALLUT, L., BONNEAU, F. & LE HIR, H. 2008. NMD factors UPF2 and UPF3 bridge UPF1 to the exon junction complex and stimulate its RNA helicase activity. *Nat Struct Mol Biol,* 15**,** 85-93.

CHAVATTE, L., SEIT-NEBI, A., DUBOVAYA, V. & FAVRE, A. 2002. The invariant uridine of stop codons contacts the conserved NIKSR loop of human eRF1 in the ribosome. *EMBO J,* 21**,** 5302-11.

CHENG, J., BELGRADER, P., ZHOU, X. & MAQUAT, L. E. 1994. Introns are cis effectors of the nonsense-codon-mediated reduction in nuclear mRNA abundance. *Mol Cell Biol,* 14**,** 6317-25.

CHENG, J. & MAQUAT, L. E. 1993. Nonsense codons can reduce the abundance of nuclear mRNA without affecting the abundance of pre-mRNA or the half-life of cytoplasmic mRNA. *Mol Cell Biol,* 13**,** 1892-902.

CHOI, K. M. & BRIMACOMBE, R. 1998. The path of the growing peptide chain through the 23S rRNA in the 50S ribosomal subunit; a comparative cross-linking study with three different peptide families. *Nucleic Acids Res,* 26**,** 887-95.

CHOW, L. T., GELINAS, R. E., BROKER, T. R. & ROBERTS, R. J. 1977. An amazing sequence arrangement at the 5' ends of adenovirus 2 messenger RNA. *Cell,* 12**,** 1-8.

COLGAN, D. F. & MANLEY, J. L. 1997. Mechanism and regulation of mRNA polyadenylation. *Genes Dev,* 11**,** 2755-66.

CORDEN, J. L. 2013. RNA polymerase II C-terminal domain: Tethering transcription to transcript and template. *Chem Rev,* 113**,** 8423-55.

COSSON, B., COUTURIER, A., CHABELSKAYA, S., KIKTEV, D., INGE-VECHTOMOV, S., PHILIPPE, M. & ZHOURAVLEVA, G. 2002. Poly(A)-binding protein acts in translation termination via eukaryotic release factor 3 interaction and does not influence [PSI(+)] propagation. *Mol Cell Biol,* 22**,** 3301-15.

COSTELLO, J., CASTELLI, L. M., ROWE, W., KERSHAW, C. J., TALAVERA, D., MOHAMMAD-QURESHI, S. S., SIMS, P. F., GRANT, C. M., PAVITT, G. D., HUBBARD, S. J. & ASHE, M. P. 2015. Global mRNA selection mechanisms for translation initiation. *Genome Biol,* 16**,** 10.

CULBERTSON, M. R. 1999. RNA surveillance. Unforeseen consequences for gene expression, inherited genetic disorders and cancer. *Trends Genet,* 15**,** 74-80.

CULBERTSON, M. R., UNDERBRINK, K. M. & FINK, G. R. 1980. Frameshift suppression in *Saccharomyces cerevisiae.* II. Genetic properties of group II suppressors. *Genetics,* 95**,** 833-853.

CZAPLINSKI, K., RUIZ-ECHEVARRIA, M. J., PAUSHKIN, S. V., HAN, X., WENG, Y., PERLICK, H. A., DIETZ, H. C., TER-AVANESYAN, M. D. & PELTZ, S. W. 1998. The surveillance complex interacts with the translation release factors to enhance termination and degrade aberrant mRNAs. *Genes Dev,* 12**,** 1665-77.

CZAPLINSKI, K., WENG, Y., HAGAN, K. W. & PELTZ, S. W. 1995. Purification and characterization of the Upf1 protein: a factor involved in translation and mRNA degradation. *RNA,* 1**,** 610-23.

DAHLBERG, J. E. & LUND, E. 2004. Does protein synthesis occur in the nucleus? *Curr Opin Cell Biol,* 16**,** 335-8.

DAI, M. S., ARNOLD, H., SUN, X. X., SEARS, R. & LU, H. 2007. Inhibition of c-Myc activity by ribosomal protein L11. *EMBO J,* 26**,** 3332-45.

DANCHIN, E., VITIELLO, V., VIENNE, A., RICHARD, O., GOURET, P., MCDERMOTT, M. F. & PONTAROTTI, P. 2004. The major histocompatibility complex origin. *Immunol Rev,* 198**,** 216-32.

DAVID, A., DOLAN, B. P., HICKMAN, H. D., KNOWLTON, J. J., CLAVARINO, G., PIERRE, P., BENNINK, J. R. & YEWDELL, J. W. 2012. Nuclear translation visualized by ribosome-bound nascent chain puromycylation. *J Cell Biol,* 197**,** 45-57.

DE, S., VARSALLY, W., FALCIANI, F. & BROGNA, S. 2011. Ribosomal proteins' association with transcription sites peaks at tRNA genes in Schizosaccharomyces pombe. *RNA,* 17**,** 1713-26.

DE TURRIS, V., NICHOLSON, P., OROZCO, R. Z., SINGER, R. H. & MUHLEMANN, O. 2011. Cotranscriptional effect of a premature termination codon revealed by live-cell imaging. *RNA,* 17**,** 2094-107.

DELPY, L., SIRAC, C., MAGNOUX, E., DUCHEZ, S. & COGNE, M. 2004. RNA surveillance down-regulates expression of nonfunctional kappa alleles and detects premature termination within the last kappa exon. *Proc Natl Acad Sci U S A,* 101**,** 7375-80.

DEVER, T. E. & GREEN, R. 2012. The elongation, termination, and recycling phases of translation in eukaryotes. *Cold Spring Harb Perspect Biol,* 4**,** a013706.

DIETZ, H. C., VALLE, D., FRANCOMANO, C. A., KENDZIOR, R. J., JR., PYERITZ, R. E. & CUTTING, G. R. 1993. The skipping of constitutive exons in vivo induced by nonsense mutations. *Science,* 259**,** 680-3.

DOSTIE, J. & DREYFUSS, G. 2002. Translation is required to remove Y14 from mRNAs in the cytoplasm. *Curr Biol,* 12**,** 1060-7.

DURAND, S. & LYKKE-ANDERSEN, J. 2013. Nonsense-mediated mRNA decay occurs during eIF4F-dependent translation in human cells. *Nat Struct Mol Biol,* 20**,** 702-9.

EBERLE, A. B., STALDER, L., MATHYS, H., OROZCO, R. Z. & MUHLEMANN, O. 2008. Posttranscriptional gene regulation by spatial rearrangement of the 3' untranslated region. *PLoS Biol,* 6**,** e92.

ERICKSON, H. P. 2009. Size and shape of protein molecules at the nanometer level determined by sedimentation, gel filtration, and electron microscopy. *Biol Proced Online,* 11**,** 32-51.

EVERS, D. L., FOWLER, C. B., CUNNINGHAM, B. R., MASON, J. T. & O'LEARY, T. J. 2011. The effect of formaldehyde fixation on RNA: optimization of formaldehyde adduct removal. *J Mol Diagn,* 13**,** 282-8.

FATSCHER, T., BOEHM, V. & GEHRING, N. H. 2015. Mechanism, factors, and physiological role of nonsense-mediated mRNA decay. *Cell Mol Life Sci,* 72**,** 4523-44.

FERRAIUOLO, M. A., LEE, C. S., LER, L. W., HSU, J. L., COSTA-MATTIOLI, M., LUO, M. J., REED, R. & SONENBERG, N. 2004. A nuclear translation-like factor eIF4AIII is recruited to the mRNA during splicing and functions in nonsense-mediated decay. *Proc Natl Acad Sci U S A,* 101**,** 4118-23.

FEWELL, S. W. & WOOLFORD, J. L., JR. 1999. Ribosomal protein S14 of Saccharomyces cerevisiae regulates its expression by binding to RPS14B pre-mRNA and to 18S rRNA. *Mol Cell Biol,* 19**,** 826-34.

FIORINI, F., BOUDVILLAIN, M. & LE HIR, H. 2013. Tight intramolecular regulation of the human Upf1 helicase by its N- and C-terminal domains. *Nucleic Acids Res,* 41**,** 2404-15.

FONG, N. & BENTLEY, D. L. 2001. Capping, splicing, and 3' processing are independently stimulated by RNA polymerase II: different functions for different segments of the CTD. *Genes Dev,* 15**,** 1783-95.

FORSBURG, S. L. & RHIND, N. 2006. Basic methods for fission yeast. *Yeast,* 23**,** 173-83.

FRISCHMEYER, P. A. & DIETZ, H. C. 1999. Nonsense-mediated mRNA decay in health and disease. *Hum Mol Genet,* 8**,** 1893-900.

GALLIE, D. R. & TANGUAY, R. 1994. Poly(A) binds to initiation factors and increases cap-dependent translation in vitro. *J Biol Chem,* 269**,** 17166-73.

GAO, Q., DAS, B., SHERMAN, F. & MAQUAT, L. E. 2005. Cap-binding protein 1-mediated and eukaryotic initiation factor 4E-mediated pioneer rounds of translation in yeast. *PNAS,* 102**,** 4258-4263.

GATFIELD, D., UNTERHOLZNER, L., CICCARELLI, F. D., BORK, P. & IZAURRALDE, E. 2003. Nonsense-mediated mRNA decay in Drosophila: at the intersection of the yeast and mammalian pathways. *EMBO J,* 22**,** 3960-70.

GEHRING, N. H., NEU-YILIK, G., SCHELL, T., HENTZE, M. W. & KULOZIK, A. E. 2003. Y14 and hUpf3b form an NMD-activating complex. *Mol Cell,* 11**,** 939-49.

GIBSON, R. A., HAJIANPOUR, A., MURER-ORLANDO, M., BUCHWALD, M. & MATHEW, C. G. 1993. A nonsense mutation and exon skipping in the Fanconi anaemia group C gene. *Hum Mol Genet,* 2**,** 797-9.

GOIDL, J. A. & ALLEN, W. 1978. Does protein synthesis occur within the nucleus? . *Trends Biol. Sci.,* 3**,** N225-N228.

GOIDL, J. A., CANAANI, D., BOUBLIK, M., WEISSBACH, H. & DICKERMAN, H. 1975. Polyanion-induced release of polyribosomes from HeLa cell nuclei. *J Biol Chem,* 250**,** 9198-205.

GONZALEZ, C. I., RUIZ-ECHEVARRIA, M. J., VASUDEVAN, S., HENRY, M. F. & PELTZ, S. W. 2000. The yeast hnRNP-like protein Hrp1/Nab4 marks a transcript for nonsense-mediated mRNA decay. *Mol Cell,* 5**,** 489-99.

GOSS, D. J. & KLEIMAN, F. E. 2013. Poly(A) binding proteins: are they all created equal? *Wiley Interdiscip Rev RNA,* 4**,** 167-79.

GRAIFER, D., MALYGIN, A., ZHARKOV, D. O. & KARPOVA, G. 2014. Eukaryotic ribosomal protein S3: A constituent of translational machinery and an extraribosomal player in various cellular processes. *Biochimie,* 99**,** 8-18.

GRANDI, P., RYBIN, V., BASSLER, J., PETFALSKI, E., STRAUSS, D., MARZIOCH, M., SCHAFER, T., KUSTER, B., TSCHOCHNER, H., TOLLERVEY, D., GAVIN, A. C. & HURT, E. 2002. 90S pre-ribosomes include the 35S pre-rRNA, the U3 snoRNP, and 40S subunit processing factors but predominantly lack 60S synthesis factors. *Mol Cell,* 10**,** 105-15.

GREEN, M. R. & SAMBROOK, J. 2012. *Molecular Cloning: A Laboratory Manual (Fourth Edition),* New York, Cold Spring Harbor Laboratory Press.

GRIMSON, A., O'CONNOR, S., NEWMAN, C. L. & ANDERSON, P. 2004. SMG-1 is a phosphatidylinositol kinase-related protein kinase required for nonsense-mediated mRNA Decay in Caenorhabditis elegans. *Mol Cell Biol,* 24**,** 7483-90.

GROLLMAN, A. P. 1966. Structural basis for inhibition of protein synthesis by emetine and cycloheximide based on an analogy between ipecac alkaloids and glutarimide antibiotics. *Proc Natl Acad Sci U S A,* 56**,** 1867-74.

GROLLMAN, A. P. 1968. Inhibitors of protein biosynthesis. V. Effects of emetine on protein and nucleic acid biosynthesis in HeLa cells. *J Biol Chem,* 243**,** 4089-94.

GUAN, Q., ZHENG, W., TANG, S., LIU, X., ZINKEL, R. A., TSUI, K. W., YANDELL, B. S. & CULBERTSON, M. R. 2006. Impact of nonsense-mediated mRNA decay on the global expression profile of budding yeast. *PLoS Genet,* 2**,** e203.

HAGAN, K. W., RUIZ-ECHEVARRIA, M. J., QUAN, Y. & PELTZ, S. W. 1995. Characterization of cis-acting sequences and decay intermediates involved in nonsense-mediated mRNA turnover. *Mol Cell Biol,* 15**,** 809-23.

HALL, G. W. & THEIN, S. 1994. Nonsense codon mutations in the terminal exon of the beta-globin gene are not associated with a reduction in beta-mRNA accumulation: a mechanism for the phenotype of dominant beta-thalassemia. *Blood,* 83**,** 2031-7.

HAMID, F. M. & MAKEYEV, E. V. 2014. Emerging functions of alternative splicing coupled with nonsense-mediated decay. *Biochem Soc Trans,* 42**,** 1168-73.

HE, F., BROWN, A. H. & JACOBSON, A. 1997. Upf1p, Nmd2p, and Upf3p are interacting components of the yeast nonsense-mediated mRNA decay pathway. *Mol Cell Biol,* 17**,** 1580-94.

HEITZ, E. 1931. Die ursache der gesetzmassigen zahl, lage, form und grosse pflanzlicher nukleolen. *Planta,* 12**,** 775-884.

HILLEREN, P. & PARKER, R. 1999. mRNA surveillance in eukaryotes: kinetic proofreading of proper translation termination as assessed by mRNP domain organization? *RNA,* 5**,** 711-9.

HINNEBUSCH, A. G. & LORSCH, J. R. 2012. The mechanism of eukaryotic translation initiation: new insights and challenges. *Cold Spring Harb Perspect Biol,* 4.

HIRATA, M. & OKAMOTO, Y. 1987. Enumeration of terminal deoxynucleotidyl transferase positive cells in leukemia/lymphoma by flow cytometry. *Leuk Res,* 11**,** 509-18.

HIROKAWA, G., KIEL, M. C., MUTO, A., SELMER, M., RAJ, V. S., LILJAS, A., IGARASHI, K., KAJI, H. & KAJI, A. 2002. Post-termination complex disassembly by ribosome recycling factor, a functional tRNA mimic. *EMBO J,* 21**,** 2272-81.

HODGKIN, J., PAPP, A., PULAK, R., AMBROS, V. & ANDERSON, P. 1989. A new kind of informational suppression in the nematode Caenorhabditis elegans. *Genetics,* 123**,** 301-13.

HOLT, C. E. & SCHUMAN, E. M. 2013. The central dogma decentralized: new perspectives on RNA function and local translation in neurons. *Neuron,* 80**,** 648-57.

HOSHINO, S., IMAI, M., KOBAYASHI, T., UCHIDA, N. & KATADA, T. 1999. The eukaryotic polypeptide chain releasing factor (eRF3/GSPT) carrying the translation termination signal to the 3'-Poly(A) tail of mRNA. Direct association of erf3/GSPT with polyadenylate-binding protein. *J Biol Chem,* 274**,** 16677-80.

HOSODA, N., KIM, Y. K., LEJEUNE, F. & MAQUAT, L. E. 2005. CBP80 promotes interaction of Upf1 with Upf2 during nonsense-mediated mRNA decay in mammalian cells. *Nat Struct Mol Biol,* 12**,** 893-901.

HSIN, J. P. & MANLEY, J. L. 2012. The RNA polymerase II CTD coordinates transcription and RNA processing. *Genes Dev,* 26**,** 2119-37.

IBORRA, F. J., ESCARGUEIL, A. E., KWEK, K. Y., AKOULITCHEV, A. & COOK, P. R. 2004. Molecular cross-talk between the transcription, translation, and nonsense-mediated decay machineries. *J Cell Sci,* 117**,** 899-906.

IBORRA, F. J., JACKSON, D. A. & COOK, P. R. 2001. Coupled transcription and translation within nuclei of mammalian cells. *Science,* 293**,** 1139-42.

IOANNOU, M., COUTSOGEORGOPOULOS, C. & SYNETOS, D. 1998. Kinetics of inhibition of rabbit reticulocyte peptidyltransferase by anisomycin and sparsomycin. *Mol Pharmacol,* 53**,** 1089-96.

ISHIGAKI, Y., LI, X., SERIN, G. & MAQUAT, L. E. 2001. Evidence for a pioneer round of mRNA translation: mRNAs subject to nonsense-mediated decay in mammalian cells are bound by CBP80 and CBP20. *Cell,* 106**,** 607-17.

ISKEN, O., KIM, Y. K., HOSODA, N., MAYEUR, G. L., HERSHEY, J. W. & MAQUAT, L. E. 2008. Upf1 phosphorylation triggers translational repression during nonsense-mediated mRNA decay. *Cell,* 133**,** 314-27.

ITO, K., UNO, M. & NAKAMURA, Y. 2000. A tripeptide 'anticodon' deciphers stop codons in messenger RNA. *Nature,* 403**,** 680-4.

JACKSON, R. J., HELLEN, C. U. & PESTOVA, T. V. 2010. The mechanism of eukaryotic translation initiation and principles of its regulation. *Nat Rev Mol Cell Biol,* 11**,** 113-27.

KAPP, L. D. & LORSCH, J. R. 2004. The molecular mechanics of eukaryotic translation. *Annu Rev Biochem,* 73**,** 657-704.

KASHIMA, I., YAMASHITA, A., IZUMI, N., KATAOKA, N., MORISHITA, R., HOSHINO, S., OHNO, M., DREYFUSS, G. & OHNO, S. 2006. Binding of a novel SMG-1-Upf1-eRF1-eRF3 complex (SURF) to the exon junction complex triggers Upf1 phosphorylation and nonsense-mediated mRNA decay. *Genes Dev,* 20**,** 355-67.

KHARE, A. K., SINGH, B. & SINGH, J. 2011. A fast and inexpensive method for random spore analysis in Schizosaccharomyces pombe. *Yeast,* 28**,** 527-33.

KIEL, M. C., KAJI, H. & KAJI, A. 2007. Ribosome recycling: An essential process of protein synthesis. *Biochem Mol Biol Educ,* 35**,** 40-4.

KIETRYS, A. M., SZOPA, A. & BAKOWSKA-ZYWICKA, K. 2009. Structure and function of intersubunit bridges in procaryotic ribosome. *Biotechnologia,* 1**,** 48-58.

KIM, S. H., KOROLEVA, O. A., LEWANDOWSKA, D., PENDLE, A. F., CLARK, G. P., SIMPSON, C. G., SHAW, P. J. & BROWN, J. W. 2009. Aberrant mRNA transcripts and the nonsense-mediated

decay proteins UPF2 and UPF3 are enriched in the Arabidopsis nucleolus. *Plant Cell,* 21**,** 2045-57.

KISLINGER, T., COX, B., KANNAN, A., CHUNG, C., HU, P., IGNATCHENKO, A., SCOTT, M. S., GRAMOLINI, A. O., MORRIS, Q., HALLETT, M. T., ROSSANT, J., HUGHES, T. R., FREY, B. & EMILI, A. 2006. Global survey of organ and organelle protein expression in mouse: combined proteomic and transcriptomic profiling. *Cell,* 125**,** 173-86.

KOBAYASHI, T., NOMURA, M. & HORIUCHI, T. 2001. Identification of DNA cis elements essential for expansion of ribosomal DNA repeats in Saccharomyces cerevisiae. *Mol Cell Biol,* 21**,** 136-47.

KOMARNITSKY, P., CHO, E. J. & BURATOWSKI, S. 2000. Different phosphorylated forms of RNA polymerase II and associated mRNA processing factors during transcription. *Genes Dev,* 14**,** 2452-60.

KONDRASHOV, N., PUSIC, A., STUMPF, C. R., SHIMIZU, K., HSIEH, A. C., XUE, S., ISHIJIMA, J., SHIROISHI, T. & BARNA, M. 2011. Ribosome-mediated specificity in Hox mRNA translation and vertebrate tissue patterning. *Cell,* 145**,** 383-97.

KOPP, K., GASIOROWSKI, J. Z., CHEN, D., GILMORE, R., NORTON, J. T., WANG, C., LEARY, D. J., CHAN, E. K., DEAN, D. A. & HUANG, S. 2007. Pol I transcription and pre-rRNA processing are coordinated in a transcription-dependent manner in mammalian cells. *Mol Biol Cell,* 18**,** 394-403.

KOROSTELEV, A., ASAHARA, H., LANCASTER, L., LAURBERG, M., HIRSCHI, A., ZHU, J., TRAKHANOV, S., SCOTT, W. G. & NOLLER, H. F. 2008. Crystal structure of a translation termination complex formed with release factor RF2. *Proc Natl Acad Sci U S A,* 105**,** 19684-9.

KOZAK, M. 1999. Initiation of translation in prokaryotes and eukaryotes. *Gene,* 234**,** 187-208.

KOZAK, M. 2001. Constraints on reinitiation of translation in mammals. *Nucleic Acids Res,* 29**,** 5226-32.

KUPERWASSER, N., BROGNA, S., DOWER, K. & ROSBASH, M. 2004. Nonsense-mediated decay does not occur within the yeast nucleus. *RNA,* 10**,** 1907-15.

LAGE, H. 2003. ABC-transporters: implications on drug resistance from microorganisms to human cancers. *Int J Antimicrob Agents,* 22**,** 188-99.

LE HIR, H., GATFIELD, D., IZAURRALDE, E. & MOORE, M. J. 2001. The exon-exon junction complex provides a binding platform for factors involved in mRNA export and nonsense-mediated mRNA decay. *EMBO J,* 20**,** 4987-97.

LE HIR, H., IZAURRALDE, E., MAQUAT, L. E. & MOORE, M. J. 2000a. The spliceosome deposits multiple proteins 20-24 nucleotides upstream of mRNA exon-exon junctions. *EMBO J,* 19**,** 6860-9.

LE HIR, H., MOORE, M. J. & MAQUAT, L. E. 2000b. Pre-mRNA splicing alters mRNP composition: evidence for stable association of proteins at exon-exon junctions. *Genes Dev,* 14**,** 1098-108.

LEBARON, S., SCHNEIDER, C., VAN NUES, R. W., SWIATKOWSKA, A., WALSH, D., BOTTCHER, B., GRANNEMAN, S., WATKINS, N. J. & TOLLERVEY, D. 2012. Proofreading of pre-40S ribosome maturation by a translation initiation factor and 60S subunits. *Nat Struct Mol Biol,* 19**,** 744-53.

LEEDS, P., PELTZ, S. W., JACOBSON, A. & CULBERTSON, M. R. 1991. The product of the yeast UPF1 gene is required for rapid turnover of mRNAs containing a premature translational termination codon. *Genes Dev,* 5**,** 2303-14.

LEEDS, P., WOOD, J. M., LEE, B. S. & CULBERTSON, M. R. 1992. Gene products that promote mRNA turnover in Saccharomyces cerevisiae. *Mol Cell Biol,* 12**,** 2165-77.

LEJEUNE, F., ISHIGAKI, Y., LI, X. & MAQUAT, L. E. 2002. The exon junction complex is detected on CBP80-bound but not eIF4E-bound mRNA in mammalian cells: dynamics of mRNP remodeling. *EMBO J,* 21**,** 3536-45.

LELIVELT, M. J. & CULBERTSON, M. R. 1999. Yeast Upf proteins required for RNA surveillance affect global expression of the yeast transcriptome. *Mol Cell Biol,* 19**,** 6710-9.

LESNIK, C., GOLANI-ARMON, A. & ARAVA, Y. 2015. Localized translation near the mitochondrial outer membrane: An update. *RNA Biol,* 12**,** 801-9.

LI, B., WACHTEL, C., MIRIAMI, E., YAHALOM, G., FRIEDLANDER, G., SHARON, G., SPERLING, R. & SPERLING, J. 2002. Stop codons affect 5' splice site selection by surveillance of splicing. *Proc Natl Acad Sci U S A,* 99**,** 5277-82.

LI, Q., KIM, Y., NAMM, J., KULKARNI, A., ROSANIA, G. R., AHN, Y. H. & CHANG, Y. T. 2006. RNA-selective, live cell imaging probes for studying nuclear structure and function. *Chem Biol,* 13**,** 615-23.

LING, C. & ERMOLENKO, D. N. 2016. Structural insights into ribosome translocation. *Wiley Interdiscip Rev RNA,* 7**,** 620-36.

LONGMAN, D., PLASTERK, R. H., JOHNSTONE, I. L. & CACERES, J. F. 2007. Mechanistic insights and identification of two novel factors in the C. elegans NMD pathway. *Genes Dev,* 21**,** 1075-85.

LOSSON, R. & LACROUTE, F. 1979. Interference of nonsense mutations with eukaryotic messenger RNA stability. *Proc Natl Acad Sci U S A,* 76**,** 5134-7.

LYKKE-ANDERSEN, J., SHU, M. D. & STEITZ, J. A. 2000. Human Upf proteins target an mRNA for nonsense-mediated decay when bound downstream of a termination codon. *Cell,* 103**,** 1121-31.

LYKKE-ANDERSEN, J., SHU, M. D. & STEITZ, J. A. 2001. Communication of the position of exon-exon junctions to the mRNA surveillance machinery by the protein RNPS1. *Science,* 293**,** 1836-9.

MAGUIRE, B. A. & ZIMMERMANN, R. A. 2001. The ribosome in focus. *Cell,* 104**,** 813-6.

MAQUAT, L. E. 1995. When cells stop making sense: effects of nonsense codons on RNA metabolism in vertebrate cells. *RNA,* 1**,** 453-65.

MAQUAT, L. E. 2002. NASty effects on fibrillin pre-mRNA splicing: another case of ESE does it, but proposals for translation-dependent splice site choice live on. *Genes Dev,* 16**,** 1743-53.

MAQUAT, L. E. & LI, X. 2001. Mammalian heat shock p70 and histone H4 transcripts, which derive from naturally intronless genes, are immune to nonsense-mediated decay. *RNA,* 7**,** 445-56.

MARTIN, W. & KOONIN, E. V. 2006. Introns and the origin of nucleus-cytosol compartmentalization. *Nature,* 440**,** 41-5.

MATLIN, A. J., CLARK, F. & SMITH, C. W. 2005. Understanding alternative splicing: towards a cellular code. *Nat Rev Mol Cell Biol,* 6**,** 386-98.

MATSUO, Y., ASAKAWA, K., TODA, T. & KATAYAMA, S. 2006. A rapid method for protein extraction from fission yeast. *Biosci Biotechnol Biochem,* 70**,** 1992-4.

MATSUYAMA, A., ARAI, R., YASHIRODA, Y., SHIRAI, A., KAMATA, A., SEKIDO, S., KOBAYASHI, Y., HASHIMOTO, A., HAMAMOTO, M., HIRAOKA, Y., HORINOUCHI, S. & YOSHIDA, M. 2006. ORFeome cloning and global analysis of protein localization in the fission yeast Schizosaccharomyces pombe. *Nat Biotechnol,* 24**,** 841-7.

MCCLINTOCK, B. 1934. The relation of a particular chromosomal element to the development of the nucleoli in Zea mays. *Z. Zellforschung und Mikrosk Anat,* 21**,** 294-326.

MCCRACKEN, S., FONG, N., YANKULOV, K., BALLANTYNE, S., PAN, G., GREENBLATT, J., PATTERSON, S. D., WICKENS, M. & BENTLEY, D. L. 1997. The C-terminal domain of RNA polymerase II couples mRNA processing to transcription. *Nature,* 385**,** 357-61.

MCGARY, K. & NUDLER, E. 2013. RNA polymerase and the ribosome: the close relationship. *Curr Opin Microbiol,* 16**,** 112-7.

MCKEEHAN, W. & HARDESTY, B. 1969. The mechanism of cycloheximide inhibition of protein synthesis in rabbit reticulocytes. *Biochem Biophys Res Commun,* 36**,** 625-30.

MCLEOD, T., ABDULLAHI, A., LI, M. & BROGNA, S. 2014. Recent studies implicate the nucleolus as the major site of nuclear translation. *Biochem Soc Trans,* 42**,** 1224-8.

MEHLIN, H., DANEHOLT, B. & SKOGLUND, U. 1992. Translocation of a specific premessenger ribonucleoprotein particle through the nuclear pore studied with electron microscope tomography. *Cell,* 69**,** 605-13.

MELERO, R., BUCHWALD, G., CASTANO, R., RAABE, M., GIL, D., LAZARO, M., URLAUB, H., CONTI, E. & LLORCA, O. 2012. The cryo-EM structure of the UPF-EJC complex shows UPF1 poised toward the RNA 3' end. *Nat Struct Mol Biol,* 19**,** 498-505, S1-2.

MELNIKOV, S., BEN-SHEM, A., GARREAU DE LOUBRESSE, N., JENNER, L., YUSUPOVA, G. & YUSUPOV, M. 2012. One core, two shells: bacterial and eukaryotic ribosomes. *Nat Struct Mol Biol,* 19**,** 560-7.

MENDELL, J. T. & DIETZ, H. C. 2001. When the message goes awry: disease-producing mutations that influence mRNA content and performance. *Cell,* 107**,** 411-4.

MENDELL, J. T., SHARIFI, N. A., MEYERS, J. L., MARTINEZ-MURILLO, F. & DIETZ, H. C. 2004. Nonsense surveillance regulates expression of diverse classes of mammalian transcripts and mutes genomic noise. *Nat Genet,* 36**,** 1073-8.

MOORE, M. J. & PROUDFOOT, N. J. 2009. Pre-mRNA processing reaches back to transcription and ahead to translation. *Cell,* 136**,** 688-700.

MOROZOV, I. Y., JONES, M. G., GOULD, P. D., CROME, V., WILSON, J. B., HALL, A. J., RIGDEN, D. J. & CADDICK, M. X. 2012. mRNA 3' tagging is induced by nonsense-mediated decay and promotes ribosome dissociation. *Mol Cell Biol,* 32**,** 2585-95.

MUHLEMANN, O., EBERLE, A. B., STALDER, L. & ZAMUDIO OROZCO, R. 2008. Recognition and elimination of nonsense mRNA. *Biochim Biophys Acta,* 1779**,** 538-49.

MUHLEMANN, O., MOCK-CASAGRANDE, C. S., WANG, J., LI, S., CUSTODIO, N., CARMO-FONSECA, M., WILKINSON, M. F. & MOORE, M. J. 2001. Precursor RNAs harboring nonsense codons accumulate near the site of transcription. *Mol Cell,* 8**,** 33-43.

MUHLRAD, D. & PARKER, R. 1999. Aberrant mRNAs with extended 3' UTRs are substrates for rapid degradation by mRNA surveillance. *RNA,* 5**,** 1299-1307.

NAEGER, L. K., SCHOBORG, R. V., ZHAO, Q., TULLIS, G. E. & PINTEL, D. J. 1992. Nonsense mutations inhibit splicing of MVM RNA in cis when they interrupt the reading frame of either exon of the final spliced product. *Genes Dev,* 6**,** 1107-19.

NAG, A., NARSINH, K. & MARTINSON, H. G. 2007. The poly(A)-dependent transcriptional pause is mediated by CPSF acting on the body of the polymerase. *Nat Struct Mol Biol,* 14**,** 662-9.

NATHANSON, L., XIA, T. & DEUTSCHER, M. P. 2003. Nuclear protein synthesis: a re-evaluation. *RNA,* 9**,** 9-13.

NOLLER, H. F., HOFFARTH, V. & ZIMNIAK, L. 1992. Unusual resistance of peptidyl transferase to protein extraction procedures. *Science,* 256**,** 1416-9.

NURENBERG, E. & TAMPE, R. 2013. Tying up loose ends: ribosome recycling in eukaryotes and archaea. *Trends Biochem Sci,* 38**,** 64-74.

NYIKO, T., KERENYI, F., SZABADKAI, L., BENKOVICS, A. H., MAJOR, P., SONKOLY, B., MERAI, Z., BARTA, E., NIEMIEC, E., KUFEL, J. & SILHAVY, D. 2013. Plant nonsense-mediated mRNA decay is controlled by different autoregulatory circuits and can be induced by an EJC-like complex. *Nucleic Acids Res,* 41**,** 6715-28.

OHNISHI, T., YAMASHITA, A., KASHIMA, I., SCHELL, T., ANDERS, K. R., GRIMSON, A., HACHIYA, T., HENTZE, M. W., ANDERSON, P. & OHNO, S. 2003. Phosphorylation of hUPF1 induces formation of mRNA surveillance complexes containing hSMG-5 and hSMG-7. *Mol Cell,* 12**,** 1187-200.

OKADA-KATSUHATA, Y., YAMASHITA, A., KUTSUZAWA, K., IZUMI, N., HIRAHARA, F. & OHNO, S. 2012. N- and C-terminal Upf1 phosphorylations create binding platforms for SMG-6 and SMG-5:SMG-7 during NMD. *Nucleic Acids Res,* 40**,** 1251-66.

PALACIOS, I. M., GATFIELD, D., ST JOHNSTON, D. & IZAURRALDE, E. 2004. An eIF4AIII-containing complex required for mRNA localization and nonsense-mediated mRNA decay. *Nature,* 427**,** 753-7.

PANSE, V. G. & JOHNSON, A. W. 2010. Maturation of eukaryotic ribosomes: acquisition of functionality. *Trends Biochem Sci,* 35**,** 260-6.

PARKER, M. S., SAH, R., BALASUBRAMANIAM, A., SALLEE, F. R., PARK, E. A. & PARKER, S. L. 2014. On the expansion of ribosomal proteins and RNAs in eukaryotes. *Amino Acids,* 46**,** 1589-604.

PASSMORE, L. A., SCHMEING, T. M., MAAG, D., APPLEFIELD, D. J., ACKER, M. G., ALGIRE, M. A., LORSCH, J. R. & RAMAKRISHNAN, V. 2007. The eukaryotic translation initiation factors eIF1 and eIF1A induce an open conformation of the 40S ribosome. *Mol Cell,* 26**,** 41-50.

PAULSEN, I. T., BROWN, M. H. & SKURRAY, R. A. 1996. Proton-dependent multidrug efflux systems. *Microbiol Rev,* 60**,** 575-608.

PELTZ, S. W., BROWN, A. H. & JACOBSON, A. 1993. mRNA destabilization triggered by premature translational termination depends on at least three cis-acting sequence elements and one trans-acting factor. *Genes Dev,* 7**,** 1737-54.

PENDLE, A. F., CLARK, G. P., BOON, R., LEWANDOWSKA, D., LAM, Y. W., ANDERSEN, J., MANN, M., LAMOND, A. I., BROWN, J. W. & SHAW, P. J. 2005. Proteomic analysis of the Arabidopsis nucleolus suggests novel nucleolar functions. *Mol Biol Cell,* 16**,** 260-9.

PEREIRA, K. D., TAMBORLIN, L., MENEGUELLO, L., DE PROENCA, A. R., ALMEIDA, I. C., LOURENCO, R. F. & LUCHESSI, A. D. 2016. Alternative Start Codon Connects eIF5A to Mitochondria. *J Cell Physiol,* 231**,** 2682-9.

PEREZ CANADILLAS, J. M. & VARANI, G. 2003. Recognition of GU-rich polyadenylation regulatory elements by human CstF-64 protein. *EMBO J,* 22**,** 2821-30.

PESTKA, S. 1971. Inhibitors of ribosome functions. *Annu Rev Microbiol,* 25**,** 487-562.

PETROPOULOS, A. D., MCDONALD, M. E., GREEN, R. & ZAHER, H. S. 2014. Distinct roles for release factor 1 and release factor 2 in translational quality control. *J Biol Chem,* 289**,** 17589-96.

PETROV, A. S., GULEN, B., NORRIS, A. M., KOVACS, N. A., BERNIER, C. R., LANIER, K. A., FOX, G. E., HARVEY, S. C., WARTELL, R. M., HUD, N. V. & WILLIAMS, L. D. 2015. History of the ribosome and the origin of translation. *Proc Natl Acad Sci U S A,* 112**,** 15396-401.

PISAREV, A. V., HELLEN, C. U. & PESTOVA, T. V. 2007. Recycling of eukaryotic posttermination ribosomal complexes. *Cell,* 131**,** 286-99.

PISAREV, A. V., SKABKIN, M. A., PISAREVA, V. P., SKABKINA, O. V., RAKOTONDRAFARA, A. M., HENTZE, M. W., HELLEN, C. U. & PESTOVA, T. V. 2010. The role of ABCE1 in eukaryotic posttermination ribosomal recycling. *Mol Cell,* 37**,** 196-210.

POLLICE, A. A., MCCOY, J. P., JR., SHACKNEY, S. E., SMITH, C. A., AGARWAL, J., BURHOLT, D. R., JANOCKO, L. E., HORNICEK, F. J., SINGH, S. G. & HARTSOCK, R. J. 1992. Sequential

paraformaldehyde and methanol fixation for simultaneous flow cytometric analysis of DNA, cell surface proteins, and intracellular proteins. *Cytometry,* 13**,** 432-44.

PRESUTTI, C., CIAFRE, S. A. & BOZZONI, I. 1991. The ribosomal protein L2 in S. cerevisiae controls the level of accumulation of its own mRNA. *EMBO J,* 10**,** 2215-21.

PREVOT, D., DARLIX, J. L. & OHLMANN, T. 2003. Conducting the initiation of protein synthesis: the role of eIF4G. *Biol Cell,* 95**,** 141-56.

RAJAVEL, K. S. & NEUFELD, E. F. 2001. Nonsense-mediated decay of human HEXA mRNA. *Mol Cell Biol,* 21**,** 5512-9.

RAM, O. & AST, G. 2007. SR proteins: a foot on the exon before the transition from intron to exon definition. *Trends Genet,* 23**,** 5-7.

RAMAGOPAL, S. & ENNIS, H. L. 1981. Regulation of synthesis of cell-specific ribosomal proteins during differentiation of Dictyostelium discoideum. *Proc Natl Acad Sci U S A,* 78**,** 3083-7.

RAMANI, A. K., NELSON, A. C., KAPRANOV, P., BELL, I., GINGERAS, T. R. & FRASER, A. G. 2009. High resolution transcriptome maps for wild-type and nonsense-mediated decay-defective Caenorhabditis elegans. *Genome Biol,* 10**,** R101.

RAMESH, M. & WOOLFORD, J. L., JR. 2016. Eukaryote-specific rRNA expansion segments function in ribosome biogenesis. *RNA,* 22**,** 1153-62.

REHWINKEL, J., LETUNIC, I., RAES, J., BORK, P. & IZAURRALDE, E. 2005. Nonsense-mediated mRNA decay factors act in concert to regulate common mRNA targets. *RNA,* 11**,** 1530-44.

ROBBINS, E. & BORUN, T. W. 1967. The cytoplasmic synthesis of histones in hela cells and its temporal relationship to DNA replication. *Proc Natl Acad Sci U S A,* 57**,** 409-16.

ROUQUETTE, J., CHOESMEL, V. & GLEIZES, P. E. 2005. Nuclear export and cytoplasmic processing of precursors to the 40S ribosomal subunits in mammalian cells. *EMBO J,* 24**,** 2862-72.

RUBIN, G. M. & SULSTON, J. E. 1973. Physical linkage of the 5 S cistrons to the 18 S and 28 S ribosomal RNA cistrons in Saccharomyces cerevisiae. *J Mol Biol,* 79**,** 521-30.

RUFENER, S. C. & MUHLEMANN, O. 2013. eIF4E-bound mRNPs are substrates for nonsense-mediated mRNA decay in mammalian cells. *Nat Struct Mol Biol,* 20**,** 710-7.

RUGJEE, K. N., ROY CHAUDHURY, S., AL-JUBRAN, K., RAMANATHAN, P., MATINA, T., WEN, J. & BROGNA, S. 2013. Fluorescent protein tagging confirms the presence of ribosomal proteins at Drosophila polytene chromosomes. *PeerJ,* 1**,** e15.

RUIZ-ECHEVARRIA, M. J. & PELTZ, S. W. 1996. Utilizing the GCN4 leader region to investigate the role of the sequence determinants in nonsense-mediated mRNA decay. *EMBO J,* 15**,** 2810-9.

SAINI, P., EYLER, D. E., GREEN, R. & DEVER, T. E. 2009. Hypusine-containing protein eIF5A promotes translation elongation. *Nature,* 459**,** 118-21.

SAINT-LEGER, A. & RIBAS DE POUPLANA, L. 2015. The importance of codon-anticodon interactions in translation elongation. *Biochimie,* 114**,** 72-9.

SAULIERE, J., MURIGNEUX, V., WANG, Z., MARQUENET, E., BARBOSA, I., LE TONQUEZE, O., AUDIC, Y., PAILLARD, L., ROEST CROLLIUS, H. & LE HIR, H. 2012. CLIP-seq of eIF4AIII reveals transcriptome-wide mapping of the human exon junction complex. *Nat Struct Mol Biol,* 19**,** 1124-31.

SAUNDERS, A., CORE, L. J. & LIS, J. T. 2006. Breaking barriers to transcription elongation. *Nat Rev Mol Cell Biol,* 7**,** 557-67.

SCHNELL, U., DIJK, F., SJOLLEMA, K. A. & GIEPMANS, B. N. 2012. Immunolabeling artifacts and the need for live-cell imaging. *Nat Methods,* 9**,** 152-8.

SCHRODER, P. A. & MOORE, M. J. 2005. Association of ribosomal proteins with nascent transcripts in S. cerevisiae. *RNA,* 11**,** 1521-9.

SCHUWIRTH, B. S., BOROVINSKAYA, M. A., HAU, C. W., ZHANG, W., VILA-SANJURJO, A., HOLTON, J. M. & CATE, J. H. 2005. Structures of the bacterial ribosome at 3.5 A resolution. *Science,* 310**,** 827-34.

SCHWEINGRUBER, C., RUFENER, S. C., ZUND, D., YAMASHITA, A. & MUHLEMANN, O. 2013. Nonsense-mediated mRNA decay - mechanisms of substrate mRNA recognition and degradation in mammalian cells. *Biochim Biophys Acta,* 1829**,** 612-23.

SELMER, M., DUNHAM, C. M., MURPHY, F. V. T., WEIXLBAUMER, A., PETRY, S., KELLEY, A. C., WEIR, J. R. & RAMAKRISHNAN, V. 2006. Structure of the 70S ribosome complexed with mRNA and tRNA. *Science,* 313**,** 1935-42.

SHANDILYA, J. & ROBERTS, S. G. 2012. The transcription cycle in eukaryotes: from productive initiation to RNA polymerase II recycling. *Biochim Biophys Acta,* 1819**,** 391-400.

SHATKIN, A. J. 1976. Capping of eucaryotic mRNAs. *Cell,* 9**,** 645-53.

SHAW, P. & BROWN, J. 2012. Nucleoli: composition, function, and dynamics. *Plant Physiol,* 158**,** 44-51.

SHAW, P. J. & JORDAN, E. G. 1995. The nucleolus. *Annu Rev Cell Dev Biol,* 11**,** 93-121.

SHEPPARD, D. N., OSTEDGAARD, L. S., RICH, D. P. & WELSH, M. J. 1994. The amino-terminal portion of CFTR forms a regulated Cl- channel. *Cell,* 76**,** 1091-8.

SHI, M., ZHANG, H., WANG, L., ZHU, C., SHENG, K., DU, Y., WANG, K., DIAS, A., CHEN, S., WHITMAN, M., WANG, E., REED, R. & CHENG, H. 2015. Premature Termination Codons Are Recognized in the Nucleus in A Reading-Frame Dependent Manner. *Cell Discov,* 1.

SHIBUYA, T., TANGE, T. O., SONENBERG, N. & MOORE, M. J. 2004. eIF4AIII binds spliced mRNA in the exon junction complex and is essential for nonsense-mediated decay. *Nat Struct Mol Biol,* 11**,** 346-51.

SHIGEOKA, T., LU, B. & HOLT, C. E. 2013. Cell biology in neuroscience: RNA-based mechanisms underlying axon guidance. *J Cell Biol,* 202**,** 991-9.

SINGH, G., KUCUKURAL, A., CENIK, C., LESZYK, J. D., SHAFFER, S. A., WENG, Z. & MOORE, M. J. 2012. The cellular EJC interactome reveals higher-order mRNP structure and an EJC-SR protein nexus. *Cell,* 151**,** 750-64.

SOUDET, J., GELUGNE, J. P., BELHABICH-BAUMAS, K., CAIZERGUES-FERRER, M. & MOUGIN, A. 2010. Immature small ribosomal subunits can engage in translation initiation in Saccharomyces cerevisiae. *EMBO J,* 29**,** 80-92.

STRUNK, B. S., LOUCKS, C. R., SU, M., VASHISTH, H., CHENG, S., SCHILLING, J., BROOKS, C. L., 3RD, KARBSTEIN, K. & SKINIOTIS, G. 2011. Ribosome assembly factors prevent premature translation initiation by 40S assembly intermediates. *Science,* 333**,** 1449-53.

STRUNK, B. S., NOVAK, M. N., YOUNG, C. L. & KARBSTEIN, K. 2012. A translation-like cycle is a quality control checkpoint for maturing 40S ribosome subunits. *Cell,* 150**,** 111-21.

SUSOROV, D., MIKHAILOVA, T., IVANOV, A., SOKOLOVA, E. & ALKALAEVA, E. 2015. Stabilization of eukaryotic ribosomal termination complexes by deacylated tRNA. *Nucleic Acids Res,* 43**,** 3332-43.

TARUN, S. Z., JR. & SACHS, A. B. 1995. A common function for mRNA 5' and 3' ends in translation initiation in yeast. *Genes Dev,* 9**,** 2997-3007.

TARUN, S. Z., JR. & SACHS, A. B. 1996. Association of the yeast poly(A) tail binding protein with translation initiation factor eIF-4G. *EMBO J,* 15**,** 7168-77.

TASHEVA, E. S. & ROUFA, D. J. 1995. Regulation of human RPS14 transcription by intronic antisense RNAs and ribosomal protein S14. *Genes Dev,* 9**,** 304-16.

TOPISIROVIC, I., SVITKIN, Y. V., SONENBERG, N. & SHATKIN, A. J. 2011. Cap and cap-binding proteins in the control of gene expression. *Wiley Interdiscip Rev RNA,* 2**,** 277-98.

TRCEK, T., SATO, H., SINGER, R. H. & MAQUAT, L. E. 2013. Temporal and spatial characterization of nonsense-mediated mRNA decay. *Genes Dev,* 27**,** 541-51.

TSCHOCHNER, H. & HURT, E. 2003. Pre-ribosomes on the road from the nucleolus to the cytoplasm. *Trends Cell Biol,* 13**,** 255-63.

UDEM, S. A. & WARNER, J. R. 1973. The cytoplasmic maturation of a ribosomal precursor ribonucleic acid in yeast. *J Biol Chem,* 248**,** 1412-6.

URLAUB, G., MITCHELL, P. J., CIUDAD, C. J. & CHASIN, L. A. 1989. Nonsense mutations in the dihydrofolate reductase gene affect RNA processing. *Mol Cell Biol,* 9**,** 2868-80.

VEINOT-DREBOT, L. M., SINGER, R. A. & JOHNSTON, G. C. 1988. Rapid initial cleavage of nascent pre-rRNA transcripts in yeast. *J Mol Biol,* 199**,** 107-13.

VENEMA, J. & TOLLERVEY, D. 1999. Ribosome synthesis in Saccharomyces cerevisiae. *Annu Rev Genet,* 33**,** 261-311.

VESPER, O., AMITAI, S., BELITSKY, M., BYRGAZOV, K., KABERDINA, A. C., ENGELBERG-KULKA, H. & MOLL, I. 2011. Selective translation of leaderless mRNAs by specialized ribosomes generated by MazF in Escherichia coli. *Cell,* 147**,** 147-57.

WAGNER, R. R. & HUANG, A. S. 1965. Reversible inhibition of interferon synthesis by puromycin: evidence for an interferon-specific messenger RNA. *Proc Natl Acad Sci U S A,* 54**,** 1112-8.

WAHL, M. C., WILL, C. L. & LUHRMANN, R. 2009. The spliceosome: design principles of a dynamic RNP machine. *Cell,* 136**,** 701-18.

WANG, H., YU, J., ZHANG, L., XIONG, Y., CHEN, S., XING, H., TIAN, Z., TANG, K., WEI, H., RAO, Q., WANG, M. & WANG, J. 2014. RPS27a promotes proliferation, regulates cell cycle progression and inhibits apoptosis of leukemia cells. *Biochem Biophys Res Commun,* 446**,** 1204-10.

WARNER, J. R. & MCINTOSH, K. B. 2009. How common are extraribosomal functions of ribosomal proteins? *Mol Cell,* 34**,** 3-11.

WEN, J. 2009. *Characterization of nonsense mediated mRNA decay in Schizosaccharomyces pombe.* PhD Thesis, University of Birmingham.

WEN, J. & BROGNA, S. 2010. Splicing-dependent NMD does not require the EJC in Schizosaccharomyces pombe. *EMBO J,* 29**,** 1537-51.

WENG, Y., CZAPLINSKI, K. & PELTZ, S. W. 1996. Genetic and biochemical characterization of mutations in the ATPase and helicase regions of the Upf1 protein. *Mol Cell Biol,* 16**,** 5477-90.

WILL, C. L. & LUHRMANN, R. 2011. Spliceosome structure and function. *Cold Spring Harb Perspect Biol,* 3.

WONG, W., BAI, X. C., BROWN, A., FERNANDEZ, I. S., HANSSEN, E., CONDRON, M., TAN, Y. H., BAUM, J. & SCHERES, S. H. 2014. Cryo-EM structure of the Plasmodium falciparum 80S ribosome bound to the anti-protozoan drug emetine. *Elife,* 3.

WU, R. S. & WARNER, J. R. 1971. Cytoplasmic synthesis of nuclear proteins. Kinetics of accumulation of radioactive proteins in various cell fractions after brief pulses. *J Cell Biol,* 51**,** 643-52.

XUE, S. & BARNA, M. 2012. Specialized ribosomes: a new frontier in gene regulation and organismal biology. *Nat Rev Mol Cell Biol,* 13**,** 355-69.

YOON, J. H., LOVE, D. C., GUHATHAKURTA, A., HANOVER, J. A. & DHAR, R. 2000. Mex67p of Schizosaccharomyces pombe interacts with Rae1p in mediating mRNA export. *Mol Cell Biol,* 20**,** 8767-82.

YOUNGMAN, E. M., HE, S. L., NIKSTAD, L. J. & GREEN, R. 2007. Stop codon recognition by release factors induces structural rearrangement of the ribosomal decoding center that is productive for peptide release. *Mol Cell,* 28**,** 533-43.

YUSUPOVA, G. & YUSUPOV, M. 2014. High-resolution structure of the eukaryotic 80S ribosome. *Annu Rev Biochem,* 83**,** 467-86.

ZAVIALOV, A. V., HAURYLIUK, V. V. & EHRENBERG, M. 2005. Splitting of the posttermination ribosome into subunits by the concerted action of RRF and EF-G. *Mol Cell,* 18**,** 675-86.

ZHANG, S., RUIZ-ECHEVARRIA, M. J., QUAN, Y. & PELTZ, S. W. 1995. Identification and characterization of a sequence motif involved in nonsense-mediated mRNA decay. *Mol Cell Biol,* 15**,** 2231-44.

ZORIO, D. A. & BENTLEY, D. L. 2004. The link between mRNA processing and transcription: communication works both ways. *Exp Cell Res,* 296**,** 91-7.

APPENDICES

Appendix 1 Media and solutions

S. Pombe media (recipes available from http://www-bcf.usc.edu/~forsburg/media.html)

YES

5 g yeast extract and 225 mg each of the amino acid and nucleotide supplements (adenine, histidine, leucine, uracil, arginine and lysine hydrochloride) were dissolved in 900 mL of purified H_2O. The media was sterilised by autoclaving at 121°C for 30 minutes. 3% glucose from 30% liquid stock was added after autoclaving.

Agar YES media was made by adding 2% agar to the media before autoclaving. 3% glucose was added to the media after autoclaving and thoroughly mixed before dispensing in 25 mL volumes into 9 cm petri dishes. Plates were allowed to cool in a laminar flow for at least 30 minutes and stored at 4°C.

EMM without leucine

3 g potassium hydrogen phthalate, 2.2 g Na2HPO4, 5 g NH4Cl and 225 mg of each of the amino acid and nucleotide supplements (adenine, histidine, uracil, arginine and lysine hydrochloride) were dissolved in 950 mL of purified H_2O and sterilized by autoclaving at 121°C for 30 minutes. After autoclaving, 2% glucose from 40% liquid stock and 1 X of each of salt, vitamin and mineral stocks (see recipes below) was added to cooled media.

EMM agar media was made by adding 2% agar to the media before autoclaving. After autoclaving, 2% glucose was added to the media and thoroughly mixed before dispensing in 25 mL volumes into 9 cm petri dishes.

SPAS mating plates

1g KH_2PO_4, 1 X vitamins, 10 g glucose, 45 mg/mL of each of the amino acid and nucleotide supplements (adenine, histidine, leucine, arginine, uracil and lysine hydrochloride) and 3% agar were dissolved in 1L purified H2O and sterilized by autoclaving 121°C for 30 minutes. Media was then dispensed in 25 mL volumes into 9 cm petri dishes.

E. coli media (recipes as described in Molecular Cloning 4th edition (Green and Sambrook, 2012))

LB liquid broth and agar media

10 g Bacto-tryptone, 5 g yeast extract, and 10 g NaCl were dissolved in 800 mL purified H_2O and the pH was adjusted to 7.5 with NaOH. The volume was brought to 1L with purified H_2O and the media was sterilised by autoclaving at 121°C for 30 minutes. Antibiotics were added to cold media at the required concentration just before use.

For agar media, 1% agar was added to the liquid media before autoclaving. Antibiotics were added when the media had cooled to 55°C. 25 mL media was poured into 9 cm Petri dishes and was allowed to set in a laminar flow hood for at least 30 minutes. Plates were stored at 4 °C.

NZY media

5 g NaCl, 2 g $MgSO_4 \cdot 7H_20$, 5 g yeast extract and 10 g NZ amine (Casein hydrolysate) were dissolved in 1L purified H_2O. The pH was adjusted to 7.5 with NaOH and the media was sterilised by autoclaving at 121°C for 30 minutes.

Stocks for use with media

(recipes available from http://www-bcf.usc.edu/~forsburg/media.html)

1. 30% Glucose stock

300 g glucose dissolved in 1L purified H_2O, autoclaved and stored at RT.

2. 40% Glucose stock

400 g glucose dissolved in 1L purified H_2O, autoclaved and stored at RT.

3. 50× Salt stock

52.5 g $MgCl_2 \cdot 6H_2O$, 0.735 g $CaCl_2 \cdot 2H_2O$, 50 g KCl and 2 g Na_2SO_4 dissolved in 1 L purified H_2O, autoclaved and stored at RT.

4. 1000× Vitamin stock

0.1 g pantothenic acid, 1 g nicotinic acid, 1 g inositol and 1 mg biotin in dissolved in 100 mL purified H_2O, autoclaved and stored in a dark environment.

5. 10000× Mineral stock

0.5 g boric acid, 0.4 g $MnSO_4$, 0.4 g $ZnSO_4 \cdot 7H_2O$, 0.2 g $FeCl_2 \cdot 6H_2O$, 40 mg molybdic acid, 0.1 g KI, 40 mg $CuSO_4 \cdot 5H_2O$ and 1 g citric acid dissolved in 100 mL purified H_2O, autoclaved and stored in a dark environment.

6. Antibiotic stocks

Antibiotic stocks were prepared as below and filter sterilised before use. Stocks were stored at -20°C.

- Ampicillin - 100 mg/mL stock in sterile purified H_2O. Working concentration 100 µg/mL in LB media.
- G418 (Sigma) – 100 mg/mL stock in sterile purified H_2O. Working concentration 100 µg/mL.
- Puromycin (Caltag Medsystems) - 50 mg/mL stock in sterile purified H_2O. Working concentration 250 µg/mL in YES media unless otherwise stated.
- Emetine (Sigma) – 100 mg/mL stock in sterile purified H_2O. Working concentration 100 µg/mL in YES media unless otherwise stated.

- Cycloheximide (Sigma) – 100 mg/mL stock in sterile purified H_2O. Working concentration 100 µg/mL in YES media unless otherwise stated.
- Anisomycin (Sigma) – 20 mg/mL stock in DMSO. Working concentration 250 µg/mL in YES media unless otherwise stated.

Appendix 2 *S. pombe* strains used in this study

Stock reference	Strain name	Alternative reference	Genotype	Source
TLM001	wt	SPJK001	h+ ade6-210 arg3D his3D leu1-32 ura4DS/E	Janet Partridge
TLM093	Cbc2-3HA	DB4	h- cbp20-3HA::kanMx6 ade6-M216 leu1-32 ura4-D18	Sandip De stocks
TLM095	Rpl7-3HA (h-)	DB1	h- rpl7-3HA::kanMx6	Sandip De stocks
TLM097	Rpl11-3HA (h-)	DB2	h- rpl11-3HA::kanMx6	Sandip De stocks
TLM099	Rpl25-3HA (h-)	DB3	h- rpl25-3HA::kanMx6	Sandip De stocks
TLM011	pUpf3-GFP	-	h+*upf3*Δ::KanMX4 ade6-M210 ura4-D18 leu1-32 (pREP41 Upf3-GFP::LEU2)	This study
TLM101	Gar2-GFP	DB8	h- gar2-GFP::kanMX6 leu1 ura4	Sandip De stocks
TLM103	ptr1-1	SPJK010	h- leu1-32 ptr1-1 ts for mRNA export	Jikai Wen stocks
TLM105	ptr3-1	SPJK013	h- leu1-32 ptr3-1 ts for mRNA export	Jikai Wen stocks
TLM107	ptr4-1	SPJK014	h- leu1-32 ptr4-1 ts for mRNA export	Jikai Wen stocks
TLM109	Rae1-167	SPJK049	h(-) leu1-32 ura4-D18 rae1-167	Jikai Wen stocks
TLM111	Rpl7-3HA (h+)		h+ rpl7-3HA::kanMx6	This study
TLM113	Rpl25-3HA (h-)		h+ rpl25-3HA::kanMx6	This study

Appendix 3 Optimisation of ChIP sonication conditions

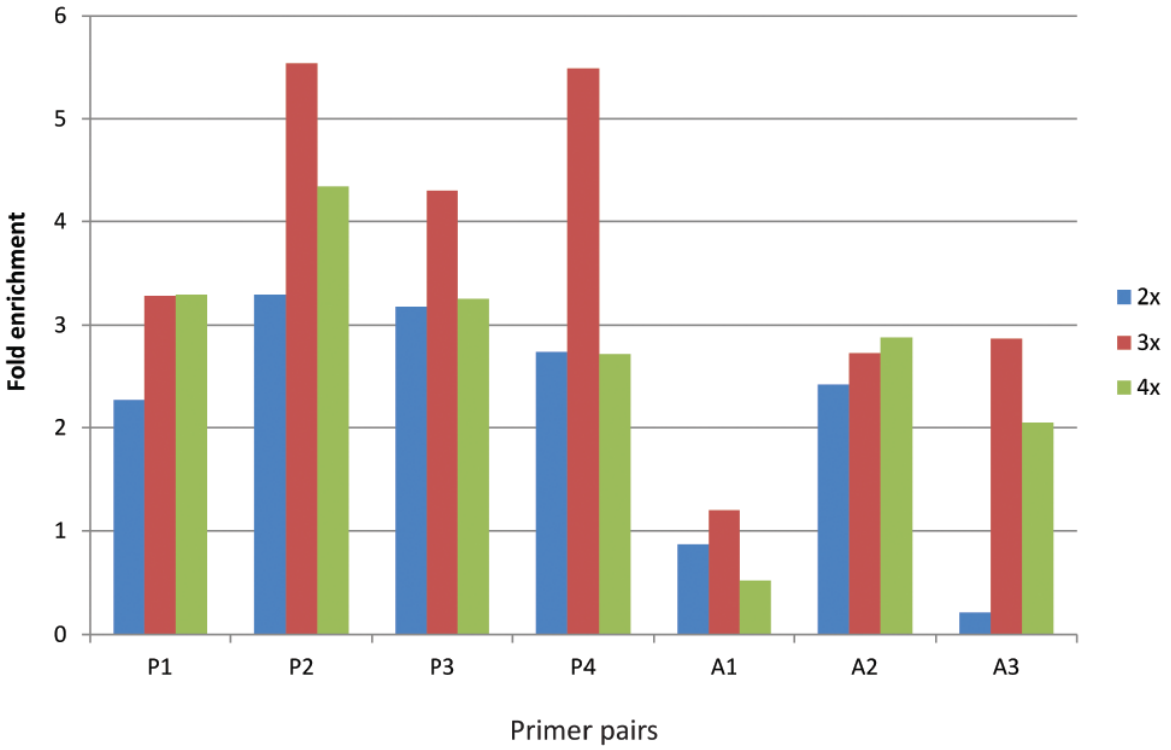

Histogram showing enrichment of Cbc2 at the *pma1* and *act1* loci following qRT-PCR of ChIP samples from a Cbc2-3HA strain (De et al., 2011) that had been sonicated either 2, 3 or 4 times for 20s. Primer pairs used at each locus are indicated below the histogram and are listed in Appendix 4. The fold enrichment of Cbc2 at different regions of each locus is calculated using the ΔΔct method (described in Materials and Methods) in comparison to the intergenic region in (A). ChIP was with a 12CA5 anti-HA antibody (CRUK) using ChIP protocol I in Materials and Methods.

Appendix 4 Primers used in ChIP-qRT-PCR analysis & gene loci information

Gene name & primer stock reference	Primer pair	Primer Sequence
Intergenic region	Forward	GCGAAACCAGTATGGACGAT
	Reverse	AACGGGCAAATGTAAAGACG
*pma*1	P1 F	CTCTAGAACATACGTTATTTAATCTCGA
	P1 R	GTATTACCGACAATAGAAAAGGGG
Sandip De stocks	P2 F	GTCTTCGTGATTGGGTCGAT
	P2 R	GGGGTCACCATAGTGCTTGT
	P3 F	ATCCCGTTTCCAAGAAGGTT
	P3 R	GAGGATCGGAACAAGGCATA
	P4 F	GTCTTTCCACCGTCATTGGT
	P4 R	ACGGAGAACGGCAACAATAG
*act*1	A1 F	GCTCAATGTTATCCGTTTCCG
	A1 R	GTAGTTGGTAAACGGTAAGTTATAACAC
Sandip De stocks	A2 F	GGAAGAAGAAATCGCAGCGT
	A2 R	ACATATCATCCCAGTTGTTGACAATAC
	A3 F	GAAATGTGATGTTGATATTCGTAAAG
	A3 R	GCTCTCATCATACTCTTGCTTGG
*fba*1	F1 F	CCCTGCCATTAACGTCACCT
	F1 R	CCAGCAAAGAAGTGAGCACC
T77-T82	F2 F	CTGGGATGTCTACCGTGAGC
This study	F2 R	GTGTTGACCCAAAAGAGCGG
	F3 F	CGACAAGCCCGTTTTCTTCG
	F3R	AGGCGAATTGGGTATCAGTGT
*gpd*3	G1 F	CTCACTGGCAAGATCCAAGTTGTCG
	G1 R	ACCGTGGGTAGAGTCGTACTTGAAC
JM80-JM83	G2 F	CAAGCGTGTCATCATCTCTGCTCCT
Jianming Wang stocks	G2 R	GTGCAAGAGGCGTTGGAGATAACC
*pgk*1	PG1 F	TAAGCTCGCTATCACCGACG
	PG1 R	ACGATACGGGCATTGTTGGT
T87-T92	PG2 F	CTCGTCCCTTCCTTGCCAT
This study	PG2 R	GCCATACCACCGCAGATGAT
	PG3 F	ACGGATGGATGGGTTTGGAC
	PG3 R	CAAACTCAAAGACACCAGCGG
*pdc*101	PD1 F	CCCAACACCAATGACCTTAGC
	PD1 R	CCTCAGCTCTCTTGATGGCA
T93-T98	PD2 F	ACTGGGGTGAAGTTAGCAGC
This study	PD2 R	AAGATGTTGGGGTTGGGAGC
	PD3 F	GGGGTCACATTGGTTGGTCT
	PD3 R	GCTTGTGGCGGATCATTTGA
*tdh*1	T1 F	CCGTAACGCTTTGGTCGCTA
	T1 R	CCGTGGGTAGAGTCGTACTTG
T105-T110	T2 F	CACTGTCCACGCTACCACTG
This study	T2 R	GAGGAGGGGATGATGTTGGC

	T3 F	GCCAAGCCTACCAACTACGA
	T3 R	TGTCACCGCAGAAGTCAGTG
*Ubc*4	U1 F	ACCCACCGTCTTCTTGTTCC
	U1 R	GCTGCACAATCCTAGCAAGC
T155-T160	U2 F	GCTTGTGAATCGGAGGAGGA
This study	U2 R	GCATCACTGTCAACCATACCG
	U3 F	TCCATCCAAGTGAAGCGAGG
	U3 R	ACCGTTTGAATTGATGTTGGGA
*ecm*33	E1 F	CTCTTCTTTTCGCCGCAGC
	E1 R	GCCAGAGTTACCAGCATCAGAA
T161-T166	E2 F	TCCGCTAACTCTAAGGGTGT
This study	E2 R	ACAAGTTACCAGCAGCACTCT
	E3 F	GGTTTCCCCGTCATCTCTGA
	E3 R	TGGACCAAGGGCAAGTGAAA
*tif*52	TI1 F	GCTGCTCCTCCTGAAATTCCT
	TI1 R	CCTCGCCCGTACTACCTTTC
T181-T186	TI2 F	CCTGCCACTTCAATCTCGGT
This study	TI2 R	TTCCTCCAATGCTGCTTCCC
	TI3 F	CGCTGTGCTACTATGCTGGA
	TI3 R	TTGACACCAAGCTGTTCAGC
*clu*1	C1 F	CCTCTCTTCCTGGCTCCTCT
	C1 R	CAGGGTCTGCGTATGATCGG
T187-T192	C2 F	GAGATTCTGCCGCCTACTCC
This study	C2 R	GACCAGCATAATCAACGACGC
	C3 F	ACAGAACACCACGAATAGGCA
	C3 R	TGCTTCCAATGATTCTTGAGCT
*tif*32	TF1 F	GCTCAGGAGAAGGCAGACAA
	TF1 R	TCTGTGCGGCTCTTGGAAAG
T193-T198	TF2 F	CTGGTGTTGAACAGGAGCGT
This study	TF2 R	ACTCGGCTTCAGATTCTTGCT
	TF3 F	CGTGCTTATCGTCGTGAAGC
	TF3 R	TGCGTTGTTTCTCCCTCTCG
*eft*201	EF1 F	AAGGCTGGTGATGCTCGTTT
	EF1 R	CAGTACCATCAGCAGGCTCC
T199-T204	EF2 F	GTTTTCCGTCTCCCCAGTCG
This study	EF2 R	GGTCGGATTTGGAAAGACGC
	EF3 F	GCTGACGAGTTTGGATGGGA
	EF3 R	CCAGGCAAAAGCAGCAACAA
*tef*3	TE1 F	TTGTACCTGGTTGCGTCCTC
	TE1 R	ACGACACCACCACCAAAGTT
T205-T210	TE2 F	GTCTACCCTTATGCGTGCCA
This study	TE2 R	GGAGTGTCGGCTTCAGACTC
	TE3 F	TTGTACCTGGTTGCGTCCTC
	TE3 R	ACGACACCACCACAAAGTT

Details of gene loci analysed by qPCR

Gene	Systematic name	Locus	Length (nt) Transcription unit (CDS)	Product	RNA copy number per cell	Protein copy number per cell
pma1	SPAC1071.10c	Chr I 3876176 - 3871642	4535 (2760)	P-type proton ATPase, P3-type Pma1	190	438967
act1	SPBC32H8.12c	Chr II 1477317 – 1475485	1833 (1128)	actin Act1	180	464684
fba1	SPBC19C2.07	Chr II 1688336 – 1689599	1264 (1077)	fructose-bisphosphate aldolase Fba1	520	1376321
gpd3	SPBC354.12	Chr II 578063 – 580056	1994 (1008)	glyceraldehyde 3-phosphate dehydrogenase Gpd3	110	151540
pgk1	SPBC14F5.04c	Chr II 4159543 – 4157821	1723 (1245)	phosphoglycerate kinase Pgk1 (predicted)	250	1079504
pdc101	SPAC1F8.07c	Chr I 103594 – 101715	1880 (1709)	pyruvate decarboxylase (predicted)	310	852089
tdh1	SPBC32F12.11	Chr II 2807534 – 2809051	1518 (1011)	glyceraldehyde-3-phosphate dehydrogenase Tdh1	560	1021180
ecm33	SPAC1705.03c	Chr I 1571567 - 1569613	1955 (1266)	cell wall protein Ecm33	48	97610
ubc4	SPBC119.02	Chr II 715227 – 716311	1085 (894)	APC ubiquitin conjugating enzyme E2 Ubc4/UbcP1	52	305467
tif52	SPAC56F8.03	Chr I 1129519 – 1133089	3571 (3240)	translation initiation factor eIF5B Tif52 (predicted)	16	24083
clu1	SPBC530.06c	Chr II 802902 – 798995	3908 (3710)	clustered mitochondria (cluA/CLU1) homolog Clu1 (predicted)	1.9	74.66
tif32	SPBC17D11.05	Chr II 3314293 – 3317452	3160 (2844)	translation initiation factor eIF3a	18	58060
eft201	SPAC513.01c	Chr I 2910274 – 2907643	2632 (2529)	translation elongation factor 2 (EF-2) Eft2,A	59	670805
tef3	SPCC417.08	Chr III 1685599 – 1688951	3353 (3144)	translation elongation factor eEF3	160	277776

Appendix 5 Additional RPM-ChIP results

A

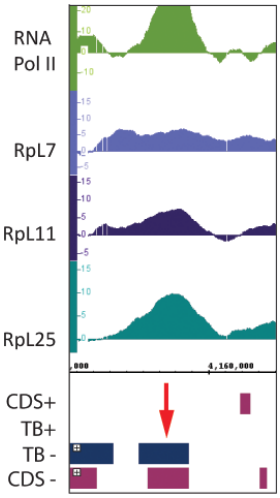

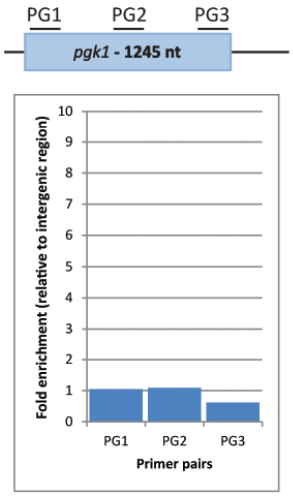

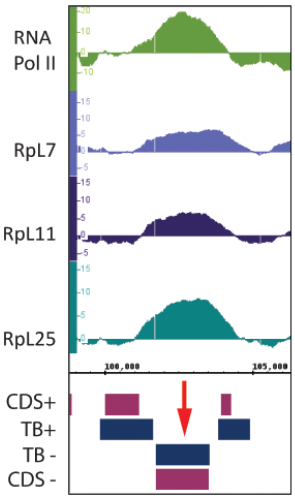

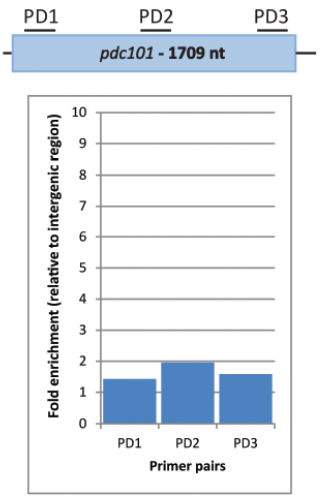

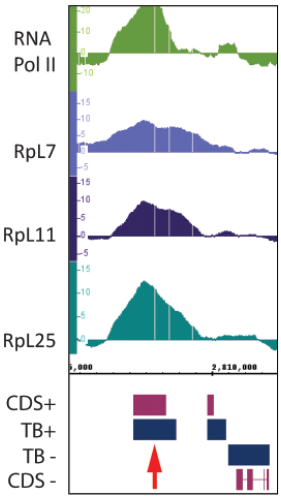

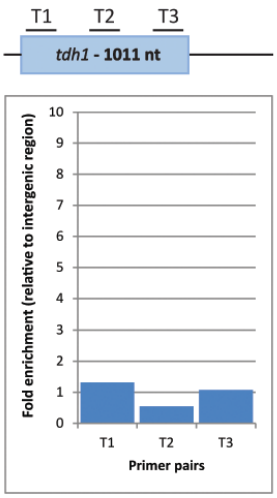

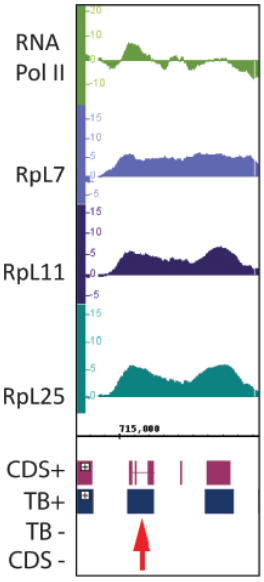
RNA
Pol II
RpL7
RpL11
RpL25
715,080
CDS+
TB+
TB -
CDS -

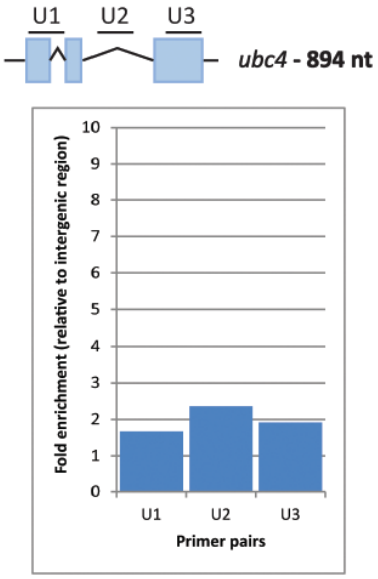
U1
U2
U3
ubc4 - 894 nt
Fold enrichment (relative to intergenic region)
0
1
2
3
4
5
6
7
8
9
10
U1
U2
U3
Primer pairs

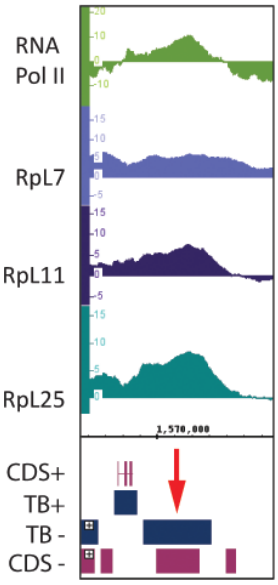
RNA
Pol II
RpL7
RpL11
RpL25
1,570,000
CDS+
TB+
TB -
CDS -

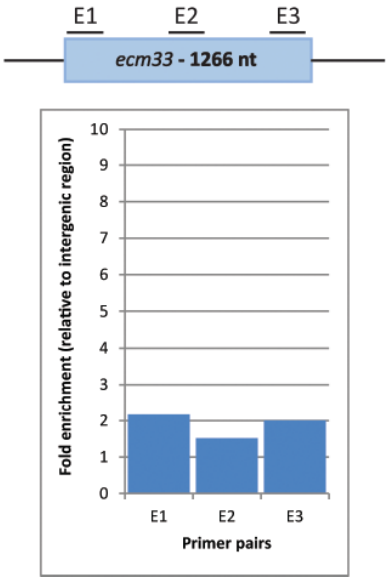
E1
E2
E3
ecm33 - 1266 nt
Fold enrichment (relative to intergenic region)
0
1
2
3
4
5
6
7
8
9
10
E1
E2
E3
Primer pairs

B

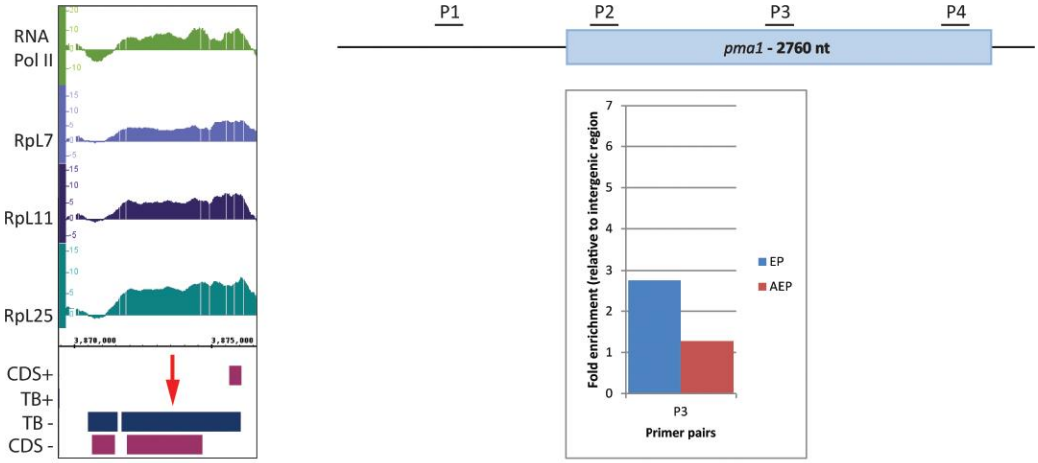
RNA Pol II
RpL7
RpL11
RpL25
CDS+
TB+
TB -
CDS -
P1
P2
P3
P4
pma1 - 2760 nt
Fold enrichment (relative to intergenic region)
EP
AEP
P3
Primer pairs

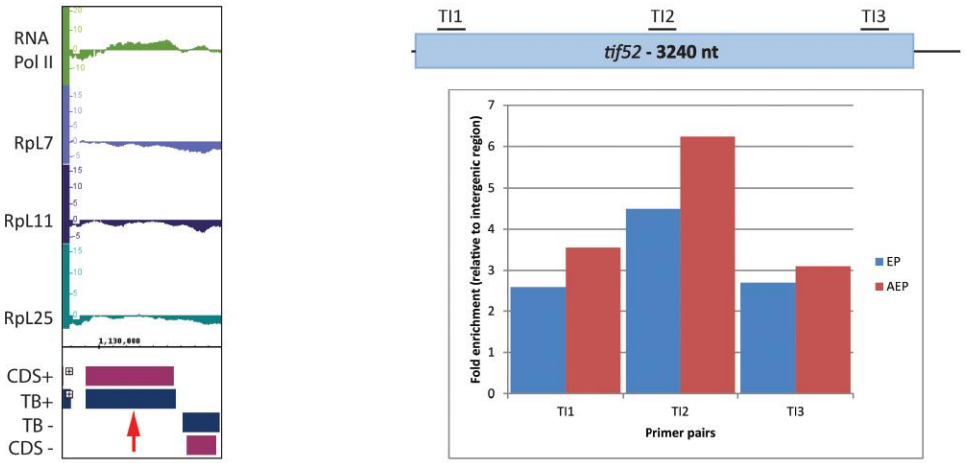
RNA Pol II
RpL7
RpL11
RpL25
CDS+
TB+
TB -
CDS -
TI1
TI2
TI3
tif52 - 3240 nt
Fold enrichment (relative to intergenic region)
EP
AEP
TI1
TI2
TI3
Primer pairs

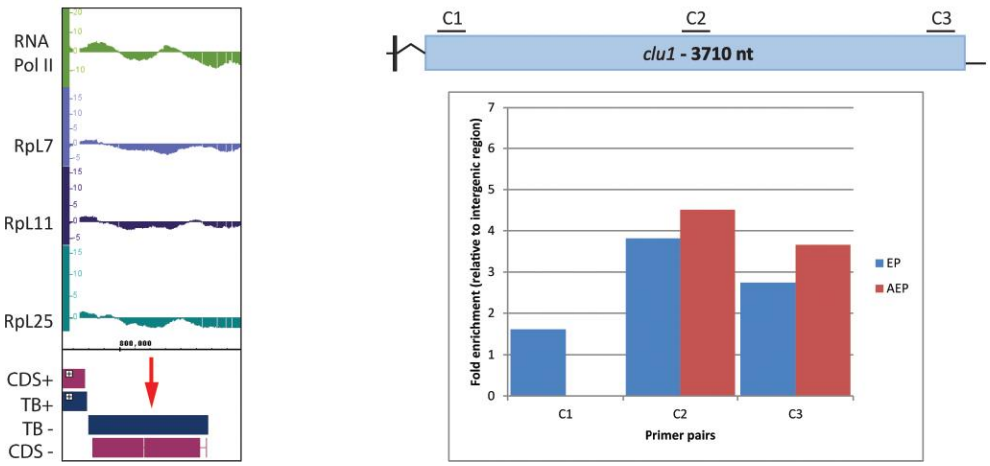
RNA Pol II
RpL7
RpL11
RpL25
CDS+
TB+
TB -
CDS -
C1
C2
C3
clu1 - 3710 nt
Fold enrichment (relative to intergenic region)
EP
AEP
C1
C2
C3
Primer pairs

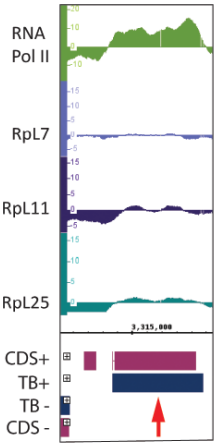
RNA
Pol II
RpL7
RpL11
RpL25
CDS+
TB+
TB -
CDS -

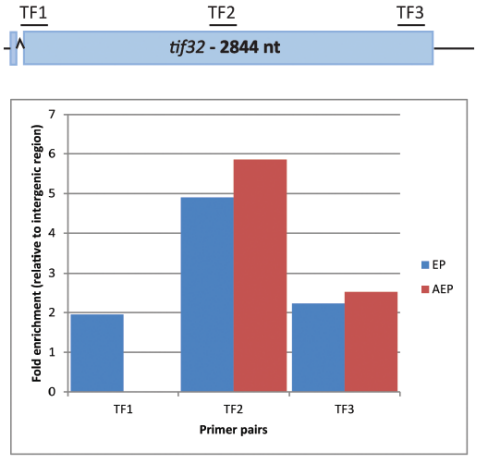
TF1
TF2
TF3
tif32 - 2844 nt
Fold enrichment (relative to intergenic region)
Primer pairs
EP
AEP

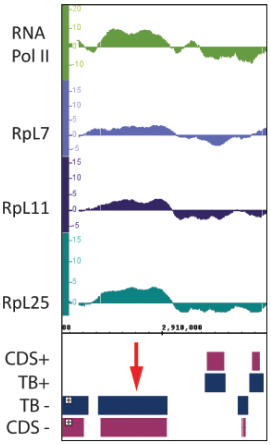
RNA
Pol II
RpL7
RpL11
RpL25
CDS+
TB+
TB -
CDS -

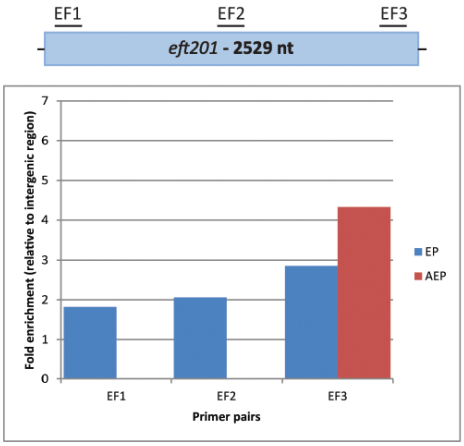
EF1
EF2
EF3
eft201 - 2529 nt
Fold enrichment (relative to intergenic region)
Primer pairs
EP
AEP

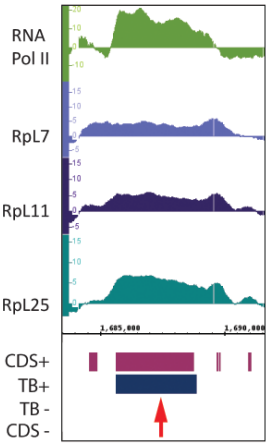
RNA
Pol II
RpL7
RpL11
RpL25
CDS+
TB+
TB -
CDS -

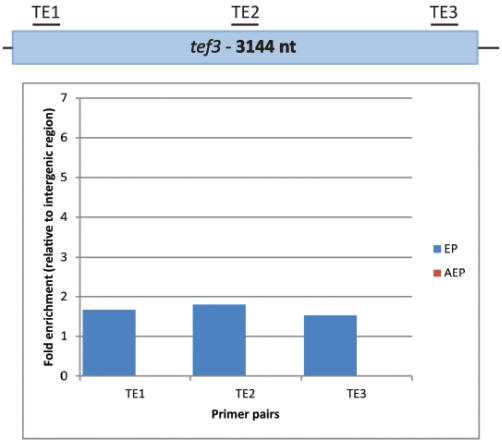
TE1
TE2
TE3
tef3 - 3144 nt
Fold enrichment (relative to intergenic region)
Primer pairs
EP
AEP

Appendix 5 Enrichment profiles of Pol II, RpL7, RpL11 and RpL25 at several *S. pombe* loci, as determined by analysis of ChIP-chip data (De et al., 2011). (A) Histograms in each panel show qRT-PCR analysis of enrichment of ribopuromycylated peptides at the named loci when wild-type cultures had been treated with 200 μg/mL emetine for 30 minutes followed by 250 μg/mL puromycin for 15 minutes. (B) Histograms show enrichment with puromycylated peptides both without (blue) and with (red) anisomycin alongside emetine treatment. ChIP was carried out with an anti-puromycin antibody (clone 5B12) using ChIP protocol II in (A) and ChIP protocol III in (B) (see Materials and Methods). Schematic of each gene shows the locations of primer pairs (Appendix 4) used at each locus.

Appendix 6 Preliminary analysis of the association of puromycylated peptides with polysome fractions

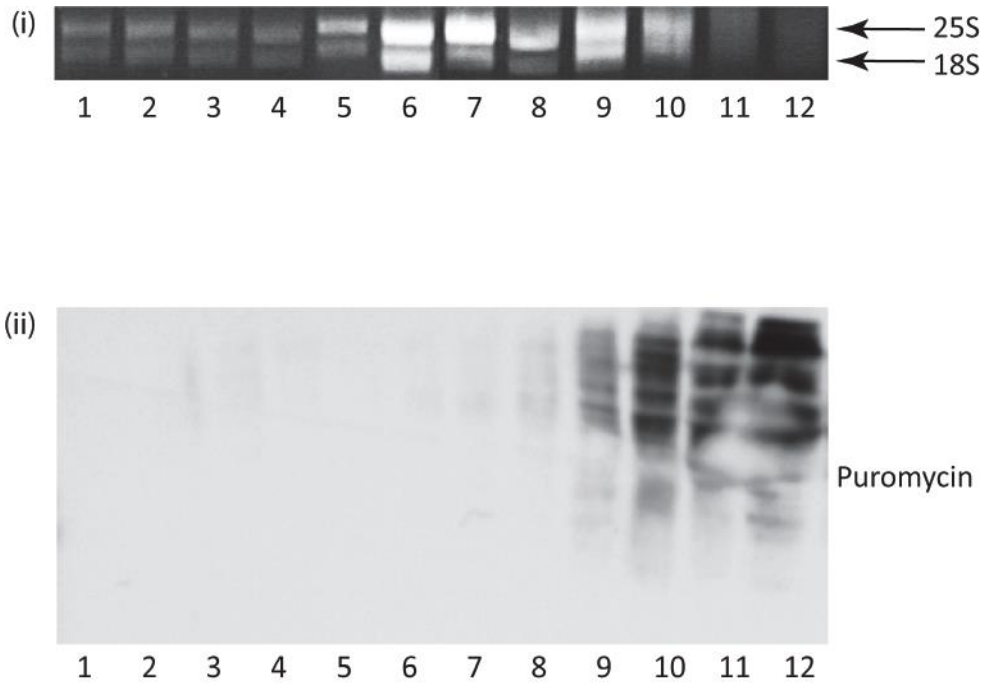

(i) A 1% native agarose gel showing RNA contained within 10 µL of each of the polysomal fractions from cells that had been ribopuromycylated by treatment with emetine at 200 µg/mL for 30 minutes, followed by treatment with puromycin at 250 µg/mL for 15 minutes. (ii) Western blot showing distribution of puromycylated peptides in protein extracts from the same polysomal fractions shown above (ii). Detection of puromycylated peptides was performed by probing the nitrocellulose membrane with a mouse anti-puromycin antibody (clone 5B12, see Material and Methods).

Appendix 7 Additional polysome profiles

A

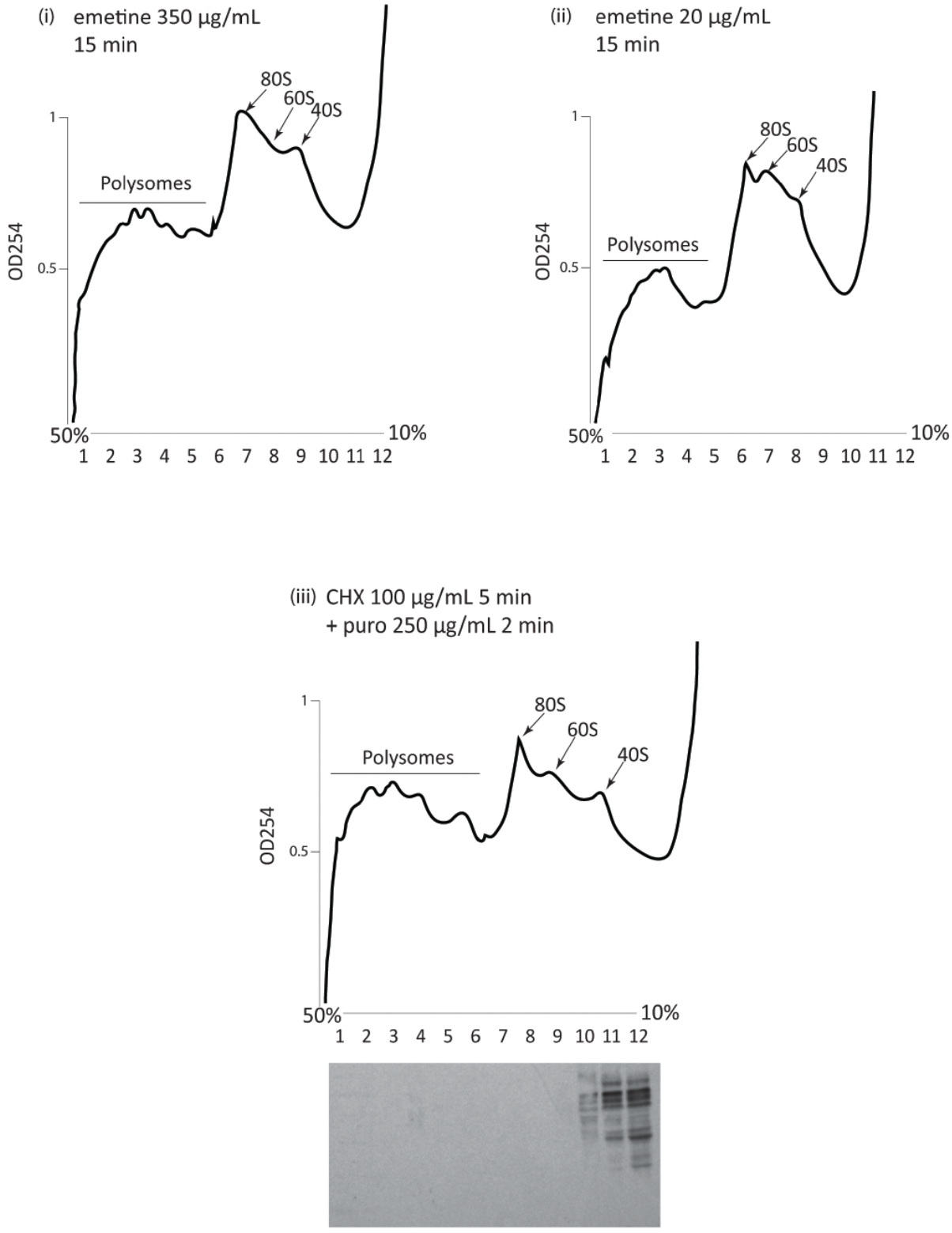

B

(i)

No drug

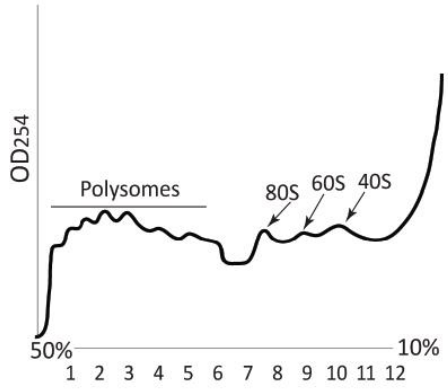

(ii)

Emetine 100 µg/ml 5 min

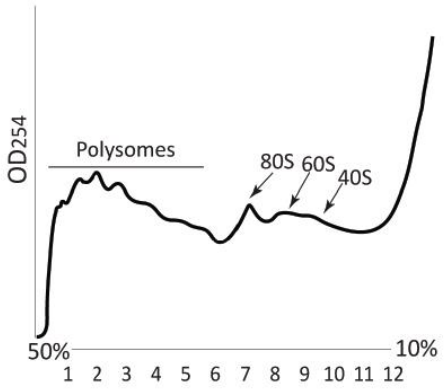

(iii)

CHX 100 µg/ml 5 min

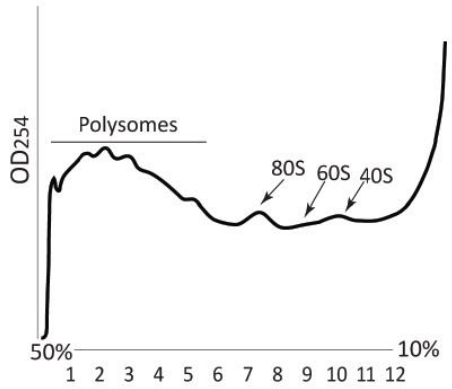

(iv)

Puro 50 µg/ml 30 s

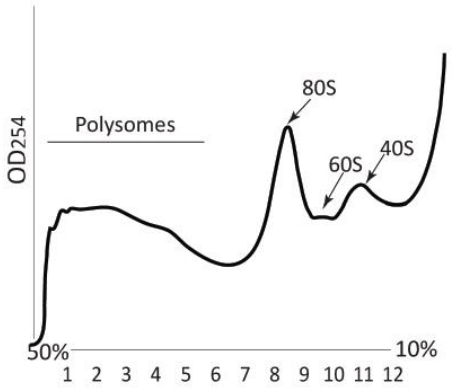

(v)

Emetine 100 µg/ml 5 min
+ puro 50 µg/ml 30 s

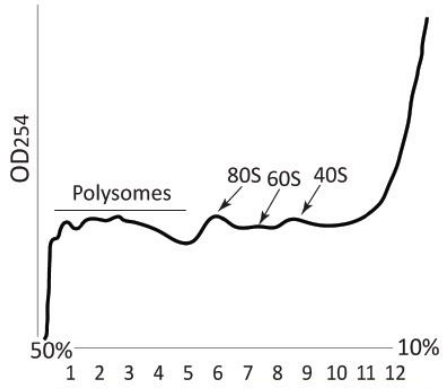

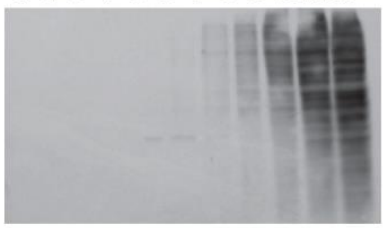

(vi)

CHX 100 µg/ml 5 min
+ puro 50 µg/ml 30 s

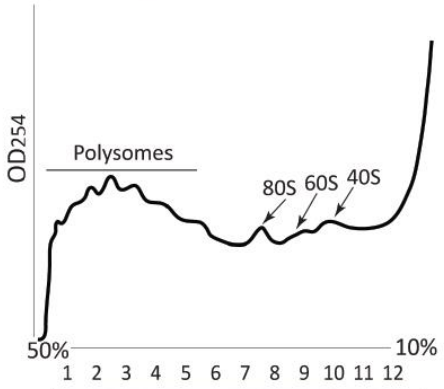

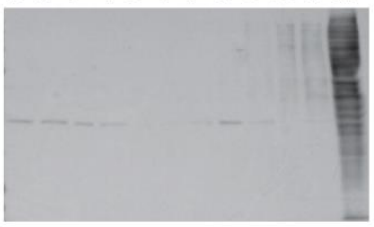

Appendix 7 Additional preliminary polysome profiles. (A) *S. pombe* cells were treated with translation inhibitors at the concentrations and durations indicated and polysome profiling was carried out as in Figure 4.2 to assess the stabilisation of polysomes. Data represents only one experimental run and therefore no statistical analysis was carried out. (B) Polysome profiling of HeLa cells, treated with translation inhibitors at the concentrations and durations indicated. Data represents only one experimental run and therefore no statistical analysis was carried out. Western blots in (A) and (B) show the detection of puromycylated peptides with the fractions and was carried out as in Figure 4.3.

Appendix 8 Primers used for cloning upf3 into prep41-GFP

Primer stock reference	Primer sequence	Comments
T1 This study	cccGCTAGCaccATGGCTCCTGATATCTCAA	Forward primer for amplification of *S. pombe* upf3, after ATG, with Nhe1 restriction site added at 5' end
T2 This study	cccGCTAGCAACATTATCAGTTGTTAG	Reverse primer for amplification of *S. pombe* upf3, before stop codon, with Nhe1 restriction site added at 5' end

Appendix 9 Plasmid maps & list of ribosomal proteins being tagged with GFP

The ribosomal proteins currently being tagged with GFP for episomal expression are listed below:-

Rps2	Rps1201
Rps3	Rps13
Rps5	Rps1502
Rps602	Rps1602
Rps1102	Rps1801

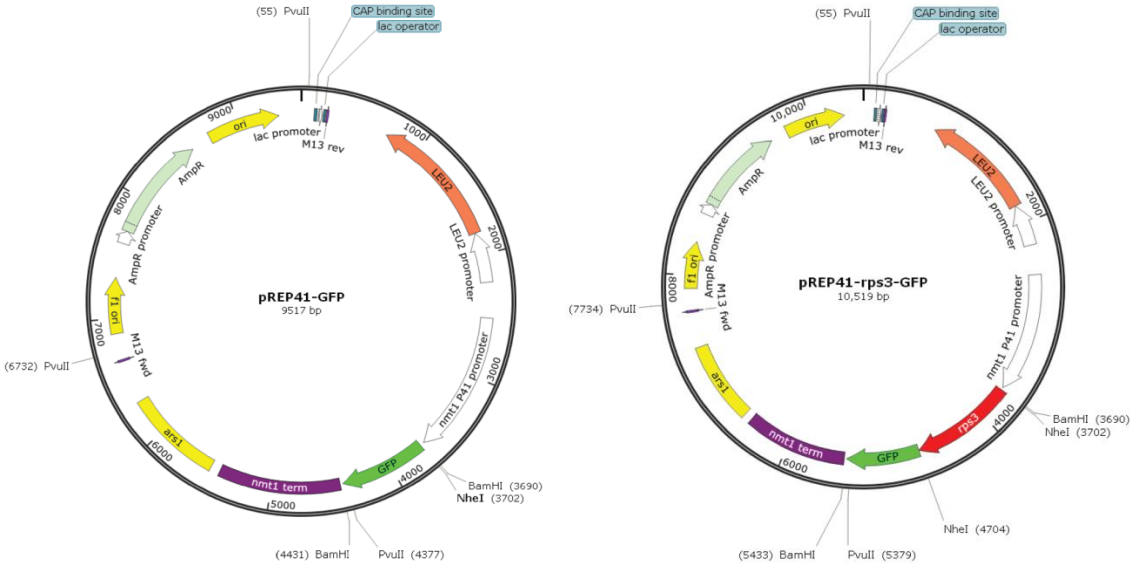

Plasmid map of the prep41-GFP vector (left) used for episomal tagging of Upf3 with GFP and also for current work to tag ribosomal proteins. An example of a plasmid map for GFP-tagged Rps3 is also shown (right). Cloning of the Upf3 and RP sequences was at the Nhe1 restriction site, immediately after the ATG of GFP, as described in Materials and Methods.